



UNIVERSITAT
POLITÈCNICA
DE VALÈNCIA



Modelling and experimental validation of an innovative coaxial helical borehole heat exchanger for a dual source heat pump system

PhD Thesis

Antonio Cazorla Marín

Supervisors

Dr. José Miguel Corberán Salvador

Dr. Carla Isabel Montagud Montalvá

June 2019

Acknowledgements

I would like to say thank you to all the people that has accompanied me during this long period. It would have not been possible without your support.

I would like to especially thank my supervisors Carla and José Miguel, for all the valuable help and guidance that they offered me during my PhD and for offering the opportunity of working in the GEOTeCH project and developing my thesis. To Felix, for guiding me in the beginning with the B2G model and introducing me to the work in the IIE. To Javi, for all the work that we have shared in the GEOTeCH project and helping me with the heat pump model and to Ximo. To Pepe, Emilio, Jorge, Carla, José Miguel and Rafa, for giving me the opportunity of helping in the lessons in the Master. To my office colleague Daniela, for all the conversations and all her help. To Rafa and Jorge, for all the funny conversations at the mid-morning. To all my colleagues in the IIE, present and past, for all the lunches, dinners, beers, nights, Colpbol matches and all the moments that we have shared, especially to Fran, Alex, Abdel, Estefania, Fernando, Miquel, Leti, Bárbara.

Thanks to Henk, for all his help and guidance during my stay at Groenholland and afterwards, to Guus, for making it possible and helping me so much and also to Roy. Thanks to Francesco for offering me the opportunity of staying in UNIBO and all his help, as well as to the Saras, Kristina and Carlo. I would also like to thank all the partners in the GEOTeCH project, it has been a pleasure to work with you. Thanks to José Acuña for providing me with the data of the borehole in KTH, to Giulio and Alessandro from HiRef, Marco, Stefano, Emanuele and Davide, from UNIPD and Francesco, from UNIBO, for providing me with the data from the Tribano demo-site and all the help, and to GEOTHEX, for the information regarding the helical BHE and the experimental data.

Thanks to my father, my sister and my mother, for all their support since the beginning and for helping me in everything, also to my friends, who have encouraged me and understand my lack of time, as well as to Ángela, for helping me during the final steps.

Finally, I would like to acknowledge the financial support that has made this PhD thesis possible. The present work has been supported by the European Community Horizon 2020 Program for European Research and Technological Development (2014-2020) inside the framework of the project 656889 – GEOTeCH (Geothermal Technology for Economic Cooling and Heating), also by the Generalitat Valenciana inside the program “Ayudas para la contratación de personal investigador en formación de carácter predoctoral (ACIF/2016/131)” and by the Institute for Energy Engineering of the Universitat Politècnica de València.

Abstract

Due to the growing increase in energy demand in buildings and the need for an energy transition to renewable and more efficient systems, low enthalpy geothermal energy is considered as an efficient and renewable alternative to conventional systems to provide heating, cooling and domestic hot water production in a sustainable way.

Within this context, the GEOTeCH project was created, a European project that proposes the development of more efficient geothermal heat pump systems with a lower cost compared to the market. To this end, a new type of coaxial Borehole Heat Exchanger (BHE) with helical flow through the outer tube has been developed, which presents a higher efficiency and allows to reduce the length of the heat exchanger to be installed, as well as a Dual Source Heat Pump (DSHP) with variable speed compressor, capable of working with the ground or air as a source / sink, selecting the one that provides the best performance of the system. These components are used in the new "plug and play" system DSHP developed. The main objective is to develop efficient and replicable systems to provide heating, cooling and producing domestic hot water in the market sector of small buildings with a smaller size of the BHE field and an increase in the efficiency. To demonstrate the applicability of these systems, three demonstration facilities have been installed in different countries in Europe: Italy, the Netherlands and the United Kingdom.

In this PhD thesis, a complete dynamic model of the system has been developed in the TRNSYS software, capable of reproducing the behaviour of the different components and the system in general. This model is a useful tool for the development and analysis of different control strategies without the need to implement them in real installations, as well as analyse the behaviour of the system operating under different conditions. For this purpose, it is necessary to develop detailed models of the new components developed in the project: the helical coaxial BHE and the DSHP; to be able to couple them to the rest of the components in the complete model of the system.

For this reason, a dynamic model of the new BHE with helical flow has been developed, able to accurately reproduce the short-term behaviour of the BHE, focused on the evolution of the fluid temperature, and has been validated with experimental data in different operating conditions. In order to reproduce not only the dynamic behaviour of the BHE, but also the long-term response of the ground and the interaction between BHEs in a field, another model has been developed in TRNSYS that performs this function. In this way, by coupling both models, it is possible to reproduce the short-term behaviour of the BHE as well as the long-term response of the ground.

On the other hand, a model of the DSHP, previously developed from data obtained in an experimental campaign, has been implemented in TRNSYS. With this model, it is possible to calculate the capacity of the heat pump depending on the operating mode in which it is

operating (producing heating, cooling, domestic hot water, working with the ground, air, etc.), the frequency of the compressor and other variables and operating conditions.

The model of the hybrid system in TRNSYS has been used to make an analysis of its behaviour working in different climatic conditions, for which three cities have been selected in Spain and three in Europe, with different climatic characteristics. So, different simulations of the system have been carried out in each city for one year. The efficiency of the system in each city has been analysed, as well as the use of each of the sources (air / ground).

On the other hand, one of the demonstration facilities of the GEOTeCH project, including the air-conditioned office building and the coupling with the fan coils, has also been modelled in TRNSYS. With this model, it is intended to study a new strategy to control the frequency of the compressor based on the temperature of the rooms, instead of controlling it based on the supply temperature, with the aim of reducing the consumption of the compressor when the rooms are already in comfort conditions. In addition, other optimization strategies have been tested with the model, analysing the savings obtained with each of them.

Therefore, the models developed, both for the BHE and the system, are able to reproduce their operation and can be used as virtual installations, constituting useful tools to help in the design of the system and the different components, the analysis of their behaviour and the development of optimization strategies.

Resum

A causa del creixent augment de la demanda energètica en edificis i la necessitat d'una transició energètica cap a sistemes renovables i més eficients, l'energia geotèrmica de baixa entalpia es planteja com una alternativa eficient i renovable als sistemes convencionals per proporcionar calefacció, refrigeració i produir aigua calenta sanitària de forma sostenible.

Dins d'aquest context naix el projecte GEOTeCH, un projecte europeu que planteja el desenvolupament de sistemes amb bomba de calor geotèrmica més eficients i amb un cost menor en comparació amb el mercat. Per a això, s'ha desenvolupat un nou tipus d'intercanviador enterrat coaxial amb flux helicoidal en el tub extern que presenta una major eficiència i permet reduir la longitud d'intercanviador a instal·lar, així com una bomba de calor dual amb compressor de velocitat variable, capaç de treballar amb el terreny o l'aire com a font, seleccionant la que proporcione un millor rendiment del sistema. Aquests components s'utilitzen en el nou sistema "plug and play" amb bomba de calor dual desenvolupat. El principal objectiu és desenvolupar un sistema eficient i replicable per proporcionar calefacció, refrigeració i produir aigua calenta sanitària en el sector de mercat d'edificis xicotets amb una grandària menor en el camp d'intercanviadors soterrats i un augment de l'eficiència. Per demostrar l'aplicabilitat d'aquests sistemes, s'han construït tres instal·lacions demostració en diferents països d'Europa: Itàlia, Països Baixos i Regne Unit.

En aquesta tesi doctoral s'ha desenvolupat un model dinàmic complet del sistema en el programari TRNSYS, capaç de reproduir el comportament dels diferents components i del sistema en general. Aquest model constitueix una eina útil per al desenvolupament i anàlisi de diferents estratègies de control sense la necessitat d'implementar-les en instal·lacions reals, així com analitzar el comportament del sistema funcionant sota condicions diferents. Per a aquest propòsit, cal desenvolupar models detallats dels nous components desenvolupats en el projecte: l'intercanviador enterrat coaxial helicoidal i la bomba de calor dual; per poder acoblar-los a la resta de components en el model complet del sistema.

Per això, s'ha desenvolupat un model dinàmic del nou intercanviador enterrat coaxial amb flux helicoidal, capaç de reproduir amb precisió el comportament a curt termini de l'intercanviador, enfocat a l'evolució de la temperatura del fluid, i s'ha validat amb dades experimentals en diferents condicions d'operació. Per a poder reproduir no només el comportament dinàmic de l'intercanviador soterrat, sinó també la resposta a llarg termini del terreny i la interacció entre intercanviadors en un camp, s'ha desenvolupat un altre model en TRNSYS que realitza aquesta funció. D'aquesta manera, en acoblar els dos models és possible reproduir el comportament a curt termini de l'intercanviador enterrat, al mateix temps que la resposta a llarg termini del terreny.

D'altra banda, s'ha implementat en TRNSYS un model de la bomba de calor dual desenvolupat prèviament a partir de dades obtingudes en una campanya experimental. Amb aquest model és possible calcular la capacitat de la bomba de calor dependent del mode

d'operació en què estiga funcionant (produint calefacció, refrigeració, aigua calenta sanitària, treballant amb el terreny, l'aire, etc.), de la freqüència del compressor i altres variables i condicions d'operació.

El model del sistema dual en TRNSYS s'ha utilitzat per a fer una anàlisi del seu comportament funcionant en diferents condicions climàtiques, per a això s'han seleccionat tres ciutats a Espanya i tres a Europa amb diferents característiques climàtiques i s'han realitzat simulacions del sistema funcionant en cada ciutat durant un any. S'ha analitzat l'eficiència del sistema en cada ciutat, així com l'ús de cadascuna de les fonts (aire / terreny).

D'altra banda, també s'ha modelat en TRNSYS una de les instal·lacions demostració del projecte GEOTECH, incloent l'edifici d'oficines climatitzat i l'acoblament amb els fan coils. Amb aquest model es pretén estudiar una nova estratègia per a controlar la freqüència del compressor d'acord amb la temperatura de les habitacions, en lloc de controlar-la en base a la temperatura de subministrament, amb l'objectiu de reduir el consum del compressor quan les habitacions ja es troben en condicions de confort. A més, altres estratègies d'optimització s'han provat amb el model, analitzant els estalvis que s'obté amb cadascuna d'elles.

Per tant, els models desenvolupats, tant de l'intercanviador enterrat com els del sistema són capaços de reproduir el seu funcionament i es poden utilitzar com a instal·lacions virtuals, constituint eines útils per ajudar en el disseny del sistema i els diferents components, l'anàlisi del seu comportament i el desenvolupament d'estratègies d'optimització.

Resumen

Debido al creciente aumento de la demanda energética en edificios y a la necesidad de una transición energética hacia sistemas renovables y más eficientes, la energía geotérmica de baja entalpía se plantea como una alternativa eficiente y renovable a los sistemas convencionales para proporcionar calefacción, refrigeración y producir agua caliente sanitaria de forma sostenible.

Dentro de este contexto nace el proyecto GEOTeCH, un proyecto europeo que plantea el desarrollo de sistemas con bomba de calor geotérmica más eficientes y con un coste menor en comparación con el mercado. Para ello, se ha desarrollado un nuevo tipo de intercambiador enterrado coaxial con flujo helicoidal en el tubo externo que presenta una mayor eficiencia y permite reducir la longitud de intercambiador a instalar, así como una bomba de calor dual con compresor de velocidad variable, capaz de trabajar con el terreno o el aire como fuente/sumidero, seleccionando la que proporcione un mejor rendimiento del sistema. Estos componentes se utilizan en el nuevo sistema “plug and play” con bomba de calor dual desarrollado. El principal objetivo es desarrollar un sistema eficiente y replicable para proporcionar calefacción, refrigeración y producir agua caliente sanitaria en el sector de mercado de pequeños edificios con un tamaño menor en el campo de intercambiadores enterrados y un aumento de la eficiencia. Para demostrar la aplicabilidad de estos sistemas, se han construido tres instalaciones demostración en diferentes países de Europa: Italia, Países Bajos y Reino Unido.

En esta tesis doctoral se ha desarrollado un modelo dinámico completo del sistema en el software TRNSYS, capaz de reproducir el comportamiento de los diferentes componentes y del sistema en general. Este modelo constituye una herramienta útil para el desarrollo y análisis de diferentes estrategias de control sin la necesidad de implementarlas en instalaciones reales, así como analizar el comportamiento del sistema funcionando bajo condiciones diferentes. Para este propósito, es necesario desarrollar modelos detallados de los nuevos componentes desarrollados en el proyecto: el intercambiador enterrado coaxial helicoidal y la bomba de calor dual; para poder acoplarlos al resto de componentes en el modelo completo del sistema.

Por ello, se ha desarrollado un modelo dinámico del nuevo intercambiador enterrado coaxial con flujo helicoidal, capaz de reproducir con precisión el comportamiento a corto plazo del intercambiador, enfocado a la evolución de la temperatura del fluido, y se ha validado con datos experimentales en diferentes condiciones de operación. Para poder reproducir no solo el comportamiento dinámico del intercambiador enterrado, sino también la respuesta a largo plazo del terreno y la interacción entre intercambiadores en un campo, se ha desarrollado otro modelo en TRNSYS que realiza esta función. De esta manera, al acoplar ambos modelos es posible reproducir el comportamiento a corto plazo del intercambiador enterrado a la vez que la respuesta a largo plazo del terreno.

Por otro lado, se ha implementado en TRNSYS un modelo de la bomba de calor dual desarrollado previamente a partir de datos obtenidos en una campaña experimental. Con este modelo es posible calcular la capacidad de la bomba de calor dependiendo del modo de operación en que esté funcionando (produciendo calefacción, refrigeración, agua caliente sanitaria, trabajando con el terreno, el aire, etc.), de la frecuencia del compresor y otras variables y condiciones de operación.

El modelo del sistema dual en TRNSYS se ha utilizado para hacer un análisis de su comportamiento funcionando en diferentes condiciones climáticas, para ello se han seleccionado tres ciudades en España y tres en Europa con diferentes características climáticas y se han realizado simulaciones del sistema funcionando en cada ciudad durante un año. Se ha analizado la eficiencia del sistema en cada ciudad, así como el uso de cada una de las fuentes (aire/terreno).

Por otro lado, también se ha modelado en TRNSYS una de las instalaciones demostración del proyecto GEOTeCH, incluyendo el edificio de oficinas climatizado y el acoplamiento con los fan coils. Con este modelo se pretende estudiar una nueva estrategia para controlar la frecuencia del compresor en base a la temperatura de las habitaciones, en lugar de controlarla en base a la temperatura de suministro, con el objetivo de reducir el consumo del compresor cuando las habitaciones ya se encuentran en condiciones de confort. Además, otras estrategias de optimización se han probado con el modelo, analizando los ahorros que se obtiene con cada una de ellas.

Por tanto, los modelos desarrollados, tanto del intercambiador enterrado como los del sistema son capaces de reproducir su funcionamiento y se pueden utilizar como instalaciones virtuales, constituyendo herramientas útiles para ayudar en el diseño del sistema y los diferentes componentes, el análisis de su comportamiento y el desarrollo de estrategias de optimización.

Contents

Acknowledgements	i
Abstract	iii
Resum	v
Resumen	vii
List of figures	xiii
List of tables	xvii
Nomenclature	xxi
1 Introduction	1
1.1 Motivation.....	1
1.2 State of the art	4
1.3 Aim of the study.....	8
1.3.1 Methodology	8
1.4 Structure of the thesis.....	9
2 Description of the DSHP system	11
2.1 Introduction.....	11
2.2 System components	12
2.2.1 Layout of the system	12
2.2.2 Borehole heat exchanger	15
2.2.3 Dual source heat pump	16
2.2.4 Control system of the dual source heat pump system	19
2.3 Tribano demo-site	23
2.3.1 Tribano office building.....	26
2.3.2 Tribano Dual Source Heat Pump.....	30
2.3.3 Tribano Borehole Heat Exchangers field	31
2.3.4 Operation and control of the system.....	37
3 Modelling of the coaxial BHE.....	39
3.1 State of the art of BHE modelling.....	39
3.1.1 Modelling the ground mass: common analytical models	39
3.1.2 g-function model	41
3.1.3 Numerical and analytical modelling of the BHE	42
3.1.4 Computer programs used in the simulation of BHEs and GSHP systems	43
3.1.5 Modelling of BHE fields and long-term response of the ground	44
3.1.6 Approach to the new BHE modelling	45

3.2	B2G BHE dynamic model	46
3.2.1	U-tube B2G model	47
3.3	Standard and helical coaxial B2G dynamic model	48
3.3.1	Parameters calculation.....	50
3.3.2	Numerical resolution	54
3.3.3	Pressure loss calculation.....	56
3.4	Optimal location of the ground nodes.....	57
3.4.1	Methodology	58
3.4.2	Calculation of the ground nodes position.....	61
3.5	Coaxial B2G model implementation in TRNSYS	69
3.6	Experimental validation of the coaxial B2G dynamic model under different operating conditions	70
3.6.1	TRT coaxial helical BHE	71
3.6.2	DTRT standard coaxial BHE in KTH (Stockholm)	74
3.6.3	System operation conditions validation of a standard coaxial BHE in Tribano... ..	87
3.7	Long-term BHE field model	95
3.7.1	Background	95
3.7.2	Line Source Approach model.....	96
3.7.3	LSA model implementation in TRNSYS	99
4	Modelling of the dual source heat pump system.....	105
4.1	Introduction.....	105
4.1.1	Dynamic modelling of GSHP and DSHP systems	105
4.1.2	Control of systems.....	106
4.1.3	Approach to the dual source heat pump system modelling	107
4.2	Hybrid dual source heat pump model	109
4.2.1	Experimental tests and characterisation	109
4.2.2	Polynomial correlations for the DSHP performance calculation	112
4.2.3	Fan characterization	116
4.2.4	DSHP parasitic consumption.....	116
4.2.5	BPHEs pressure drop.....	117
4.2.6	Free-cooling BPHE model	118
4.2.7	TRNSYS implementation of the DSHP model	120
4.3	Integrated DSHP system modelling	122
4.3.1	User loop	124
4.3.2	DHW loop	128
4.3.3	Ground loop.....	129
4.3.4	Weather	132
4.3.5	Compressor control	132
4.3.6	DSHP control	134
4.3.7	Components power consumption	138
4.3.8	Performance assessment of the system.....	139
4.4	Tribano demo-site model: office building and heat pump control.....	140

4.4.1	Heat pump model adaptation.....	142
4.4.2	Office building modelling	143
4.4.3	Internal circuit	149
4.4.4	Fan coils modelling	149
4.4.5	Compressor control	154
4.4.6	Heat pump parameters.....	158
4.4.7	Outputs: power consumption and comfort	160
5	Applications of the system model	163
5.1	Assessment of the DSHP system in different climates	163
5.1.1	Assessment for different locations in Spain	165
5.1.2	Assessment for different locations in Europe.....	174
5.1.3	DSHP system operation.....	181
5.2	Room temperature control	185
5.2.1	Parametric analysis.....	185
5.2.2	Tribano system operation	191
6	Conclusions	197
6.1	Future research.....	200
	References.....	203
	Publications	213
	Appendixes	215
A.	Computer Codes of the TRNSYS types	215
A.1.	Coaxial B2G model.....	215
A.1.1.	Parameters, inputs and outputs of the B2G coaxial TRNSYS type.....	215
A.1.2.	External files B2G coaxial TRNSYS type	216
A.1.3.	B2G coaxial FROTRAN code.....	217
A.2.	Dual Source Heat Pump (DSHP) model	232
A.2.1.	Parameters, inputs and outputs of the DSHP TRNSYS type	232
A.2.2.	DSHP FROTRAN code.....	233
A.3.	Line Source Approach (LSA) model	247
A.3.1.	Parameters, inputs and outputs of the LSA TRNSYS type	247
A.3.2.	External file LSA TRNSYS type	247
A.3.3.	LSA FORTRAN code	247
A.4.	Pipe model	253
A.4.1.	Parameters, inputs and outputs of the pipe TRNSYS type.....	253
A.4.2.	Pipe FORTRAN code.....	254
A.5.	Room Temperature Control (RTC) model.....	258
A.5.1.	Parameters, inputs and outputs of the RTC TRNSYS type.....	258
A.5.2.	RTC FORTRAN code	258
B.	Coefficients for the DSHP model	263

C. Tribano office building characteristics.....	267
D. Parametrical studies Room temperature control.....	269

List of figures

Figure 1.1. Ground Source Heat Pump system in cooling and heating mode [16]	3
Figure 1.2. GEOTeCH consortium.....	7
Figure 2.1. Plug and play system layout [42]	13
Figure 2.2. Coaxial spiral BHE, GEOTHEX ® [46].....	15
Figure 2.3. Gap between the spiral rib and the outer pipe wall	16
Figure 2.4. Basic structure and components of the dual source heat pump [48]	18
Figure 2.5. Thermal source control.....	21
Figure 2.6. Compressor frequency control for heating/DHW mode (only P control)	22
Figure 2.7. Map of the system distribution of the Tribano demo-site in the HiRef S.p.A, factory. (Source: google maps).....	24
Figure 2.8. Data acquisition and monitoring system	25
Figure 2.9. Flow meter (magnetic).....	25
Figure 2.10. West façade of the office building of the Tribano demo-site (Source: Google maps).....	27
Figure 2.11. North façade of the office building of the Tribano demo-site.....	27
Figure 2.12. Map of the offices that are air-conditioned by the DSHP system	28
Figure 2.13. Fan coil Galletti FLAT S-20 installed in the meeting room.....	29
Figure 2.14. DSHP installed in the Tribano demo-site	30
Figure 2.15. Back side of the DSHP unit: connecting pipes and sensors.....	31
Figure 2.16. Distance from the collector pit of the BHE field to the DSHP.....	32
Figure 2.17. Collector pit of the BHE field	32
Figure 2.18. Diagram of the coaxial BHEs installed in Tribano	33
Figure 2.19. Map of the BHE field in the Tribano demo-site. Temperature sensors are located in OB 1, OB 2 and OB 3 (blue), as well as on the head of BHE 8 and COL (yellow) [51]	35
Figure 2.20. Geology strata in the region of Tribano (Padova). Data extracted from [52] ..	36
Figure 3.1. Temperature response factors (g-functions) for various multiple borehole configurations compared to the temperature response curve for a single borehole [71]	42
Figure 3.2. Thermal network model adopted: (a) 2D model; (b) 3D model [119]	47
Figure 3.3. Thermal network of the coaxial configuration model: a) borehole layout; b) vertical discretization.....	49
Figure 3.4. Cross-sectional area of the helical flow path.....	52
Figure 3.5. Semi-spherical thermal resistances at the bottom of the borehole	54
Figure 3.6. Thermal network used for the calculation of the penetration radii	59
Figure 3.7. Penetration radii: results for GEOTHEX BHE: a) Ground nodes temperature optimization; b) Heat transfer rate optimization	63

Figure 3.8. Penetration radii: comparison of simulated results for two scenarios: a) Ground nodes temperature optimization; b) Heat transfer rate optimization.....	65
Figure 3.9. Preliminary correlation calculated with the heat transfer optimization.....	67
Figure 3.10. Comparison between the penetration radii correlations and calculated points	68
Figure 3.11. Schematics of the model layout on the TRNSYS visual platform.....	69
Figure 3.12. B2G helical: results of the simulation in two scenarios a) fluid following the spiral path, b) Part of the fluid through the gap, enhancement factor=1.25.	73
Figure 3.13. B2G coaxial (KTH) short term simulation in the three scenarios.....	78
Figure 3.14. B2G coaxial (KTH) short term: Vertical temperature profiles in the three scenarios for different heat injection times.	80
Figure 3.15. B2G coaxial (KTH) extended time simulation in the three scenarios.	84
Figure 3.16. B2G coaxial (KTH) extended time: Vertical temperature profiles in the three scenarios.....	86
Figure 3.17. BHE field pipes distribution in Tribano.....	88
Figure 3.18. B2G coaxial summer day operation (13/09/2018): simulation results	91
Figure 3.19. B2G coaxial winter day operation (19/11/2018): simulation results.....	91
Figure 3.20. B2G coaxial five winter days operation (19/11/2018-23/11/2018): a) simulation results for the five days; b) zoom on the fourth day.....	92
Figure 3.21. Ground loop TRNSYS model, comprising the 8 BHEs	94
Figure 3.22. Simulation of circulating temperature for the ground loop with the eight BHEs in cooling mode during one day (13/09/2018).....	95
Figure 3.23. Ground load profile divided in thermal load pulses [130].....	97
Figure 3.24. Superposition of piecewise heat steps. The actual heat steps are superimposed in time [130].....	97
Figure 3.25. Load aggregation [130].....	99
Figure 3.26. TRNSYS layout for the coupling between the B2G and the LSA models.....	100
Figure 3.27. Comparison between LSA model and other simulation models.....	101
Figure 3.28. Comparison between the LSA model and g-function: Borehole wall temperature	103
Figure 3.29. Comparison between the LSA model and g-function coupled with B2G model: BHE outlet temperature	104
Figure 4.1. Condenser capacity, compressor power input and compressor COP in M5-Winter Ground operating mode ($T_{ci}=40^{\circ}\text{C}$, $dT_c=5\text{ K}$, $T_{ei}=0^{\circ}\text{C}$, $dT_e=3\text{K}$) [48].....	110
Figure 4.2. Condenser capacity, compressor power input and compressor COP in M4-Winter Air operating mode ($T_{ci}=40^{\circ}\text{C}$, $dT_c=5\text{ K}$, $T_{air}=7(6)^{\circ}\text{C}$, $ffan=50\%$) [48].....	111
Figure 4.3. Comparison between experimental measurements and polynomial correlations for M5- Winter Ground mode: compressor consumption and condenser capacity [48]	112
Figure 4.4. DSHP independent variables for mode M1-Summer Air [50].....	113

Figure 4.5. DSHP independent variables for modes M4-Winter Air, M6 and M7-DHW Air [50].....	114
Figure 4.6. DSHP independent variables for modes M2-Summer Ground, M3 DHW-User, M5-Winter Ground, M8 and M9-DHW Ground [50].....	115
Figure 4.7. Compressor and global COP maps at different supply water temperatures ($T_{co}=45^{\circ}\text{C}$ on the left side, $T_{co}=35^{\circ}\text{C}$ on the right side) in the operating mode M5-Winter Ground, ($f_{comp} = 50 \text{ Hz}$, $T_{ei}=0^{\circ}\text{C}$) [48].....	116
Figure 4.8. Free-cooling BPHE effectiveness correlation. Comparison with simulated results	119
Figure 4.9. Pressure drop (dP) in each side of the free-cooling BPHE: a) ground side; b) user side	120
Figure 4.10. DSHP TRNSYS type connections	122
Figure 4.11. User loop macro in TRNSYS	125
Figure 4.12. User circuit Circulation pump macro in TRNSYS.....	128
Figure 4.13. DHW loop macro in TRNSYS.....	129
Figure 4.14. Ground loop macro in TRNSYS	130
Figure 4.15. LSA reset signal.....	131
Figure 4.16. Weather file type in TRNSYS	132
Figure 4.17. Compressor control macro in TRNSYS.....	133
Figure 4.18. Heat Pump control macro in TRNSYS	134
Figure 4.19. Season signal example (1=summer, 0=winter)	135
Figure 4.20. Source control macro in TRNSYS.....	136
Figure 4.21. Flux diagram for the operating mode selection.....	137
Figure 4.22. SPFs macro in TRNSYS	139
Figure 4.23. TRNSYS layout of the Tribano demo-site model	142
Figure 4.24. Heat balance on the zone air node [167].....	143
Figure 4.25. Tribano building macro in TRNSYS	144
Figure 4.26. Tribano building modelling. Thermal zones scheme	145
Figure 4.27. TABULA Webtool [168]	146
Figure 4.28. Tribano building model in TRNBuild.....	147
Figure 4.29. Tribano building natural ventilation control.....	148
Figure 4.30. Internal circuit and fan coils macro in TRNSYS.....	149
Figure 4.31. Fan coils connection in TRNSYS.....	150
Figure 4.32. Fan coil TRNSYS modelling in cooling mode	151
Figure 4.33. Fan coil TRNSYS modelling in heating mode.....	152
Figure 4.34. Fan speed controller for heating mode	153
Figure 4.35. Pressure drop in the fan coils.....	154
Figure 4.36. Water temperature control in TRNSYS	155
Figure 4.37. Scheme of the compressor frequency control using the room temperature approach	156
Figure 4.38. Room temperature control in TRNSYS.....	158

Figure 4.39. Heat pump parameters macro in TRNSYS	160
Figure 4.40. Outputs macro in TRNSYS	162
Figure 5.1. Thermal loads in different locations in Spain: a) Valencia; b) Madrid; c) Bilbao	166
Figure 5.2. Thermal energy provided by the heat pump in the different working modes for the three cities in Spain	168
Figure 5.3. Share of the thermal energy produced by the heat pump in the three Spanish cities	170
Figure 5.4. Seasonal Performance Factors obtained for the three cities in Spain	172
Figure 5.5. System Seasonal Performance Factor 4 (SPF4) for the three locations in Spain	173
Figure 5.6. Thermal loads in the three cities in Europe: a) Athens; b) Strasbourg; c) Stockholm.....	175
Figure 5.7 Thermal energy produced by the heat pump in the different working modes for the three cities in Europe.....	177
Figure 5.8. Share of thermal energy produced by the heat pump for the three European cities	178
Figure 5.9. System Seasonal Performance Factor (SPF4) for the three cities in Europe...	180
Figure 5.10. Change of working mode during one week in winter for Bilbao.....	181
Figure 5.11. Winter day in Valencia: a) temperatures in the heat pump, buffer tank and supply set point; b) compressor frequency and temperature difference in the internal circuit.....	183
Figure 5.12. Summer day in Valencia: a) temperatures in the heat pump, buffer tank and supply set point; b) Temperature from DHW tank, operating mode and heat pump switch	184
Figure 5.13. Operation of the system for a heating day (12 th March): a) supply and return and operative temperature in the zones; b) outdoor temperature and compressor frequency.....	193
Figure 5.14. Operation of the system for a cooling day in spring (5 th June): a) supply and return and operative temperature in the zones; b) outdoor temperature and compressor frequency.....	194
Figure 5.15. Operation of the system for a cooling day in summer (10 th July): a) supply and return and operative temperature in the zones; b) outdoor temperature and compressor frequency.....	195
Figure A. 1. External file 1: definition of the ground layers thermal properties	216
Figure A. 2. External file 2: definition of the initial ground nodes temperatures	217
Figure A. 3. External file with the BHEs coordinates in the field (x, y)	247

List of tables

Table 2.1. Heat pump and system operating modes	19
Table 2.2. Technical specifications of the Tribano demo-site [51]	26
Table 2.3. Information about the different conditioned spaces	29
Table 2.4. Rated technical data of fan coil Galletti FLAT S-20	30
Table 2.5. Technical specifications of the Tribano demo-site BHE field [51]	34
Table 2.6. Thermophysical characteristics of the soil. Data extracted from [53]	36
Table 3.1. Main parameters calculation of penetration radii for GEOTHEX BHE	62
Table 3.2. Penetration radii for the two optimization scenarios	65
Table 3.3. Parameters values to calculate the penetration radii correlations.....	65
Table 3.4. Coefficients of the preliminary correlation used as initial point (x_0)	68
Table 3.5. Calculated coefficients for the final penetration radii correlations.....	68
Table 3.6. Main parameters of the BHE.....	71
Table 3.7. B2G spiral coaxial: Comparison between experimental and calculated results..	74
Table 3.8. Main parameters of the coaxial BHE with no grout [135].....	75
Table 3.9. Undisturbed ground temperature at different depths used in the B2G coaxial model.....	75
Table 3.10. Penetration diameters for the short term simulations in the three scenarios..	77
Table 3.11. B2G coaxial (KTH) short term: Comparison between experimental and calculated results.....	79
Table 3.12. B2G coaxial (KTH) short term vertical profiles: absolute temperature values error between simulated and experimental results (average and maximum values)..	81
Table 3.13. Penetration diameters for the extended time simulations in the three scenarios	81
Table 3.14. B2G coaxial (KTH) extended time: Comparison between experimental and calculated results.....	84
Table 3.15. B2G coaxial (KTH) extended time vertical profiles: absolute temperature values error between simulated and experimental results (average and maximum values)..	86
Table 3.16. Mass flow rate calculation	88
Table 3.17. Ground thermal properties at different depths used in the B2G model	89
Table 3.18. Main parameters used in the B2G coaxial model for the Tribano BHE	90
Table 3.19. Penetration diameters for the Tribano BHE model at different heat injection times	90
Table 3.20. B2G coaxial daily operation in Tribano: calculated errors	93
Table 3.21. Error in applying the aggregation algorithm to the LSA model.....	101
Table 3.22. U-tube BHE parameters.....	102
Table 4.1. Coefficients for the calculation of the pressure drop at the BPHE of the DSHP	117
Table 4.2. Coefficients for the calculation of the density and viscosity of the fluids	117

Table 4.3. Coefficients for the calculation of the circulation pumps consumption.....	139
Table 4.4. Internal gains definition in TRNBuild for the thermal zones	147
Table 5.1. Main inputs for the different locations in Spain.....	167
Table 5.2. Total energy provided by the heat pump for the three cities in Spain	168
Table 5.3. Heat extraction and injection in the ground for the three cities in Spain	171
Table 5.4. Return temperature from the ground loop in the three cities in Spain	171
Table 5.5. U-value extracted from the TABULA database for each representative city in Europe.....	174
Table 5.6. Main inputs for the different locations in Europe	176
Table 5.7. Total energy provided by the heat pump for the three cities in Spain	177
Table 5.8. Heat extraction and injection in the ground for the three cities in Spain	179
Table 5.9. Return temperature from the ground loop in the three cities in Spain	179
Table 5.10. First results of the system working under the water temperature control (base scenario underlined)	187
Table 5.11. Best results of the system working under the water temperature control. The base scenario is underlined	188
Table 5.12. Results from the best scenarios for the parametric analysis for comfort category II: supply temperature limits, temperature difference for the circulation pump control, savings with respect to original scenario and hours out of comfort.....	189
Table 5.13. Results from the best scenarios for the parametric analysis for comfort category III: supply temperature limits, temperature difference for the circulation pump control, savings with respect to original scenario and hours out of comfort.....	189
Table 5.14. Power consumption of each component: total consumption (kWh) and percentage with respect to the base scenario (underlined).....	190
Table A. 1. Parameters of the B2G coaxial TRNSYS type	215
Table A. 2. Inputs of the B2G coaxial TRNSYS type.....	215
Table A. 3. Outputs of the B2G coaxial TRNSYS type.....	216
Table A. 4. Parameters of the DSHP TRNSYS type.....	232
Table A. 5. Inputs of the DSHP TRNSYS type.....	232
Table A. 6. Outputs of the DSHP TRNSYS type.....	232
Table A. 7. Parameters of the LSA TRNSYS type	247
Table A. 8. Inputs of the LSA TRNSYS type.....	247
Table A. 9. Outputs of the LSA TRNSYS type.....	247
Table A. 10. Parameters of the pipe TRNSYS type	253
Table A. 11. Inputs of the pipe TRNSYS type.....	253
Table A. 12. Outputs of the pipe TRNSYS type.....	253
Table A. 13. Parameters of the RTC TRNSYS type.....	258
Table A. 14. Inputs of the RTC TRNSYS type. The number of inputs 1, 2 and 3 will depend on the number of rooms in parameter 1.....	258
Table A. 15. Outputs of the RTC TRNSYS type	258
Table B. 1. M1-Summer Air coefficients	263

Table B. 2. M2-Summer Ground coefficients	263
Table B. 3. M3-DHW User (Full recovery) coefficients	263
Table B. 4. M4-Winter Air coefficients	264
Table B. 5. M5-Winter Ground coefficients	264
Table B. 6. M6 and M7 - DHW Air coefficients	265
Table B. 7. M8 and M9 - DHW Ground coefficients	265
Table C. 1. Walls distribution	267
Table C. 2. Windows distribution	268
Table C. 3. Walls characteristics	268
Table C. 4. Windows characteristics	268
Table D. 1. Parametric analysis. List of simulations	269
Table D. 2. Parametric analysis. Power consumption (% respect simulation 1) and number of hours out of comfort in each thermal zone	274
Table D. 3. Parametric analysis. Electric energy consumption of each component (kWh)	278

Nomenclature

Symbols

Symbol	Description	Units
α	Thermal diffusivity	m^2/s
c_v	Volumetric thermal capacity	$J/(m^3 \cdot K)$
C	Thermal capacitance	J/K
C_p	Specific heat	$J/(kg \cdot K)$
D	Diameter	m
Fo	Fourier number; $Fo = \frac{\alpha \cdot t}{L^2}$	-
H	Borehole depth	m
h	Convective heat transfer coefficient	$W/(m^2 \cdot K)$
k	Thermal conductivity	$W/(m \cdot K)$
k_a	Aggregation factor	-
L	Representative distance in Fo (r , r_b or H)	m
λ	Thermal conductivity	$W/(m \cdot K)$
\dot{m}	Mass flow rate	kg/s
m_a	Margin value	-
n	Number of nodes	-
Nu	Nusselt number; $Nu = \frac{h \cdot D}{\lambda}$	-
q	Heat transfer rate per unit length	W/m
\dot{Q}	Heat transfer rate / heat capacity	W
R	Thermal resistance	K/W
r	Radial distance	m
ρ	Density	kg/m^3
t	Time	s
T	Temperature	$^{\circ}C$
v	Velocity	m/s
\dot{W}	Electric power	W
z	Vertical direction coordinate	m

Subscripts

Symbol	Description
0	Initial
∞	Far-field
<i>b</i>	Borehole / grout zone
<i>bg1</i>	Grout node to short term ground node
<i>c</i>	Conduction
<i>ci</i>	Inner diameter of the inner pipe
<i>co</i>	Outer diameter of the inner pipe
<i>e</i>	Spherical
<i>ef</i>	Effective
<i>ei</i>	Inner diameter of the outer pipe
<i>eo</i>	Outer diameter of the outer pipe
<i>eq</i>	Equivalent
<i>g</i>	Ground
<i>g1</i>	Ground node (short term)
<i>g2</i>	Ground node (mid-term)
<i>g1g2</i>	Short term to mid-term ground nodes
<i>g2ug</i>	Mid-term to undisturbed ground nodes
<i>gp1</i>	Ground penetration for short term ground node
<i>gp2</i>	Ground penetration for mid-term ground node
<i>h</i>	Convection
<i>i</i>	Inner pipe zone
<i>ip</i>	Inner pipe
<i>in</i>	Inlet
<i>io</i>	Inner pipe node to outer pipe node
<i>j</i>	j-node
<i>o</i>	Outer pipe zone
<i>ob</i>	Outer pipe zone to borehole backfilling node
<i>op</i>	Outer pipe
<i>out</i>	Outlet
<i>r</i>	Rib
<i>ug</i>	Undisturbed ground
<i>v</i>	Vertical
<i>x</i>	Borehole node position

Acronyms

Acronym	Description
B2G	Borehole-to-Ground (BHE dynamic model)
BHE	Borehole Heat Exchanger
BPHE	Brazed Plate Heat Exchanger
COP	Coefficient Of Performance
DHW	Domestic Hot Water
DSHP	Dual Source Heat Pump
DTRT	Distributed Thermal Response Test
GSHE	Ground Source Heat Exchanger
GSHP	Ground Source Heat Pump
LSA	Line Source Approach (ground response model)
MPG	Mono Propylene Glycol
OB	Observation Borehole
RMSE	Root Mean Square Error
SPF	Seasonal Performance Factor
TRT	Thermal Response Test

Chapter 1

1 Introduction

1.1 Motivation

Currently, environmental issues as carbon emissions and global warming, but also oil dependency are a big concern that is necessary to be solved. In this framework, the use of non-contaminant and renewable energies is key in order to reduce the pollutants emissions and the dependency on fossil fuels for the energetic supply, but also the improvement of the energy efficiency of the systems.

Regarding this concern, the European regulation has adopted different strategies during the last years in order to reduce the carbon emissions and other pollutants, stimulate the use of renewable energies and increase the efficiency of the systems. For example, the Renewable Energy Directive 2009/28/EC (RES Directive) on the promotion of the use of energy from renewable sources [1], which sets the targets for the Member States to achieve the overall target of using a 20% of renewable energy in the final energy consumption by 2020, or the Decision no 406/2009/EC, which sets the commitments of the different Member States on the reduction of their greenhouse gas emissions [2]. Both following the Europe 2020 strategy, which sets as targets for climate change and energy the reduction of greenhouse gas emissions by at least a 20% compared to 1990 levels, achieving a 20% of the final energy consumption from renewable sources and an increase of 20% in the energy efficiency [3].

In this direction, the European commission created the Horizon 2020 programme, the biggest European Union (EU) Research and Innovation programme, available over 7 years (2014-2020) and nearly €80 billion of funding available. Inside it, the Energy Challenge supports a transition to a reliable, sustainable and competitive energy system, including the development and introduction to market of affordable cost-effective and resource-efficient technology solutions to decarbonize the energy system in a sustainable way, secure energy supply and complete the energy internal market, with the geothermal energy among the proposed solutions [4]. The targets for 2030 are a cut of 40% in greenhouse gas emissions, compared to 1990 levels, at least a 32% share of renewable energy consumption and a 32.5% improvement in energy efficiency at EU level [5], after some revisions on the original framework [6]. The European Commission also presented a long-term strategy, in which it is included a climate-neutral economy by 2050 [7], in line with the Paris Agreement objective to keep the global temperature increase well below 2°C and pursue efforts to keep it to 1.5°C.

As well, the United Nations, in one of its Sustainable Development Goals to promote prosperity while protecting the planet, set to “Ensure the access to affordable, reliable, sustainable and modern energy” [8]. Stating that increase energy efficiency and the use of renewable energy is crucial for achieving its objectives of sustainable communities in an environmentally friendly way.

In this context, buildings account for almost one third of the final global energy consumption, according to the International Energy Agency [9] being an important source of carbon emissions. In this sector, Heating, Ventilating and Air-Conditioning (HVAC) systems represent an important and growing part of the total energy consumption [10] and, as stated in the Strategic Research and Innovation Agenda for Renewable Heating & Cooling [11], achieving Europe’s 2020 and 2050 targets on greenhouse emissions, renewable energy and energy efficiency, will require the spreading of new technologies with a high energy efficiency. The contribution of renewable HVAC systems to the EU energy targets by 2020 and 2050 strongly depends on the availability of reliable, efficient and affordable technology, and the replacement of energy systems using fossil fuels.

Concerning space heating and cooling in buildings, Ground Source Heat Pump (GSHP) systems become one of the most efficient heating and cooling renewable technologies currently available, representing an efficient alternative to conventional systems [12]–[14]. These systems consists of a water-to-water heat pump, the user circuit through which the supply water that has been heated up (heating mode) or cooled down (cooling mode) flows to the emission system (underfloor heating, fan coils, radiators, etc.), and the ground circuit. The main difference with a conventional air-to-water heat pump is that they use the ground as a heat source or heat sink, depending on the season, in order to provide heating or cooling to buildings, respectively, as it is shown in Figure 1.1. Furthermore, with GSHP systems, it is possible to reach around 40% energy savings in comparison to air-to-water heat pump systems [15]. This higher efficiency is achieved thanks to a more stable temperature of the ground during the year in comparison with the air and, in most cases, also more favourable (warmer in winter and cooler in summer). In order to carry out this heat exchange between the heat pump and the ground, one or several Ground Source Heat Exchangers (GSHEs) are used. A GSHE usually consists of one or more long plastic pipes buried in the ground through which the heat carrier fluid flows. The fluid that comes from the GSHP is heated up (heating mode) or cooled down (cooling mode) when flowing through the GSHE thanks to the temperature difference with the surrounding ground, then extracting or injecting heat in the ground, respectively.

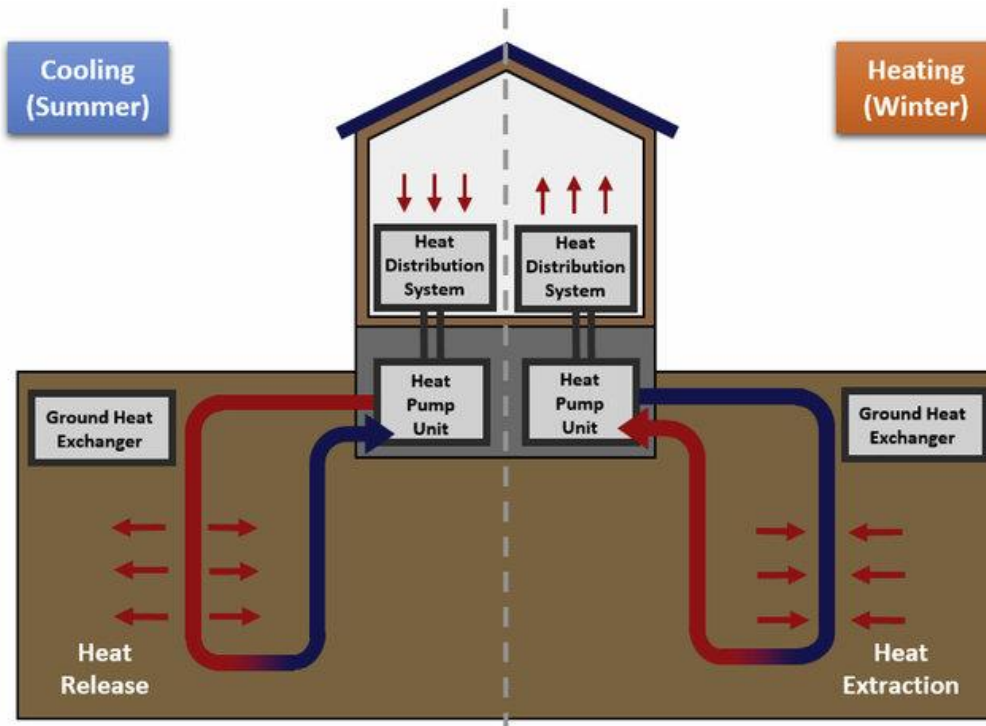


Figure 1.1. Ground Source Heat Pump system in cooling and heating mode [16]

The GSHE component is one of the more expensive parts of the system, due to the high cost involved in manufacturing so long pipes and burying them below the ground level (sometimes more than 200 m deep). For this reason, in the design of these GSHEs, the necessary length should be optimized in order to obtain a good efficiency in the heat transfer with the ground, at a reasonable cost. This means that the heat exchanger should not be under-sized (low efficiency) nor over-sized (high cost). Different solutions are used in order to obtain a good efficiency and reducing the length of GSHE as much as possible:

- Studying different GSHE configurations with higher efficiency.
- Combining different sources into hybrid energy systems, so the heat transfer with the ground would decrease.
- Using different simulation and design software in order to optimize the design and operation of the GSHEs and the entire system.

The efficient operation of the system is also key in, not only reducing the necessary heat transfer with the ground, but also the energy consumption of the system. For this purpose, the development of optimization control strategies would contribute in increasing the feasibility of these GSHP systems. In this context, the development of dynamic simulation models, able to reproduce the behaviour of the different components (among them, the GSHE and the heat pump) and the entire system, can contribute in testing the different control strategies developed without the need of implanting them on site.

1.2 State of the art

The high investment cost that involves the GSHP systems in comparison with other more conventional systems, despite being more efficient, has led to a low implementation of these systems in zones like the South of Europe, especially in comparison with northern countries, where the use of GHSPs for heating applications is widespread. In 2008, Sweden represented more than one third of the total GSHPs in European countries, where GSHP systems supplied around a 20% of the heating demand (reaching around 35% of savings in greenhouse gases emissions), followed by Norway (around 9%) and Finland (around 7%), while in southern countries they supplied less than 1% of the total heating demand [17]. It is also important to mention that the national regulations in the different European countries concerning geothermal systems are diverse, and an unified legislative framework and guidelines would be necessary [18]. Another study by Rivoire et al. [14], in which different building are simulated in different climates in Europe, concluded that GSHP systems present a higher economic feasibility in colder climates, like the north and east of Europe than warmer climates, like the South of Europe, and that subsidies are necessary for becoming economically feasible in GSHP designed to cover the entire heating demand. Nonetheless, the use of GSHP systems is increasing globally. By 2014, the capacity of GHSPs in the world have increased by more than 9 times compared to 2000 [18].

Despite this, the use of GSHP systems in southern Europe, would exploit one of the main advantages of reversible GSHPs: the underground thermal storage. As it is possible to use the ground as a thermal storage, injecting heat in summer and extracting it during the winter, providing a thermal balance in the ground and then maintaining the system efficiency over the years. Therefore, the use of this technology in the south of Europe can reach high levels of efficiency, as demonstrated by the European projects GEOCOOL 'Geothermal Heat Pump For Cooling And Heating Along European Coastal Areas' [19] and GROUND-MED 'Advanced ground source heat pump systems for heating and cooling in Mediterranean climate' [20].

Regarding the most important part inside the GSHP systems, the GSHE, there exist a wide variety of configurations [21], [22]. In the case of open loop systems, the water from a lake or pond is directly extracted by using wells (the environmental risk is higher and it is restricted by law, depending on the local regulation). Closed loop systems are the most used systems, as the environmental impact is quite lower in comparison with open loops. Among the closed loop systems, horizontal GSHEs are quite less complex than vertical and more economical, however, they require more land area to meet the same heat exchange requirement, but still they are used for residential and smaller non-residential applications [23].

On the other hand, vertical GSHEs, also called Borehole Heat Exchangers (BHEs), are the predominant GSHEs used for both residential and non-residential GSHP applications [12]. In this configuration, a borehole is drilled vertically into the soil and a heat exchanger is introduced, the gap between the heat exchanger and the borehole wall is normally filled with a grouting material. The most extended BHE configuration is the single U-tube, in

which two straight pipes (downward and upward) are connected by a U-turn at the bottom, as it presents the lowest cost. This is why it is also installed two pipes (double U-pipe) or even three in the same borehole. Other configurations are also used, like the coaxial, consisting in two concentric pipes: the inner pipe and the outer pipe, forming two channels: the inner channel formed by the inner pipe and the outer channel, formed by the annular space between the outer and the inner pipes. The aim of using a coaxial BHE is to reduce the borehole thermal resistance increasing the contact area between the fluid in the outer pipe and the surrounding ground, expecting a reduction in the required length and then, reducing the cost of drilling, other benefits expected are a longer fluid residence time and a reduced overall pressure drop [24]. However, turbulent flow regime is difficult to achieve in the annulus (turbulent flow is desired to increase the heat transfer with the ground), this is why sometimes the outer flow path is modified by using multiple smaller flow paths or considering a helical design [25]. Moreover, it is desired to reduce the short circuit between the inner and outer channels, in order to improve the BHE thermal efficiency. The popularity of this configuration has grown during the last years, considering the increasing number of related research publications [25]. For example, Kurevija et al. [26] studied the suitability of coaxial BHEs for active and passive cooling, determining that they need to be designed with active cooling option; Acuña [27] studied different configurations (U-pipes, coaxial, multi-pipe and multi-chamber BHEs) in order to reduce the temperature difference between the fluid and the surrounding ground, carrying out several experimental tests with these configurations. Other improvements have also been studied, like the immersion of the vertical probes in an artificial fluid inside a case, increasing the heat transfer within the borehole due to natural convection [28].

One of the main solutions in order to reduce the BHE length needed and to save energy in GSHP systems is to combine the ground source with another thermal source, resulting in a hybrid system. For heating systems, GSHPs are combined with solar collectors, resulting in lower costs due to the shorter BHEs. In addition, when the cooling demand is low in summer, solar collectors can inject heat into the ground, preventing a possible overheating of the collectors [29], but also preventing the ground temperature to decrease too much, what would mean a decrease in the heat pump efficiency. An example of a GSHP with BHEs combined with solar collectors can be found in [30]. In the case of additional heat sinks, the cooling tower is the most common solution [31], using the ambient air as a heat sink. It is also possible to combine GSHP systems with several systems, for example, in [32], a combined system consisting of a power generation unit, an absorption machine, two ground source heat pumps a storage tank and two electric chillers is described.

Hybrid systems also contribute to reduce the greenhouse gases emissions, for example, combining GSHP systems with photovoltaic systems could lead to increase the economic feasibility of GSHP systems while reducing the emissions [33]; another example in which a GSHP system is combined with thermal storage and supported by an air-to-water heat pump for a cooling dominated office building is described in [34], reducing the electrical

energy consumption of the system. A recent review on hybrid ground source heat pumps is presented in [35] and also in [36].

The use of a hybrid system combining ground and air sources presents two main advantages. First, the reduction in the GSHE length, which has a higher cost than an air heat exchanger, leading to economic savings. Second, the system operation could be optimized, selecting in each moment the more favourable source/sink and then, increasing the overall efficiency of the system and the seasonal performance. An example of energy savings when using a dual source heat pump ground/air in comparison with a GSHP system can be found in [37]. In order to reduce the size of the system, its cost and simplify the operation, the implementation of a Dual Source Heat Pump (DSHP) in a unique unit has been studied. A DSHP able to work using ground water or the air as a source/sink was presented in [38]. It was studied how selecting the more favourable source/sink during the heat pump operation could lead to energy savings and a better annual performance of the system, with improvements in the annual performance factor from 2% to 7% in comparison with the groundwater source system and from 4% to 18% in comparison with the air source system. Another conclusion from this study was that the system performance could be improved by adapting the compressor and pump frequencies. In another work [39], it was study the use of different control and operation strategies for the operation of a hybrid GSHP for cooling dominated applications, combined with a supplemental heat rejecter, like a cooling tower, reaching important economic savings.

On the other hand, the use of GSHPs involves the use of refrigerants in the refrigeration cycle, which may have an impact in the ozone layer depletion and global warming. However, the technology is progressing in the switch to new refrigerants with no impact in the ozone layer and low Global Warming Potential (GWP). The current GSHPs are using this type of refrigerants, such as HFCs and HFOs (for example, R32).

In all this context, the GEOTeCH project 'GEOthermal Technology for economic Cooling and Heating' [40], a four years duration project funded by the European Commission inside the Horizon 2020 program, was created to demonstrate the next generation of GSHP systems with a high energy efficiency but also lower system costs in comparison with the market. The project consortium is formed by several industrial and research partners from different European countries, presented in Figure 1.2.



Figure 1.2. GEOTeCH consortium

One of the main objectives of the project is to develop system solutions with hybrid heat pump and control technologies, in order to offer efficient and replicable ‘plug and play’ systems to the housing and small buildings market sector.

For this purpose, a compact DSHP unit was developed, capable of providing heating, cooling and producing DHW, working with the air or the ground as a source/sink. It incorporates a variable speed compressor, so the heat pump capacity can be adapted to the thermal demand, working with R32 as a refrigerant, which presents a low GWP. In addition, an innovative coaxial BHE with helical flow path through the outer tube was created in order to be included in these plug and play systems. This BHE incorporates a helical rib attached to the inner tube wall, so the fluid follows a helical path through the annular channel. Moreover, the inner pipe is insulated, so the thermal interference between the inner and outer pipes is minimized. The main objective of this new BHE is to achieve high levels of thermal performance with low pressure losses and increasing the efficiency at low Reynolds numbers.

In order to test the performance of the ‘plug and play’ system, three demonstration facilities (called demo-sites) were installed in Italy, the Netherlands and the United Kingdom. Different control strategies have been developed in order to optimize the operation of the system and the selection of the air or the ground as a source/sink. Therefore optimizing the seasonal performance of the system, with a shorter length of BHE, in comparison with a full GSHP system, and the consequent decrease in the investment cost. Furthermore, a new dry drilling technology, effective, economic and easy to implement was developed, in order to install the new BHEs with reduced environmental impact, better operating conditions and lower safety risks.

Inside the framework of this project, a dynamic model of the new coaxial helical BHE and a complete model of the plug and play system have been developed in order to test different control and optimization strategies without the need of implementing them on site, being able to carry out parametric analysis with different control parameters values

easily and in a fast way and carry out an energetic assessment, as part of this PhD dissertation.

1.3 Aim of the study

The main aim of this PhD thesis is the dynamic modelling of an innovative coaxial BHE with helical flow path through the outer tube and its validation with experimental data under different conditions and for different geometries. The model must be able to predict the short-term behaviour of the BHE, focused on the temperature evolution of the fluid inside the pipes. The new BHE has been developed in the framework of the European project GEOTeCH [40], with an insulated inner pipe and a spiral rib attached to the inner pipe outer wall. Furthermore, the long-term response of the ground must also be addressed in order to obtain the complete response of the BHE and surrounding ground, both on the short- and long-term.

The secondary objective is to develop a complete dynamic model of a DSHP system (also designed in the GEOTeCH project), using the previously developed BHE model for the ground loop and a model of the specific DSHP, coupled to the rest of components of the system; and to develop another dynamic model of the system, focused on the building and the coupling with the heat pump by the fan coils emission system and adapt it to the demonstration installation of Tribano, installed in the framework of the GEOTeCH project. These models would provide a useful tool in order to reproduce the dynamic behaviour of the system and the interaction between components, making it possible to carry out an energy assessment of the system under various conditions and test different control and optimization strategies. In this context, those conditions in which this innovative DSHP system would be more suitable compared to a standard ground source heat pump system could be determined. Finally, the model could be used as a tool for developing and testing a new control strategy for heating and cooling in an office building based on setting the compressor frequency depending directly on the room temperatures evolution instead of the water supply temperature.

1.3.1 Methodology

The analysis of the experimental data used in the validation of the BHE model, as well as the analysis of the results obtained by the different models, was carried out in the Microsoft Excel software.

The modelling of the DSHP systems models were developed in the software TRNSYS. The standard components already available in the program were used. However, several new *types* were created in order to model specific new components: the dynamic coaxial BHE, the long-term ground response model, the DSHP and some controllers used in the creation of new control strategies. All the TRNSYS *types* were written in FORTRAN language using the Microsoft Visual Studio software and the Intel Fortran compiler.

For the calculation of the ground nodes optimum position, the MATLAB software was used.

1.4 Structure of the thesis

This PhD dissertation is structured in the following chapters:

- In chapter 2, the DSHP system and its different components is described in detail.
- The chapter 3 represents the core of the thesis, here it is described the dynamic model of the coaxial helical BHE, as well as the model of the long-term ground response. The experimental validation of the BHE model is also presented.
- In chapter 4, a detailed description of the DSHP system model in TRNSYS and its different subsystems is presented, including the model of the DSHP and the control strategies. In addition, the description of the TRNSYS system focused on the building modelling and its coupling to the fan coils emission system is also described, together with the new room temperature control strategy.
- The applications of these TRNSYS models is presented in chapter 5, where an energy assessment of the DSHP system in different climates is carried out and a new control strategy is applied to the system model focused on the building and the fan coils emission system.
- The main conclusions extracted from the results obtained are detailed in chapter 6.

Chapter 2

2 Description of the DSHP system

2.1 Introduction

The GEOTeCH project (Geothermal Technology for Economic Cooling and Heating) [40] is a Horizon 2020 European project that started in 2015, with the objective of spreading the use of shallow geothermal systems for providing heating and cooling to buildings in a renewable, efficient and cost-effective way.

One of the main outcomes of the GEOTeCH project is the development of efficient and replicable “plug and play” entire systems that can be introduced in the market sectors of housing and small buildings. These systems will provide buildings with the needs of heating, cooling and Domestic Hot Water (DHW) at a low cost and a high energy efficiency. This is possible thanks to some innovative technologies developed and improved inside the project: dry drilling technology, borehole heat exchangers, dual source heat pumps (DSHP) and also a robust system control.

With the new dry drilling technology, it is possible to improve the drilling operating conditions and lower the safety risks, resulting in a solution with a high efficiency, cost-effective, easy to implement and more environmentally friendly than the conventional technologies. This dry drilling technology is combined with an innovative BHE coaxial configuration, developed by GEOTHEX BV[41], with an insulated inner pipe and helical fluid flow path. This new BHE solution improves the thermal efficiency, especially at low Reynolds number, allowing the use of shorter boreholes.

Regarding the hybrid heat pump, the innovative DSHP is able to operate with the ground or the ambient air as a heat/sink source, selecting the optimal one according to the operating and climatic conditions in each moment. In this way, the seasonal performance of the system is increased, as the heat pump will select the heat source/sink in order to work with the most favourable one during its operation. Furthermore, as the heat pump system will work, not only with the ground, but also with the air, the required area of GSHE will decrease in comparison with a standard GSHP system, since the amount of heat exchanged with the ground will be smaller, leading to a lower cost of the installation.

In order to assess the performance of this “plug and play” system solution, three demonstration facilities (also called “demo-sites”) were constructed in three different locations in Europe, with the aim of being monitored during a minimum time of 12 months. The three demo-sites that were installed are the following:

- Amsterdam small-scale office building. Located at the offices of the company Groenholland BV, in Amsterdam (Netherlands).

- Tribano small-scale office building. Installed in the offices of the company HiRef S.p.A., in Tribano, province of Padova (Italy).
- Leicester small-scale household. Located at Leicester (United Kingdom).

In this PhD dissertation, data from the demo-sites of Amsterdam and Tribano has been used. The preliminary planned installation of Amsterdam was firstly used in order to model the plug and play system, but due to a delay in the construction of the final demo-site, the Tribano demo-site was the one finally used to validate the BHE dynamic model with monitored data in section 3.6.3, as well as to develop control strategies in section 5.2.

2.2 System components

2.2.1 Layout of the system

The plug and play system consists of a variable speed heat pump that heats up or cools down water in order to provide the building with the required need of DHW, heating or cooling. For this purpose, the heat pump is able to operate both as an air-to-water heat pump (using the air as a thermal source/sink) or a water-to-water heat pump (using the ground). Inside the building, the rooms are being heated or cooled by the use of a number of terminal units (normally fan coils), heating or cooling the air in the room with the water coming from the heat pump. This system consists of three main hydraulic loops, interconnected by the DSHP:

- User side loop.
- Domestic Hot Water (DHW) loop.
- Ground loop.

Additionally, a free-cooling Brazed Plate Heat Exchanger (BPHE) is connecting the ground loop and the user loop, bypassing the heat pump, in order to cool down the building when the fluid temperature coming from the ground loop is low enough to provide the required cooling without the need of operating the heat pump. The layout of the system is shown in Figure 2.1.

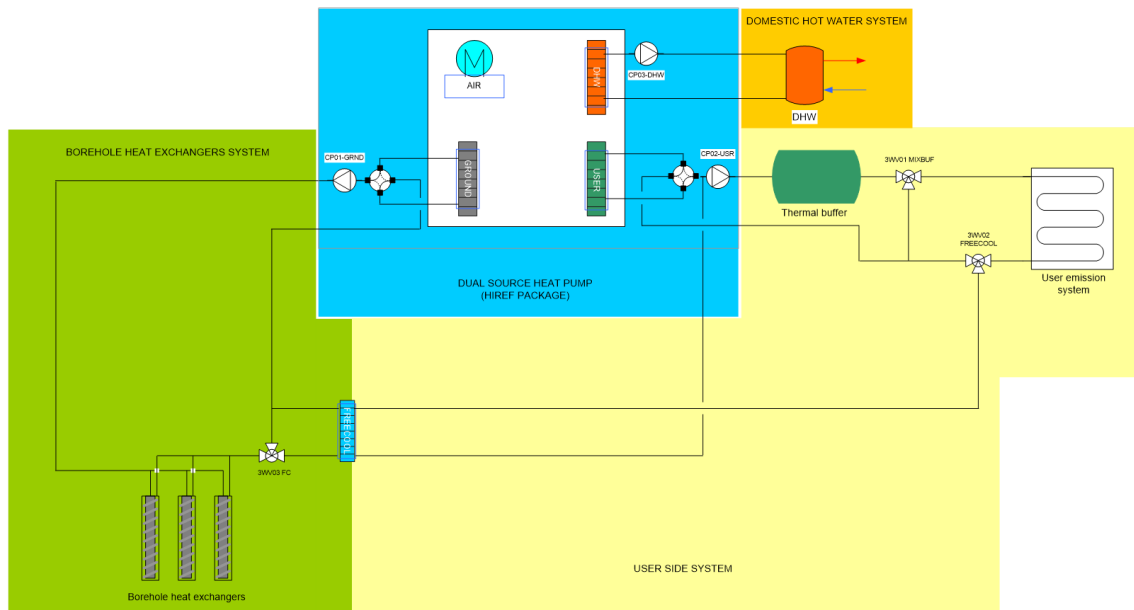


Figure 2.1. Plug and play system layout [42]

2.2.1.1 User side loop

The user side system is the hydraulic loop by which the heat transfer fluid that has been heated up or cooled down by the heat pump is transported to the terminal units in the building in order to heat/cool the conditioned space air. The usual heat transfer fluid is water. In some periods during the summer season, the fluid coming from the ground loop is cold enough to provide the required cooling to the building, therefore, a free-cooling BPHE is used to cool down the water in the user side loop directly without the need of switching on the heat pump, bypassing it. A three-way valve in the circuit is used in order to switch between the free-cooling BPHE or the DSHP.

Optionally, it is possible to install a buffer tank at the outlet of the DSHP, in order to provide some extra thermal inertia to the circuit. There are several advantages in having a buffer tank in the circuit: from the point of view of the control, since it provides a higher thermal inertia, placing a temperature sensor at the outlet of the tank leads to a smoother temperature change when the compressor starts/stops, compared to placing it at the outlet of the heat pump. This allows the unit to remain on/off a minimum time, which is necessary to allow the oil to return to the compressor and prevent the compressor to cycle too often, reducing the number of starts per hour, too. Therefore, the life of the compressor will increase [43]. These advantages will be more significant with a fixed speed compressor heat pump, as it will work with the compressor cycling all the time at approximately its nominal capacity, while a variable speed compressor will adapt its frequency to the thermal demand. However, the variable speed compressor cannot work below the minimum frequency. In this case, it will start cycling, switching on/off with the minimum frequency. It is then, when the thermal inertia of a buffer tank might help assuring that the compressor will be on/off the required minimum time. Nevertheless, as a variable speed heat pump cycle at the minimum capacity, the required volume of water will be small in comparison to a fixed speed heat pump, where the buffer tank must be sized for the nominal capacity. Therefore,

in some cases the water inside the circuit pipes provides enough thermal inertia and there is no need of a buffer tank.

In the demo-site of Tribano, as well as the one in Leicester, no buffer tank was installed, while in the Amsterdam demo-site a tank of 150 litres was installed.

Concerning the emission system inside the building, several fan coil units are placed in the conditioned rooms, so the water flowing through the user circuit will heat up or cool down the air inside the rooms. For this purpose, this water is flowing through a coil inside the unit, while a fan moves the room air through the coil, so the temperature of this air is increased or decreased in order to provide thermal comfort inside the space. The number of fan coils will depend on the thermal load of the conditioned space: internal gains as occupancy, lighting or equipment; thermal losses with the outside air and adjacent rooms, solar gains through windows, infiltrations, ventilation, etc.

2.2.1.2 Domestic Hot Water loop

When the heat pump is working in DHW mode, it will heat up the water in the DHW circuit so the temperature of the water inside the storage tank will be increased in order to keep the water hot enough (around 50°C) to provide the domestic hot water. The hot water inside the tank will afterwards be mixed with cold water from the supply network in order to reach the temperature desired by the user when there is demand.

The main component of this hydraulic circuit is the storage tank. This tank must be coupled indirectly to the heat pump BPHE, according to EN 1717:2000 [44], in order to prevent the potable water from being polluted. The main options to couple the storage tank to the heat pump is to use a tank with an integrated coil heat exchanger inside, to use an intermediate heat exchanger between the heat pump and the tank or using a double wall condenser in the heat pump (not applicable to this case, because the BPHE is already defined in the heat pump). Despite the fact that the most inefficient case is the use of a storage tank with an integrated coil heat exchanger, it is the most used option for this purpose [45].

In the plug and play systems designed in the framework of the GEOTeCH project, the DHW storage tanks installed in the demo-sites are tanks with integrated coil heat exchanger.

2.2.1.3 Ground loop

The DSHP will work switching between the air and the ground as the thermal source, depending on which is the most favourable. When it works with the ground, a heat transfer fluid flows from the heat pump to several Borehole Heat Exchangers (BHEs) through the ground hydraulic loop. Thanks to these BHEs buried in the ground, the fluid is heated up or cooled down due to the temperature difference between the fluid and the ground around them and it will flow back to the heat pump.

The main parts of the ground hydraulic loop are the field of BHEs and the connecting pipes. There is one pipe through which the total fluid flows from the heat pump to the BHE field, then it is split into the different BHE lines, carrying the fluid to each BHE and back to a collector where the fluid is mixed and then, the total fluid flow returns to the heat pump.

The number of BHEs in the BHE field and their geometry will depend on the thermal load of the building. It must be previously estimated in order to size correctly the heat pump and also the BHE field. The geometry and number of BHEs will depend on the amount of heat that will be exchanged with the ground (injected or extracted), in order to prevent the ground from increasing or decreasing too much its temperature. This is because a big alteration in the ground temperature could cause a deterioration in the operating conditions of the heat pump, thus the efficiency of the system would decrease. Furthermore, the BHE field must be big enough to handle the thermal load peaks in the system.

Regarding the GSHE configuration, there exist several types, as shown in Chapter 1. In the framework of the project, a new coaxial BHE was developed in order to be installed in these plug and play systems. A more detailed explanation of the BHE is explained in section 2.2.2.

2.2.2 Borehole heat exchanger

A new configuration of coaxial BHE was initially developed by the company GEOTHEX BV [41] and further improved in the GEOTeCH project, in order to be installed in the plug and play systems, increasing the cost-effectiveness of the system. It consists of a coaxial BHE, with an insulated inner pipe and helical fluid flow path through the outer pipe. A drawing of the BHE is shown in Figure 2.2.

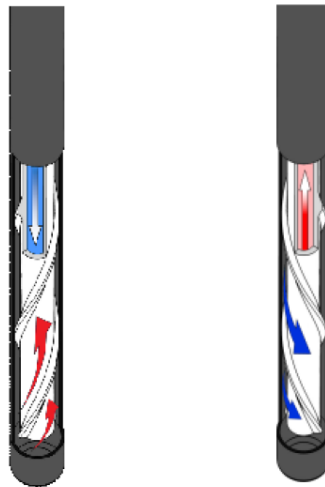


Figure 2.2. Coaxial spiral BHE, GEOTHEX ® [46]

This innovative configuration was designed to achieve high levels of thermal performance with low pressure losses, with a reduction in the thermal losses between the fluid inside the inner and the outer tube and an increase of the efficiency at low Reynolds numbers. This will allow designs with shorter boreholes, improving the hydraulic performance, thus reducing the pumping energy costs and emissions, improving the short-timescale response and thermal storage capacity. Additionally, it is possible to integrate it completely with the new dry auger-based drilling technology developed inside the GEOTeCH project [40].

Preliminary studies concluded that the efficiency was significantly increased in comparison with conventional heat exchanger designs, especially at low Reynolds numbers [46]. This configuration has been further studied and optimized inside the framework of the GEOTeCH project.

As it can be seen in Figure 2.2, the Geothex ® heat exchanger consists of a coaxial BHE with an insulated inner pipe to minimize the heat loss between the inner and outer flow channel. Regarding the outer channel, one or more helical vanes are attached on the outer part of the inner pipe, so the fluid will follow a helical flow path, increasing the effective length and increasing the heat transfer, especially at low Reynolds.

As shown in Figure 2.3, the edge of the spiral vane and the inner wall of the outer pipe are not in full contact, but there is a small gap. Therefore, although the vanes will touch the outer pipe inner wall at different places along the length of the BHE, the helical path is not completely closed.

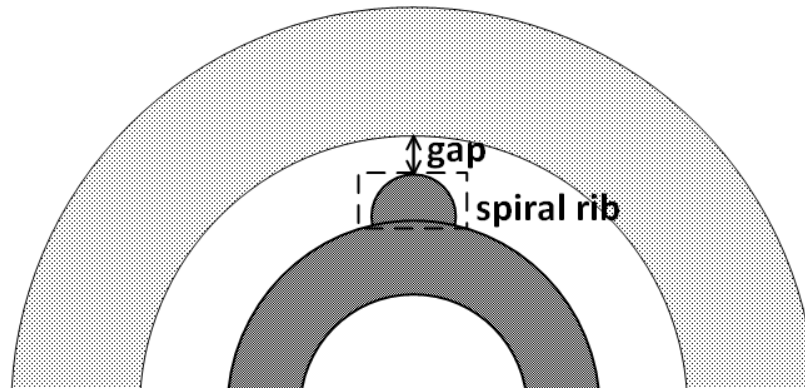


Figure 2.3. Gap between the spiral rib and the outer pipe wall

The reasons that explain this gap are two: first of all, manufacturing tolerances of the special inner pipe material, as they are not as high as in conventional extruded pipes. But even more important, if the fit is very tight it would be very hard to insert the inner pipe inside the outer pipe due to the friction, especially with long heat exchangers.

The existence of this gap means that some part of the fluid flowing through the outer channel will flow through the gap, therefore a local turbulence may be generated, producing an increase in the convective heat transfer between the fluid and the grout/ground that surrounds the BHE. This phenomenon will be studied in section 3.6.1.

2.2.3 Dual source heat pump

The heat pump used in the plug and play systems is a new technology developed by the Italian company HiRef S.p.A. [47] and further designed and tested inside the framework of the GEOTeCH project. The main innovation introduced is the dual source concept, so it is capable of working both with the air or the ground as thermal source, all integrated in the same refrigerant circuit. With this compact solution, it is possible to operate either with the air or the ground, choosing the best thermal source/sink from an efficiency point of view, depending on the real-time operating and climatic conditions. This will lead to a higher seasonal performance if compared with current technology. Additionally, as the heat pump will work not only with the ground, but also with the air, the heat injection/extraction to

the ground will be reduced in comparison with a GSHP system, therefore the size of BHE that is required in order for the system to work properly will be smaller, leading to a reduction on the system cost.

The new DSHP works with R32 as refrigerant and a variable speed compressor, so the heat pump capacity can be adapted to the thermal demand. It is a reversible heat pump, so it can produce heating during winter and cooling during summer, but also DHW during all the year. Regarding the main target, it was conceived for satisfying the demand of a small multifamily house or an office building, thus it is simple to operate and very automatic.

Three prototypes were designed, manufactured and tested by different partners involved in the project in order to improve the final design. The prototypes #1 and #2 have a nominal capacity of 8 kW, while the prototype #3 has a nominal capacity of 16 kW. The prototype #1 was tested in the facilities of the Universitat Politècnica de València and some improvements were suggested for the following prototypes. In this PhD dissertation, the prototype #1 has been considered as the reference, as it has been tested in the installations of the Institute of Energy Engineering in the Universitat Politècnica de València, also designed and modelled by the same research group. However, as the DSHP installed in the demo-site of Tribano was the 16 kW prototype, the heat pump model developed for prototype #1 was adapted to prototype #3. The prototypes #2 and #3 have very similar components than prototype #1, but different size, for example, the BPHEs or the compressor. A more detailed description of the DSHP can be found in [48], also its design was described in [49] and the test campaign and modelling in [50].

2.2.3.1 Design and components of the DSHP

The reason for using R32 as refrigerant instead of a more conventional one is the current status of the European F-gas regulation, together with the volatile evolution of the refrigerants regulations at an international level. The use of HFCs is going to be restricted progressively, but the alternatives to the current refrigerants are not clear, because there are not commercially available components yet to install in the units. Despite the fact that other refrigerants were also considered (R410A or R1234ze), R32 was chosen as the best solution for short and medium term, due to its considerable low Global Warming Potential.

The DSHP is a reversible heat pump, able to provide heating or cooling to the user, depending on the season, but also satisfy the DHW demand. Furthermore, it can use either the air or the ground as thermal source/sink, depending on the most favourable one. All of this in a single compact unit for domestic use. For this purpose, an air to water heat pump was selected with two extra BPHEs: one for the ground loop and another one for producing DHW independently from the user BPHE. Resulting in a compact outdoor unit with four heat exchangers:

- The air coil consists of a Round Tube and Plate Fin (RTPF) heat exchanger. On the outer part of the coil, two Electronically Commutated Motor (ECM) fans were situated with continuous variable speed control.

- Ground BPHE. It is used both as evaporator and condenser, depending if the heat pump is working in heating or cooling mode, respectively. The model selected is the F85 by SWEP.
- User BPHE. It is used both as evaporator and condenser, too. The model is the F80AS, by SWEP.
- DHW BPHE. It is always used as a condenser. The model installed is the B26, by SWEP.

The basic structure of the DSHP is shown in Figure 2.4.

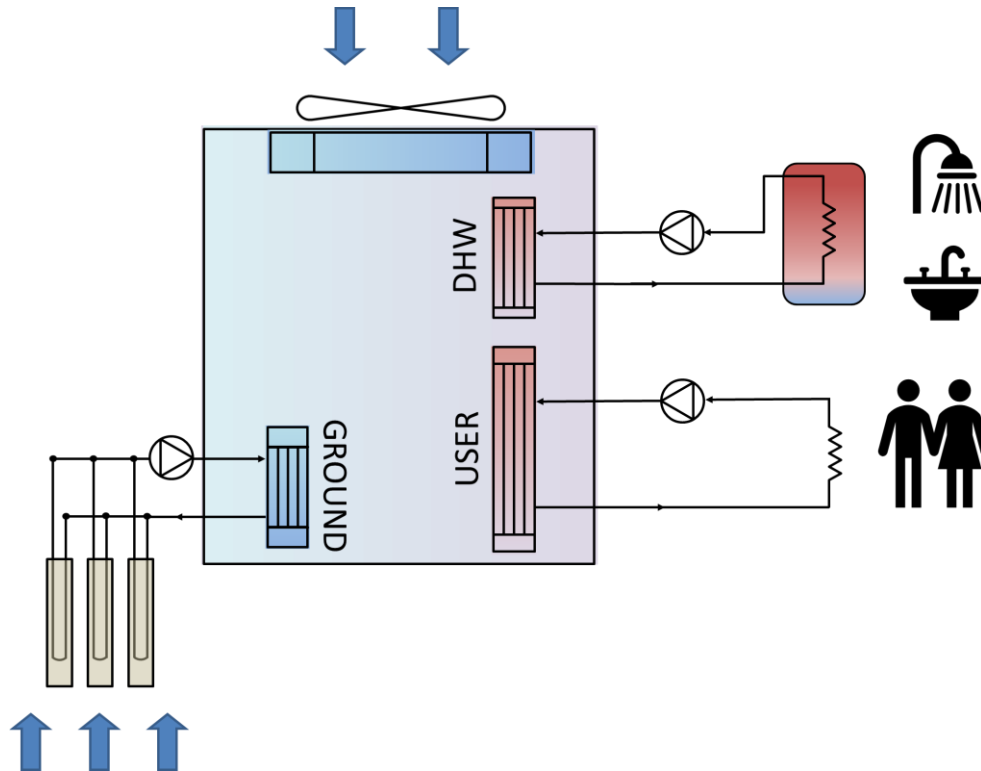


Figure 2.4. Basic structure and components of the dual source heat pump [48]

The unit incorporates a variable speed compressor in order to adapt the capacity of the heat pump to the wide range of operating conditions and therefore, minimize the partial load losses. In order to achieve the highest efficiency at these operating conditions, a scroll compressor was selected. The main issue was to find a compressor available in the market able to work with the refrigerant R32, as there were few available at the moment of designing the first prototype. In the end, the installed compressor for the prototype #1 was the model XHV-25 (25 cc), by Copeland. For the prototype #3, a bigger model was installed (38 cc), since the capacity of the heat pump is bigger (8 kW against 16 kW).

The circulation pumps that are required in the three hydraulic loops are already included in the frame of the DSHP: DHW, user and ground loops.

2.2.3.2 DSHP and system operating modes

The DSHP is designed in such a way that it can provide heating or cooling to the user, depending on the season, but also DHW during the whole year. Since the main market sectors of this unit are houses and small offices, the heating and cooling periods are

completely separated by intermediate seasons, while the DHW demand will exist during the whole year, simultaneously with the heating or cooling demands.

In order to specify the different operating modes in which the heat pump can work, two different seasons are defined: summer season, where there will be a cooling demand (unit will operate as a chiller) as well as DHW demand; and winter season, where there will be a heating demand (unit working as a heat pump) and DHW demand. Using these definitions, eight modes could be defined. In addition, there is another operating mode in which it is possible to produce chilled water in order to provide cooling to the building during the summer season, and at the same time the unit is producing DHW. This mode will be called full recovery (operating mode M3).

Apart from these nine heat pump operating modes, the system is capable of working in free-cooling conditions. The system incorporates a free-cooling heat exchanger in order to cool down the water in the user loop directly, without using the heat pump, when the fluid coming from the ground loop is cold enough to handle the cooling demand. This free-cooling mode is the M10. Additionally, the free-cooling mode can operate at the same time that the heat pump is producing DHW with the air; this will be the operating mode M11. All the operating modes of the heat pump and the plug and play system are shown in Table 2.1.

Table 2.1. Heat pump and system operating modes

	Condenser	Evaporator	Operating mode
Summer	Air	User	M1-Summer Air
	Ground	User	M2-Summer Ground
	--	--	M10- Free cooling
	DHW	User	M3-DHW User (Full Recovery)
	DHW	Air	M6-DHW Air
	DHW	Ground	M8-DHW Ground
	DHW	Air	M11-Free-cooling+ DHW Air
Winter	User	Air	M4-Winter Air
	User	Ground	M5-Winter Ground
	DHW	Air	M7-DHW Air
	DHW	Ground	M9-DHW Ground

2.2.4 Control system of the dual source heat pump system

As it was shown in section 2.2.3.2, the DSHP system can operate in quite a lot of different modes, depending on what is producing: heating, cooling or DHW, which thermal source/sink it is going to use: air or ground and if the free-cooling mode can be used. Therefore a control system is necessary for selecting the operating mode in which the heat pump is going to work each time, but it must be simple and easy to handle by the user. In addition, other variables are needed to be controlled in order to achieve the highest efficiency of the system: the frequency of the compressor must be adapted to the thermal

demand, as well as the fan speed, also the speed of the circulation pump of the different circuits. For the moment, some simple strategies have been implemented in the demo-sites, some of them have not been able to be tested, due to the fact that the demo-sites are still in a testing phase and some operating modes are not being used, for example, the system in Tribano was not producing DHW, yet. Furthermore, some control strategies are suggested and tested in the model of the system in this PhD dissertation.

2.2.4.1 Selection of operating mode

In order to select the operating mode in which the heat pump will work, first the controller must know what is going to produce: heating, cooling or DHW. Then, it will select the thermal source (air or ground) depending on their temperatures.

The user is the one that specifies if the heat pump will work in winter mode (producing heating when needed) or summer mode (producing cooling). Usually, the user will switch the heat pump to winter mode in the transition period between the warm season to the cold season during the year and it will switch back to summer mode in the transition to the warm season. These periods will depend on the climatology of the location.

Regarding the DHW production, it will be produced during the whole year. Currently, the control system will prioritise the DHW production against the heating or cooling, selecting the DHW production mode whenever there is a need of DHW (the temperature in the DHW storage tank decreases below a specific value, for example, 40°C). As the DHW production is not implemented in the demo-sites yet, this control has not been tested. Another control for the DHW production is suggested in this PhD dissertation and it will be explained in the section 4.3, mainly consisting in filling the DHW tank with hot water during the night and provide heating/cooling during the day.

Regarding the source selection, the temperature of the two thermal sources is compared, and the most favourable will be selected (the hotter in winter and the cooler in summer). For the air source, the ambient air temperature measured at the heat pump is used, while for the ground source, the temperature of the fluid coming from the ground loop is used, measured at the inlet of the heat pump. The control will use a hysteresis band (for example $\pm 2\text{K}$) in order to prevent the heat pump from switching the source very rapidly. Figure 2.5 shows an example of the source selection control.

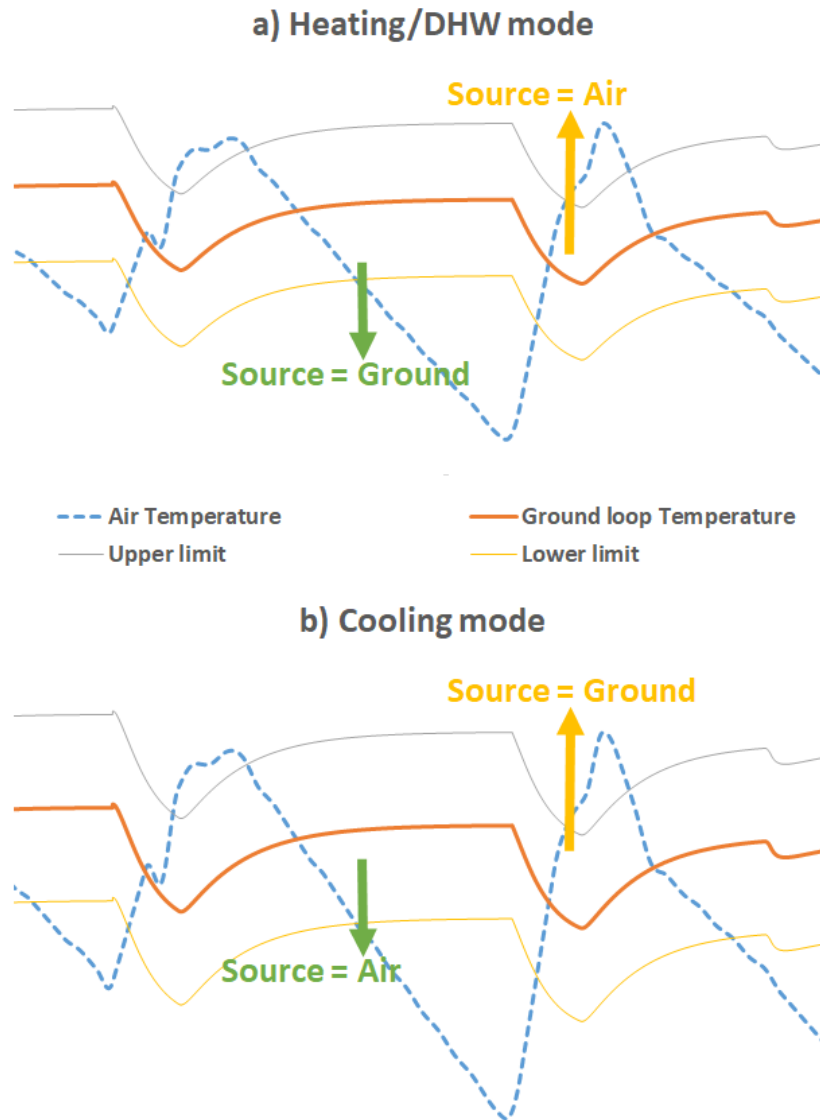


Figure 2.5. Thermal source control

Regarding the full-recovery mode, if there is a need of cooling, but also of producing DHW, the heat pump will select the full-recovery mode (M3), providing cold water to the user loop and at the same time heating up the water in the DHW loop.

The free-cooling mode will operate when there is a need of cooling and the return temperature from the ground loop is lower than a specific value (for example, 10 °C). Then, the heat pump will stop, and it will be bypassed, so the fluid in the ground loop will flow through the free-cooling heat exchanger, cooling down the water in the user loop.

2.2.4.2 Frequency control

The frequency of the compressor must be adapted to the demand, so the capacity of the heat pump will change in order to handle the thermal load. In order to adapt the frequency of the compressor to the demand, it will vary between the minimum and maximum frequencies in order to maintain a constant temperature in the user circuit (supply or return temperature). When the frequency of the compressor reaches the minimum value, and the

demand is still low, the compressor will cycle, switching on/off, until the demand increases, so the compressor frequency must increase. In order to control this cycling of the compressor, a hysteresis band is set. In order to carry out this control, a PI controller is used together with a differential controller with hysteresis. This control is described in Figure 2.6, but only considering the proportional action.

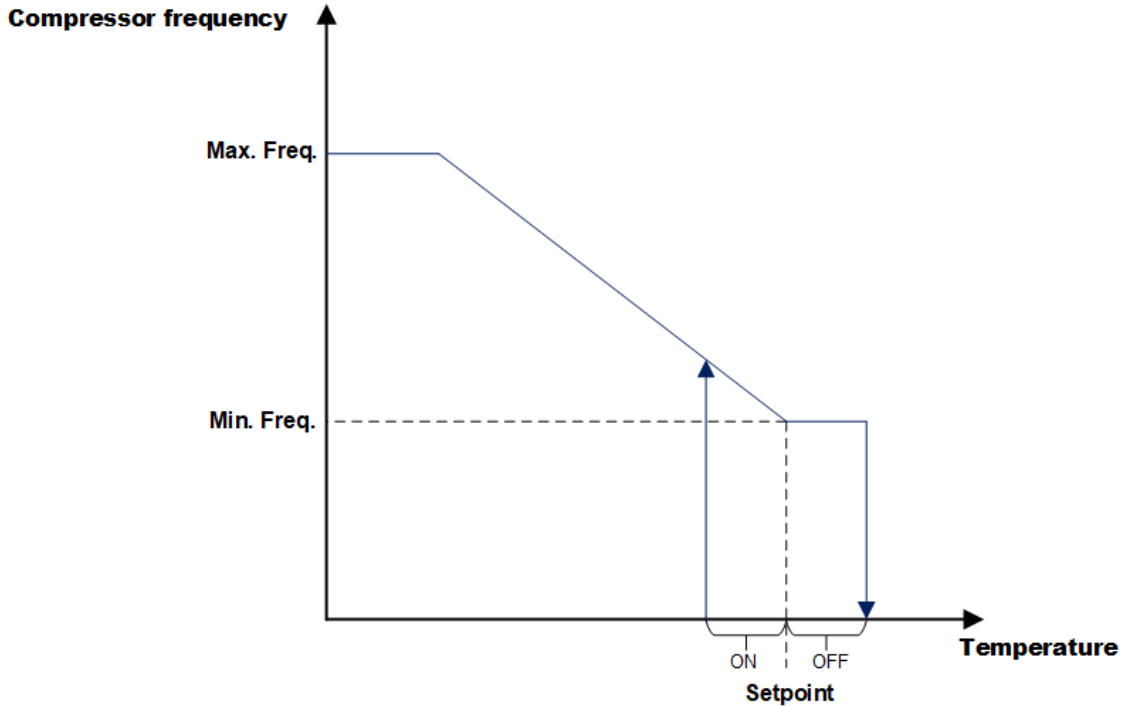


Figure 2.6. Compressor frequency control for heating/DHW mode (only P control)

The current controlled temperature in the user circuit is the return temperature, so the PI controller will try to maintain the temperature of the water coming back to the heat pump from the user circuit. An example of set points for this control is the following:

- Setpoint for cooling= 12°C.
- Setpoint for heating= 45°C.
- Setting for DHW production= 45°C.
- Hysteresis ON= 1K.
- Hysteresis OFF= 1K.
- Maximum frequency= 80 Hz.
- Minimum frequency= 20 Hz.

It would also be possible to control the supply temperature, but the main problem is that this temperature will present a sharp change when the compressor starts/stops. In order to solve this problem, a small buffer tank would soften the temperature change and thus, it will help to control the supply temperature, as well as to provide some thermal inertia to keep the compressor on/off the minimum required time and prevent too many start-ups, as explained in section 2.2.1.1.

Therefore, there are two main monitored temperatures that can be controlled in the user circuit: the supply temperature at the outlet of the buffer tank or the return temperature (inlet to the heat pump). Usually the return temperature is controlled because it is simpler to implement the PID controller and the temperature sensor inside the same heat pump unit and the inlet temperature is more constant, what is good for the compressor life. On the other hand, controlling the supply temperature is more efficient from the point of view of the user comfort, because the water entering the emission system will have a more constant temperature, maintaining the comfort inside the air-conditioned spaces. If the controlled temperature is the return temperature, the supply temperature will vary depending on the instant thermal demand.

The frequency of the circulation pumps of the three circuits (user, ground and DHW) could be kept fixed, so the mass flow rate would be constant through the circuit. Another possible control strategy is to vary the pump speed in order to maintain a constant temperature difference in the circuit with a PI controller, so the temperature difference in the BPHE of the heat pump will be approximately constant.

Regarding the fan frequency, it can be varied proportionally to the compressor frequency or change it as a function of the air temperature.

2.3 Tribano demo-site

The Tribano demo-site is one of the demonstration facilities installed in the framework of the GEOTeCH project, located at the factory of the company HiRef S.p.A. in the municipality of Tribano, in the province of Padova (Italy). The DSHP system was installed in the second half of the year 2017 and it started working around January 2018. It provides heating and cooling to some spaces of the office building located at the factory. It could produce DHW as well, although currently it is deactivated the DHW production. The DSHP installed in the system is the prototype #3 developed inside the framework of the GEOTeCH project. The heat pump is located outside of the building and connected to the BHEs field 20 m far from the heat pump. The BHEs field consists of eight coaxial BHEs with a length of 30 m each. The DHW tank, the distribution of the pipes, as well as the control and data acquisition system are located inside a technical room next to the DSHP.

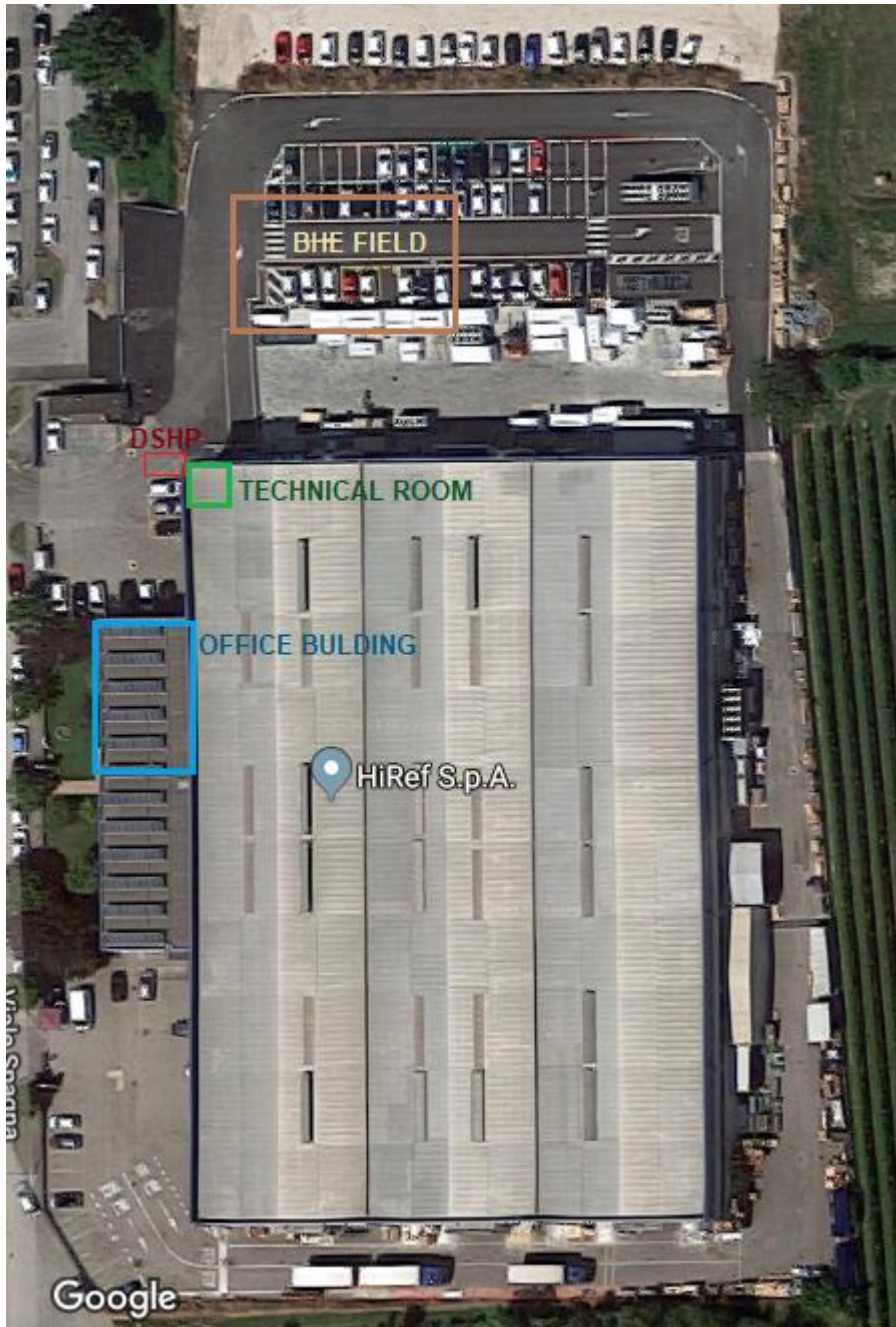


Figure 2.7. Map of the system distribution of the Tribano demo-site in the HiRef S.p.A, factory.
(Source: google maps)

The system is fully monitored since the beginning, although it was working in a testing period during the first months of operation and there is no reliable data of the system working until July 2018, due to several issues in the data acquisition system, as well as the control system.

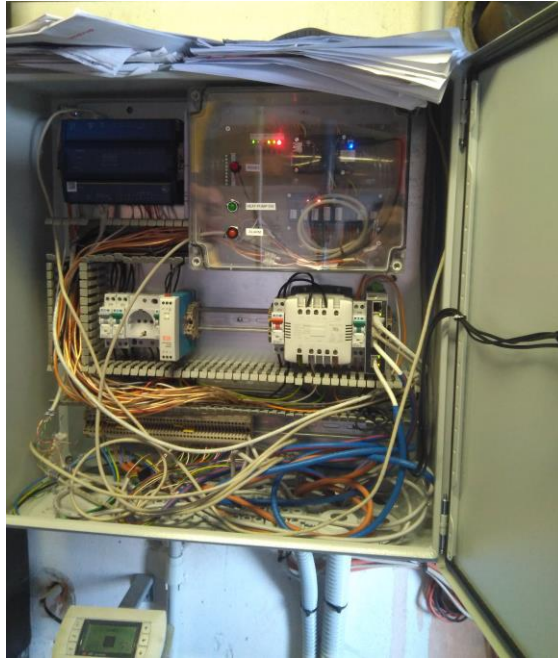


Figure 2.8. Data acquisition and monitoring system

The flow rates of each circuit (user, ground and DHW) are measured with magnetic flowmeters (Figure 2.9), the inlet and outlet temperatures of each circuit from the heat pump side are measured with PT100 temperature sensors. The expected accuracy of the magnetic flowmeters is 0.5-1%, regarding the temperature sensors, it is $\pm 0.1\text{K}$.

Additionally, some other temperature sensors were installed in the BHE field by the University of Bologna inside the framework of the GEOTeCH project, in order to analyse the temperature of the surrounding ground and the inlet and outlet temperatures of one of the BHEs [51].



Figure 2.9. Flow meter (magnetic)

Some of the technical details of the system are specified in Table 2.2.

Table 2.2. Technical specifications of the Tribano demo-site [51]

Heat pump nominal capacity	Heating: 16 kW Cooling: 14 kW
Tanks	Number of tanks: 2 <ul style="list-style-type: none"> • DHW buffer tank: 300 l • Expansion tank: 18 l
Circulation pumps	Number of pumps: 3 (1 per hydraulic loop) <ul style="list-style-type: none"> • Max. delivery head: 12 m • Max. volume flow: 10 m³/h
Sensors	Number of pressure sensors: 3 (1 per hydraulic loop) Number of flow sensors: 3 (1 per hydraulic loop) <ul style="list-style-type: none"> • Nominal flow: 5m³/h Number of temperature sensors: 6 (2 per hydraulic loop: inlet and outlet in the heat pump)
BHE field	8 coaxial BHEs 30 m deep each BHE

The Tribano demo-site has been used as a reference installation in the development of this PhD dissertation, and data from the system and the office building was used in the modelling and simulation of the system. In addition, data from the BHE field was used in order to validate the coaxial BHE dynamic model developed in this PhD thesis.

2.3.1 Tribano office building

2.3.1.1 Office building

The air-conditioned building corresponds to an office building, built in the 90s, next to the production workshop, as shown in Figure 2.7, and corresponding with the main offices of the HiRef factory. The west façade and the main entrance is shown in Figure 2.10 and the north façade is shown in Figure 2.11.



Figure 2.10. West façade of the office building of the Tribano demo-site (Source: Google maps)



Figure 2.11. North façade of the office building of the Tribano demo-site

2.3.1.2 Conditioned spaces

The conditioned rooms are three offices and one meeting room located at the second floor of the building (top floor), the names of the offices are the following (with the original name in Italian):

- Research and Development office (Ricerca E Sviluppo).
- Sales office (Commerciale).
- Administration office (Amministrazione).
- Meeting room (Meta' Sala Incontri).

The layout of these rooms is shown in Figure 2.12, with the dimensions of each one. The conditioned rooms are coloured in red. The corridor and rooms adjacent to these rooms (coloured in light brown) are not conditioned, but the rest of the offices in the other part of the building are. Furthermore, there are eight inverters installed in the corridor connected to several photovoltaic panels on the roof, which are switched on whenever there is solar radiation, so there will be a heat gain in the corridor because of the inverters. The production building (coloured in grey) is adjacent to the Research and Development room. This room is oriented to the north, the Sales office is oriented to the north and west, while the Administration office and the meeting room, to the west.

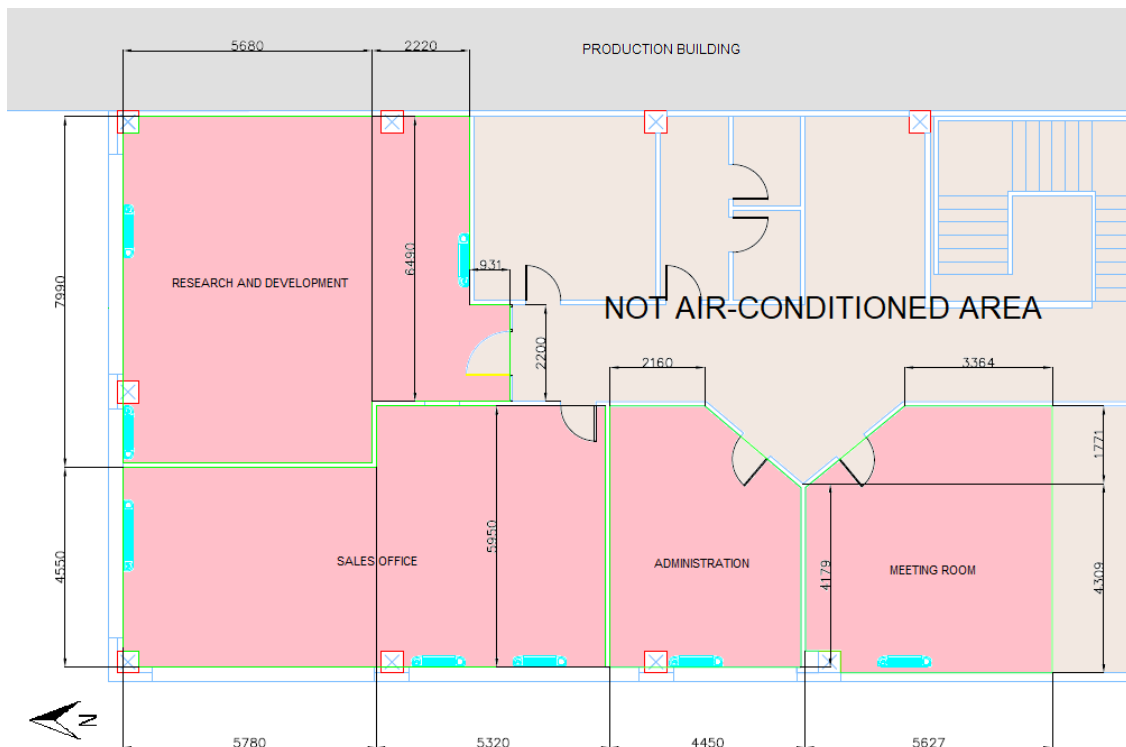


Figure 2.12. Map of the offices that are air-conditioned by the DSHP system

All the exterior walls have some windows, oriented to the north and west, as shown in Figure 2.11. However, the external wall of the meeting room is entirely glazed, as shown in Figure 2.10.

The offices of the company are open from Monday to Friday, the occupancy and equipment of each room is different, as well as the number of fan coils installed. This information is gathered in Table 2.3.

Table 2.3. Information about the different conditioned spaces

Room	Schedule (Monday – Friday)	Occupancy and equipment	Fan coils
Research and Development	8 h – 18 h	8 people 8 computers	3
Sales office	8 h – 18 h	7 people 7 computers	3
Administration	8 h – 18 h	4 people 4 computers	1
Meeting room	3 h per day	1 projector 1 laptop 4 people	1

2.3.1.3 Fan coils

In total, there are eight fan coils installed in the four conditioned rooms. They are all connected in parallel to the user circuit, so the water coming from this circuit will be the one used to heat up or cool down the air moved by the fans in the fan coils. The fan coils were manufactured by the company Galletti, the model is the FLAT S-20, a wall-mounted fan coil with vertical air flow (Figure 2.13). They are switched on from 7:30 in the morning to 20:00 in the evening, independently if the heat pump is working or not.



Figure 2.13. Fan coil Galletti FLAT S-20 installed in the meeting room

The fan coil is able to operate at three different fan speeds, so the air flow rate will change depending on this speed. Each fan coil includes its own thermostat, so it will change its speed automatically depending on the temperature difference with the comfort temperature. The main technical data of the fan coils is specified in Table 2.4.

Table 2.4. Rated technical data of fan coil Galletti FLAT S-20

Fan speed		min	med	max
Total cooling capacity (1)	kW	1.09	1.34	1.75
Sensible cooling capacity (1)	kW	0.75	0.93	1.22
Water flow (1)	l/h	186	230	300
Heating capacity (2)	kW	1.21	1.47	1.93
Air flow	m ³ /h	135	170	225
Power input	W	14	20	27

(1) Water temperature 7/12 °C, air temperature dry bulb 27°C, wet bulb 19°C (47% relative humidity).

(2) Inlet water temperature 50 °C, same water flow as in cooling mode, air temperature 20°C.

2.3.2 Tribano Dual Source Heat Pump

The DSHP installed at the Tribano demo-site is the prototype #3 developed inside the GEOTeCH project. Its nominal capacity is 16 kW for heating and 14 kW for cooling. It is a reversible heat pump that can provide heating, cooling and DHW to a small house or office building. It is an outdoor air-to-water heat pump unit with two extra BPHE in order to be capable of working either with the air or ground as thermal source, and to provide DHW independently from the heating/cooling production. It works with R32 as refrigerant and a variable speed scroll compressor manufactured by Copeland of 38 cc. The main components of the heat pump were further detailed in section 2.2.3, as well as the main control and operation system. The DSHP was installed very close to the technical room, next to the production workshop in the HiRef factory in Tribano, as can be seen in Figure 2.14, where the front part of the unit with the two fans is shown, as well as the different hydraulic connections with the different circuits: ground loop, user loop and DHW loop.

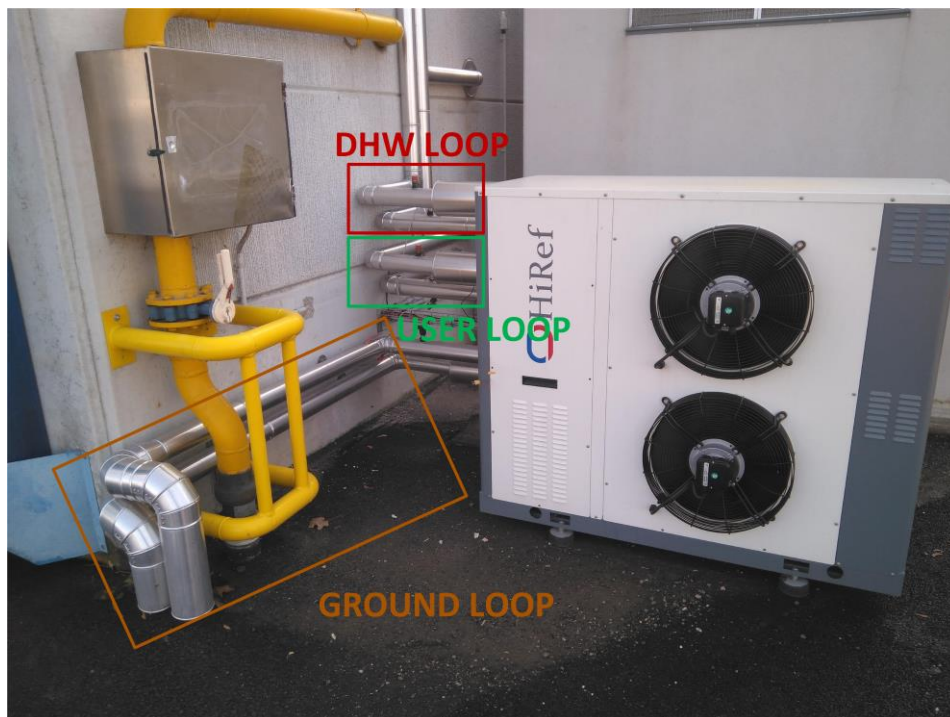


Figure 2.14. DSHP installed in the Tribano demo-site

On the back side of the unit (Figure 2.15), the connection pipes with the three circuits are placed: inlet and outlet of the heat pump. It is also possible to see the different temperature sensors, flow meters and pressure switches.



Figure 2.15. Back side of the DSHP unit: connecting pipes and sensors

2.3.3 Tribano Borehole Heat Exchangers field

2.3.3.1 BHEs field

The field of BHEs is located around 20 m far from the DSHP (Figure 2.16) under the parking of the factory, as shown in Figure 2.7. It consists of eight coaxial BHEs, in a rectangular configuration, connected in parallel in eight different hydraulic lines, using water as circulating fluid. Each BHE hydraulic line is distributed from a collector (Figure 2.17), where the total water coming from the heat pump is split in the different BHE pipe lines. Later on, the water coming from each BHE is mixed in the collector and flowing back to the heat pump. A map of the distribution of the BHEs field is presented in Figure 2.19.



Figure 2.16. Distance from the collector pit of the BHE field to the DSHP



Figure 2.17. Collector pit of the BHE field

The installed BHEs are standard coaxial BHEs, 30 m deep, not the spiral coaxial BHE configuration developed inside the GEOTeCH project. This is because the new BHE configuration was not fully available at the time that this facility was installed.

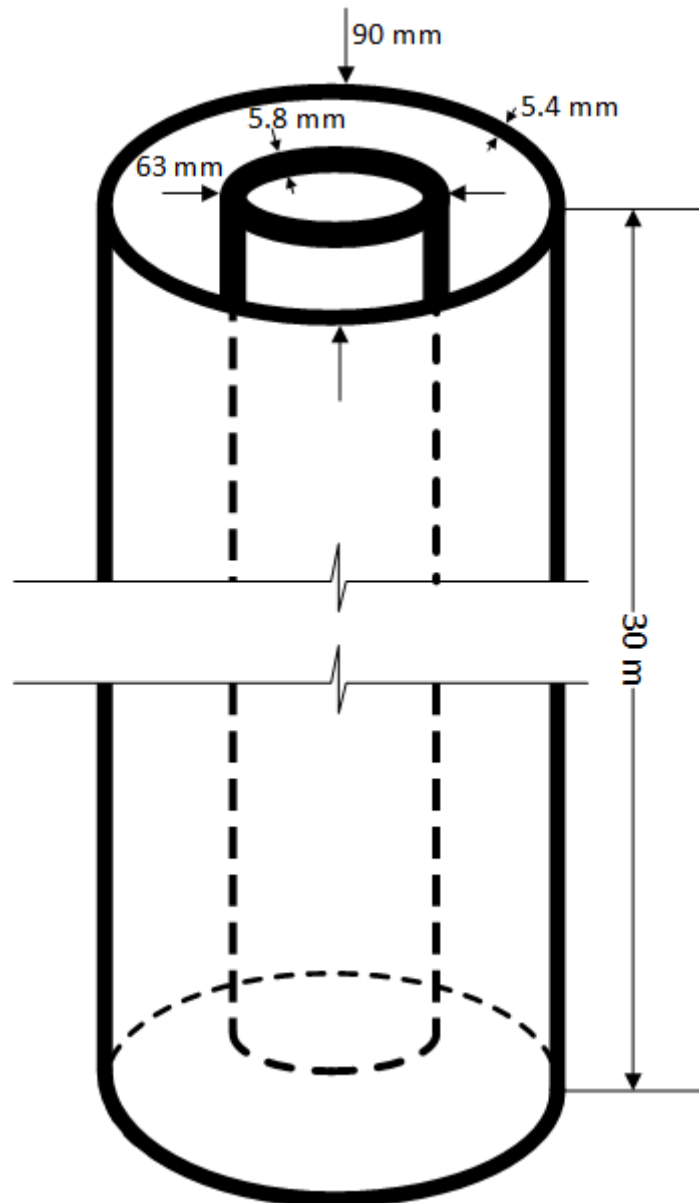


Figure 2.18. Diagram of the coaxial BHEs installed in Tribano

The BHEs were not grouted, as a hydrogeological study proved that it was not necessary and the hollow stem auger drilling developed in the GEOTeCH project was not equipped with the grouting devices at the moment of the installation. The absence of grouting caused the surrounding ground to collapse around each BHE when the drilling rods that contained it were removed. The excavated ground consisted mostly of very fine sand with some clayey banding on the top of the borehole. In addition, in order to contain intrusions of rainwater and pollutants, dry pellets were released from the top. The characteristics of the BHEs field and the monitoring system are further detailed in the work [51]. The technical specifications about the BHEs field (geometry, materials, etc.) are shown in Table 2.5.

Table 2.5. Technical specifications of the Tribano demo-site BHE field [51]

Borehole Heat Exchanger	Standard coaxial BHE Fluid used: water Absence of grouting: Borehole filled with soil collapsed Drill bit outer diameter (OD): 170 mm Drill rod outer diameter: 135 mm
Outer pipe	Type: PE100 SDR17 Outer diameter: 90 mm Thickness: 5.4 mm Length: 30 meter coiled Number of coils: 8
Inner pipe	Type: PP SDR11 Outer diameter: 63 mm Thickness: 5.8 mm Length: 30 m assembled in welded bars Length of bars: 4 meters Number of bars: 7.5
Geometry of the BHE field	Number of BHEs: 8 Displacement geometry: Rectangular Distance among BHEs: 6 m Type of connection: parallel Number of BHEs lines: 8 Type of BHEs line: PE100 SDR 11 DN32 Type of connections: electrofusion welding couplings
Centralizers	Number of centralizers: 15 Distance between two centralizers: 2 m

2.3.3.2 Monitoring system of the BHEs field

Apart from the monitoring system already implemented in the heat pump unit, several temperature sensors were installed in different parts of the BHEs field by the University of Bologna [51]:

- Inlet and outlet of BHE 8.
- Inlet and outlet of Collector (COL).
- Three observation boreholes (OB1, OB2 and OB3).

A map with the distribution of the BHEs and the temperature sensors is shown in Figure 2.19. Two PT100 sensors were installed on the head of BHE 8 with the purpose of collecting measurements of the inlet/outlet temperature of one of the BHEs and then, analysing the thermal behaviour of the BHE. These measurements were used in order to validate the BHE dynamic model (B2G model) of the coaxial configuration, as explained in section 3.6.3. Two PT100 sensors were installed in the collector, measuring the mixed water temperature flowing to/from the BHE 8.

Regarding the observation boreholes, they were installed with the purpose of studying the thermal evolution of the surrounding ground at different depths due to the climatic influence, as well as the heat injected/extracted by the BHEs. They consist of three pipes (PE100 SDR11 OD63) installed at different distances and orientations from the BHE 8 in a straight line (see Figure 2.19). One of them was installed between BHE8 and BHE6 (OB1), and two out of the BHEs field, west to the BHE8, at distances of 1 m (OB2) and 3 m (OB3). In this way, the thermal interaction between BHEs can be observed at OB1, while the OB2 and OB3 are mostly influenced only by BHE8. OB2 was installed as close to BHE8 as possible in order to study the influence of heat injection/extraction of one BHE in the local closest surrounding ground. The temperature measured in OB3 represents better the undisturbed ground temperature evolution.

Each observation borehole is filled with water and four temperature sensors are placed at depths of 2, 5, 10 and 15 meters each. The temperature sensors that were used are Therm Links, based on Modular Underground Monitoring System (MUMS) technology developed by ASE S.r.l. The accuracy of the Therm Links is $\pm 0.5\text{K}$, and the PT100 sensors have a tolerance of 0.15K at 0°C [51].



Figure 2.19. Map of the BHE field in the Tribano demo-site. Temperature sensors are located in OB 1, OB 2 and OB 3 (blue), as well as on the head of BHE 8 and COL (yellow) [51]

No mass flow rate sensors were installed in the BHE field, therefore there are available only measurements of the total mass flow rate flowing from the heat pump, but not the mass flow rate through each BHE, which would not be equal, as the hydraulic distribution system is not balanced and the length of the pipes between the collector and each BHE is different. More details about the monitoring system and the sensors can be found in the work [51].

2.3.3.3 Geology of the soil

Regarding the geology of the soil, the information was extracted from a hydro-geological study in the region of Tribano [52]. It mainly consists of unconsolidated, alluvial soil, with very fine grain size (silt and clay) and a low permeability, with sandy layers interspersed at different depths [51], as shown in Figure 2.20.

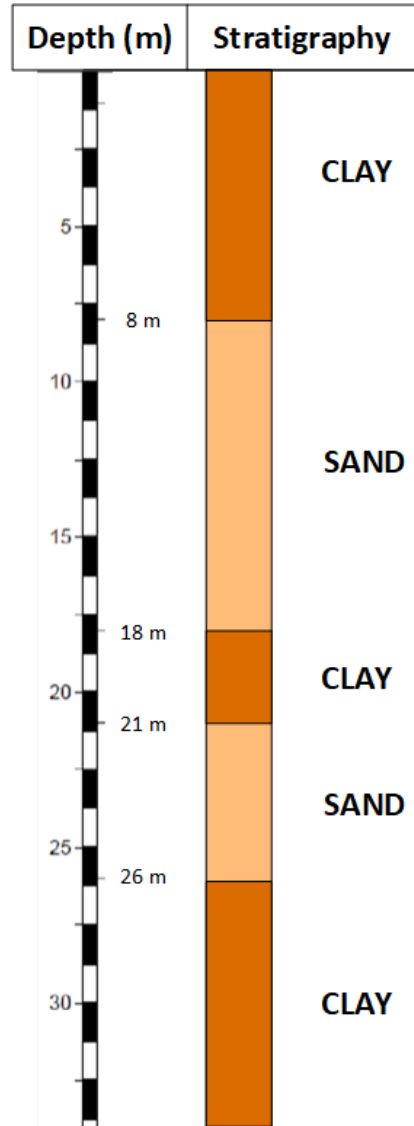


Figure 2.20. Geology strata in the region of Tribano (Padova). Data extracted from [52]

Regarding the thermal properties of the materials of the ground layers, they were extracted from the norm UNI11466:2012 [53] and are shown in Table 2.6.

Table 2.6. Thermophysical characteristics of the soil. Data extracted from [53]

Material	Thermal conductivity [W/(m K)]		Volumetric thermal capacity [MJ/(m ³ K)]
		Average value	
Wet clay/silt	1.1 - 3.1	1.8	2.0 - 2.8
Wet sand	2.0 - 3.0	2.4	2.2 - 2.8

2.3.4 Operation and control of the system

As explained in section 2.2.4, several control strategies can be used in order to operate the DSHP system. During the first months of operation, simple control strategies were used:

- The compressor frequency is controlled using a PI controller, trying to maintain the return temperature in the user circuit at the defined setpoint.
- The season switch is selected manually, this is, the change from heating to cooling and vice versa.
- The heat pump is always providing heating or cooling when demanded. This means that even during the night and the weekends the heat pump can start up in order to maintain the user circuit temperature.
- The DHW production is switched off for the moment, but it could be switched on.
- The flow rates at the user loop and ground loop are kept constant during the whole day, every day. Thus, the circulation pumps do not switch off, so they are working all the time at constant speed. The user loop flow rate is kept around 3000 kg/h, while the ground loop flow rate is maintained at roughly 4000 kg/h.
- The selection of the source is carried out as explained in 2.2.4.1. The water temperature coming from the ground loop is compared with the ambient air temperature and, depending on the temperatures difference, the best source is selected, with a hysteresis of $\pm 2\text{K}$.
- The main parameters that are used are the following:
 - Setpoint for cooling= 12°C .
 - Setpoint for heating= 45°C .
 - Setting for DHW production= 40°C .
 - Hysteresis ON= 1K.
 - Hysteresis OFF= 1K.
 - Maximum compressor frequency= 80 Hz.
 - Minimum compressor frequency=20 Hz.

Different control strategies were tested in the model of the system in order to improve the performance of the system, trying to reduce the energy consumption. One of the main control strategies in order to reduce the consumption is to control the speed of the circulation pumps in order to keep a constant temperature difference along the circuit, so the speed will adapt to the demand and not kept at a value that is normally too high. Another optimization strategy that will be simulated is the controlling of the heat pump compressor frequency based on the room temperature instead of controlling the supply/return temperature, then decreasing the supply temperature (in heating mode) whenever the thermal demand is low, decreasing then the consumption but assuring the thermal comfort. A brief introduction on the control of these systems is presented in section 4.1.

Chapter 3

3 Modelling of the coaxial BHE

3.1 State of the art of BHE modelling

The main component that differentiates a GSHP system from a conventional heat pump system is the field of Borehole Heat Exchangers (BHEs). This component is one of the most important components of the system, but also one of the most relatively expensive parts, as it implies drilling in the ground (several tens or hundreds of meters) and installing long pipes below the ground level in order to extract/inject heat from/to the ground. For this reason, a correct design of this BHE field is key in order to reduce the cost of the system as much as possible, always assuring a good thermal performance in the ground side in order to achieve a high energy efficiency of the entire system. In practice, this trade-off between efficiency and cost means that the BHE should not be under-sized (low efficiency) or over-sized (high cost). Furthermore, the operation of the system should be optimized, considering all the components, in order to achieve the highest possible efficiency of the entire GSHP system and compete with other conventional technologies.

Regarding the design and optimization of the GSHP systems, dynamic models are a very useful tool, as they are able to predict the behaviour of the whole integrated system, considering the interaction between components. Focusing on the most important component in GSHP systems, the BHE, an accurate short-term dynamic model is necessary, especially in an ON/OFF operation GSHP system, where it is key to reproduce accurately the cycling of the system, since the performance of the heat pump will strongly depend on the return temperature coming from the ground loop.

In this framework, several approaches regarding the BHE modelling have been used based on different assumptions and complexity levels, as well as the coupling with GSHP systems. Furthermore, different computer programs have also been used to simulate BHEs and GSHP systems. The main models and computer programs in order to simulate BHEs and GSHP systems are described in a high number of research works, for example [54]–[57].

3.1.1 Modelling the ground mass: common analytical models

To start with, the most commonly used analytical models for calculating the ground temperature outside of the BHE are based on the point heat source model of Carslaw and Jaeger [58]: Infinite Line Source (ILS), Infinite Cylindrical Source (ICS) and Finite Line Source (FLS). With these models it is possible to calculate the ground temperature outside the BHE, simulating the heat conduction in a homogeneous soil mass with a constant heat flow rate from a BHE, under different assumptions and levels of complexity. These models

have been used as the base to develop a great part of the current analytical and semi-analytical models [59].

The Infinite Line Source model is based on the Kelvin's line source theory [60], in which a constant heat flux from an imaginary infinite line is injected in the radial direction to an infinite medium at an initial uniform temperature. This model was used by Ingersoll and Plass [61] to provide practical applications for BHE modelling, so the BHE is represented by an infinite line that injects heat in the radial direction at a constant rate to an infinite ground mass, simplifying the heat injection into the ground as a one-dimensional process. The solution for calculating the ground temperature T , at a radial distance r , at time t , with a constant heat flux per meter q_0 , is presented in the equation (3.1).

$$T(r, t) - T_0 = \frac{q_0}{4\pi\lambda} \int_{\frac{r^2}{4\alpha t}}^{\infty} \frac{e^{-u}}{u} du = \frac{q_0}{4\pi\lambda} E_1\left(\frac{r^2}{4\alpha t}\right) \quad (3.1)$$

where T_0 is the initial temperature of the ground, λ is the soil thermal conductivity and α is the soil thermal diffusivity, and E_1 is the exponential integral function. This integral can be expressed as expansion series [62], according to the equation (3.2).

$$E_1(x) = -\gamma - \ln(x) - \sum_{n=1}^{\infty} \frac{(-1)^n x^n}{n n!} \quad (3.2)$$

Where $x = r^2 / (4\alpha t)$ and γ is the Euler constant ($\gamma \sim 0.5772$). Several approximations of the exponential integral function (E_1) have been developed in order to provide simpler algebraic solutions, one of the most known is the formulas developed by Abramowitz and Stegun [63]. Other examples have been presented, for example, Ingersoll and Plass [64] provided an approximation of the integral with tabulated values. On the other hand, Hart and Couvillion [65], proposed an algebraic approximation of the equation (3.1), assuming a hypothetical far-field radius where the effect of the line source vanishes, r_{∞} , depending on the heat injection time and thermal properties of the ground [59].

In the Infinite Cylindrical Source model, a constant heat flux from an imaginary infinite hollow cylinder is injected in the radial direction to an infinite medium at an initial uniform temperature. The solution for calculating the ground temperature at a specific radial distance and heat injection time is presented in the equation (3.3).

$$T(r, t) - T_0 = -\frac{q_0}{\pi^2 r_b \lambda} \int_0^{\infty} (1 - e^{-\alpha u^2 t}) \frac{J_0(ur) Y_1(ur_b) - Y_0(ur) J_1(ur_b)}{u^2 [J_1^2(ur_b) + Y_1^2(ur_b)]} du \quad (3.3)$$

where r_b is the borehole radius and J_0, J_1, Y_0 and Y_1 are Bessel functions.

As it happens with the ILS model, solving the integral in equation (3.3) is not straight forward. Therefore, some approximate solutions were provided by Carslaw and Jaeger depending on the time scale. On the other hand, tabulated and graphical values for this integral were provided by Ingersoll et al. [64] and Kavanaugh [66].

Regarding the FLS model, the BHE is approximated by a finite line source constituting a series of point sources, with the top corresponding to the ground surface. The solution of the continuous point source is integrated over the length of the BHE (H) in order to calculate

the ground temperature. The ground mass is modelled as semi-infinite, so the temperature variation in the surface will have an influence on the ground temperature. In order to model the ground as a semi-infinite region and impose a determined temperature at the soil surface, Carslaw and Jaeger used the method of images [58]. Therefore, a virtual line source of the same length as the BHE, with an opposite heat flux is placed above the ground surface symmetrically to the original line source. Eskilson [67] proposed a solution for calculating the temperature field around a finite line, according to the equation (3.4).

$$T(r, z, t) - T_0 = \frac{q_0}{4\pi\lambda} \int_0^H \left[\frac{\operatorname{erfc}\left(\frac{\sqrt{r^2 + (z-h)^2}}{2\sqrt{\alpha t}}\right)}{\sqrt{r^2 + (z-h)^2}} - \frac{\operatorname{erfc}\left(\frac{\sqrt{r^2 + (z+h)^2}}{2\sqrt{\alpha t}}\right)}{\sqrt{r^2 + (z+h)^2}} \right] dh \quad (3.4)$$

The three analytical solutions (ILS, ICS and FLS) have been studied and compared in several studies [57], [68]–[70], in order to find the valid time ranges in which each one is suitable to be applied, depending on different variables, mainly the Fourier number ($Fo = \alpha t/L^2$, where L would be the radial distance r in the ILS, the borehole radius r_b in the ICS and the borehole length H in the FLS), based on the thermal properties of the ground, the injection time and the radial distance. In general, the ICS is recommended for short injection periods (up to 34 hours) for typical operation conditions [68], as it considers that the heat is injected at the borehole radius, while the FLS is the most suitable for very long injection times (in the range of some years), as it considers two-dimensional effects [68].

3.1.2 g-function model

Based on the FLS model, Eskilson [67] introduced the concept of *g-function*. A non-dimensional thermal response function that represents the temperature at the borehole wall, according to the equation (3.5).

$$T_b - T_0 = \frac{q_0}{2\pi\lambda} g\left(\frac{t}{t_s}, \frac{r_b}{H}\right), \quad t_s = \frac{H^2}{9\alpha} \quad (3.5)$$

where T_b is the temperature on the borehole surface and t_s is a steady-state time scale. The *g-functions* are valid for times greater than $5r_b^2/\alpha$. For a typical borehole, this implies times between 3 and 6 hours [71].

The *g-function* concept has been used by many researchers in the field of GSHP modelling, leading to a great number of models with different levels of complexity and computational efficiency. For this purpose, *g-functions* have been treated not only analytically, but also numerically. Among the analytical solutions, Claesson and Eskilson gave two asymptotic approximations [67], Zeng et al. suggested a non-dimensional *g-function*, similar to the Eskilson one [72]. Lamarche and Beauchamp [73] calculated their analytical *g-function* similarly, but using the integral mean temperature along the BHE

depth. More recently, other authors have developed analytical or semi-analytical approaches based on the FLS analytical approach [74]–[76]. Regarding the numerical calculation of *g-functions*, several approximations have been considered, depending on the boundary condition assumed: imposition of the heat flux condition, imposition of the temperature conditions, combination of both, etc. Some examples of *g-functions* calculated with a heat flux boundary condition and a temperature boundary condition can be found in [77], [78], respectively.

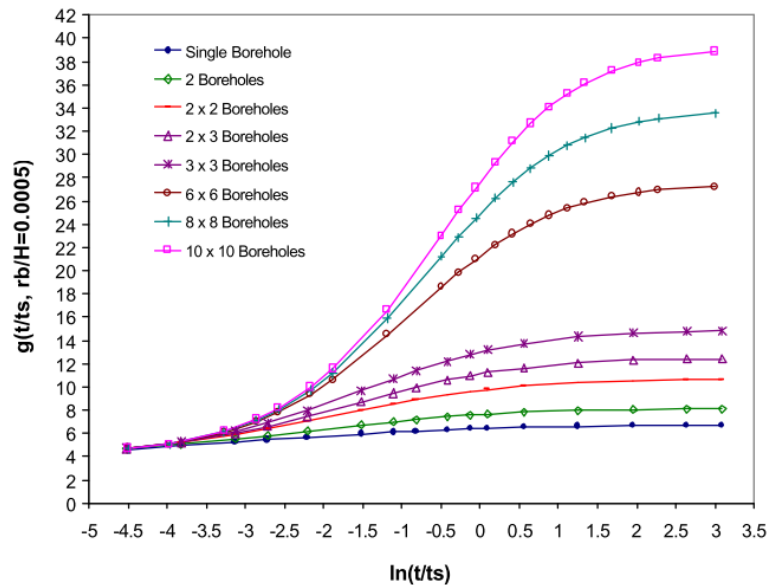


Figure 3.1. Temperature response factors (*g-functions*) for various multiple borehole configurations compared to the temperature response curve for a single borehole [71]

Although initially the *g-function* models were mainly focused on the prediction of the ground thermal response on the mid-long-term, they have been improved to predict shorter time injection periods. Because it is important to predict not only the long-term response, but also the short-term response, as it will have an impact on the performance of the heat pump, which is influenced by the temperature of the fluid coming from the BHEs. In this regard, Yavuzturk and Spitler developed a short time-step model [58], extending Eskilson's concept of non-dimensional temperature response factors. So they developed *g-functions* that are suitable for shorter time periods (hourly or less) using a numerical approach with a two dimensional implicit finite volume. Lamarche and Beauchamp [59] developed an analytical approach to reproduce the short-term response of the BHE, solving the exact solution for coaxial BHE and a good approximation for a U-tube configuration.

3.1.3 Numerical and analytical modelling of the BHE

Several numerical and analytical models with a higher level of detail have been developed, modelling not only the surrounding ground, but also the behaviour of the borehole in terms of the fluid temperature evolution. Numerical models, most of them based on the finite difference and the finite element (FEM) methods [59], are usually more precise

and flexible than analytical models, but they have a higher computational cost and it is more difficult to couple them with dynamic simulation programs. The finite difference method is the traditional used to solve heat and fluid flow problems, so it is more widespread [59]. Some of the most known finite difference methods are [71], [79]. Regarding FEM, its use is not so much widespread, but it is increasing [59]. One of the first important works is the one of Muraya [80], afterwards, some other FEM models were developed, for example, [81]–[84].

On the other hand, analytical and semi-analytical methods are limited to some assumptions and simplifications that reduce their accuracy. However, they present a lower computational cost and they can be coupled into design/simulation programs more easily [56]. Several of these models use a thermal network based on thermal resistances and capacitances in order to model the heat transfer between the different parts of the borehole and also the surrounding ground [28], [79], [85]–[91]. Among them, Zarrella et al. [87] presented the CaRM (Capacity and Resistance) model, considering the thermal capacitance of the borehole: grout and fluid, also Pasquier and Marcotte [90] proposed a thermal network model, improving the TRCM (Thermal Resistance Capacity Model) developed by Bauer et al. [88], integrating the thermal capacitance of the heat carrier fluid and pipe.

In addition, short-term analytical solutions have also been developed, for example the one developed by Li and Lai [92]. It can be used in time scales greater than one hour (up to several years), but not in very short-term scales (in the range of minutes) needed to reproduce the dynamic behaviour of an on/off GSHP. Another short-term analytical solution was developed by Javed and Claesson [93], studying the BHE heat transfer and the boundary conditions in the Laplace domain, also using a thermal network. Additionally, they developed a numerical solution.

3.1.4 Computer programs used in the simulation of BHEs and GSHP systems

Apart from all of these analytical and numerical models, there also exist some other computer programs that can be used in order to assist in the design and simulation of GSHP systems and BHEs [55], [56], [94]. Among them, GLHEPRO [95], EED [96], EnergyPlus [97], Modelica [98], [99] or TRNSYS [100]. In order to simulate the behaviour of, not only the BHE itself, but the entire GSHP system and the coupling between the different components, a transient simulation program (like TRNSYS) is a powerful tool, since it is able to connect the models of the different components and solve the simultaneous equations of the system model, displaying the results [101].

It is possible to find several BHE models already implemented in TRNSYS [102], two of the most commonly used are the Superposition Borehole Model (SBM), developed by Eskilson [67], [103] and implemented in TRNSYS by Pahud [104], [105] (type 281); and the Duct Storage model (DST), developed by Hellström [106], [107] and implemented in TRNSYS by Pahud [108], [109] (Type 557). The main drawback of these models is that they neglect the heat capacity of the fluid and the grout existing in the BHE, and show a low accuracy during the short-term injection period [102]. Apart from these models, it is

possible to find another less common BHE models, like the *Erdwärmesonden* model (EWS), developed by Huber and Schuler for double U-pipes BHEs [110], in order to improve the transient prediction of the behaviour compared to the existing BHE models, reducing the simulation time [102] and implemented in TRNSYS by Wetter and Huber [111] as the type 451.

3.1.5 Modelling of BHE fields and long-term response of the ground

Concerning the modelling of BHE fields on the long term, three main issues should be taken into account: first, it is necessary to predict the long-term response of the ground due to the heat injection from the BHE (not only reproduce the short-term dynamic response of the BHE), second, it is necessary to account for time-varying loads (as the heat injected in the ground will vary with the time, depending on the heat pump operation) and third, it is necessary to consider the thermal interaction between the different BHEs located in the field.

For this purpose, a long-term ground model must be used to calculate the temperature variation of the ground due to the heat injection load from the BHEs on the long term. Then, time and space superposition techniques must be used to account for the time-varying heat loads and different BHEs in the field, respectively.

Regarding the long term model, it is possible to use one of the analytical solutions given by Carslaw and Jaeger (ILS, ICS or FLS, depending on the Fourier number, being the FLS model the most suitable for longer terms simulations) and apply space and time superposition techniques. The space superposition technique consists in summing up the temperature alterations of all the BHEs in the field at the desired point [70]. In order to account for time-varying boundary conditions and/or time-dependent heat injection/extraction by using the ground temperature response solution with time-independent conditions, the Duhamel's theorem can be used [112]. So the heat injection/extraction is divided in a series of single, constant, unitary heat pulses and the solution is applied for the corresponding time-steps, superimposing the response in each step. Some examples of the application of this theorem can be found in [57], [70].

In this framework, one of the frequently used methodologies to calculate the long-term response of the ground, especially implemented in computer programs like EED, GLHEPRO or EnergyPlus, is to calculate the ground temperature variation with pre-generated *g-functions*. Therefore, these functions are calculated previously with analytical or numerical methods for different common BHEs field configurations. The pre-calculated *g-function* already includes the interaction between the different BHEs in the field, so it is only necessary to apply a time superposition technique in order to account for the different time-varying heat loads injected into the ground. As long as the time operation increases in the simulation, the number of heat injection steps will increase too. Therefore, for long time operating simulations, the computational cost will be very high. In order to address this issue, load-aggregation algorithms are used in order to reduce the computational cost [55], so the unitary heat loads are lumped together into larger blocks, considering that the most

recent loads will have a greater influence in the ground response than the past heat loads. In the literature, several aggregation techniques have been presented, for example, the method developed by Yavuzturk and Spitler [113], the Multiple Load Aggregation Algorithm (MLAA) developed by Bernier et al. [114] or the aggregation algorithm used by Ruiz-Calvo et al. [115]. The American Society of Heating and Air-Conditioning Engineers (ASHRAE) recommended the method developed by Kavanaugh and Rafferty, allowing to design a BHE system considering three representative building heat loads, the thermal resistances, based on ICS model, and a temperature penalty variable (T_p), considering the effect of the interaction between BHE on the long term [116], some corrections have been provided to the original method by Bernier [117] or Fossa [118], and an improved method was suggested by Fossa and Rolando for a 10 years horizon [116].

3.1.6 Approach to the new BHE modelling

Within this framework, a dynamic model for a U-tube BHE configuration was developed, called B2G model [119], [120]. The main purpose of this model was to predict the short-term dynamic response of a U-tube BHE in terms of the heat carrier fluid temperature, so it could be used in the modelling of a GSHP system in TRNSYS environment at a low computational cost. The main issue was to develop a BHE model able to simulate the dynamic evolution of the fluid temperature in order to couple it to a water-to-water heat pump model. This short-term dynamic response of the BHE is especially important in the on/off operation of the heat pump, as the cycling times may be in the range of a few minutes.

In this regard, the B2G model is able to predict the outlet fluid temperature of the BHE when the inlet temperature and mass flow rate are known, together with the geometric and thermophysical characteristics of the BHE and surrounding ground. Therefore, the outlet fluid temperature could be used in the heat pump model in order to predict its performance. This model is based on a thermal network approach, with thermal resistances and capacitances in order to simulate the heat transfer processes between the different parts of the BHE. The thermal network selected was simple enough to carry out simulations with a low computational cost, but detailed enough to reproduce the short-term response of the BHE with a high accuracy.

On the other hand, the long-term response of the surrounding ground can be calculated with an external ground model, optimized to calculate the long-term response of the ground with a low computational cost, so when coupled both the short- and long-term models, it is possible to simulate the behaviour of the BHE, as well as the surrounding ground, with an overall low computational cost. In a previous work, the U-tube B2G model was coupled to a *g-function* previously generated for a specific BHE field configuration [115].

In this PhD dissertation, the B2G dynamic model has been adapted to an innovative coaxial configuration with helical flow through the outer pipe, developed inside the framework of the GEOTeCH Horizon2020 project [40], as well as to a standard coaxial configuration. Additionally, some improvements were integrated in the form of new features available in the model. The new coaxial B2G model was also implemented in

TRNSYS, so it can be used for modelling the integrated dual source heat pump system described in section 2. The modelling of the whole system will be described in section 4.

Apart from this, a different long-term model for the ground response was implemented in TRNSYS based on an approach of the ILS model, so it is possible to calculate the thermal interactions between BHEs in a field without the need of having a pre-calculated *g-function* for a specific BHE field configuration.

In summary, the innovations of the new BHE model are the following:

- Adaptation of the thermal network to a coaxial BHE configuration.
- Thermodynamic modelling of the helical fluid flow path along the outer pipe.
- Consideration of the vertical heat conduction through the ground and grout.
- Consideration of a heterogeneous layered ground with different thermal properties.
- Estimation of the heat transfer at the bottom of the BHE.
- Calculation of the pressure loss in the BHE for the standard coaxial configuration.
- Increase of the number of ground nodes in the definition of the affected ground around the BHE: from only one ground node formerly considered in the previous B2G version, to three ground nodes in order to reproduce the very-short term behaviour of the BHE with a high accuracy, as well as the short/mid-term behaviour and the undisturbed ground.
- Development of a methodology to calculate the optimal position of the ground nodes, depending on the BHE geometry, expected operating conditions (heat injection time during a day) and the ground thermal properties.
- Implementation in TRNSYS of the new helical coaxial B2G model.
- Implementation in TRNSYS of a long-term ground response model in order to consider any BHE field configuration without the need of a pre-calculated *g-function*.

3.2 B2G BHE dynamic model

The B2G (Borehole-to-Ground) model was originally developed to predict the thermal interaction between a BHE and the surrounding ground, focused on the short-term evolution of the fluid temperature. It is based on a thermal network approach together with a vertical discretization of the BHE in a way that the radial heat transfer between the different parts of the borehole (fluid inside the pipes, grout and ground) is modelled by a 2D thermal network at each depth. The advection of the fluid is modelled, so the vertical temperature distribution is calculated. In order to reproduce the thermal evolution of the fluid with a computational cost as low as possible, the simplest thermal network that is able to reproduce the BHE behaviour with accuracy enough ($RMSE < 0.1K$) was used. For this purpose, only the portion of surrounding ground mostly affected by the heat transfer at the end of the heat injection/extraction period is considered in the thermal network.

The thermal network consists of different nodes, representing each part of the BHE and considering their thermal properties. The thermal interaction between nodes is calculated

by the use of thermal resistances. These thermal resistances model the conductive and convective heat transfer between the different parts involved. Furthermore, the thermal inertia of the fluid, the grout and the ground is represented by a thermal capacitance in each node.

3.2.1 U-tube B2G model

The B2G model was initially developed for a single U-tube BHE configuration and presented in previous research works, where it was validated experimentally with several BHEs under different conditions: in [119], the B2G model was validated using a step-test from a BHE located in Stockholm (Sweden); in [120], the B2G model was validated using experimental data (normal operation and a step-test) from a BHE of a GSHP located in Valencia (Spain) and in [115], the coupling between the B2G model and a *g-function* model was validated for the BHE field of the GSHP located in Valencia. The 2D thermal network consisted of five thermal capacitances and six thermal resistances, forming a 5C6R-*n* model, where *n* is the number of vertical divisions. This system can be solved numerically, solving the system of ordinary differential equations, as shown in [119]. The thermal network is presented in Figure 3.2, where T_1 and T_2 represent the upward and downward fluid inside the pipe, T_{b1} and T_{b2} represent the grout (it is divided in two regions) and T_g represents the surrounding ground affected by the heat injected/extracted in the daily working period of the BHE.

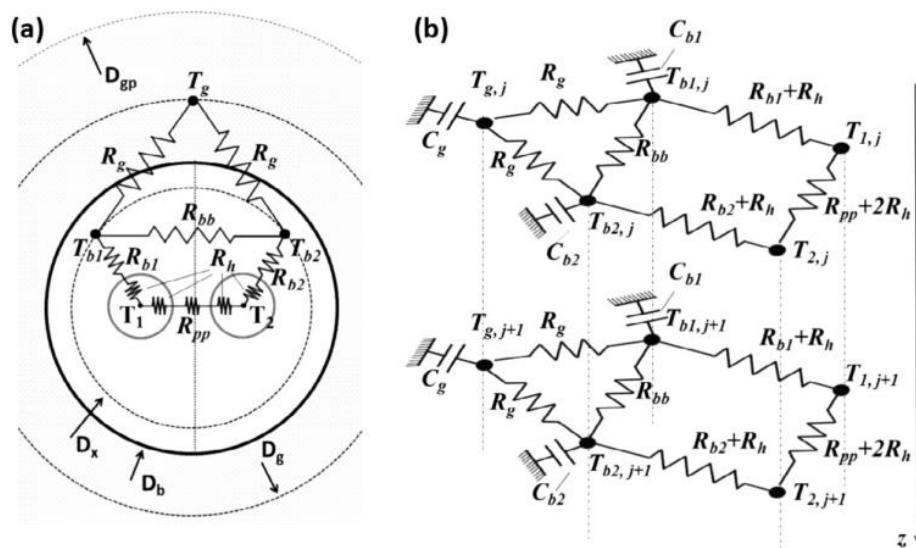


Figure 3.2. Thermal network model adopted: (a) 2D model; (b) 3D model [119]

The vertical conduction (axial transport) is neglected, but the fluid advection in the vertical direction is taken into account in the transient energy balance equations.

The model was able to calculate the short-term behaviour of different BHEs with a high accuracy (absolute error within 0.15°C), as well as predicting the dynamic behaviour of a BHE during the operation of a GSHP facility when coupled with a long-term BHE model, as the *g-function* model [115].

3.3 Standard and helical coaxial B2G dynamic model

A new coaxial helical BHE has been developed in the framework of the GEOTeCH project, it was detailed in section 2.2.2. In order to simulate this new BHE, and aid in its design and the operation of the GSHP system, the B2G model was adapted, first to a standard coaxial BHE configuration and then to the innovative coaxial helical configuration. The main difference between these two models is the equivalent section and the hydraulic diameter in the outer pipe, as the fluid will flow vertically straight in the standard coaxial BHE, whereas it will follow a helical path in the new BHE. A first approach to these configurations was presented previously, both for the standard coaxial [121], [122] and coaxial helical BHE [123]–[125]. In this work, the thermal network has been extended in order to include three ground nodes: close ground (ground node 1), further ground (ground node 2) and undisturbed ground (undisturbed ground node). In addition, a new methodology for the calculation of the ground nodes position has been used.

The new thermal network consists of five nodes with their five thermal capacitances; together with an additional node, that represents the undisturbed ground (therefore, presenting an infinite capacitance and constant temperature). Each node represents one part of the BHE: T_i represents the fluid flowing inside the inner pipe, T_o represents the fluid in the outer pipe, T_b represents the grout of the borehole, T_{g1} represents the first ground node, T_{g2} represents the second ground node and T_{ug} represents the undisturbed ground node. In this model, three ground nodes are used instead of only one (as in the U-tube B2G model). With these three ground nodes, it is possible to have a higher accuracy of the BHE thermal response during the different heat injection periods, without greatly incrementing the complexity of the model:

- The first ground node (T_{g1}) represents the closer ground region in contact with the borehole, which has a higher influence in the short-term response of the BHE. This region covers the annulus area between the borehole wall diameter (D_b) and the first ground penetration diameter (D_{gp1}).
- The second ground node (T_{g2}) represents the further ground region, with a lower influence in the short-term response but a higher influence in the mid-term response. This region covers the annulus area between the first ground penetration diameter (D_{gp1}) and the second ground penetration diameter (D_{gp2}).
- The undisturbed ground node (T_{ug}) represents the far surrounding ground, which keeps a constant temperature, as it remains undisturbed during the heat injection period assumed in the model. This node is located at the undisturbed ground diameter (D_{ug}).

The convective and conductive heat transfer between the different nodes was calculated by the use of radial thermal resistances between nodes (R_{io} , R_{ob} , R_{bg1} , R_{g1g2} and R_{g2ug}). The heat conduction between the vertically adjacent grout and ground nodes has also been considered by the use of vertical thermal resistances (R_{vb} , R_{vg1} and R_{vg2}).

In Figure 3.3 a), the thermal network used for calculating the heat transfer between the different parts of the BHE at a specific depth (z) is shown, while the vertical discretization of the BHE, showing three adjacent vertical divisions and the vertical thermal resistances is shown in Figure 3.3 b).

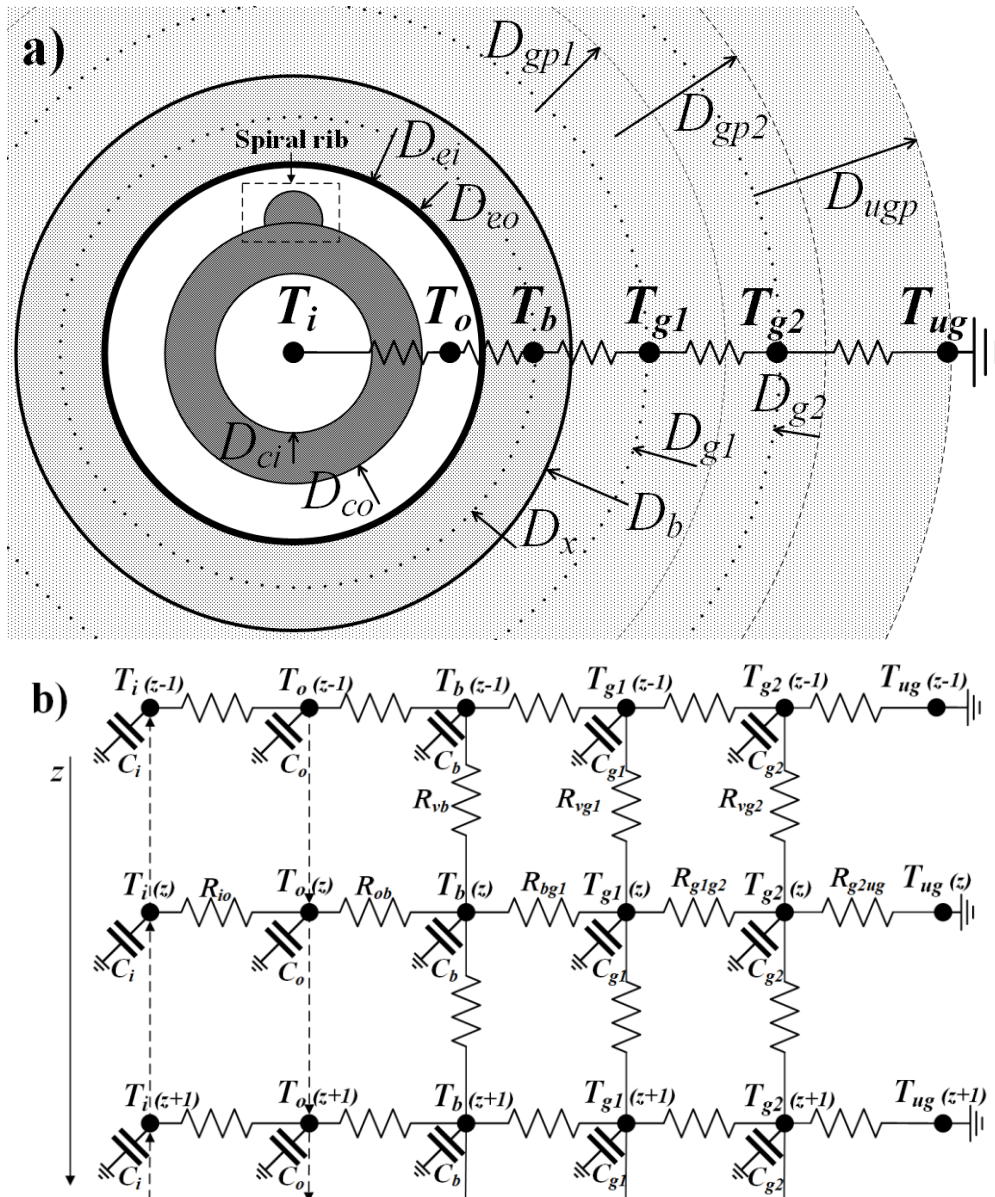


Figure 3.3. Thermal network of the coaxial configuration model: a) borehole layout; b) vertical discretization

The energy balance equations that describe the system are described as follows:

- For the fluid nodes, the axial heat conduction is neglected, but the vertical direction advection is considered. In the case of the fluid inside the inner pipe, the transient energy balance equation will consider not only the vertical advection (represented by its vertical velocity, v_i), but also the heat exchange with the fluid in the outer pipe (equation (3.6)). In the case of the fluid inside the outer pipe, the transient energy balance equation will consider its vertical advection (v_o) and also the heat exchange with the fluid in the inner pipe and the grout (equation (3.7)).

$$\frac{\partial T_i(z)}{\partial t} = v_i \frac{\partial T_i(z)}{\partial z} - \frac{1}{C_i} \left(\frac{T_i(z) - T_o(z)}{R_{io}} \right) \quad (3.6)$$

$$\frac{\partial T_o(z)}{\partial t} = -v_o \frac{\partial T_o(z)}{\partial z} - \frac{1}{C_o} \left(\frac{T_o(z) - T_i(z)}{R_{io}} + \frac{T_o(z) - T_b(z)}{R_{ob}} \right) \quad (3.7)$$

- For the grout node, the heat exchange with the adjacent nodes in the same vertical depth is considered (fluid inside the outer pipe and the first ground node), but also the vertical heat exchange between the vertically adjacent grout nodes (at the depths immediately above and below), as shown in equation (3.8).

$$C_b \frac{\partial T_b(z)}{\partial t} = \frac{T_o(z) - T_b(z)}{R_{ob}} + \frac{T_{g1}(z) - T_b(z)}{R_{bg1}} + \frac{T_b(z-1) - T_b(z)}{R_{vb}} + \frac{T_b(z+1) - T_b(z)}{R_{vb}} \quad (3.8)$$

- For the first and second ground nodes, the heat exchange with the adjacent nodes in the same vertical depths is considered, as well as the vertical heat conduction with the vertically adjacent nodes, as shown in the equations. (3.9) and (3.10).

$$C_{g1} \frac{\partial T_{g1}(z)}{\partial t} = \frac{T_b(z) - T_{g1}(z)}{R_{bg1}} + \frac{T_{g2}(z) - T_{g1}(z)}{R_{g1g2}} + \frac{T_{g1}(z-1) - T_{g1}(z)}{R_{vg1}} + \frac{T_{g1}(z+1) - T_{g1}(z)}{R_{vg1}} \quad (3.9)$$

$$C_{g2} \frac{\partial T_{g2}(z)}{\partial t} = \frac{T_{g1}(z) - T_{g2}(z)}{R_{g1g2}} + \frac{T_{ug}(z) - T_{g2}(z)}{R_{g2ug}} + \frac{T_{g2}(z-1) - T_{g2}(z)}{R_{vg2}} + \frac{T_{g2}(z+1) - T_{g2}(z)}{R_{vg2}} \quad (3.10)$$

- The undisturbed ground node is assumed to maintain the far-field temperature (undisturbed ground temperature) at each depth: $T_{ug}(z, t) = T_{\infty}(z)$.

3.3.1 Parameters calculation

The main parameters of the model are the thermal capacitances and the thermal resistances, which can be determined based on the thermo-physical properties and the geometrical characteristics of the borehole. Furthermore, it is possible to consider different thermo-physical properties (thermal conductivity and thermal capacity) for the grout and ground at different depths in a heterogeneous layered ground. Therefore, the thermal resistances and thermal capacitances may be different at different depths.

3.3.1.1 Thermal Capacitances

The thermal Capacitances (C) are calculated considering the volumetric thermal capacitance at the corresponding depth (c) and the volume of the zone in each vertical division, of thickness dz . The grout and ground capacitances are calculated according to the equations in (3.11), where D_b represents the borehole diameter and D_{eo} represents the external diameter of the outer pipe.

$$C_b = \frac{\pi}{4}(D_b^2 - D_{eo}^2) c_b dz; \quad C_{g1} = \frac{\pi}{4}(D_{gp1}^2 - D_b^2) c_g dz; \quad C_{g2} = \frac{\pi}{4}(D_{gp2}^2 - D_{gp1}^2) c_g dz \quad (3.11)$$

The thermal capacitance of the fluid nodes is calculated based on the fluid heat capacity (C_p), the fluid density (ρ) and the volume of fluid in each vertical division, according to equation (3.12). Here, D_{ci} represents the inner diameter of the inner pipe, D_{ei} represents the inner diameter of the outer pipe and D_{co} represents the outer diameter of the inner pipe.

$$C_i = \frac{\pi}{4} D_{ci}^2 C_{p,i} \rho_i dz; \quad C_o = \frac{\pi}{4} (D_{ei}^2 - D_{co}^2) C_{p,o} \rho_o dz \quad (3.12)$$

All the fluid properties (heat capacity (C_p), density (ρ), dynamic viscosity (μ) and thermal conductivity (λ)) are calculated according to the correlations presented in [126], depending on the temperature of the fluid, the type of fluid (water or MPG and water mixture) and in the second case, the percentage of MPG in the mixture.

3.3.1.2 Thermal resistances

Thermal resistances are calculated as an addition of conductive and convective cylindrical thermal resistances. For the calculation of the conductive resistance, the nodes are located at an equivalent diameter. The equivalent diameter is calculated as the average diameter of the annulus zone according to the equations in (3.13), where D_x is the grout node diameter, D_{g1} corresponds to the short-term node diameter and D_{g2} corresponds to the mid-term node diameter.

$$D_x = \frac{D_b + D_{eo}}{2}; \quad D_{g1} = \frac{D_{gp1} + D_b}{2}; \quad D_{g2} = \frac{D_{gp2} + D_{gp1}}{2} \quad (3.13)$$

Regarding the convective thermal resistance, it is calculated using the average convective heat transfer coefficient (h) of the fluid in the inner pipe (h_i) and in the outer pipe (h_o), using the equation (3.14).

$$h = \frac{Nu k}{D} \quad (3.14)$$

The thermal conductivity of the fluid is represented by k , and the Nusselt number (Nu) is calculated depending on the flow regime, depending on the flow regime (laminar or turbulent) and the geometric configuration (circular tube in the inner pipe and concentric annular in outer pipe). These properties are calculated at the average temperature of the fluid inside each pipe (inner or outer pipe). As an example, the equations (3.15)-(3.19) are used to calculate the mean Nusselt number for the inner pipe (circular tube), assuming a constant wall temperature and depending on the flow regime [127]:

- For laminar flow:

$$Nu_{m,T} = \left\{ Nu_{m,T,1}^3 + 0.7^3 + [Nu_{m,T,2} - 0.7]^3 \right\}^{1/3} \quad (3.15)$$

$$Nu_{m,T,2} = 1.615 \sqrt[3]{Re Pr d_i / l} \quad (3.16)$$

$$Nu_{m,T,1} = 3.66 \quad (3.17)$$

- For turbulent flow:

$$Nu_m = \frac{(\xi/8) Re Pr}{1 + 12.7 \sqrt{\xi/8} (Pr^{2/3} - 1)} \left[1 + (d_i/l)^{2/3} \right] \quad (3.18)$$

$$\xi = (1.8 \log_{10} Re - 1.5)^{-2} \quad (3.19)$$

Where l represents the length of the pipe, Re the Reynolds number, Pr the Prandtl number and d_i the inner diameter of the pipe.

Regarding the outer pipe, the helical flow path is modelled assuming that the fluid flows through a rectangular duct, where L_s represents one side of the rectangular duct and $(D_{ei} - D_{co})$ represents the other side. Therefore, the equations for a regular pipe are used [127], but considering an equivalent hydraulic diameter (D_h) and an equivalent cross-sectional area of the flow (A_{eq}).

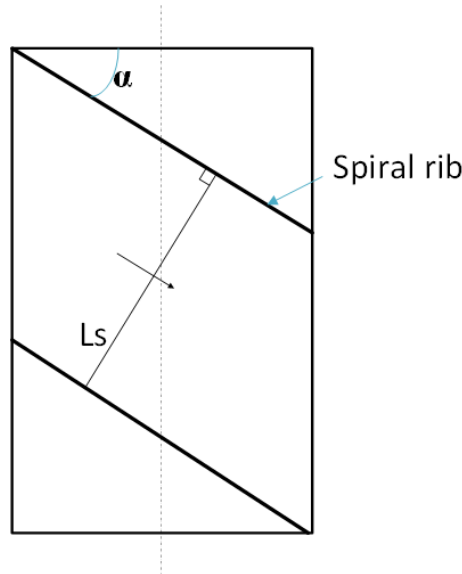


Figure 3.4. Cross-sectional area of the helical flow path

These hydraulic parameters will depend on the angle of the helix (α), the number of spiral ribs (n_r), the outer diameter of the inner pipe (D_{co}) and the inner diameter of the outer pipe (D_{ei}), according to the equations (3.20)-(3.22).

$$L_s = \frac{\pi \sin(\alpha) (D_{ei} + D_{co})}{n_r} \quad (3.20)$$

$$A_{eq} = L_s (D_{ei} - D_{co}) / 2 \quad (3.21)$$

$$D_h = \frac{4A_{eq}}{2L_s + (D_{ei} - D_{co})} \quad (3.22)$$

The equivalent length of the duct is longer than the borehole depth (L) due to the helical path, it can be calculated as $L_{eq} = L/\sin(\alpha)$.

In the case of a standard coaxial configuration, the equations for a concentric annular pipe [128] are used, where $D_h = D_{ei} - D_{co}$ and $L_{eq} = L$.

Concerning the conductive thermal resistances, they are calculated considering the conductivities of the inner pipe (k_{ip}), the outer pipe (k_{op}), the grout (k_b) and the ground (k_g) at the corresponding depth, as cylindrical thermal resistances.

The total thermal resistances between the different nodes in the radial thermal network are described in the equations (3.23) - (3.27), considering both the convective and conductive thermal resistances.

$$R_{io} = \frac{1}{\pi D_{ci} dz h_i} + \frac{\ln(D_{co}/D_{ci})}{2 \pi k_{ip} dz} + \frac{1}{\pi D_{co} dz h_o} \quad (3.23)$$

$$R_{ob} = \frac{1}{\pi D_{ei} dz h_o} + \frac{\ln(D_{eo}/D_{ei})}{2 \pi k_{op} dz} + \frac{\ln(D_x/D_{eo})}{2 \pi k_b dz} \quad (3.24)$$

$$R_{bg1} = \frac{\ln(D_b/D_x)}{2 \pi k_b dz} + \frac{\ln(D_{g1}/D_b)}{2 \pi k_g dz} \quad (3.25)$$

$$R_{g1g2} = \frac{\ln(D_{g2}/D_{g1})}{2 \pi k_g dz} \quad (3.26)$$

$$R_{g2ug} = \frac{\ln(D_{ug}/D_{g2})}{2 \pi k_g dz} \quad (3.27)$$

Regarding the vertical thermal resistances between adjacent nodes, they are calculated according to the equations (3.28)-(3.29), depending on the thermal conductivity at the corresponding depth, the vertical distance between nodes (dz) and the annulus surface. The thermal conductivity considered is the same in the vertical and radial direction.

$$R_{vb} = \frac{dz}{\frac{\pi}{4} \cdot (D_b^2 - D_{eo}^2) \cdot k_b} \quad (3.28)$$

$$R_{vg1} = \frac{dz}{\frac{\pi}{4} \cdot (D_{gp1}^2 - D_b^2) \cdot k_g} \quad ; \quad R_{vg2} = \frac{dz}{\frac{\pi}{4} \cdot (D_{gp2}^2 - D_{gp1}^2) \cdot k_g} \quad (3.29)$$

3.3.1.3 Heat transfer at the bottom of the borehole

The heat transfer at the bottom of the borehole is modelled in the form of semi-spherical thermal resistances from the bottom of the outer pipe of the BHE until the undisturbed ground. For this purpose, the last node of the vertical discretization (N node) is used. The thermal network at the bottom of the borehole is represented in Figure 3.5.

The convective semi-spherical thermal resistance from the outer pipe to the grout node is calculated according to the equation (3.30), where r_{eo} represents the outer radius of the outer tube and h the convective heat transfer coefficient. While the conductive semi-spherical thermal resistance from node $T_i(N)$ to node $T_j(N)$ is calculated using the equation

(3.31), where T_i and T_j represent the different nodes ($T_o, T_b, T_{g1}, T_{g2}, T_{ug}$) and k the thermal conductivity.

$$R_h = \frac{1}{2\pi r_{e0}^2 h} \quad (3.30)$$

$$R_{c,ij} = \frac{1/r_i - 1/r_j}{2\pi k} \quad (3.31)$$

In order to define the radius of each node in the semi-spherical thermal network, it was calculated considering the same volume of ground in the semi-sphere than in the annulus region, as described in equation (3.32):

$$\frac{4/3\pi(r_{j,e}^3 - r_{i,e}^3)}{2} = \frac{\pi}{4}(D_j^2 - D_i^2)dz \quad (3.32)$$

where $r_{j,e}$ and $r_{i,e}$ represent the semi-spherical radius of the node T_j and the node T_i , respectively, and D_j and D_i correspond to the diameters defining each region ($D_{eo}, D_b, D_{gp1}, D_{gp2}, D_{ug}$).

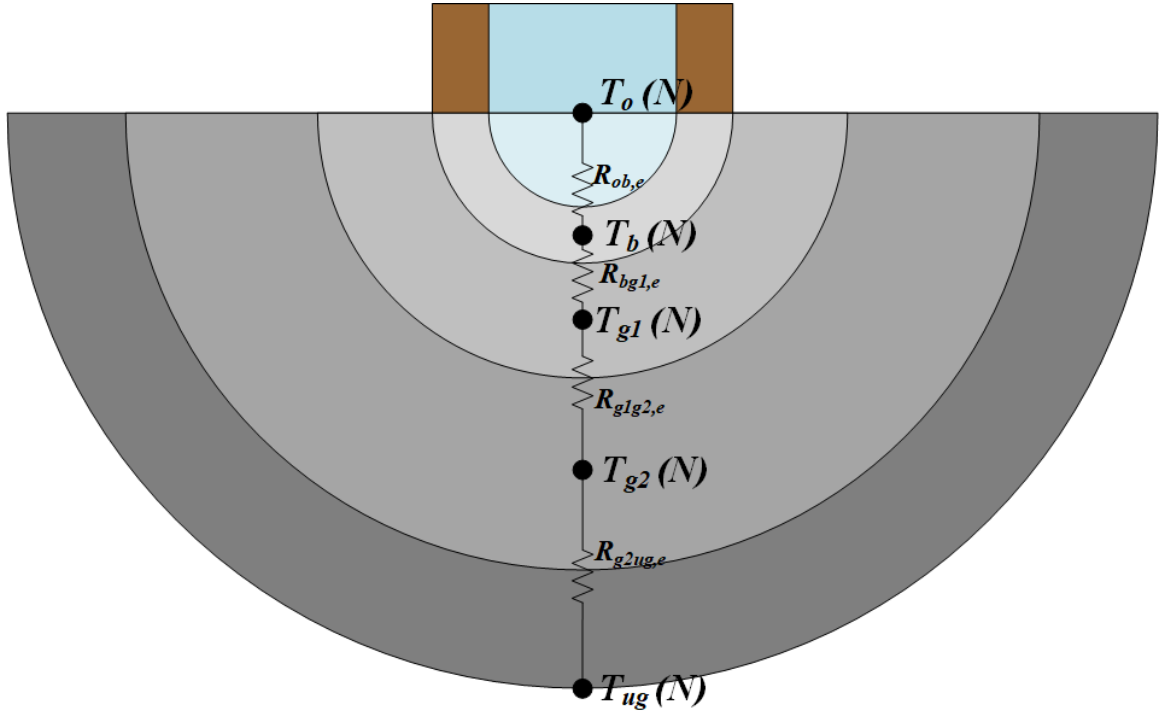


Figure 3.5. Semi-spherical thermal resistances at the bottom of the borehole

3.3.2 Numerical resolution

The energy balance equations (3.6)-(3.10) can be implemented in any simulation software once the parameters have been calculated. In order to solve the system, it is necessary to solve the equations numerically. In this work, the Lax-Wendroff method [129] has been used, and it is solved analogously to the U-tube configuration B2G model [130]. With this method, the temperatures of each node of the thermal network are calculated at a certain time ($t+1$), considering the temperature values at the previous instant (t), for each vertical section of the borehole (j), according to the equations (3.33)-(3.37). Where $j=1$

represents the surface of the borehole and $j=N$ represents the bottom of the borehole. The temperature of the fluid nodes at time $(t + 1)$ and at the vertical section j is calculated depending on the temperature at the previous instant t , in the same vertical section j , and the previous and following section $(j - 1)$ and $(j + 1)$, respectively. The grout and ground node temperatures are calculated considering the temperature value at the previous instant of the same node and the radial and vertical adjacent nodes.

$$T_i^{t+1}(j) = T_i^t(j) + \frac{\Delta t v_i}{2 dz} \left((T_i^t(j+1) - T_i^t(j-1)) + \frac{\Delta t v_i}{dz} (T_i^t(j+1) - 2 T_i^t(j) + T_i^t(j-1)) \right) - \frac{\Delta t}{C_i} \left(\frac{T_i^t(j) - T_o^t(j)}{R_{io}} \right) \quad (3.33)$$

$$T_o^{t+1}(j) = T_o^t(j) - \frac{\Delta t v_o}{2 dz} \left((T_o^t(j+1) - T_o^t(j-1)) - \frac{\Delta t v_o}{dz} (T_o^t(j+1) - 2 T_o^t(j) + T_o^t(j-1)) \right) - \frac{\Delta t}{C_o} \left(\frac{T_o^t(j) - T_i^t(j)}{R_{io}} + \frac{T_o^t(j) - T_b^t(j)}{R_{ob}} \right) \quad (3.34)$$

$$T_b^{t+1}(j) = T_b^t(j) + \frac{\Delta t}{C_b} \left(\frac{T_o^t(j) - T_b^t(j)}{R_{ob}} + \frac{T_{g1}^t(j) - T_b^t(j)}{R_{bg1}} + \frac{T_b^t(j-1) - T_b^t(j)}{R_{vb}} + \frac{T_b^t(j+1) - T_b^t(j)}{R_{vb}} \right) \quad (3.35)$$

$$T_{g1}^{t+1}(j) = T_{g1}^t(j) + \frac{\Delta t}{C_{g1}} \left(\frac{T_b^t(j) - T_{g1}^t(j)}{R_{bg1}} + \frac{T_{g2}^t(j) - T_{g1}^t(j)}{R_{g1g2}} + \frac{T_{g1}^t(j-1) - T_{g1}^t(j)}{R_{vg1}} + \frac{T_{g1}^t(j+1) - T_{g1}^t(j)}{R_{vg1}} \right) \quad (3.36)$$

$$T_{g2}^{t+1}(j) = T_{g2}^t(j) + \frac{\Delta t}{C_{g2}} \left(\frac{T_{g1}^t(j) - T_{g2}^t(j)}{R_{g1g2}} + \frac{T_{ug} - T_{g2}^t(j)}{R_{g2ug}} + \frac{T_{g2}^t(j-1) - T_{g2}^t(j)}{R_{vg2}} + \frac{T_{g2}^t(j+1) - T_{g2}^t(j)}{R_{vg2}} \right) \quad (3.37)$$

In these equations, Δt represents the time-step used for the calculations. This value should be lower than the maximum fixed by the Courant-Friedrichs-Lewy (CFL) condition. This condition should be fulfilled in order to assure that the fluid displacement in the time-step is lower than the distance between nodes, according to the equation (3.38), where dz represents the vertical division length and v the fluid velocity inside the pipe.

$$\frac{\Delta t}{\Delta t_{MAX}} = CFL \leq 1; \quad \Delta t_{MAX} = \frac{dz}{v} \quad (3.38)$$

Therefore, if the time-step of the simulation is greater than the maximum value Δt_{MAX} , the internal time-step in the BHE model (Δt) will be subdivided into smaller time-steps that satisfy the CFL condition. For this purpose a maximum value of $CFL = 0.99$ is fixed, assuring a small error margin, and the minimum Δt_{MAX} is calculated, considering the velocity of the fluid in the inner pipe (v_i) and in the outer pipe (v_o). Then, the internal time-step is calculated as expressed in the equation (3.39):

$$\Delta t = 0.99 \cdot \min\left(\frac{dz}{v_i}, \frac{dz}{v_o}\right) \quad (3.39)$$

3.3.3 Pressure loss calculation

The pressure losses through the Borehole Heat Exchanger are calculated considering it as a standard coaxial BHE. The pressure losses are calculated using the Darcy friction factor (f), the length of the BHE (L), the velocity of the fluid (v), its density (ρ) and the equivalent diameter (D_{eq}) of the pipe channel according to the equation (3.40).

$$\Delta P = \frac{f \cdot L \cdot v^2 \cdot \rho}{2 \cdot D_{eq}} \quad (3.40)$$

For the inner pipe, the equivalent diameter is the inner diameter of the inner pipe ($D_{eq} = D_{ci}$). On the other hand, for the outer pipe, the equivalent diameter is calculated using the hydraulic diameter ($D_{eq} = D_{ei} - D_{co}$).

The correlation used to calculate the Darcy friction factor (f) is the Churchill correlation, valid for both laminar and turbulent regime, as well as for the transition zone [131] is described in the equations (3.41)-(3.43).

$$f = 8 \left[\left(\frac{8}{Re} \right)^{12} + \frac{1}{(A+B)^{1.5}} \right]^{1/12} \quad (3.41)$$

$$A = \left[2.457 \ln \left(\frac{1}{\left(\frac{7}{Re} \right)^{0.9} + 0.27 \frac{\varepsilon}{D_{eq}}} \right) \right]^{16} \quad (3.42)$$

$$B = \left(\frac{37530}{Re} \right)^{16} \quad (3.43)$$

where the roughness of the pipe is represented by ε .

Regarding the outer pipe, in the calculation of the friction factor for an annular section, a correction factor is applied with the non-dimensional parameter ζ [132], as shown in the equation (3.44).

$$\zeta = \frac{(a-b)^2(a^2-b^2)}{a^4-b^4-(a^2-b^2)^2/\ln(a/b)} \quad (3.44)$$

where $a = D_{ei}/2$ and $b = D_{co}/2$. Therefore, the equivalent diameter D_{eq} must be substituted by the effective diameter, $D_{ef} = (D_{ei} - D_{co})/\zeta$, and the Reynolds number Re must be substituted by an effective Reynolds number Re_{ef} [132], according to the equation (3.45).

$$Re_{ef} = \frac{1}{\zeta} Re_{D_h} \quad (3.45)$$

where Re_{D_h} is the Reynolds number calculated for the hydraulic diameter. Therefore, the effective diameter and Reynolds number will be used in equations (3.41)-(3.43) in the calculation of the outer pipe friction factor.

3.4 Optimal location of the ground nodes

Regarding the thermal response of the ground and the amount of soil that is affected by the heat injection during a specific time period, it is usually addressed by adding a number of radial ground nodes and discretizing the soil mass in small radial steps until the far-field radius, where the effect of the heat injection vanishes. This far-field radius calculation has been addressed by several authors, from a physical or mathematical point of view, for example, Hart and Couvillion [65] defined a hypothetical far-field radius as $r_\infty = 4\sqrt{\alpha t}$, which depends on the ground thermal diffusivity (α) and the injection period (t). The addition of ground nodes inevitably leads to an increase in the complexity of the model and therefore, an increase in the computational cost. Therefore, only three ground nodes are used in the coaxial B2G model in order to model the affected surrounding ground. In this context, the location of the ground nodes position is key in order to accurately reproduce the thermal behaviour of the surrounding ground affected by the heat exchange with the BHE.

The position of the three ground nodes is defined by three penetration radii: R_{gp1} for the first ground node (short-term), R_{gp2} for the second ground node (mid-term) and R_{ug} for the undisturbed ground node. The calculation of these penetration radii is not straightforward, as they will influence in the calculation of the ground temperature and thus, in the fluid temperature calculation. For example, for the first ground node, the higher the value of the penetration radius, the greater the amount of ground that the model will consider, and as a consequence, the greater will be the heat capacity of this ground section. In the case of a greater heat capacity, the temperature of this node will vary more slowly, and it will have an influence on the short-term evolution of the water temperature. Analogously, the same will occur with the second ground node. However, the position of the undisturbed ground node will only have an influence in the heat transfer between the second ground node and the undisturbed ground node (increasing or decreasing the thermal resistance), as it only represents a temperature boundary, with no temperature variation.

The optimal position of the three ground nodes will depend on the thermo-physical properties of the ground (effective thermal conductivity and capacity), the operating conditions (heat injection period in a day) and the borehole geometry (borehole diameter), according to the equation (3.46). In the determination of the effective thermal conductivity and capacity the weighted average of the different layers has been calculated in the case of

a layered ground with different materials; in the case of groundwater flow, an increased thermal conductivity would be considered to account for this effect.

$$R_{gp1}, R_{gp2}, R_{ug} = f(k_g, c_g, t, D_b) \quad (3.46)$$

In the B2G model thermal network, the ground nodes position was defined by the penetration diameters. These diameters are defined by the penetration radii, as it is presented in the equation (3.47).

$$D_{gp1} = 2 \cdot R_{gp1} ; \quad D_{gp2} = 2 \cdot R_{gp2} ; \quad D_{ug} = 2 \cdot R_{ug} \quad (3.47)$$

3.4.1 Methodology

In order to calculate the optimal location of the ground nodes that reproduces with the highest possible accuracy the temperature variation of the ground nodes and the heat transfer along the ground, a new methodology is proposed and described in [125]. It consists in comparing the B2G model with the Infinite Cylindrical Source (ICS) model, trying to minimize the difference between the results of the two models when calculating the temperature of the first and second ground nodes.

In this comparison, a constant heat flux on the borehole wall during all the heat injection period is assumed, and the ground temperature variation is calculated for the ground nodes position and the heat transfer rate between them, for each time step. The ground nodes position (penetration radii R_{gp1} , R_{gp2} and R_{ug} ; corresponding to the ground nodes T_{g1} , T_{g2} and T_{ug} , respectively) will be optimized, so the difference between the results calculated by the two models is minimum.

For this purpose, the B2G thermal network has been adapted in order to consider a constant heat flux on the borehole wall instead of the fluid through the BHE tubes. Therefore, a node on this surface is considered (T_b), and a constant heat flux (q_0) is imposed. Figure 3.6 shows the thermal network corresponding to this problem. The ground nodes T_{g1} and T_{g2} are located, each one, at the average distance between the two concentric circumferences that form each annulus region. These positions are defined by the radii r_{g1} and r_{g2} , respectively, according to the equation (3.48).

$$r_{g1} = \frac{R_{gp1} + r_b}{2} ; \quad r_{g2} = \frac{R_{gp2} + R_{gp1}}{2} \quad (3.48)$$

where r_b represents the borehole wall radius. On the other hand, q_1 represents the heat transfer between the ground nodes T_{g1} and T_{g2} , while q_2 represents the heat transfer between T_{g2} and T_{ug} .

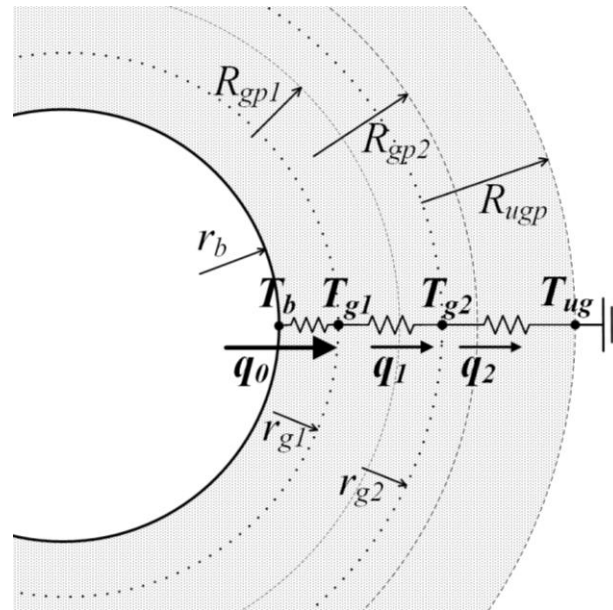


Figure 3.6. Thermal network used for the calculation of the penetration radii

The main parameters used in the models are the borehole radius (r_b), the ground thermal conductivity (λ), the ground volumetric heat capacity (c_v) and the heat flux (q_0). The main inputs are the three penetration radii (R_{gp1} , R_{gp2} and R_{ug}). The initial ground temperature is assumed to be zero, as only the temperature variation is calculated.

An optimization algorithm implemented in MATLAB® is used to find the optimal position of the three ground nodes that minimizes the difference between the B2G and the ICS models. Finally, in order to make the use of the B2G more general, polynomial correlations will be calculated to define these ground nodes positions and implemented inside the TRNSYS B2G model, so the position of the ground nodes can be calculated internally depending on the soil thermal properties, the BHE geometry and the system operating conditions. This way, the use of the B2G model can be extended to any BHE configuration, type of soil and operating conditions (total equivalent daily operating hours), enhancing its widespread use, as the user only needs to introduce these parameters as inputs to the TRNSYS type instead of estimating the ground penetration diameters. Furthermore, this methodology can be implemented for the U-tube B2G model, as the penetration diameters are calculated considering the heat injection on the borehole wall.

It is important to stress that the calculation of the ground nodes positions is not based on a physical calculation (especially the undisturbed ground node), but it is based on a mathematical calculation, comparing the results obtained by the B2G model with the ICS model for different positions of the ground nodes, choosing the positions in which the difference between the two models is minimal and defining these positions as the optimal. In any case, it is not intended to model in detail the ground behaviour, but to calculate its temperature in the portion closer to the BHE, which has a greater influence in the dynamic evolution of the fluid temperature inside the BHE, which is the final goal of the B2G model.

3.4.1.1 B2G model

In the B2G model, the temperature of the ground nodes T_{g1} and T_{g2} is calculated using the main BHE parameters and penetration radii. First, the thermal capacitances (C) of the two ground nodes are calculated according to equation (3.49), together with the UA values, which represent the thermal resistance between ground nodes, as shown in equation (3.50).

$$C_{g1} = \pi (R_{gp1}^2 - r_b^2) c_v \quad ; \quad C_{g2} = \pi (R_{gp2}^2 - R_{gp1}^2) c_v \quad (3.49)$$

$$UA_{bg1} = \frac{2 \pi \lambda}{\ln(r_{g1}/r_b)} \quad ; \quad UA_{g1g2} = \frac{2 \pi \lambda}{\ln(r_{g2}/r_{g1})} \quad ; \quad UA_{g2ug} = \frac{2 \pi \lambda}{\ln(R_{ug}/r_{g2})} \quad (3.50)$$

Second, the ground nodes temperatures (T_{g1} and T_{g2}) are calculated using the energy balance equations. The undisturbed ground temperature is defined as zero ($T_{ug} = 0$).

$$C_{g1} \frac{\partial T_{g1}(t)}{\partial t} = q_0 + UA_{g1g2} (T_{g2}(t) - T_{g1}(t)) \quad (3.51)$$

$$C_{g2} \frac{\partial T_{g2}(t)}{\partial t} = UA_{g1g2} (T_{g1}(t) - T_{g2}(t)) + UA_{g2ug} (T_{ug}(t) - T_{g2}(t)) \quad (3.52)$$

Finally, the heat transfer rate between ground nodes is calculated (q_1 and q_2) using the equations (3.53) and (3.54).

$$q_1^{B2G}(t) = UA_{g1g2} (T_{g1}^{B2G}(t) - T_{g2}^{B2G}(t)) \quad (3.53)$$

$$q_2^{B2G}(t) = UA_{g2ug} (T_{g2}^{B2G}(t) - T_{ug}^{B2G}(t)) \quad (3.54)$$

3.4.1.2 Infinite Cylindrical Source model

The Infinite Cylindrical Source (ICS) model calculates the heat transfer in the region bounded internally by a hollow circular cylinder and constant heat flux in its surface. In this case, the internal circular cylinder would correspond to the BHE, with radius r_b , and the constant heat flux through its surface would be q_0 . The solution for the calculation of the ground temperature along the radial distance was provided by Carslaw and Jaeger [58] and described in section 3.1.1. This solution is presented in equation (3.55), where the initial ground temperature is zero, and α represents the thermal diffusivity of the ground ($\alpha = \lambda/c_v$).

$$T^{ICS}(r, t) = -\frac{q_0}{\pi^2 r_b \lambda} \int_0^\infty (1 - e^{-\alpha u^2 t}) \frac{J_0(ur) Y_1(ur_b) - Y_0(ur) J_1(ur_b)}{u^2 [J_1^2(ur_b) + Y_1^2(ur_b)]} du \quad (3.55)$$

Therefore, the temperature in the ground nodes will be calculated by the equation (3.56).

$$T_{g1}^{ICS}(t) = T^{ICS}(r_{g1}, t) \quad ; \quad T_{g2}^{ICS}(t) = T^{ICS}(r_{g2}, t) \quad (3.56)$$

Regarding the heat transfer between nodes, it is calculated using the Fourier's law applied in the frontier between the ground nodes (R_{gp1} and R_{gp2}), using the equations (3.57)-(3.58), where Δr represents a very small radial distance.

$$q_1^{ICS}(t) = -2 \pi R_{gp1} \lambda \frac{T_{R_{gp1}}^{ICS}(t) - T_{R_{gp1}+\Delta r}^{ICS}(t)}{\Delta r} \quad (3.57)$$

$$q_2^{ICS}(t) = -2 \pi R_{gp2} \lambda \frac{T_{R_{gp2}}^{ICS}(t) - T_{R_{gp2}+\Delta r}^{ICS}(t)}{\Delta r} \quad (3.58)$$

3.4.2 Calculation of the ground nodes position

Both the B2G and ICS models were implemented in MATLAB®, so it is possible to calculate for each time step the temperature of the ground nodes and the heat transfer rates for a given set of parameters: borehole radius (r_b), ground properties (thermal conductivity, λ and volumetric heat capacity, c_v), heat flux (q_0) and heat injection time (t). The penetration radii (to be optimized) are introduced as inputs in the models: R_{gp1} , R_{gp2} and R_{ug} .

Regarding the infinite integral of the ICS solution, it is resolved numerically in MATLAB®. In order to reduce the computational time, instead of setting ∞ as the endpoint of the interval of integration, it was reduced to 5000, after verifying that the error in the results was negligible.

In order to compare the two models, the Root Mean Square Error (RMSE) is calculated between the results of the B2G and ICS models, considering the results of each time step during the whole heat injection time. However, it is first necessary to define which parameters will be compared in order to calculate the RMSE between the two models: the ground nodes temperature or the heat transfer rates between ground nodes. So, two scenarios were initially considered:

- a) Ground nodes temperature optimization. The temperatures of the first and second ground nodes (T_{g1} and T_{g2} , respectively) are the variables calculated by each model. So, the optimization solver will calculate the set of radii that minimizes the RMSE between these temperatures, calculated by the B2G and the ICS models. The total RMSE is defined as the sum of the RMSEs for each temperature, as shown in the equation (3.59).

$$\Sigma RMSE = \sqrt{\frac{\sum_{i=1}^t (T_{g1,i}^{B2G} - T_{g1,i}^{ICS})^2}{n}} + \sqrt{\frac{\sum_{i=1}^t (T_{g2,i}^{B2G} - T_{g2,i}^{ICS})^2}{n}} \quad (3.59)$$

- b) Heat transfer rates optimization. The heat transfer rates q_1 and q_2 are the variables to calculate. Therefore, the optimization solver finds the penetration radii that

minimize the RMSE between the heat transfer rates calculated by each model. The total RMSE is defined as the sum of the RMSEs for each heat transfer rate, as shown in the equation (3.60).

$$\Sigma RMSE = \sqrt{\frac{\sum_{i=1}^t (q_{1,i}^{B2G} - q_{1,i}^{ICS})^2}{n}} + \sqrt{\frac{\sum_{i=1}^t (q_{2,i}^{B2G} - q_{2,i}^{ICS})^2}{n}} \quad (3.60)$$

In order to find the optimal penetration radii, an optimization algorithm is used. For this study, a pattern search optimization methodology was used, using the solver *patternsearch* already implemented in the Global Optimization Toolbox in MATLAB [133]. In this solver, initial values for the penetration radii are provided, and it will search the values of the radii that minimize the sum of RMSEs ($\Sigma RMSE$), subject to the constraint that each ground node penetration radius must be lower than the next one, according to the equation (3.61).

$$R_{gp1} < R_{gp2} < R_{ug} \quad (3.61)$$

3.4.2.1 First approach: Optimization of temperatures and heat transfer rates for one configuration

First of all, the new methodology was tested for a real BHE, using the two proposed scenarios: ground nodes temperature optimization and heat transfer rates optimization, in order to check which approach was more suitable. So the penetration radii were calculated using the MATLAB optimization algorithm and tested inside the B2G model in the simulation of a Thermal Response Test (TRT) with experimental data. The BHE corresponds to the coaxial helical BHE described in section 2.2.2 and the TRT was carried out in Houten, The Netherlands [46]. The main parameters used in the calculation of the penetration radii in MATLAB are shown in Table 3.1. Additionally, a more detailed description about the TRT, the geometrical characteristics of the BHE and the simulation in TRNSYS with the B2G model can be found in section 3.6.1.

Table 3.1. Main parameters calculation of penetration radii for GEOTHEX BHE

TRT data		Model parameters	
Ground thermal conductivity (λ)	2.13 W/(m·K)	Heat injection period (t)	15 h
Ground volumetric heat capacity (c_v)	2410 kJ/(m ³ ·K)	Time step	3 min
Borehole radius (r_b)	0.044 m	Differential radial distance (Δr)	0.001 m
Average heat flux (q_0)	17.7 W/m	Initial point (x_0) [$R_{gp1,0}$ $R_{gp2,0}$ $R_{ug,0}$]	[0.1 0.2 0.3] m

The penetration radii that were calculated using the new methodology for each scenario were the following:

- Ground nodes temperature optimization: $R_{gp1}=0.163$ m, $R_{gp2}=0.362$ m, $R_{ug}=0.593$ m.
- Heat transfer rate optimization: $R_{gp1}=0.165$ m, $R_{gp2}=0.352$ m, $R_{ug}=0.517$ m.

The two scenarios produce similar results for the first and second penetration radii (R_{gp1} and R_{gp2} , respectively). Regarding the undisturbed ground radius calculated by the temperatures scenario, it takes a greater value than in the heat transfer rates scenario (0.59 m and 0.52 m, respectively). The results obtained by each model are shown in Figure 3.7, for the optimization scenarios of the ground nodes temperatures (a) and the heat transfer rates (b).

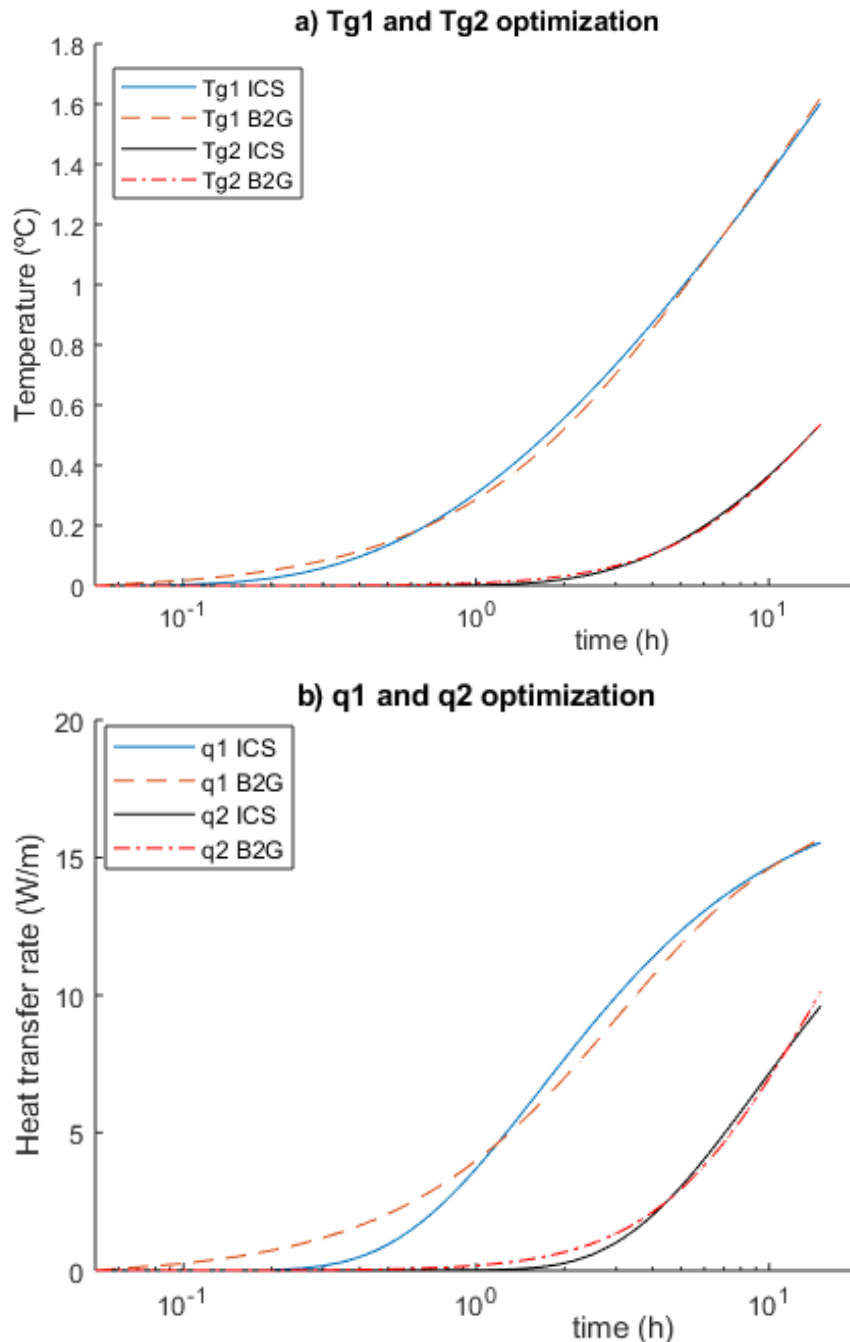
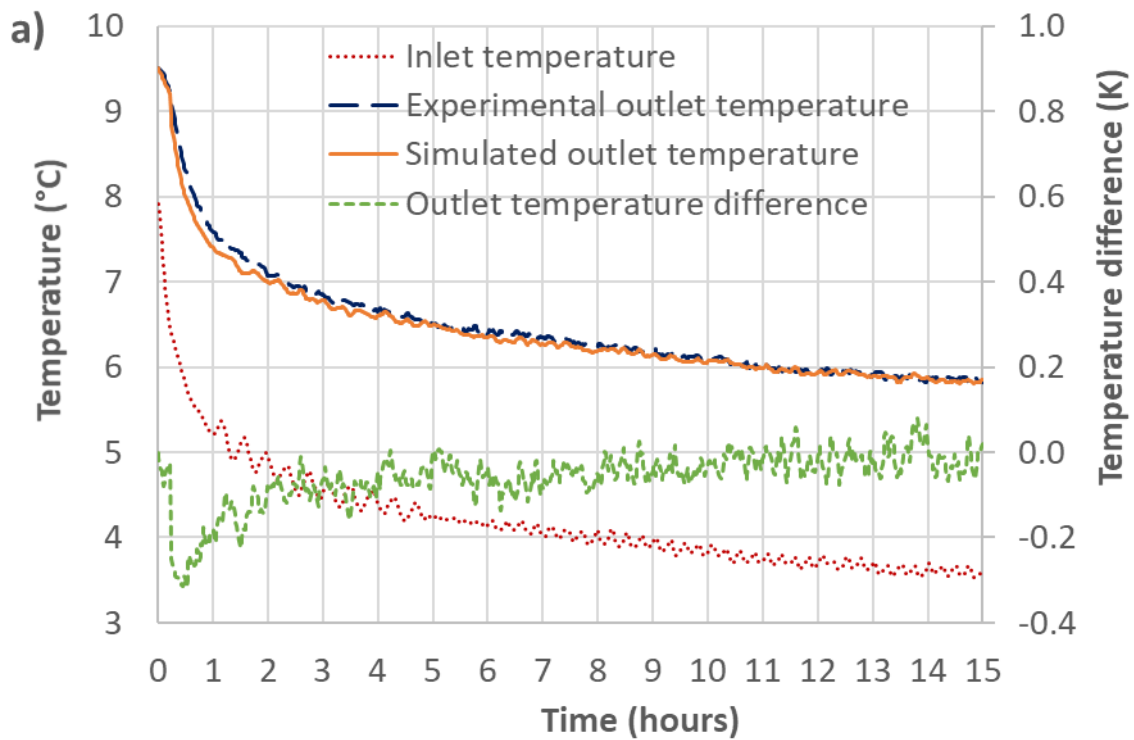


Figure 3.7. Penetration radii: results for GEOTHEX BHE: a) Ground nodes temperature optimization; b) Heat transfer rate optimization

It is possible to see that, for both cases, the results produced by the B2G model are quite similar to the results produced by the ICS model.

Once the penetration radii were calculated, they were tested as inputs in the B2G model in order to check how they influence in the accuracy of the B2G model, when simulating the behaviour of a BHE with experimental data from a TRT. So the inlet mass flow rate and fluid temperature were introduced as inputs in the B2G model and the outlet fluid temperature was simulated, together with the total heat transferred to the ground. Then, the simulated results were compared to the experimental ones by calculating the RMSE of the outlet fluid temperature and the percentage difference of the heat transferred to the ground.

For both optimization approaches, the simulated outlet temperature was quite similar to the experimental one, with a RMSE of 0.088K in the ground temperatures scenario (case a), and 0.087K in the heat transfer rate scenario (case b). Regarding the heat transfer with the ground, the simulated value was a 2.7% lower than the calculated value with experimental results in case a) and 2.5% lower in case b). The results of the simulations and the comparison with the experimental data are shown in Figure 3.8.



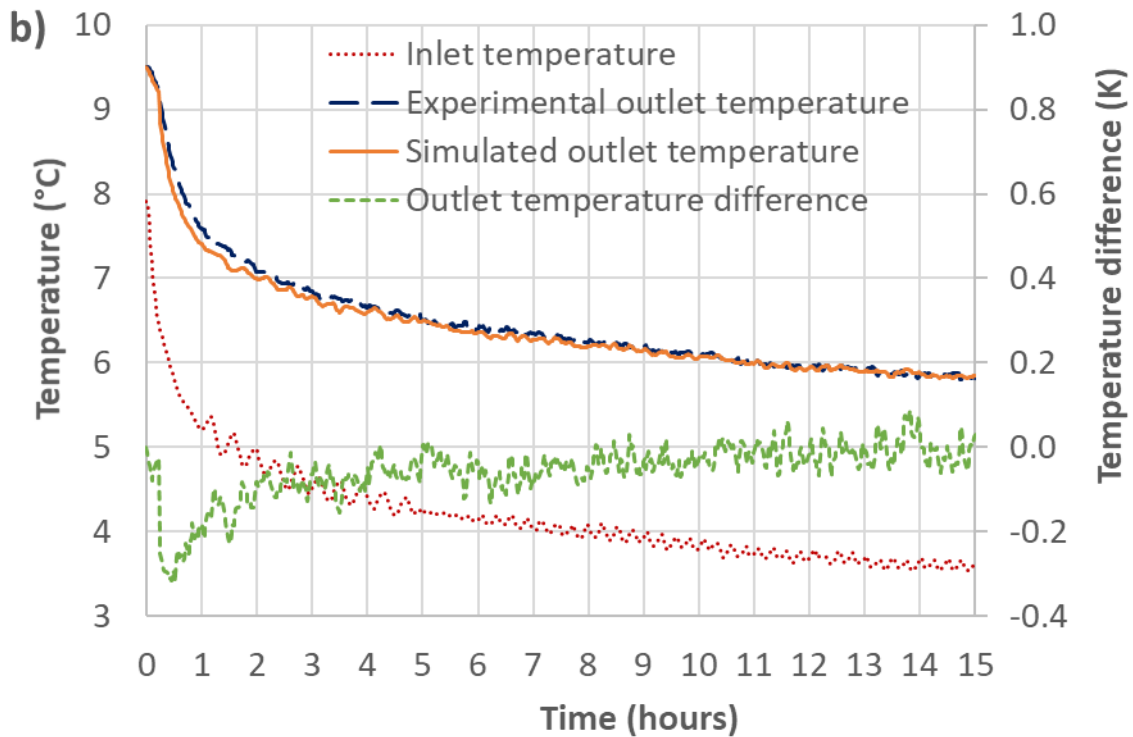


Figure 3.8. Penetration radii: comparison of simulated results for two scenarios: a) Ground nodes temperature optimization; b) Heat transfer rate optimization

Considering the results obtained for the two optimization scenarios, it can be concluded that both produce very similar results when used for simulating the BHE behaviour inside the B2G model. Furthermore, the penetration radii obtained for the two scenarios are quite similar, except for the undisturbed ground node (Table 3.2).

Table 3.2. Penetration radii for the two optimization scenarios

Scenario	R_{gp1} (m)	R_{gp2} (m)	R_{ug} (m)
a) Temperatures	0.163	0.362	0.593
b) Heat transfer	0.165	0.352	0.517

3.4.2.2 Penetration radii correlations

The proposed methodology implies long computational times for each set of variables. So, in order to facilitate this calculation for any type of soil, BHE and system operating conditions, a parametric calculation was carried out for a wide range of values of the different variables in order to obtain a polynomial correlation, easy to handle, to be implemented inside the B2G model. Therefore, it can automatically calculate the ground nodes position, introducing the values of the influencing variables as inputs. The values that were used for the parametric study are shown in Table 3.3.

Table 3.3. Parameters values to calculate the penetration radii correlations

Parameter	Values	Units
Ground thermal conductivity (λ)	[1 2 3 4]	$W/(m \cdot K)$
Ground volumetric heat capacity (c_v)	[1000 2000 3000 4000]	$kJ/(m^3 \cdot K)$

Parameter	Values	Units
Borehole radius (r_b)	[0.03 0.05 0.07 0.09]	m
Heat injection time during one day (t)	[6 12 18 24]	h

It should be mentioned that the calculation of the ground nodes position was carried out with different values of heat flux, q_0 (15, 30 and 90 W/m), producing the same optimal position of the ground nodes. Therefore, it can be concluded that this position is independent of the heat injected, but only depends on the parameters mentioned above. As a consequence, this optimal position will be valid when used inside the B2G model for a variable heat load in the BHE, also along the borehole depth. So it can be used for the modelling of a whole ground source heat pump system, where the heat load into the ground will vary.

A combination of all the values was used as inputs to the MATLAB® optimization method, with a time step of 1 minute. Several studies were carried out in order to find an accurate expression to correlate the different parameters in a single equation for each penetration radius, using both scenarios (temperatures and heat transfer rates optimizations) and different initial points in the algorithm ([0.1 0.2 0.3] m and [0.3 0.6 0.8] m). It was found that an expression that fitted with a good accuracy the calculated points is one correlating each penetration radius divided by the borehole radius as a function of the Fourier number (using the borehole radius as the representative length), as shown in the equations (3.62) - (3.65).

$$\frac{R_{gp1}}{r_b} = A_1 + B_1 \cdot Fo_b^{C_1} \quad (3.62)$$

$$\frac{R_{gp2}}{r_b} = A_2 + B_2 \cdot Fo_b^{C_2} \quad (3.63)$$

$$\frac{R_{ug}}{r_b} = A_{ug} + B_{ug} \cdot Fo_b^{C_{ug}} \quad (3.64)$$

$$Fo_b = \frac{\alpha \cdot t}{r_b^2} \quad (3.65)$$

where A_i, B_i, C_i are constants to be calculated, α is the ground thermal diffusivity, t is the heat injection time and r_b is the borehole radius.

After carrying out the parametric studies with the different scenarios and initial points, considering the results of the section 3.4.2.1, in which it is shown that both the temperatures and heat transfer rates approaches produce very accurate results (RMSE<0.1K), together with the fact that the heat transfer rates are calculated from the temperature of the ground nodes and the fact that the B2G model uses the ground nodes temperature to calculate the heat transfer to the ground and not in the other way; it was decided that the final correlations will be calculated using the ground node temperatures optimization. However,

a previous correlation using the heat transfer optimization was calculated in order to set the initial points for the calculation of the final correlation.

For these calculations, the values of the different parameters shown in Table 3.3 are used, considering a time step (Δt) of 1 minute and a differential radial distance (Δr) of 0.001 m for the heat transfer calculation. Regarding the initial point used in the optimization algorithm, a preliminary correlation was obtained based on the heat transfer optimization, it was later used in order to set an approximate starting point for the algorithm to find the optimal value. This approximation allows to provide different initial points for the different combination of variables, closer to the global optimum, rather than using a constant starting point for all the values of the parameters. For example, increasing the heat injection time will lead to higher penetration radii, so a very low value of the initial point could mean that the algorithm finds a local optimal value lower than the optimum expected. Therefore, for a higher heat injection time, it will be convenient to provide a higher initial point, rather than a constant initial point for all the injection times. The coefficients of the preliminary correlation used as initial point are shown in Table 3.4, applied in the equations (3.62)-(3.65), and the results of the preliminary correlation are shown in Figure 3.9. It is shown that some scattered points were obtained, this is one of the reasons why setting a fixed initial point could result in finding local optimum points far from the tendency calculated with the rest. These preliminary correlations were used to set the initial points in the optimization algorithm in MATLAB for the calculation of the final correlation with the ground nodes temperatures optimization.

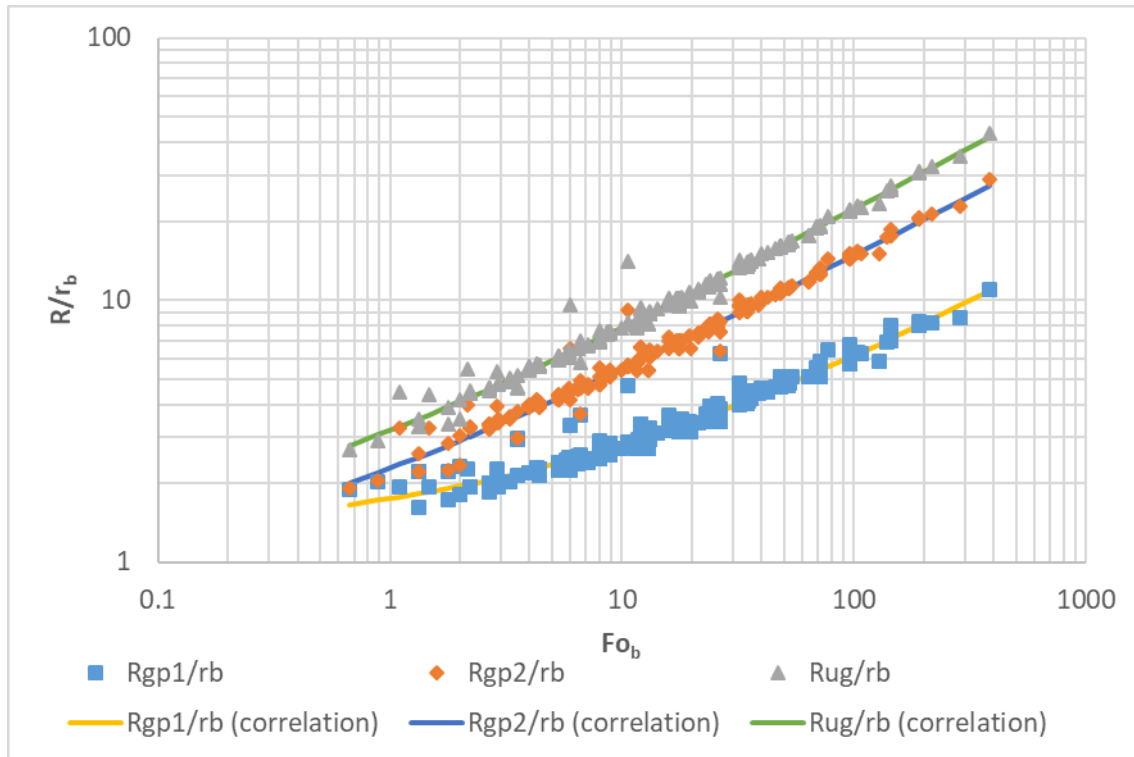


Figure 3.9. Preliminary correlation calculated with the heat transfer optimization

Table 3.4. Coefficients of the preliminary correlation used as initial point (x_0)

	R_{gp1}	R_{gp2}	R_{ug}
A_i	1.268325	0.663032	0.922542
B_i	0.482196	1.621079	2.265936
C_i	0.502414	0.470611	0.487034

The results of the final parametric study using the scenario of the ground nodes temperature optimization are shown in Figure 3.10 (plotted markers), together with the values obtained with the final correlations (plotted in solid lines). The coefficients of these correlations are shown in Table 3.5.

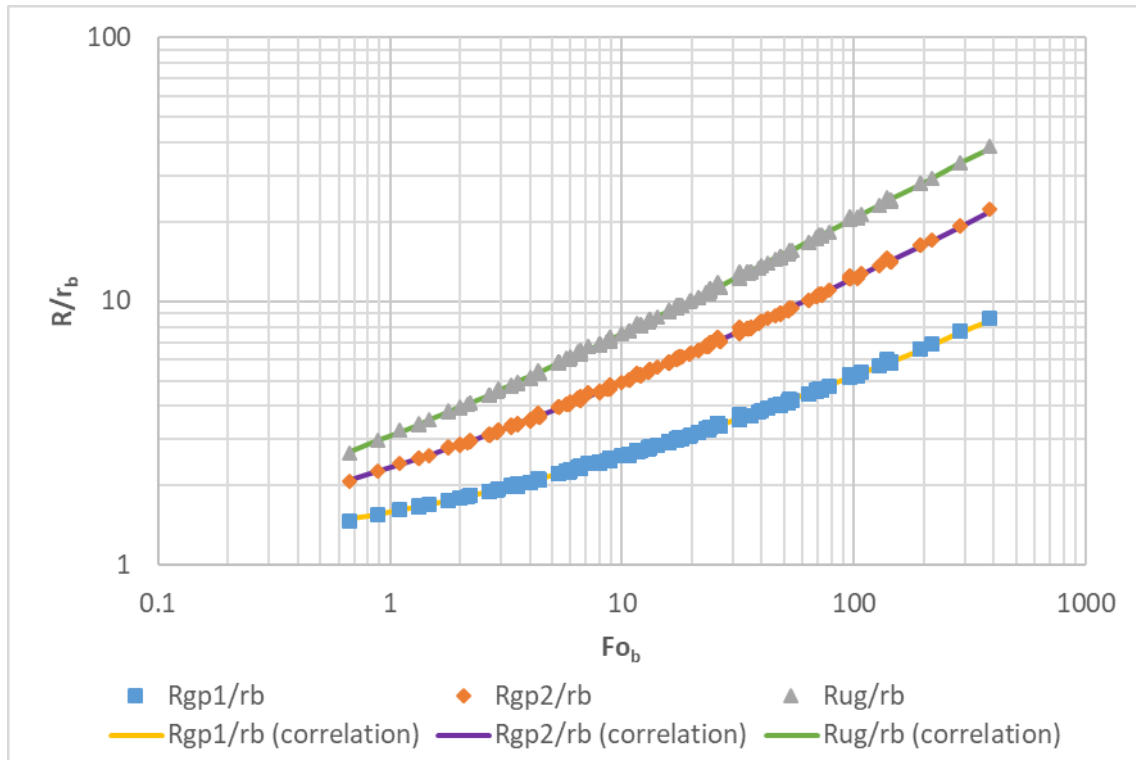


Figure 3.10. Comparison between the penetration radii correlations and calculated points

Table 3.5. Calculated coefficients for the final penetration radii correlations

	R_{gp1}	R_{gp2}	R_{ug}
A_i	0.976794	0.926305	0.767003
B_i	0.611236	1.416714	2.312549
C_i	0.420103	0.451364	0.466674

Figure 3.10 shows that the correlations fit with a good accuracy the calculated points, the RMSE for each of the penetration radii correlation was calculated, comparing the values of the 256 points calculated by the optimization algorithm with the values calculated with each correlation, obtaining a RMSE of 0.0017 m for R_{gp1} , 0.0049 m for R_{gp2} and 0.0077 m

for R_{ug} . So the correlations calculate with a good accuracy the penetration radii and are fitted to be used inside the B2G model.

The correlations were implemented inside the B2G model in order to automatically calculate the penetration radii in order to locate the ground nodes. The suitability of these correlations will be proved in section 3.6, where the whole B2G model will be validated with experimental results for different BHEs and operating conditions.

3.5 Coaxial B2G model implementation in TRNSYS

The coaxial B2G model presented in the previous section was implemented as a new TRNSYS type. It was written in FORTRAN language for the TRNSYS 16 version. Its code is shown in the appendix A.

The TRNSYS type is a black box model in which several parameters are defined, several inputs are introduced and it will calculate the outputs. Inside a whole GSHP system model, the different inputs would be introduced in the type from another types in the TRNSYS project (normally a pipe component) and the outputs would be introduced in another type as inputs (normally another pipe). In Figure 3.11, a layout in TRNSYS is shown in which a TRT test is simulated from experimental data and the error between the model and the experimental data is calculated.

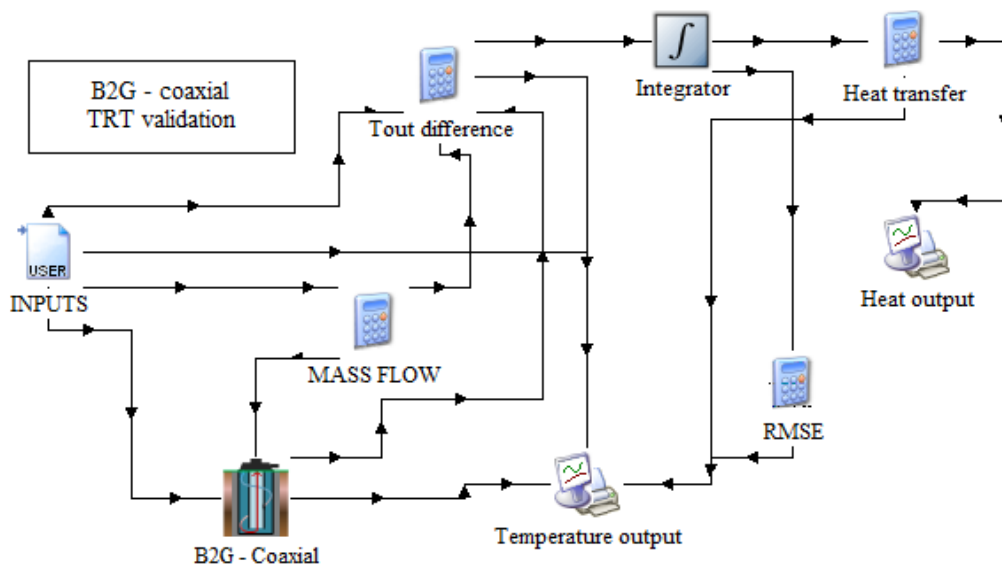


Figure 3.11. Schematics of the model layout on the TRNSYS visual platform

The main parameters that are needed to be introduced in the type are the geometrical characteristics of the BHE, the number of vertical nodes in the model, number of helical ribs and their angle (no ribs for standard coaxial BHE configuration), the type of heat carrier fluid and the roughness of the pipes.

The main inputs to be introduced in the model are the inlet temperature and mass flow rate, the sense of the flow (downwards through the outer pipe and upwards through the inner or the opposite) and the inputs needed for the calculation of the penetration radii:

effective thermal conductivity and volumetric heat capacity along the BHE and expected heat injection time during one day.

Regarding the thermal properties of the grout and ground (thermal conductivity and volumetric heat capacity), they are introduced in the model as an external text file as a function of the depth.

The main outputs simulated by the model are the outlet fluid temperature and mass flow rate (same mass flow rate as the inlet), the pressure losses in each pipe, the heat extracted/injected from/to the fluid and the average temperature of the grout and ground nodes along the depth. The model will also produce an external file with all the vertical temperature profiles of every node in the thermal network for each time step.

A list with all the parameters, inputs and outputs of the B2G coaxial model can be found in Annex A.

3.6 Experimental validation of the coaxial B2G dynamic model under different operating conditions

The B2G coaxial model has been validated against experimental data for different BHE configurations and different operating conditions with several simulations in TRNSYS. First of all, a prototype of the coaxial helical BHE, developed by GEOTHEX before the start of the GEOTeCH project, was used in order to validate the coaxial helical B2G model with experimental data from a TRT carried out in Houten (The Netherlands). After this, due to a delay in the manufacturing process of the coaxial helical BHE, it was not possible to install it in the Tribano demo-site, where standard coaxial BHE were installed instead. This is why data from standard coaxial BHEs were used in order to validate the B2G coaxial model for different geometries and conditions. It should be mentioned that the main differences between the standard and the helical coaxial BHE are the helical path through the outer pipe instead of the straight path and, in some BHE configurations, the existence of a gap between the spiral rib and the outer pipe wall that might generate a higher local turbulence, as detailed in section 2.2.2. So, a second validation was carried out using a standard coaxial BHE with no grout installed at the Royal Institute of Technology (KTH), in Stockholm (Sweden), with experimental data from a TRT. A third validation was carried out using the data from the BHE field of the Tribano demo-site described in section 2.3.3. So the B2G coaxial model was validated under normal operating conditions with the monitored data from one of the coaxial BHEs for different days.

In order to validate the model with the experimental data, the BHE and ground characteristics are specified in the B2G model and the inlet temperature and mass flow rate are introduced as inputs in the model. Then the model will simulate the outlet temperature and it is compared with the experimental results. The RMSE between the simulated and experimental outlet temperature is calculated according to the equation (3.66) and the heat transfer in the fluid is calculated, according to the equation (3.67), and compared for the experimental and simulated results.

$$RMSE = \sqrt{\frac{\sum_{t=1}^n (T_{B2G,t} - T_{experimental,t})^2}{n}} \quad (3.66)$$

$$Q (J) = \int \dot{m} C_p (T_{out} - T_{in}) dt \quad (3.67)$$

For the short-term validation of the BHE with TRTs data (sections 3.6.1 and 3.6.2.1), a heat injection interval of 15 hours was chosen, as it is a common operation time for an ON/OFF GSHP system during a day and this model is intended to predict the dynamic behaviour of the BHE during one operational day. Furthermore, a validation with an extended heat injection period was carried out (section 3.6.2.2) as well as the validation of whole days operation inside a heat pump system (section 3.6.3). The simulations were carried out in a computer with a processor Intel Core i7-7700 CPU @ 3.6 GHz and 8 GB of RAM, a simulation time step of 1 minute was used in all the simulations and the computational time will be analysed.

3.6.1 TRT coaxial helical BHE

The new coaxial helical BHE developed inside the framework of the GEOTeCH project was used in order to validate the B2G coaxial helical model with experimental data. A TRT carried out with a prototype manufactured before the start of the project was used, due to the lack of other tests with the new configuration. The TRT was carried out at the GEOTHEX BV installations, in Houten (The Netherlands) [46].

The BHE configuration was described in section 2.2.2. It consists of a coaxial BHE with insulated inner pipe and helical path through the outer channel. For this purpose, a rib is attached on the outer wall of the inner tube in order to create a helical path for the fluid to flow through the outer channel. The inner pipe is made of a foamed PE material with a thermal conductivity of 0.2 W/(m·K). The grout that fills the space between the outer pipe and the borehole wall is a mix of Thermocem and water with a thermal conductivity of around 1.56 W/(m·K). The heat carrier fluid used is a mixture of water and MPG (mono propylene glycol) with a 20% of MPG.

The main thermo-physical properties of the ground and the geometrical characteristics of the BHE are shown in Table 3.6. There is only one rib with an angle of 85.7° (see Figure 3.4 for the definition of this angle).

Table 3.6. Main parameters of the BHE

Thermo-physical properties		Geometrical characteristics	
Inner pipe conductivity	0.20 W/(m·K)	Length	44.43 m
Outer pipe conductivity	0.42 W/(m·K)	Borehole diameter	0.088 m
Ground thermal conductivity	2.13 W/(m·K)	Inner diameter of the inner pipe	0.0285 m
Grout thermal conductivity	1.56 W/(m·K)	Outer diameter of the inner pipe	0.0445 m

Thermo-physical properties		Geometrical characteristics	
Ground volumetric thermal capacitance	2410 kJ/(m ³ ·K)	Inner diameter of the outer pipe	0.057 m
Grout volumetric thermal capacitance	3500 kJ/(m ³ ·K)	Outer diameter of the outer pipe	0.063 m
Percentage of propylene-glycol in the fluid	20 %	Angle of the helical rib	85.7 °

In the TRT, the initial undisturbed ground temperature was around 9.5°C and the heat injection period was around 15 hours. The inlet temperature and mass flow rate monitored during the TRT are introduced in the model in time intervals of 1 minute (the same interval as the simulation time step considered). Then, the model calculates the outlet temperature, as well as the amount of heat transferred to the surrounding ground. During the whole test, the fluid mass flow rate flow was kept around 320 kg/h and the heat injection, around 800 W. The fluid temperature was measured with PT100 sensors with a 95% confidence interval of $\pm 0.055\text{K}$, while the error of the flow meter was $< 0.2\%$ [46].

The values shown in Table 3.6 are introduced as parameters in the BHE model, as well as the number of vertical nodes, in this case it was 150. Regarding the ground penetration diameters, they were automatically calculated with the correlations calculated in the section 3.4.2.2. The penetration diameter for the first ground node is 0.29 m, for the second ground node is 0.61 m and 0.98 m for the undisturbed ground node.

Furthermore, as was mentioned in section 2.2.2, a gap exists between the spiral rib and the wall of the outer pipe through which the fluid could flow. The part of the fluid that flows through the gap may generate a local higher turbulence, increasing the convective heat transfer coefficient from the fluid in the outer pipe to the grout/ground. In order to analyse the influence of this gap, two scenarios were studied:

- a) Without gap flow: the fluid flows in its totality following the spiral path
- b) With gap flow: part of the fluid flows through the gap between the spiral rib and the outer pipe wall, so the convective heat transfer from the outer pipe fluid to the grout is increased due to the turbulence generated by this rib.

In order to take into account this phenomenon, an enhancement factor in the convective heat transfer coefficient between the outer pipe and the grout is considered, while the convective heat transfer coefficient between the outer pipe and the inner pipe is not modified.

The enhancement factor was experimentally adjusted to a value of 1.25 (an increase of 25% in this coefficient).

The results of simulating the TRT in TRNSYS with the B2G model and the comparison with the experimental measurements is shown in Figure 3.12 for both cases: a) with an enhancement factor of 1 (no gap flow) and b) with an enhancement factor of 1.25, considering the enhanced heat transfer due to the turbulence created by the gap flow. It is

plotted the experimental inlet and outlet temperature, the outlet temperature calculated by the model and the difference between the experimental and calculated outlet temperature.

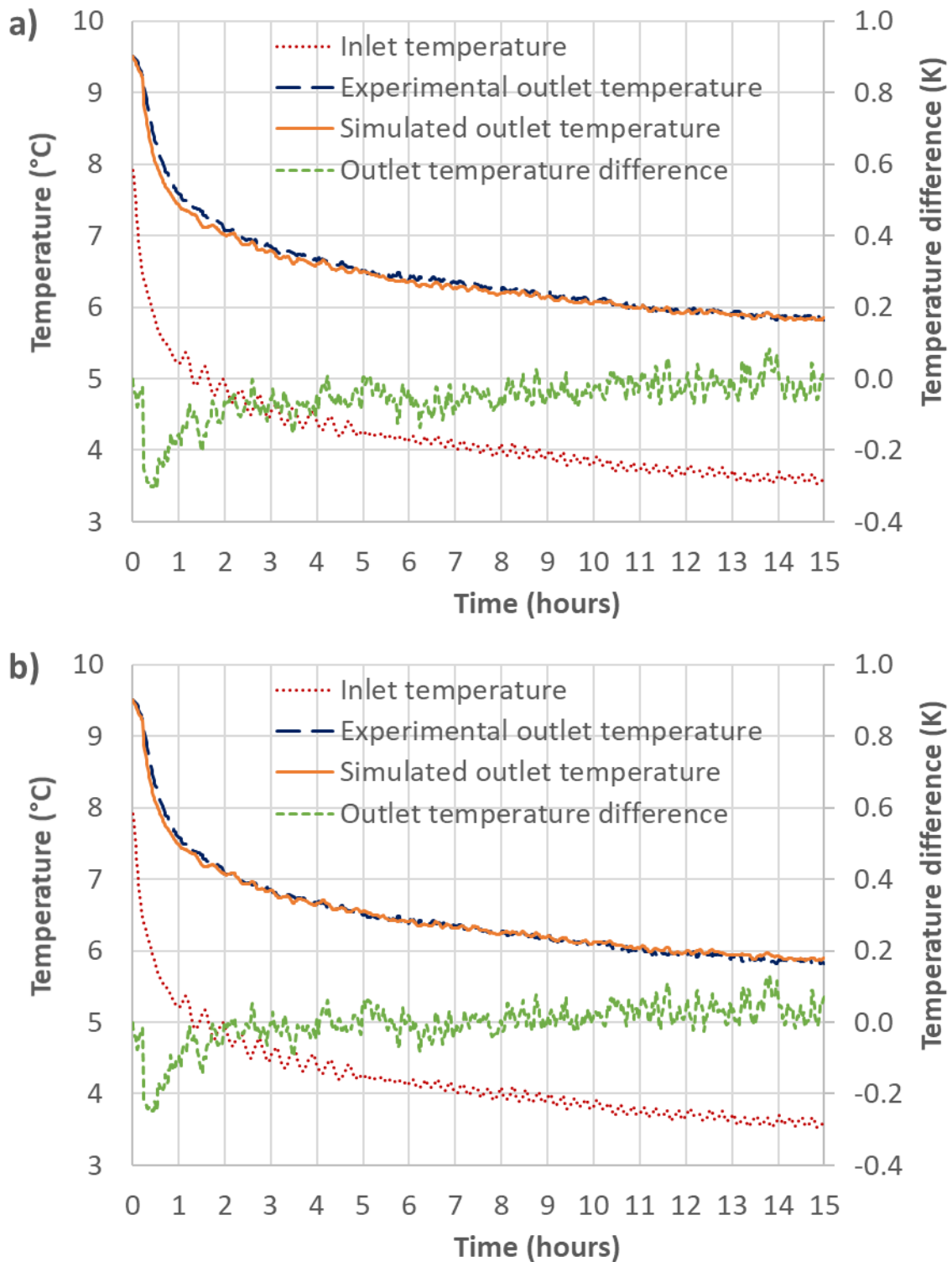


Figure 3.12. B2G helical: results of the simulation in two scenarios a) fluid following the spiral path, b) Part of the fluid through the gap, enhancement factor=1.25.

As it can be observed in Figure 3.12, the dynamic behaviour of the fluid in the BHE is well reproduced by the model. Comparing the simulated and experimental results, in both cases the RMSE is lower than 0.1K and close to the expected measurements accuracy

(0.055K), the heat extracted from the ground calculated by the model is very similar to the calculated with the experimental measurements (43022.62 kJ): less than 3% difference in case (a) and less than 0.5% in case (b). The highest difference in outlet temperature happens during the first half hour. The results of this comparison are shown in Table 3.7. The computational time to carry out each simulation was less than 2 seconds.

Table 3.7. B2G spiral coaxial: Comparison between experimental and calculated results

	RMSE (K)	Highest outlet temperature difference (K)	Calculated heat transfer (% of experimental)
Case a)	0.082	0.305	-2.48%
Case b)	0.058	0.249	-0.22%

As a conclusion, the B2G coaxial helical model is able to reproduce the behaviour of the new coaxial helical BHE during heat injection times in the range of 15 hours (a typical daily operation time for a standard GSHP system). The effect that might create the gap between the spiral rib and the outer pipe wall was studied, assuming an increase of the convective heat transfer between the annulus channel and the surrounding ground. The results showed that this increase of the convective heat transfer might happen, as the results match better in this scenario. However, the difference in the results between the scenario with and without the convective heat transfer increase is quite small. Therefore, this effect would not be very important in the final heat exchange between the fluid and the surrounding ground, this happens because there are other factors influencing to a greater extent, for example the ground and grout thermal properties.

3.6.2 DTRT standard coaxial BHE in KTH (Stockholm)

Data from a standard coaxial BHE located at the Royal Institute of Technology (KTH), in Stockholm (Sweden), was used in order to validate the B2G coaxial model with a different geometry. The BHE is a standard coaxial one, with no grout between the outer wall and the borehole wall, as the outer pipe is in contact with the borehole wall. This is possible because it is made of flexible polyethylene, so when it was filled with water, it opened until it touched the borehole wall. The inner pipe is made of medium density polyethylene (MDPE) with an outer diameter of 40 mm and a wall thickness of 2.4 mm. The bottom of the outer pipe is placed at a depth of 188 m, while the end of the internal pipe is at 182 m.

In this BHE, several DTRTs (Distributed Thermal Response Tests) were carried out, in which the circulating fluid temperature along the borehole length was measured with an optical fibre cable in the two pipes, while an inductive flow meter was used for measuring the flow rate [134]. One of the DTRTs experimental data (DTRT1 on BHE9 in [27]) was used in the experimental validation of the coaxial B2G model. The expected accuracy of absolute temperatures along the cable length is $\pm 0.1\text{K}$ [135], the expected accuracy in the flow rate measurement is around 0.5-1%.

The circulating fluid used was water and the average flow rate was 0.58 l/s. The undisturbed ground temperature along the BHE depth was measured before the start of the

DTRT, using the measurements at a depth of 17 m as the inlet and outlet conditions in order to avoid the upper segment of the BHE, where the geometry was somewhat different. This coaxial BHE with no grout is described in more detail in [135], where a model of this BHE was developed and validated with the experimental data. The main parameters used in that validation will be the starting point for the validation of the coaxial B2G model and are shown in Table 3.8.

Table 3.8. Main parameters of the coaxial BHE with no grout [135]

Thermo-physical properties		Geometrical characteristics	
Inner pipe conductivity	0.4 W/(m·K)	Active length	165-171 m
Outer pipe conductivity	0.4 W/(m·K)	Borehole diameter	0.115 m
Ground thermal conductivity	3.25 W/(m·K)	Inner/Outer diameter of the inner pipe	0.0352/0.04 m
Ground volumetric thermal capacity	2240 kJ/(m ³ ·K)	Inner/Outer diameter of the outer pipe	0.1132/0.114 m

In the B2G model, it was assumed that the active length for the whole BHE is 171 m, as it considers the same length for the inner and the outer pipe. Regarding the undisturbed ground temperature, it was estimated at different depths based on the measured vertical profile before the test. Table 3.9 shows the values used inside the B2G model at different depths for the undisturbed ground nodes.

Table 3.9. Undisturbed ground temperature at different depths used in the B2G coaxial model

Depth (m)	Temperature (°C)
0	8.9
10	8.7
20	8.5
30	8.4
40	8.3
50	8.2
60	8.1
70	8.1
80	8.1
90	8.15
100	8.2
110	8.3
120	8.4
130	8.5
140	8.65
150	8.75
160	8.85

The thermal conductivity used in [135] was 3.25 W/(m·K), in order to match the model results with the experimental data, but in the DTRTs carried out in this BHE, different values

of thermal conductivity were obtained: 3.53 W/(m·K) and 3.21 W/(m·K) in two DTRTs carried out in the same BHE, and 3.25 W/(m·K) in another BHE in the same field [27]. So, different simulations with the B2G model were carried out with slightly higher values of the ground properties in order to study the influence of these parameters, trying to match better the experimental results with the B2G model, also agreeing with the conductivity values obtained from the DTRTs. Three scenarios were proposed with the following values of ground thermal conductivity (λ) and ground volumetric heat capacity (c_v):

- Scenario a) $\lambda = 3.25 \text{ W}/(\text{m} \cdot \text{K})$ and $c_v = 2240 \text{ kJ}/(\text{m}^3 \text{K})$.
- Scenario b) $\lambda = 3.4 \text{ W}/(\text{m} \cdot \text{K})$ and $c_v = 2240 \text{ kJ}/(\text{m}^3 \text{K})$.
- Scenario c) $\lambda = 3.4 \text{ W}/(\text{m} \cdot \text{K})$ and $c_v = 2500 \text{ kJ}/(\text{m}^3 \text{K})$.

In order to carry out a complete validation of the B2G coaxial model, the short-term response of the BHE was evaluated with the model (first 15 hours of heat injection), but also the mid-term response of the BHE was evaluated with an extended time simulation of around 78 hours of heat injection.

The BHE parameters were introduced in the model: geometric characteristics according to the Table 3.8 and ground properties for the different scenarios. The number of vertical nodes used was 200 and the undisturbed ground nodes temperatures were introduced according to the Table 3.9. The inlet temperature and mass flow rates were introduced from the experimental measurements as inputs and the outlet temperature was simulated by the model. Additionally, the vertical temperature profile obtained by the B2G model was plotted for the fluid nodes (inner and outer pipe) in order to compare these values with the measured in the DTRT. The time step for the simulations was 1 minute.

The position of the ground nodes is automatically calculated by the model using the correlations described in the section 3.4.2.2, introducing the ground thermal properties, borehole radius and heat injection time (15 hours for the short-term validation and 78 hours for the extended time). Regarding the grout zone in the model, as the BHE is not grouted and this zone does not exist, the grout node was used as an extra intermediate ground node, the diameter used was an average between the outer pipe wall diameter and the first ground node diameter and the thermal properties of the ground were used.

3.6.2.1 Short-term validation

The short-term response of the BHE was simulated with the B2G model using the data from the first 15 hours of heat injection of the DTRT, considering also around five hours of water pre-circulation in the BHE. For this purpose, it was used the data from the hour 15 until the hour 35 of the test, while the heat injection started around the hour 20. The values of the penetration diameters calculated in the model are shown in Table 3.10 for each scenario. As the difference in the ground properties values are small, the calculated penetration diameters will be similar.

Table 3.10. Penetration diameters for the short term simulations in the three scenarios

	D_{gp1} (m)	D_{gp2} (m)	D_{ug} (m)
Scenario a)	0.378	0.787	1.253
Scenario b)	0.383	0.800	1.278
Scenario c)	0.371	0.767	1.219

The results obtained by the B2G model were compared with the experimental data: the outlet temperature from the BHE is shown in Figure 3.13 for the three scenarios, the difference between the simulated and experimental outlet temperatures is also plotted. The results show a very good agreement in the three cases, especially in the scenarios b) and c). The RMSE, the highest temperature difference and the percentage difference in the heat injected to the surrounding ground between the simulated and experimental results are shown in Table 3.11 (the heat injected calculated from the experimental data for this test is 364093.20 kJ). The simulations of the three scenarios produce quite accurate results, with RMSEs lower than 0.05 K in the three cases, a highest temperature difference of 0.14 K in the scenario a) and 0.1 K in scenario c) and a calculated heat injection 3% lower in the worst case. The calculation time to carry out each simulation was around 2.3 seconds.

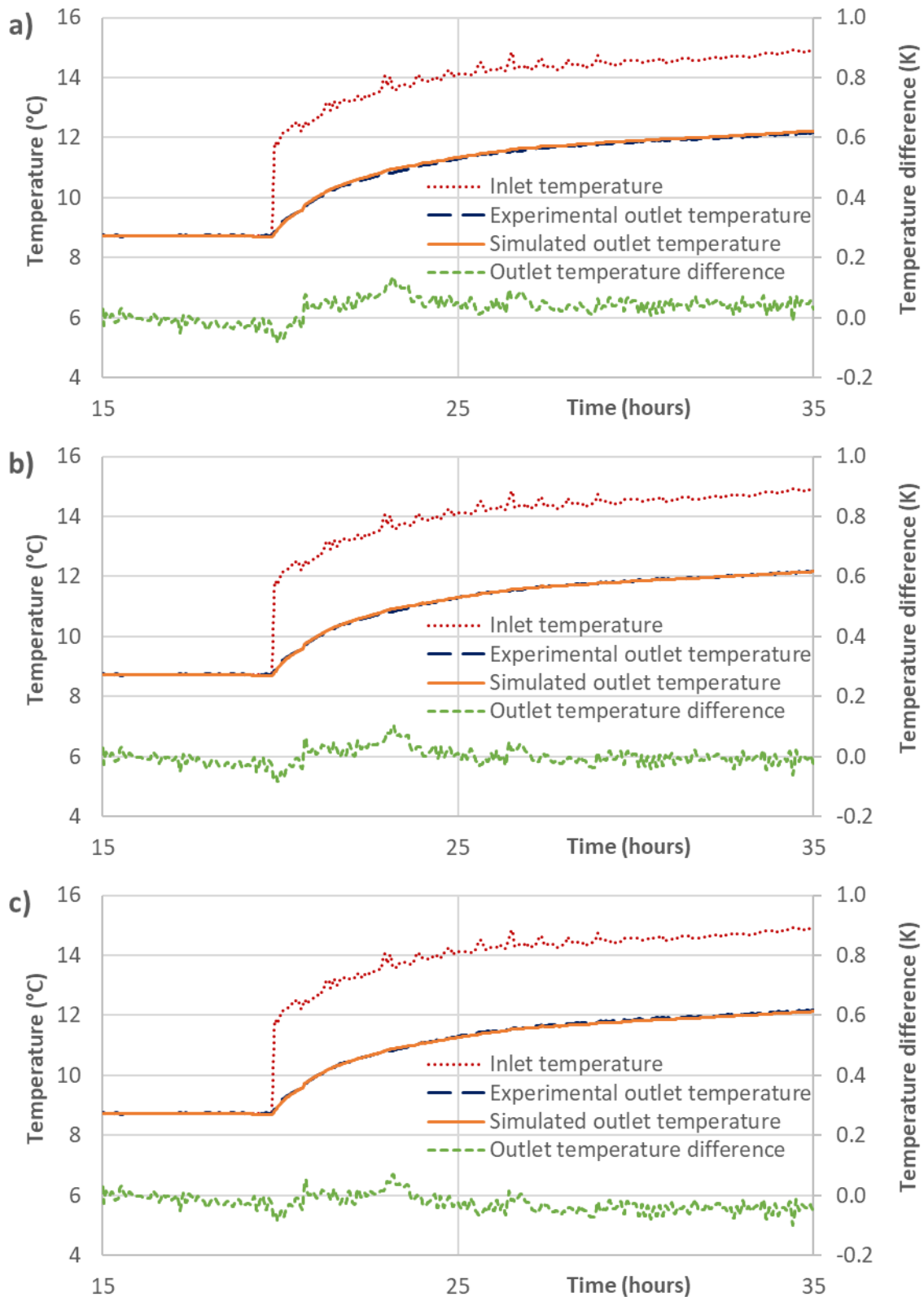
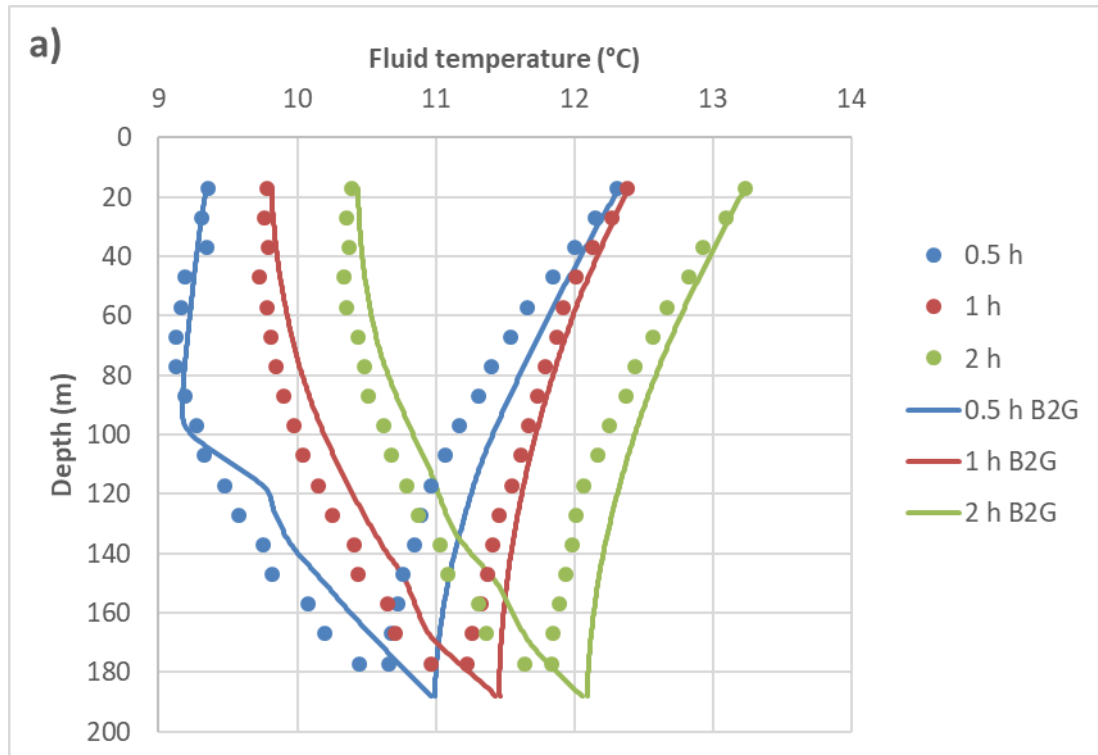


Figure 3.13. B2G coaxial (KTH) short term simulation in the three scenarios.

Table 3.11. B2G coaxial (KTH) short term: Comparison between experimental and calculated results

	RMSE (K)	Highest outlet temperature difference (K)	Calculated heat transfer (% of experimental)
Scenario a)	0.0468	0.137	-3.0%
Scenario b)	0.0263	0.104	-1.5%
Scenario c)	0.0365	0.099	-0.4%

The vertical water temperature profile inside the BHE pipes was also measured at different heat injection times (0.5 h, 1h and 2h from the start of the heat injection). So, the simulated water temperature profile was plotted against the measured data and it is shown in Figure 3.14 for the three scenarios. The absolute difference between the measured values and the corresponding simulated values was calculated. The average value for each scenario at each heat injection time is shown in Table 3.12, as well as the maximum difference value.



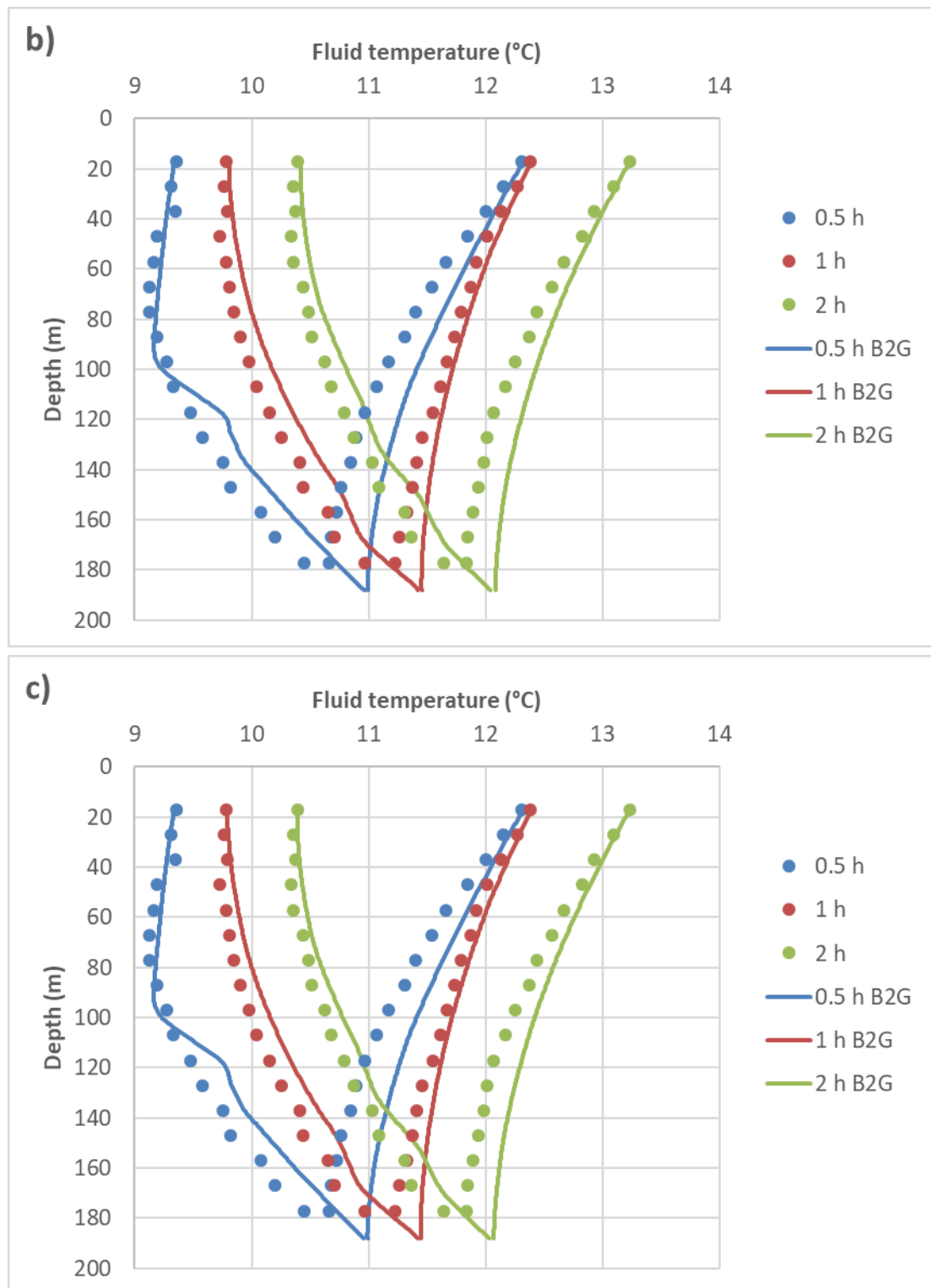


Figure 3.14. B2G coaxial (KTH) short term: Vertical temperature profiles in the three scenarios for different heat injection times.

Table 3.12. B2G coaxial (KTH) short term vertical profiles: absolute temperature values error between simulated and experimental results (average and maximum values).

	0.5 hours		1 hour		2 hours	
	Avg. (K)	Max. (K)	Avg. (K)	Max. (K)	Avg. (K)	Max. (K)
Scenario a)	0.19	0.35	0.14	0.31	0.18	0.29
Scenario b)	0.19	0.35	0.13	0.29	0.16	0.27
Scenario c)	0.18	0.35	0.12	0.27	0.14	0.25

It is possible to see that the B2G model is capable of reproducing the vertical temperature profiles with a good accuracy, despite the fact that the error is higher at the lower part of the BHE. Taking a look at the errors in Table 3.12, the maximum error at 0.5 h is 0.35 K in the three scenarios and it decreases with the heat injection time, reaching 0.25 K in the scenario c) at 2 hours of heat injection. The average error is between 0.12 K and 0.19 K in all the scenarios and heat injection periods.

Considering all the simulated results (outlet temperature, heat injection and vertical temperature profiles), it is possible to see that the scenario c) produces slightly more accurate results than scenario b), and this one slightly better results than scenario a). Nevertheless, all the three scenarios produce quite accurate results in the short term prediction of the coaxial BHE behaviour.

3.6.2.2 Extended time validation

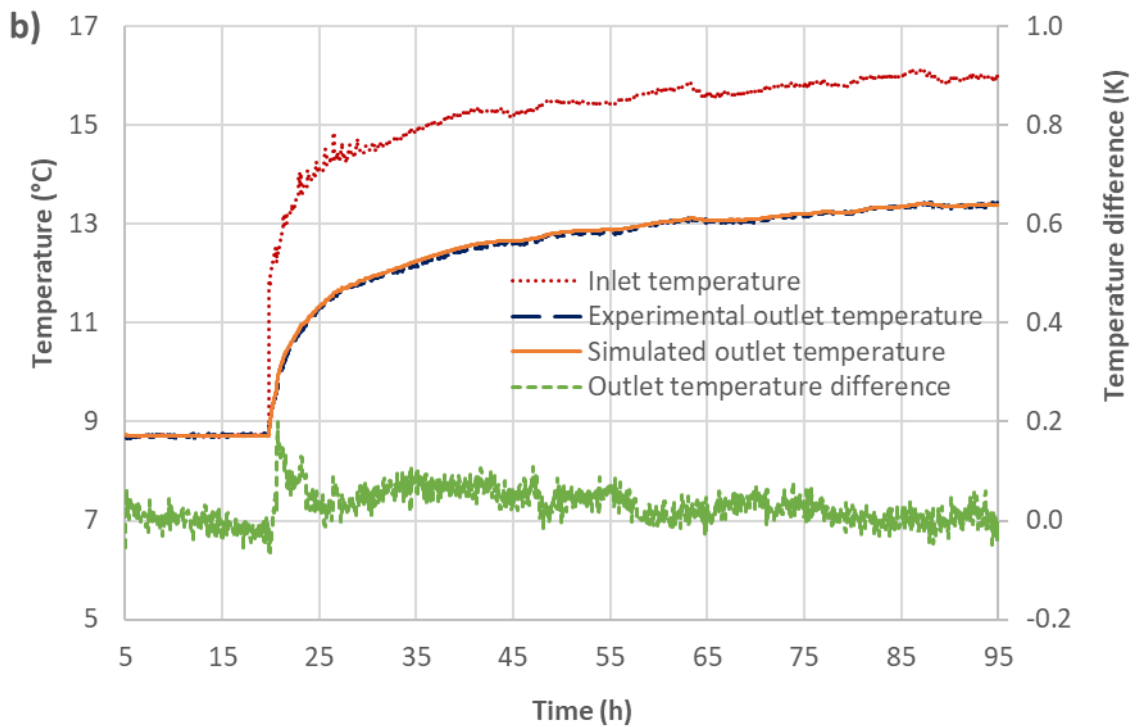
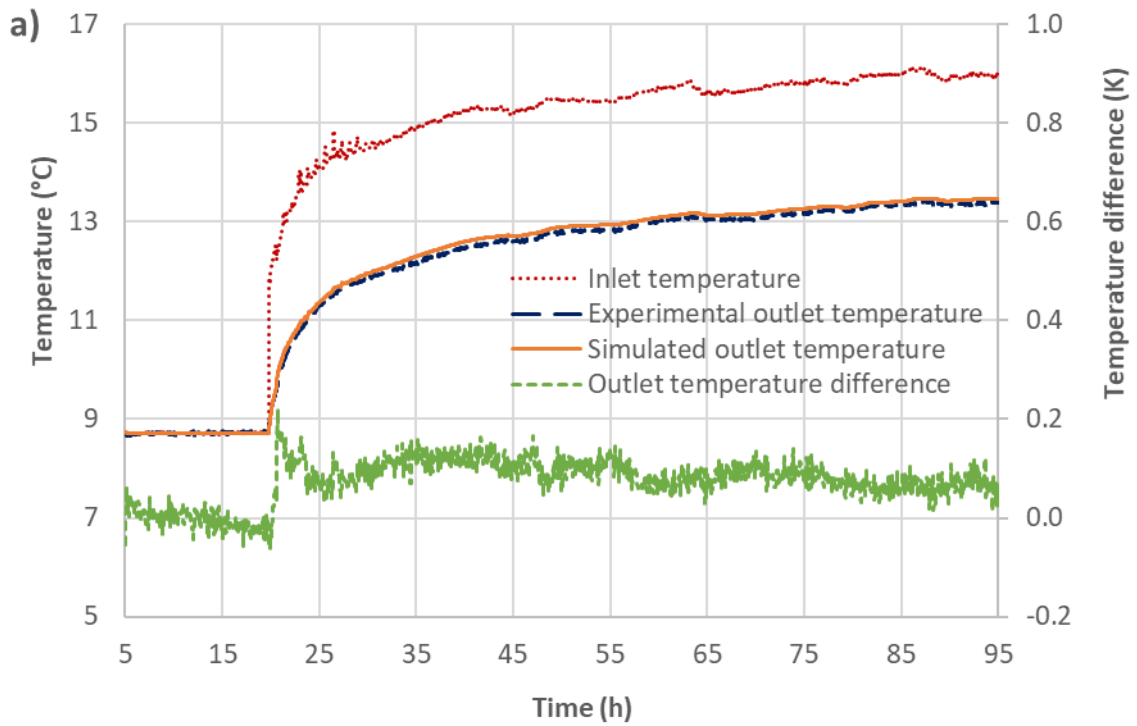
The adaptation of the B2G coaxial model to different heat injection times was studied with a simulation of a DTRT of around 78 hours of heat injection (around 95 hours of test). The DTRT is the same used for the short-term validation. In order to adapt the model to longer heat injection times, it is only necessary to change the heat injection period used for the calculation of the penetration diameters, so a bigger volume of ground will be considered, as the amount of ground affected by the heat injection in the ground will be bigger, therefore a higher ground capacity is considered. The values of the penetration diameters calculated for a heat injection period of 78 hours are shown in Table 3.13 for the three scenarios.

Table 3.13. Penetration diameters for the extended time simulations in the three scenarios

	D_{gp1} (m)	D_{gp2} (m)	D_{ug} (m)
Scenario a)	0.6435	1.5375	2.6028
Scenario b)	0.6536	1.5670	2.6563
Scenario c)	0.6292	1.4964	2.5280

The experimental data from the DTRT was used from hour 5 to hour 95, the heat injection started at hour 20, approximately, so the pre-circulation of the water was also considered. The simulated outlet temperature is plotted and compared against the experimental data in Figure 3.15, showing a good agreement in the three scenarios, especially in scenario c). The RMSE, the highest temperature difference and the percentage difference in the heat injected to the ground between the simulated and experimental

results are shown in Table 3.14 (the heat injected calculated from the experimental measurements for this test is 1772170.58 kJ). Considering the RMSEs, the scenario that produces more accurate results is the scenario c), with a RMSE of around 0.03 K for the whole simulation and a heat transfer around 1% lower than the experimental value. The RMSE obtained in scenario a) is lower than 0.09 K and lower than 0.05 in scenario b). Therefore, the three scenarios produce quite accurate results. The simulation time in order to carry out the 90 hours simulation was around 7.8 seconds.



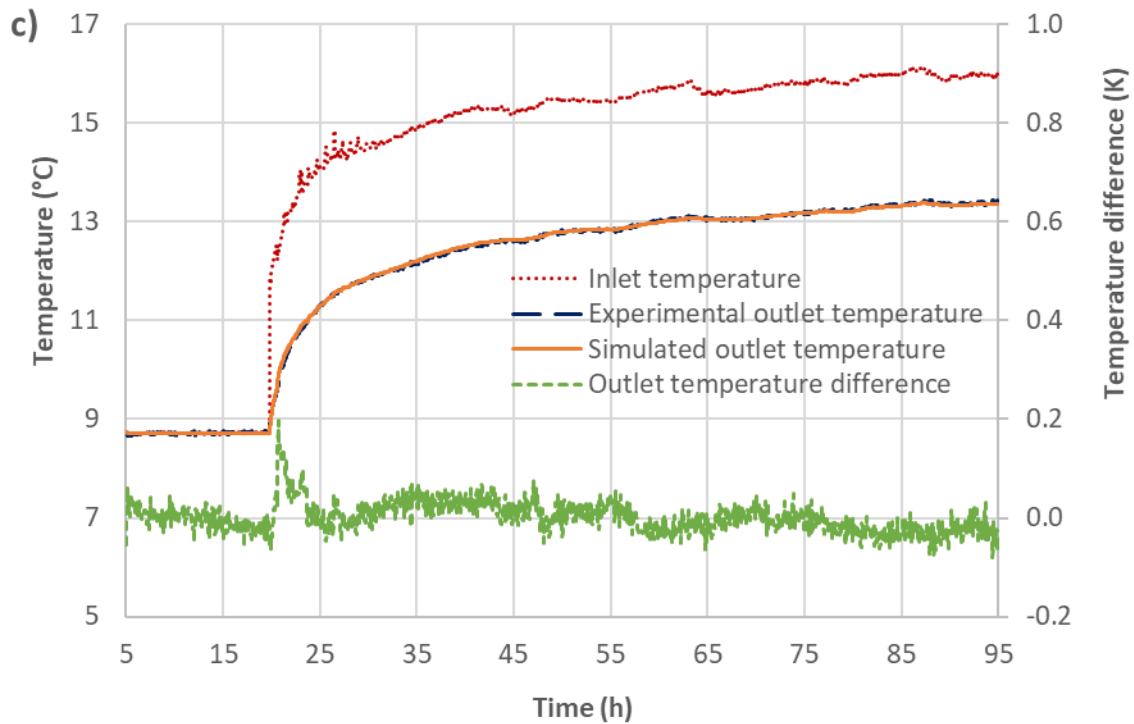
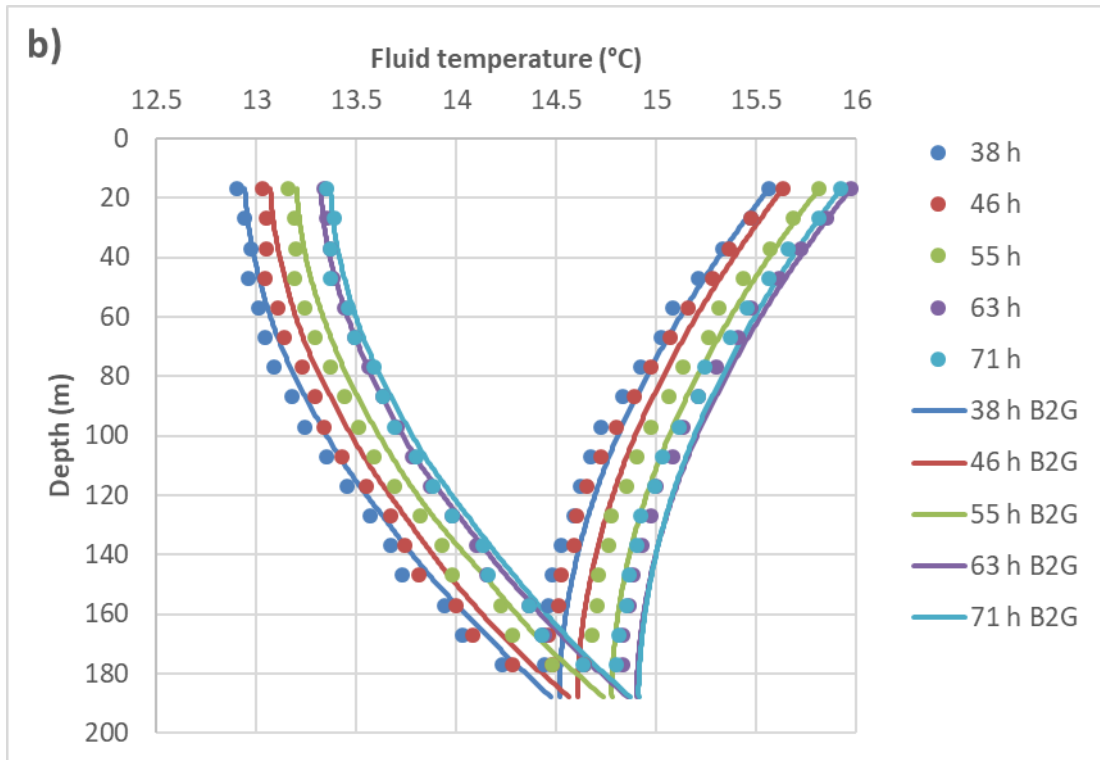
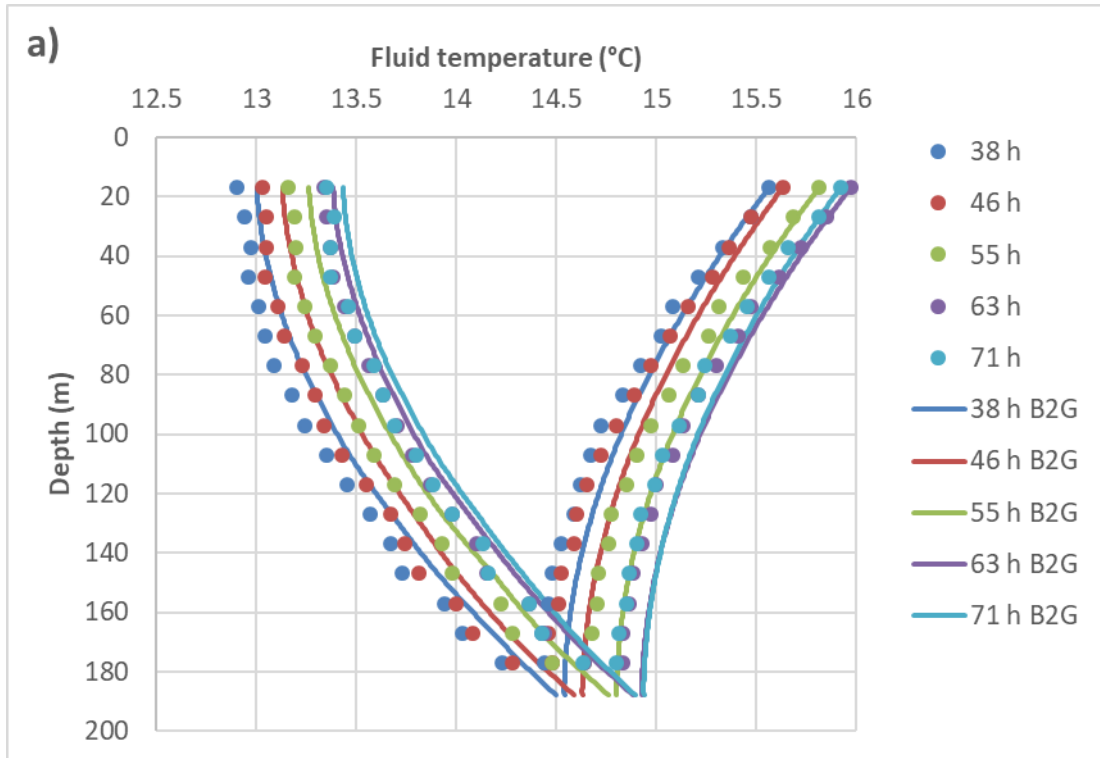


Figure 3.15. B2G coaxial (KTH) extended time simulation in the three scenarios.

Table 3.14. B2G coaxial (KTH) extended time: Comparison between experimental and calculated results

	RMSE (K)	Highest outlet temperature difference (K)	Calculated heat transfer (% of experimental)
Scenario a)	0.0867	0.220	-4.4%
Scenario b)	0.0432	0.201	-2.4%
Scenario c)	0.0297	0.197	-1.2%

Following the same methodology as in the short-term validation, the vertical water temperature profiles inside the pipes was plotted against the measured results at different heat injection times (38 h, 46 h, 55 h, 63 h and 71 h) in Figure 3.16. The absolute error between the measured points and the corresponding simulated values was calculated. The average value for each scenario and heat injection time is shown in Table 3.15, together with the maximum error value.



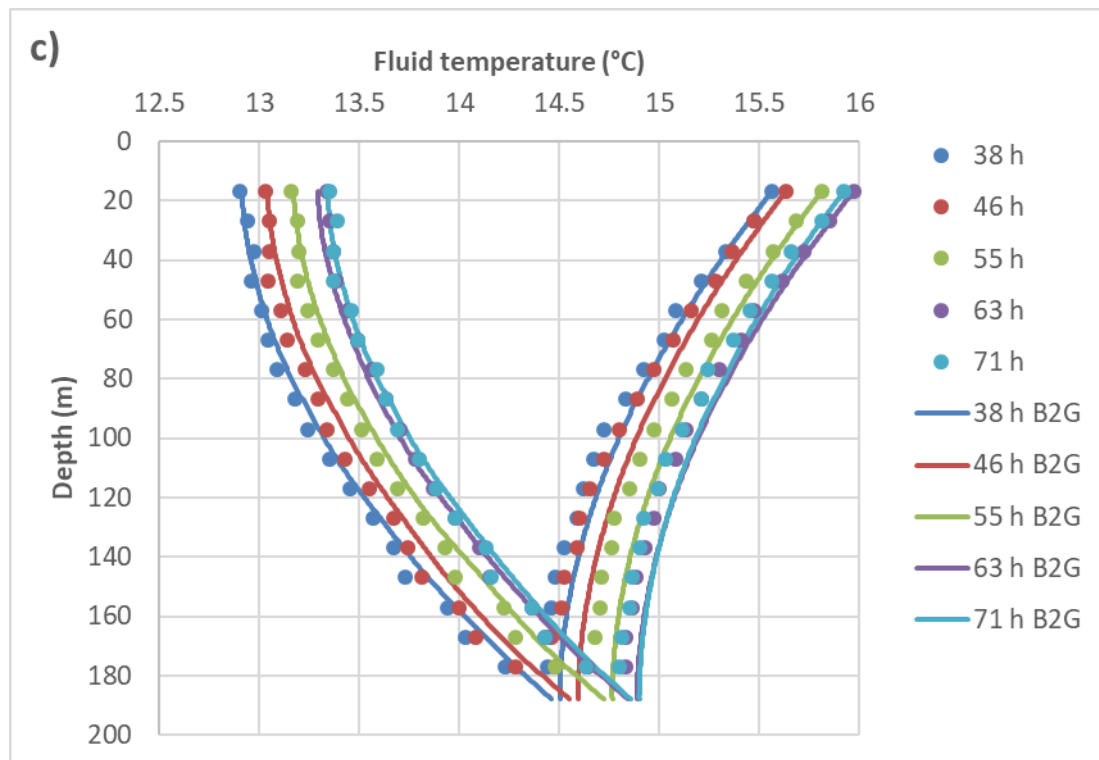


Figure 3.16. B2G coaxial (KTH) extended time: Vertical temperature profiles in the three scenarios.

Table 3.15. B2G coaxial (KTH) extended time vertical profiles: absolute temperature values error between simulated and experimental results (average and maximum values).

	38 hours		46 hours		55 hours		63 hours		71 hours	
	Avg. (K)	Max. (K)	Avg. (K)	Max. (K)	Avg. (K)	Max. (K)	Avg. (K)	Max. (K)	Avg. (K)	Max. (K)
Scenario a)	0.10	0.17	0.13	0.19	0.12	0.20	0.08	0.14	0.10	0.17
Scenario b)	0.06	0.13	0.09	0.17	0.08	0.16	0.04	0.10	0.07	0.13
Scenario c)	0.05	0.11	0.08	0.15	0.07	0.14	0.04	0.09	0.06	0.12

There is a good agreement between the simulated and measured results, although there is a higher discrepancy in the lower part of the BHE, as it happened in the short-term study. However, the average and maximum errors are quite small in the three scenarios, mainly in the scenario c), where the maximum error is around 0.15 K for a heat injection period of 46 hours and the higher average error is 0.08K.

Considering the short term and extended time validations of the model, the scenario c) produces the most accurate results, with a quite small error between the simulated and measured results. Although the other scenarios also reproduce the BHE behaviour with a high accuracy for both the short-term and mid-term heat injection periods.

Concerning the ground properties estimation, when the thermal conductivity is calculated using a TRT, an estimation is obtained and it will be slightly different in different tests, as shown in [27], where somewhat different values of the ground conductivity were obtained for the same ground. So its exact determination is not possible. In this regard, the

B2G coaxial model has proven that it is possible to provide an estimation of the ground thermal conductivity in line with the experimental results both for the short- and mid-term, as three sets of ground properties were tested in the model, concluding that the set that fitted better the experimental results was the scenario c), although all of them provide good results. Therefore, the B2G model could be a useful tool in order to aid in the estimation of the ground properties using the short-term results of a TRT, avoiding the long injection periods needed to calculate the ground conductivity with the common methodologies, reducing the cost of the test and increasing its economic feasibility.

3.6.3 System operation conditions validation of a standard coaxial BHE in Tribano

The B2G coaxial model was also validated against experimental measurements under the normal operation of the Dual Source Heat Pump (DSHP) system installed in the demonstration installation in Tribano (Italy) inside the framework of the GEOTeCH project. This installation was described in the chapter 2 and the BHE field, in section 2.3.3. The demo-site installation firstly incorporated temperature and flow sensors in the hydraulic loops in the heat pump side, among them, the ground loop. Therefore, the total mass flow rate, inlet and outlet temperatures in the ground loop were monitored, but there were no sensors placed inside the BHE field. In order to solve this, an additional monitoring system was placed by the University of Bologna in different parts of the BHEs field [51], monitoring the inlet and outlet temperature of one of the BHEs (BHE8), the collector where the flow is divided into the different BHEs and later collected, and three observation boreholes (OBs) to measure the temperature of the ground surrounding the BHE8 at different depths. These temperatures were measured with PT100 sensors and an accuracy of 0.15K at 0°C.

The monitored temperature from the inlet and outlet of the BHE8 was used in order to validate the B2G coaxial model under different operating conditions. The mass flow rate that circulates through the BHE8 was estimated based on the distribution of the BHEs in the field, and the initial and undisturbed ground temperature was estimated based on the temperature measurements from the observation boreholes. The representative days for selecting the validation data were selected based on two reasons: 1) there was monitored data for the full day, without any failure of the monitoring system during the day and 2) the predominant source used in the system during that day is the ground, as it is a dual source heat pump system and it is capable of working with the air or the ground as a source.

3.6.3.1 BHEs field in Tribano

The field mainly consists of eight coaxial BHEs with a depth of 30 m each, distributed in a rectangular configuration of 2x4 and a separation of 6 m between BHEs. The heat carrier fluid used is water, the characteristics of the BHEs are shown in Table 2.5, while the ground geology and its thermal properties are described in section 2.3.3.3. The eight coaxial BHEs are connected in parallel in eight different hydraulic lines that are distributed and collected in the collector pit. Since there are no balancing valves in the hydraulic system, the mass flow rate through each BHE will be different, due to the different pipes length between the collector and each BHE. The distribution of the BHE lines is shown in Figure 3.17.

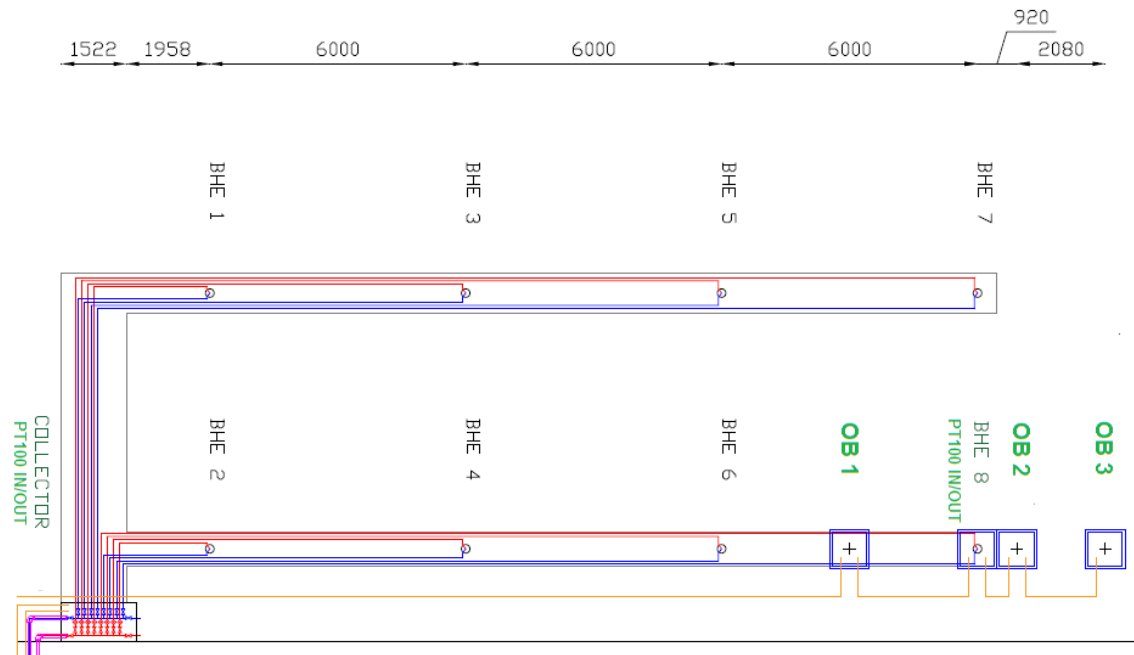


Figure 3.17. BHE field pipes distribution in Tribano

The mass flow rate through each BHE line was estimated assuming that the total pressure drop through each line (distribution pipes and BHE) would be the same in the eight lines. So, the pressure drop was calculated depending on the mass flow rate by using the methodology explained in section 3.3.3 for the BHE and the connecting pipes. An extra pressure drop of 310 Pa was considered for the head assembly and foot inversion in the BHE, based on internal studies carried out in the GEOTHEX BHE by the company Groenholland BV [136]. The calculation of the pressure drop through each line as a function of the mass flow rate was implemented in an Excel spreadsheet and then, using the Solver tool, the mass flow rate of each line is calculated by means of a mathematical algorithm in order to obtain the same pressure loss in all the lines. The total mass flow rate that was estimated corresponds to the near constant mass flow rate at which the system was working at that moment. The solution obtained by this methodology is shown in Table 3.16. The time that the water takes to flow through each entire line is also shown in the table. It can be seen that this time will be considerably different in the different BHE lines, because of the different length and different water velocity.

Table 3.16. Mass flow rate calculation

BHE	Mass flow rate (kg/h)	Percentage of total flow rate	Length of one pipe (m)	Pressure drop pipes (Pa)	Pressure drop BHE (Pa)	Total pressure drop (Pa)	Flowing time (min)
1	564	14.2%	11	1272	809	2081	14
2	765	19.3%	5	1042	1039	2081	10
3	463	11.6%	17	1371	710	2081	18
4	565	14.2%	11	1274	807	2081	14
5	400	10.1%	23	1431	651	2081	21
6	463	11.6%	17	1371	710	2081	18

BHE	Mass flow rate (kg/h)	Percentage of total flow rate	Length of one pipe (m)	Pressure drop pipes (Pa)	Pressure drop BHE (Pa)	Total pressure drop (Pa)	Flowing time (min)
7	356	9.0%	29	1474	608	2081	25
8	400	10.1%	23	1431	651	2081	21
Σ	3975	100%				2081	

The mass flow rate through each line would be quite different depending on the length of the distribution pipes, as the pressure loss will increase with the pipe length and then, the mass flow rate will decrease in order to compensate this effect, as a result, the BHE lines with longer pipes would present a lower flow rate. Focusing on the BHE8, the mass flow rate would be around a 10% of the total.

For the validation of the B2G coaxial model with the BHE8 data in different days, a constant flow rate of 400 kg/h will be assumed, together with the monitored inlet and outlet temperatures in the head of the BHE8.

3.6.3.2 Validation of B2G coaxial model under daily operating conditions

For validating the B2G coaxial model under different operating conditions, two representative days were selected: one for the summer season (cooling mode) and one for the winter season (heating mode), so the model will be validated with the system injecting heat into the ground and extracting heat from the ground, respectively. Additionally, a simulation of the BHE during five days of operation was carried out in heating mode. The day selected for the summer season was the 13th of September 2018, for the winter season it was selected the 19th of November 2018 and for the five days period it was selected from the 19th to 23rd of November 2018.

The main characteristics of the BHE are introduced in the model, according to the information described in section 2.3.3. The soil in Tribano presented different layers of wet clay and sand, so the ground thermal properties were assumed as the average values of these materials at the different depths, in five layers. The assumed values for the ground thermal conductivity and volumetric heat capacity are presented in Table 3.17.

Table 3.17. Ground thermal properties at different depths used in the B2G model

Depth (m)	Thermal conductivity (W/(m·K))	Volumetric heat capacity (kJ/(m ³ ·K))
0-8	1.8	2400
8-18	2.4	2500
18-21	1.8	2400
21-26	2.4	2500
26-30	1.8	2400

Considering these values presented in Table 3.17, the weighted average was calculated in order to determine the penetration diameters for the whole BHE depth. These average values are shown in Table 3.18, together with the main parameters used in the model.

Table 3.18. Main parameters used in the B2G coaxial model for the Tribano BHE

Thermo-physical properties		Geometrical characteristics	
Inner pipe conductivity	0.2 W/(m·K)	Length	30 m
Outer pipe conductivity	0.4 W/(m·K)	Borehole diameter	0.135 m
Average ground thermal conductivity	2.1 W/(m·K)	Inner/Outer diameter of the inner pipe	0.063/0.0514 m
Average ground volumetric thermal capacity	2450 kJ/(m ³ ·K)	Inner/Outer diameter of the outer pipe	0.09/0.0792 m

There was no grout injected in the gap between the outer pipe and the borehole wall; as a consequence, the surrounding ground collapsed and filled this gap when the drill rod was extracted. So, for the grout region in the B2G model, the properties of the ground were considered. The number of vertical divisions considered in the model were 150. The penetration diameters calculated inside the model are shown in Table 3.19 for the different heat injection periods: one day or five days, considering the average thermal properties of the ground.

Table 3.19. Penetration diameters for the Tribano BHE model at different heat injection times

Heat injection time	D_{gp1} (m)	D_{gp2} (m)	D_{ug} (m)
24 hours	0.40	0.80	1.25
120 hours	0.66	1.52	2.53

As the circulation pump of the ground loop and the heat pump in the system did not stop during the night, the initial ground temperatures were not straightforward to determine. For the summer day, an undisturbed ground temperature vertical profile was used, based on the work presented in [51], the increment of temperature due to all the heat injected and extracted during the operation of the system from the start in February was calculated using an Infinite Line Source solution approach, described in the section 3.7. With this approach it is possible to calculate the ground temperature change at different distances from the BHE, considering all the heat injection and extraction during a determined period. So, the vertical temperature profile was determined based on the undisturbed ground profile, adding the calculated temperature increase at the different ground nodes distances (determined by the penetration diameters shown in Table 3.19). This solution considers the total heat transfer in the entire BHE field (calculated from the monitored data) and the interaction between BHEs in the specified field configuration.

Regarding the initial and undisturbed ground temperatures for the winter day, an estimation was carried out based on the monitoring data measured inside the observation boreholes.

The simulations were carried out with a time step of 1 minute, the inlet temperature measured at the head of the BHE8 was introduced as an input in the model and a constant flow rate of 400 kg/h was assumed. The simulated outlet temperature was compared with the measured outlet temperature at the head of the BHE8. The results of the different

simulations are shown in Figure 3.18 for the summer day, in Figure 3.19 for the winter day and in Figure 3.20 for the simulation of the operation during five days. The simulation time for the daily simulations was around 2.5 seconds, while the simulation time of the five days operation was around 7.2 seconds.

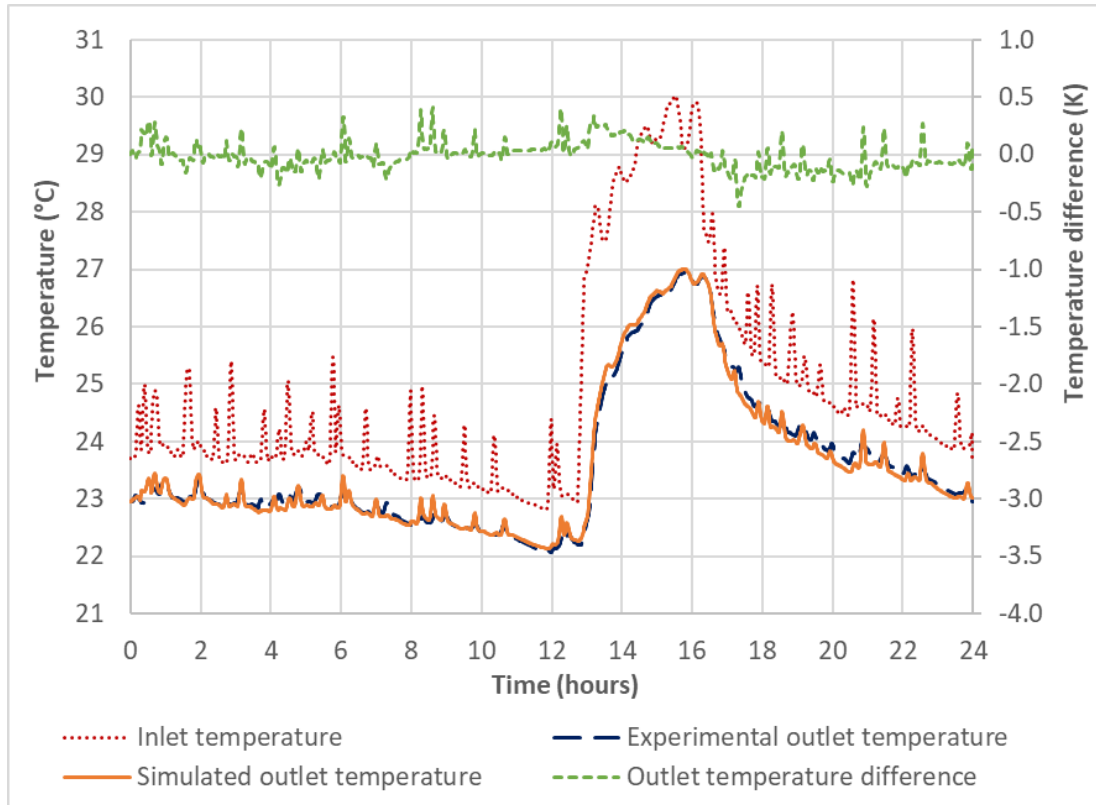


Figure 3.18. B2G coaxial summer day operation (13/09/2018): simulation results

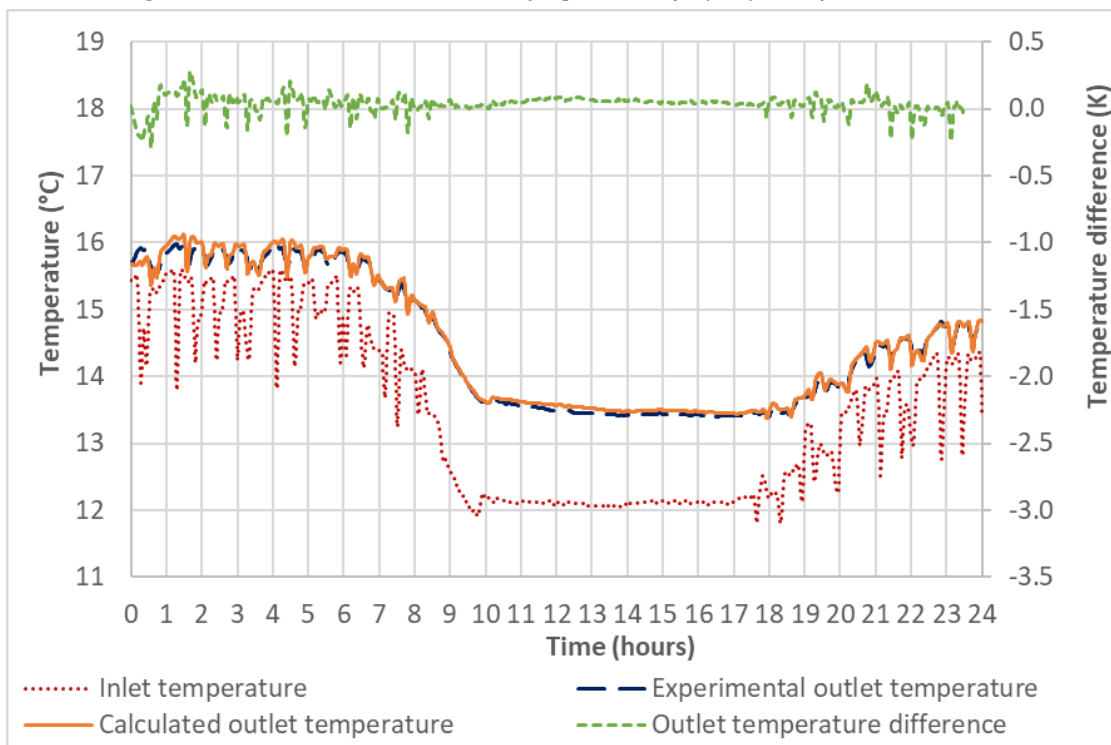


Figure 3.19. B2G coaxial winter day operation (19/11/2018): simulation results

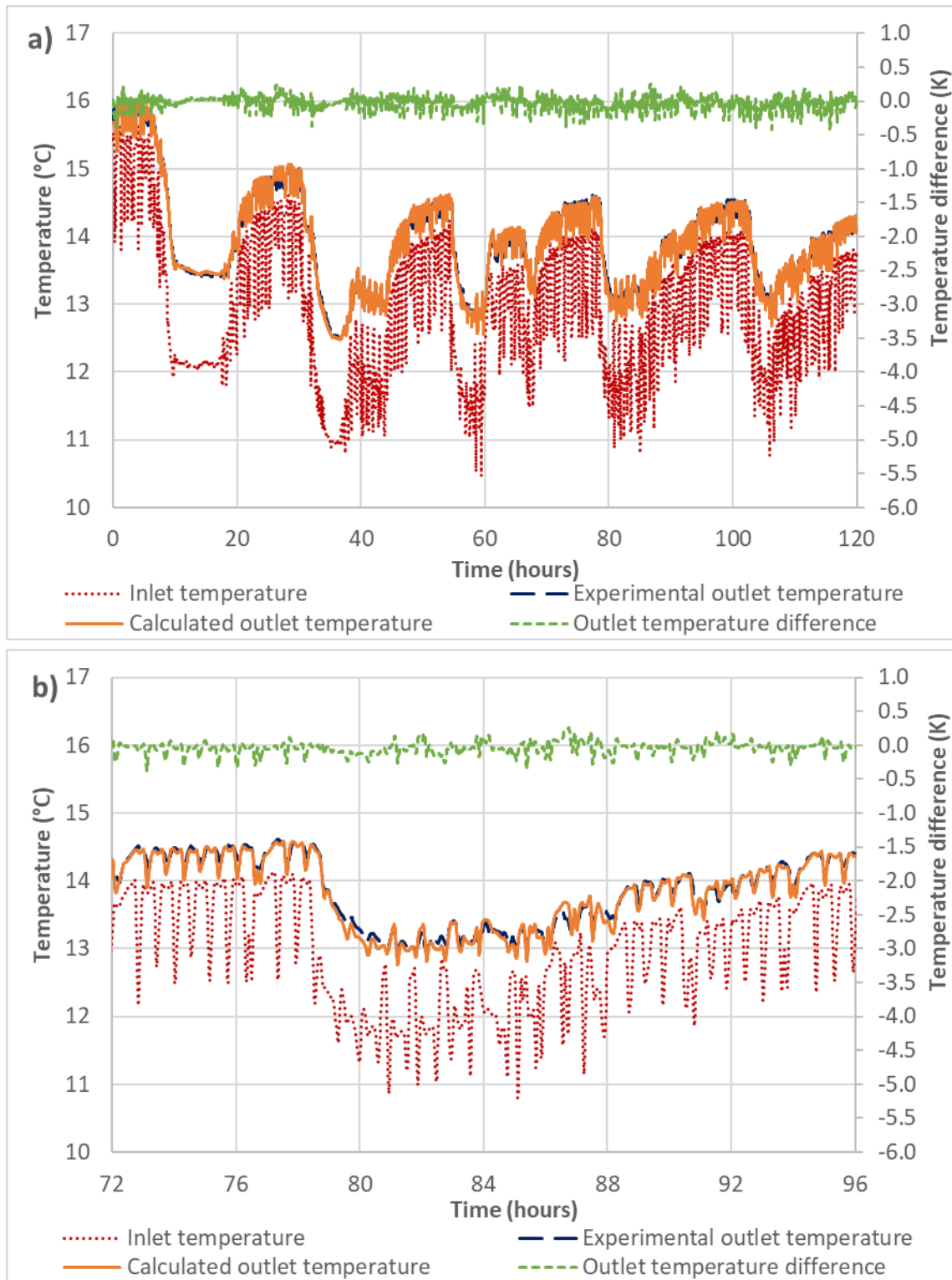


Figure 3.20. B2G coaxial five winter days operation (19/11/2018-23/11/2018): a) simulation results for the five days; b) zoom on the fourth day.

The simulated results show a good agreement with the experimental measurements in all the cases. The RMSE, the highest temperature error and the difference in the heat transfer between the simulated and experimental results are shown in Table 3.20. The RMSE are lower than 0.1 K in the winter days simulation, while it is around 0.12 K for the summer day simulation. The difference in the heat transfer is lower than 4% in all the cases.

Table 3.20. B2G coaxial daily operation in Tribano: calculated errors

	RMSE (K)	Highest outlet temperature difference (K)	Calculated heat transfer from data (kJ)	Simulated heat transfer (% of experimental)
Summer day	0.1209	0.4530	51140	+0.91%
Winter day	0.0747	0.2857	41716	+3.43%
5 winter days	0.0875	0.4177	198087	-2.06%

In conclusion, the B2G coaxial model is able to reproduce with a high accuracy the behaviour of a coaxial BHE and spiral coaxial BHE under different operating conditions: the short-term and mid-term behaviour of a TRT and the daily operation of a BHE during some days. The computational time that the TRNSYS model spent to carry out the simulations was quite short: between 2 and 8 seconds for a 15 hours or a 120 hours simulation, respectively. So, it could be used inside a complete GSHP system in TRNSYS in order to predict the behaviour of the ground loop and then, provide an accurate inlet to the heat pump in order to simulate its performance and the coupling with the rest of the system without the need of long simulation times.

3.6.3.3 Validation of the ground loop

The ground loop consisting of the eight lines of BHEs, the collector and the two pipes between the heat pump and the collector was also modelled in TRNSYS and simulated for the representative day of cooling mode. The resulting TRNSYS model is shown in Figure 3.21. The pipes between the heat pump and the collector were considered with a length of 30 m and an internal diameter of 0.1 m. It is considered that the water flow is divided in the collector to the different BHEs lines, the percentages of the total mass flow rate shown in Table 3.16 are used, as well as the pipes lengths between the collector and each BHE that are shown in this table. The thermal losses between the pipes and the ground are also simulated, considering a ground temperature of 26°C in the BHEs field and 24°C in the part between the collector and the heat pump. These values were estimated based on the temperatures monitored in the BHEs field and considering that the ground around the BHEs is more affected by the heat injection than the ground between the heat pump and the collector, where there is no heat injection but the small thermal losses from the water flowing inside the pipes.

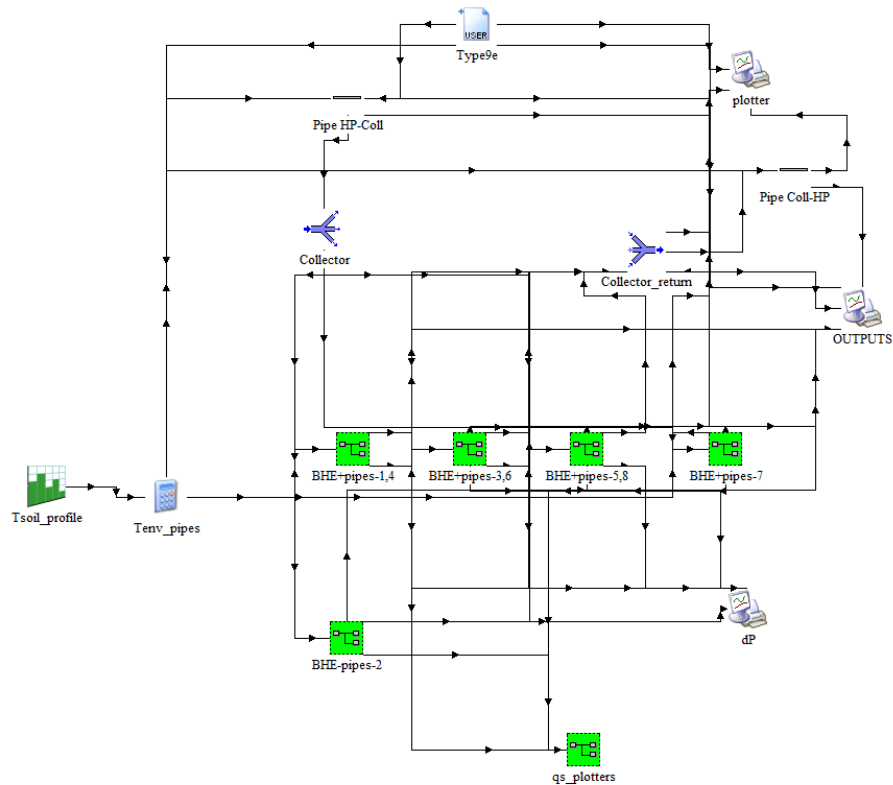


Figure 3.21. Ground loop TRNSYS model, comprising the 8 BHEs

Following the same methodology as with the BHE8, the monitored data for an entire day was used for validating the ground loop. The representative day for cooling mode was used (13/09/2018), the inlet temperature and mass flow rate from the heat pump were used, and the calculated temperature coming from the ground loop is compared with the monitored data. The results obtained in this simulation are shown in Figure 3.22.

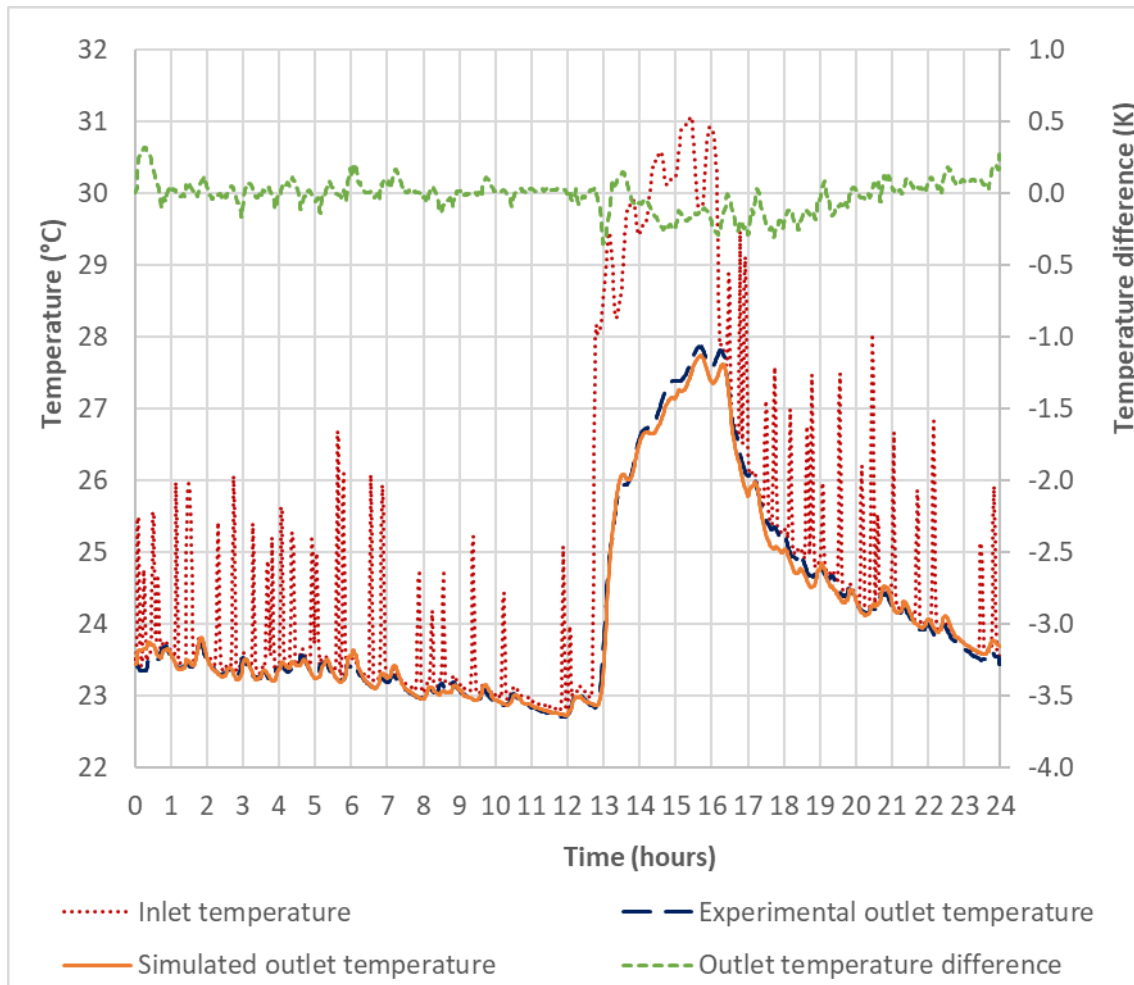


Figure 3.22. Simulation of circulating temperature for the ground loop with the eight BHEs in cooling mode during one day (13/09/2018).

In Figure 3.22, it can be seen a good agreement between the experimental and simulated results, with a RMSE of 0.11 K and the highest outlet temperature difference is 0.36K.

Despite the good agreement in considering all the BHEs in the field, an average BHE will be considered for representing all the BHEs in the entire system model. The thermal interaction between BHEs and the average temperature will be calculated by the long-term ground model described in section 3.7.

3.7 Long-term BHE field model

3.7.1 Background

The dynamic B2G coaxial model has been developed and described previously as a coaxial BHE model able to reproduce with a high accuracy the short-term response of a coaxial BHE under different operating conditions (from one day to 5 days) with a low computational cost. It was implemented in TRNSYS, so it could be used in the modelling of entire GSHP systems, by coupling it with a heat pump model and the rest of the system components. However, this model only considers the amount of surrounding ground affected by the short-term heat injection, so in order to carry out longer simulations, it

would be necessary another ground model that calculates the long-term response of the ground, as well as the interaction between BHEs in a field. In this manner, it is possible to predict, on one hand, the dynamic behaviour of the BHE for the daily operation with a low computational cost with the B2G model and on the other hand, calculate the long-term evolution of the ground temperature, considering all the heat injected into the ground and the interaction between BHEs with a time efficient long-term model. So it would be possible to predict both the short and long-term behaviour of the BHE with a low overall computational time.

In previous works, the U-tube B2G model was coupled to a pre-generated *g-function* in order to calculate this long-term response of the BHE and the interaction between BHEs for a specific BHE field configuration [115]. In this PhD dissertation, a new TRNSYS type was developed in order to model this long-term response and interaction between BHEs for any BHE field configuration, based on an algebraic approach of the ILS model and using the time superposition and load aggregation algorithm used in [115]. The new TRNSYS type was called LSA (Line Source Approach) model.

3.7.2 Line Source Approach model

A new TRNSYS type was developed adapting the tool developed by Witte [137], [138] in order to calculate the thermal interaction between BHE systems, based on the algebraic approximation of the ILS introduced by Hart and Couvillion [65], defined in the equation (3.68).

$$T(r, t) - T_0 = \frac{q_0}{2\pi\lambda} \left[\ln \frac{r_\infty}{r} - 0.9818 + \frac{4r^2}{2r_\infty^2} - \frac{1}{4 \cdot 2!} \left(\frac{4r^2}{r_\infty^2} \right)^2 + \dots \right. \\ \left. + \frac{(-1)^{N+1}}{2N \cdot N!} \left(\frac{4r^2}{r_\infty^2} \right)^N \right] \quad (3.68)$$

where r_∞ represents a hypothetical far-field radius in which the effect of the line source would disappear, according to the equation (3.69), and N represents the number of terms in the series that are considered. In the LSA model, 10 terms will be considered in order to obtain a good accuracy.

$$r_\infty = 4\sqrt{\alpha t} \quad (3.69)$$

In order to use this approach, it is assumed a constant heat injection along the borehole depth, only conductive heat transfer, no axial heat transfer, vertical orientated BHEs (not inclined) and an isotropic and homogenous ground volume (for layered ground geologies, the effective thermal properties will be assumed).

In order to consider the spatial interaction between BHEs in the field, the effects of each individual BHE are superposed, i.e. the individual temperature alterations caused by each BHE at a given position are summed up [70].

Regarding the time-dependent heat injection, the Duhamel's theorem [57], [70], [112] is normally used to evaluate the response of the ground due to this variable heat injection, dividing it in single, constant, unitary heat pulses, as shown in Figure 3.23.

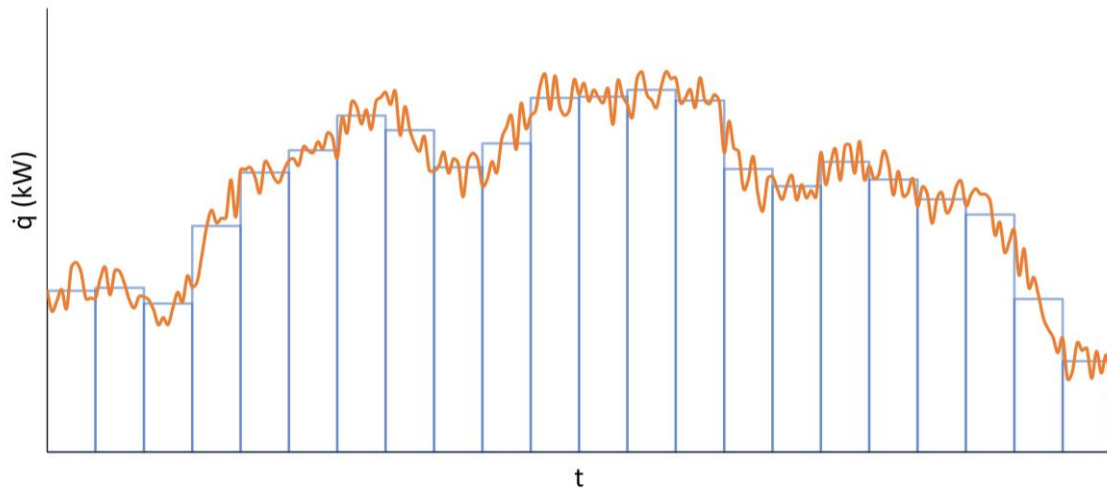


Figure 3.23. Ground load profile divided in thermal load pulses [130]

Based on this methodology, the heat injection is introduced in the model as constant, unitary heat pulses that will be superimposed in time, as shown in Figure 3.24. The “effective pulses” that will be superimposed are calculated as the difference between one block and the previous one: $\dot{q}_n^* = \dot{q}_n - \dot{q}_{n-1}$. In this manner, the heat load of one block can be obtained as the sum of the previous load steps, as it is shown in the equation (3.70).

$$\dot{q}_n = \sum_{i=1}^n \dot{q}_i^* = \sum_{i=1}^n (\dot{q}_i - \dot{q}_{i-1}) \quad (3.70)$$

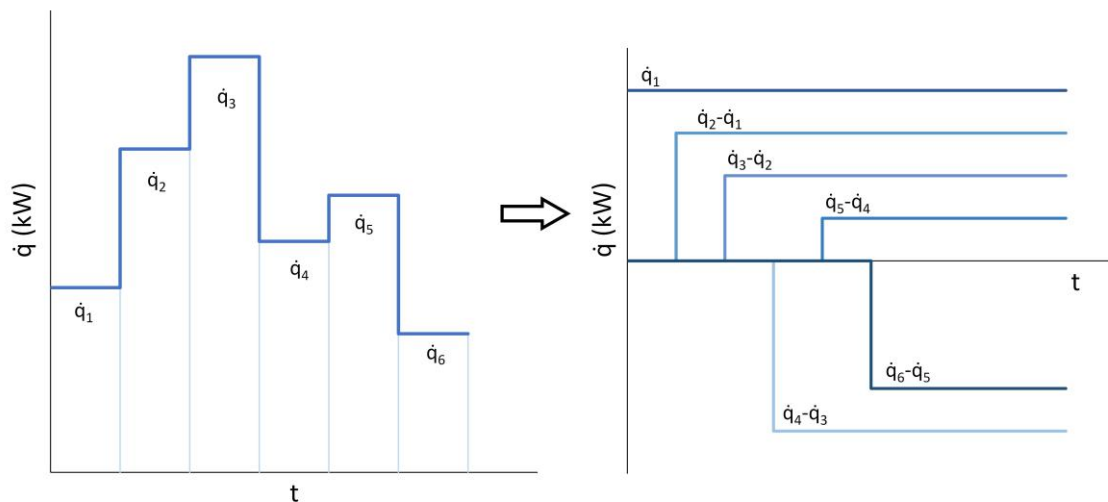


Figure 3.24. Superposition of piecewise heat steps. The actual heat steps are superimposed in time [130]

Therefore, it is possible to calculate the ground response at a certain time by superposition of the response caused by each of the accumulated heat steps until the corresponding time, considering the moment in which each step started (t_i) to calculate the

ground response corresponding to that step. So, the ground temperature alteration at the moment (t) at a radial distance (r) from the centre of each BHE will be calculated using the equations (3.71) and (3.72).

$$T(r, t) - T_0 = \sum_{i=1}^n \frac{\dot{q}_i - \dot{q}_{i-1}}{2\pi\lambda} \cdot \left[\ln \frac{r_{\infty,i}}{r} - 0.9818 + \sum_{1}^N \frac{(-1)^{N+1}}{2N \cdot N!} \left(\frac{4r^2}{r_{\infty,i}^2} \right)^N \right] \quad (3.71)$$

$$r_{\infty,i} = 4\sqrt{\alpha(t - t_i)} \quad (3.72)$$

This equation is calculated fast enough with a small number of steps, but as the simulation time increases, the number of steps increases, therefore, the computational time increases, too. In order to avoid very long computational times and decrease the memory space needed to store all the data, a load aggregation technique was used. Some examples of load aggregation algorithms are found in the work of Zhang et al. [55], Yavuzturk and Spstiler [113] and Bernier et al. [114].

In the calculation of the ground temperature alteration due to the heat injected, the most recent injected thermal loads have a higher influence in the final temperature variation, because the effect of one thermal load will be stabilized with time and the effect in the temperature alteration will be much lower. Therefore, it is possible to merge the older heat steps in averaged bigger blocks after some certain time in which the effect of these steps has been reduced significantly. With this methodology, the number of heat steps to use in the equation (3.71) will be reduced, and the accuracy of the calculation will not be greatly affected. Furthermore, the computational cost will be reduced.

In this LSA TRNSYS model, as it might involve a great number of load blocks, variable size aggregation blocks are used, instead of using bigger aggregation blocks, following the telescopic aggregation algorithm explained in [115]. This algorithm is based on two parameters: an aggregation factor, k_a , and a margin value, m_a . The duration of each initial heat step is Δt , so the steps that the algorithm follows are:

- a) Initially, the initial load blocks (with a duration of Δt) are added to the load profile as blocks of type 1 (B-1).
- b) When there are a total of $k_a + m_a$ blocks of type 1 (this is, at a time $t = (k_a + m_a) \cdot \Delta t$), the first k_a blocks of type 1 are merged in an average block of type 2 and a duration of $k_a \cdot \Delta t$. Therefore, the $k_a + m_a$ initial blocks are represented by one block of type 2 and m_a blocks of type 1.
- c) After some time equal to $k_a \cdot \Delta t$, the next k_a blocks of type 1 are assembled, so there will be two blocks of type 2 and m_a blocks of type 1.
- d) This process goes on until there are $k_a + m_a$ blocks of type 2 and m_a blocks of type 1. In this moment, the first k_a blocks of type 2 are assembled in a type 3 block, with a duration of $k_a^2 \cdot \Delta t$. Therefore, there will be one block of type 3, m_a blocks of type 2 and m_a blocks of type 1.

With this algorithm, the heat loads are aggregated forming growing blocks with time, but always keeping a minimum number of blocks of each type that ensures the accuracy of

the model, thanks to the margin value m_a . Furthermore, it is not necessary that all the type 1 blocks have the same duration, making the model more flexible. Figure 3.25 shows an example of this load aggregation method using the parameters $k_a = 5$ and $m_a = 1$.

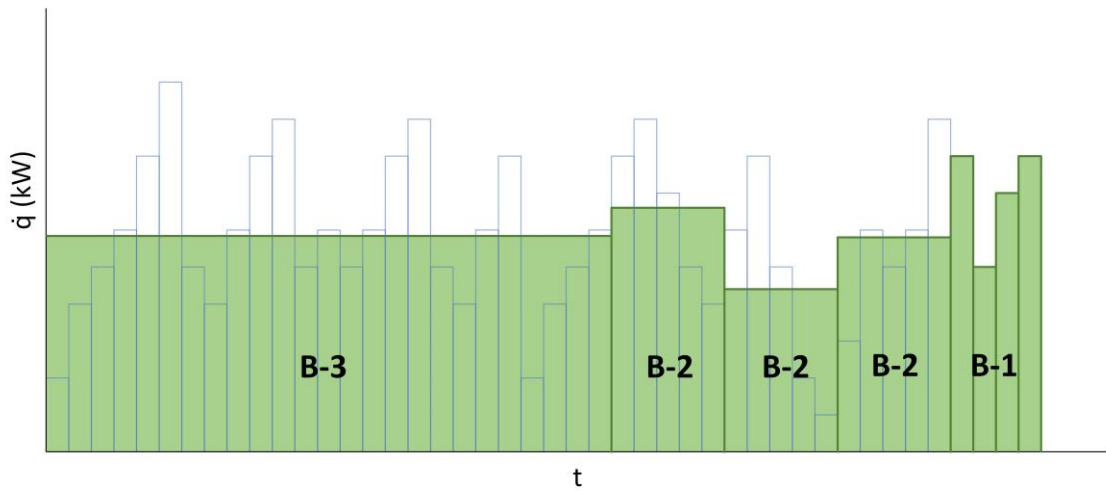


Figure 3.25. Load aggregation [130]

3.7.3 LSA model implementation in TRNSYS

The LSA model described in section 3.7.2 was implemented as a TRNSYS type using FORTRAN language. With this type, the temperature variation at the borehole wall for every BHE in a field of BHEs is calculated, considering the effect of the heat injection from all of the BHEs in the field. The average temperature is calculated and is used as the borehole wall temperature in a BHE model (in this case, the B2G model), representing all the BHEs in the field with this average BHE.

In the type, the main parameters are first introduced: number of BHEs in the field, borehole depth, undisturbed ground temperature, ground conductivity, ground volumetric capacity and the parameters k_a and m_a . Based on the previous work [115], the values of the aggregation algorithm parameters that will be used in all the simulations are $k_a = 10$ and $m_a = 5$. The BHEs field configuration is introduced as an external file, where the coordinates of the different BHEs location are defined. The distance at which the ground temperature will be calculated is also introduced as a parameter, normally it would be the borehole wall.

The heat loads will be introduced as inputs at every simulation time step and they will be integrated in order to form a unitary heat step (type 1 block), the duration of each heat step (Δt) will be defined by an input signal (step signal) and it can be different during the simulation, so the total heat injected in the simulation time step will be introduced and it will be divided by the borehole depth and it will be summed up until the time step in which the step signal changes its value, forming a heat step (in W/m) with a determined duration Δt . The heat steps will be aggregated along the simulation time according to the algorithm explained in section 3.7.2.

At the moment of each heat step aggregation, the temperature at the borehole wall is calculated for all the BHEs in the field, considering the effect of the heat injection from each BHE in the centre of the rest of the BHEs. In this way, the average borehole wall temperature is calculated and can be used in the B2G model at the start of the day in order to consider the mid- and long-term heat injection in the ground and the interaction between BHEs.

The coupling between the B2G model and the LSA is shown in Figure 3.26. The heat transfer between the BHE and the ground is calculated by the B2G model and it is introduced in the LSA model. At the start of each day's operation, the LSA recalculates the borehole wall temperature considering all the previous heat injection and it introduces this temperature as an input in the B2G model. It will consider this recalculated temperature as the ground temperature in the B2G model.

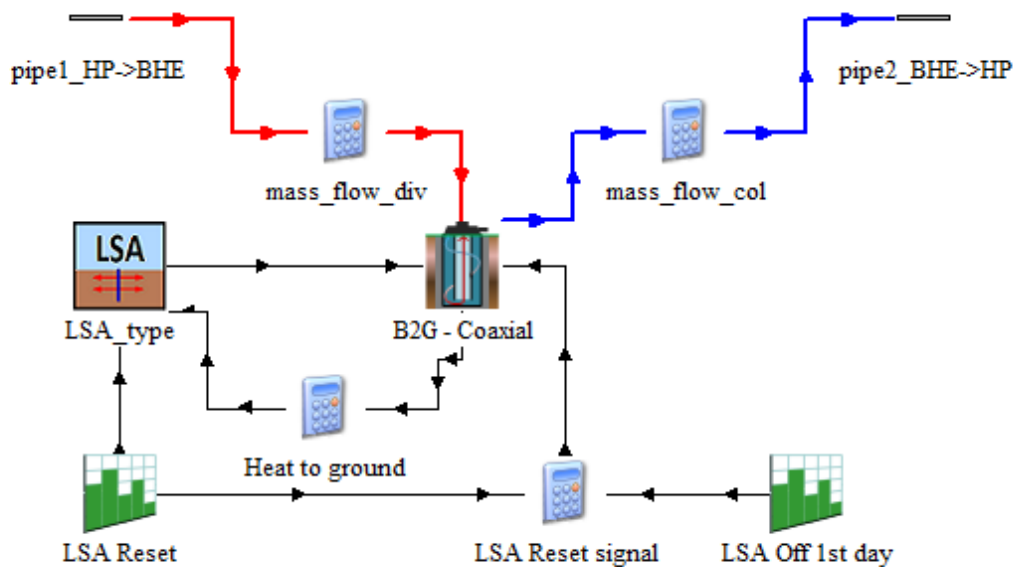


Figure 3.26. TRNSYS layout for the coupling between the B2G and the LSA models

3.7.3.1 Validation of the LSA model

In order to validate the LSA model, first it was compared with other models commonly used for the designing and simulation of BHEs: EED, DST and SBM, without using the load aggregation algorithm. Second, the accuracy of the aggregation algorithm was tested and finally, the coupling with the B2G model was analysed and compared with a pre-generated *g-function*.

For the comparison with other simulation models, a monthly thermal load was considered for 12 months (in W/m), and a 25 years simulation was carried out with the same monthly load profile. The BHE considered for the evaluation was a coaxial BHE with the geometric characteristics of the coaxial spiral BHE described in Table 3.6. A borehole resistance of 0.0982 K/(W/m) and an undisturbed ground temperature of 10°C was considered for the calculation of the fluid temperature. The comparison between models is shown in Figure 3.27, where a good agreement between the results of the different models can be seen.

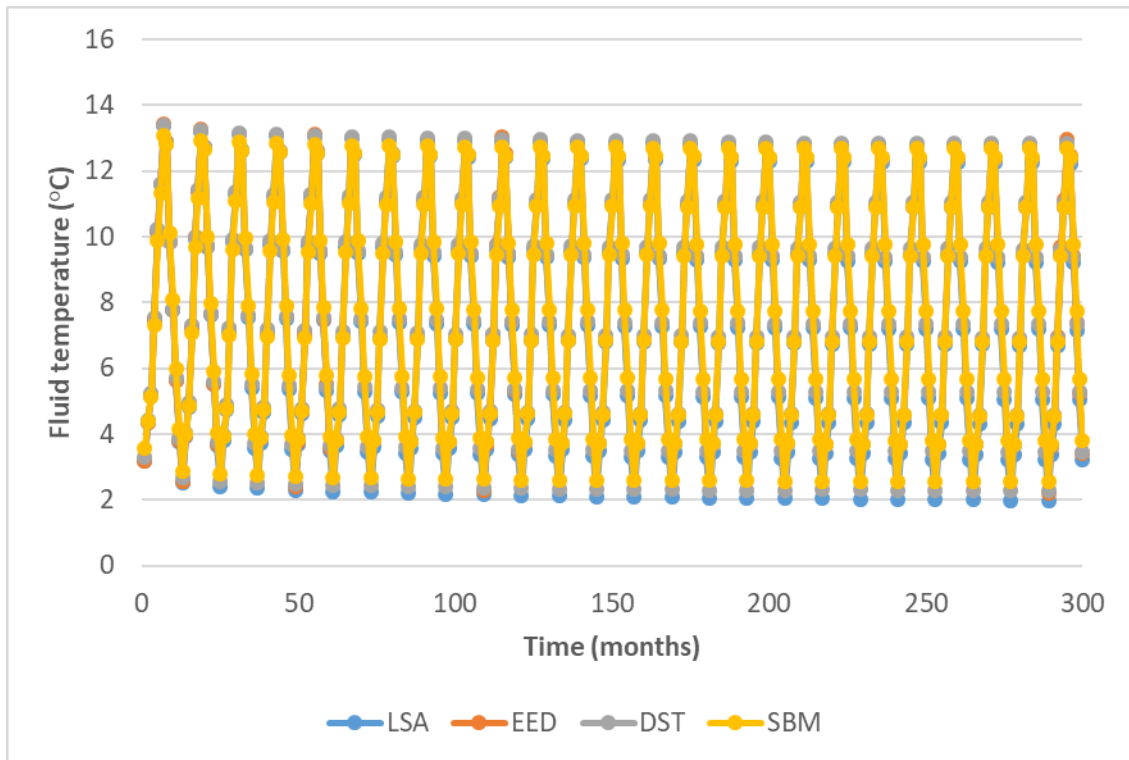


Figure 3.27. Comparison between LSA model and other simulation models

In order to check the accuracy of the load aggregation technique, several simulations with different load profiles are carried out and compared with the results obtained by the LSA tool, but instead of using the load aggregation algorithm, the temperature calculation considers all the unitary heat loads each time step. The simulation times were reduced considerably and the accuracy of applying the aggregation algorithm was quite high.

The simulated scenarios were the following:

- 1) Daily load profile for 1 month (heat extraction), repeated during 25 years.
 - a) 1 BHE and time step of 1 hour.
 - b) 9 BHEs in a 3x3 configuration and a separation of 3 m and time step of 1 hour.
- 2) Hourly load profile, repeated during 5 years.
 - a) 9 BHEs in a 3x3 configuration and a separation of 3 m.

The RMSE was calculated between the model with aggregation algorithm and without, and the simulation time of the LSA model with aggregation algorithm was measured. This is shown in Table 3.21.

Table 3.21. Error in applying the aggregation algorithm to the LSA model

	RMSE (K)	Simulation time (min)
Scenario 1 a)	0.007	3
Scenario 1 b)	0.006	3
Scenario 2	0.017	1

It can be concluded that the error produced because of the application of the aggregation algorithm to the LSA model is quite small, and the resulting simulation time is rather short.

For example, the application of the LSA without aggregation algorithm in the scenario 2 produces a simulation time of around 2 hours, whereas with the aggregation algorithm the simulation time is around 1 minute.

Finally, the coupling of the B2G model with the LSA was checked in order to validate the applicability of the LSA model for calculating the long-term response of the BHE together with the B2G model. In previous works [115], [139], the coupling between the U-tube B2G model and a pre-generated *g-function* was studied. So, this coupling was compared with the coupling between the U-tube B2G model and the LSA type in order to check the validity of this new model.

Experimental data from a GSHP system installed at the Applied Thermodynamics department, in the *Universitat Politècnica de València* was used. This installation is further described in [140]. The BHEs field consists of 6 BHEs with a depth of 50 m each one.

The simulation was carried out considering the experimental data for one BHE during 5 weeks of operation. The inlet temperature and mass flow rate for one BHE is used as inputs for the B2G model and the experimental outlet temperature is compared with the outlet temperature calculated with the B2G model when coupled with the *g-function* or the LSA model. The main parameters of the BHE are summarized in Table 3.22. Two different scenarios were considered in the LSA model: one considering only one BHE for the calculation of the borehole wall temperature and other scenario in which the BHEs field is considered (2x3 rectangular grid with a separation of 3 m between BHEs), so the interaction between BHEs is calculated and the average temperature is used as the borehole wall temperature. The heat steps are introduced in blocks of 15 and 9 hours: from 6 a.m. to 9 p.m. (heat injection period) and from 9 p.m. to 6 a.m. of the following day (recuperation period with no operation of the system) and the borehole wall temperature is calculated at 6 a.m. (the starting time of the system). The system is not working during the weekends, so this period is not considered.

Table 3.22. U-tube BHE parameters

Parameter	Value
Thermal conductivity	2.09 W/m·K
Thermal volumetric heat capacity	3500 kJ/m ³ ·K
Undisturbed ground temperature	20 °C
Borehole diameter	150 mm
Inner/Outer diameter of the pipe	25.4/32 mm
Depth	50 m

The borehole wall temperature calculated by the *g-function* is compared with the one calculated by the LSA model at the starting of the system each day for the two assumptions (LSA with one BHE field configuration and LSA with six BHEs field configuration). The results are shown in Figure 3.28. The difference between models is also plotted. The RMSE between the *g-function* simulation and the LSA model simulations are 0.03K for the BHE field configuration of 1 BHE and 0.02K in the case of the 6 BHEs configuration. In addition,

it is possible to see that the assumption of a 6 BHEs field configuration produces more accurate results during the whole simulation, whereas in the case of 1 BHE, the error is increasing during the last days.

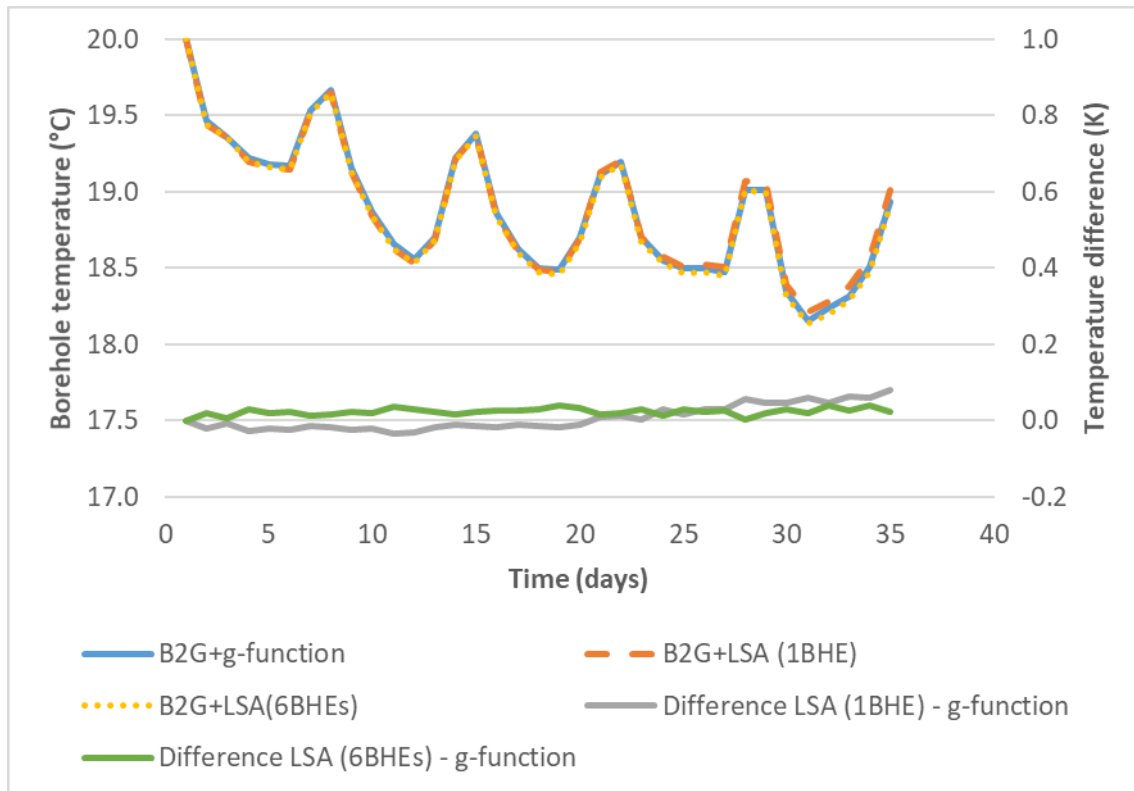


Figure 3.28. Comparison between the LSA model and g-function: Borehole wall temperature

In addition, the BHE outlet temperature was also analysed and the results obtained from the simulations using the B2G model coupled with the *g-function* and LSA models are compared. For this purpose, the daily average outlet temperature is calculated and plotted in Figure 3.29. It is possible to see that the LSA model produces results very similar to the *g-function*. Therefore, it is possible to use the LSA model as an alternative to the *g-function* with the increase in the flexibility that this implies, as there is no need of generating it previously for each specific BHE field configuration.

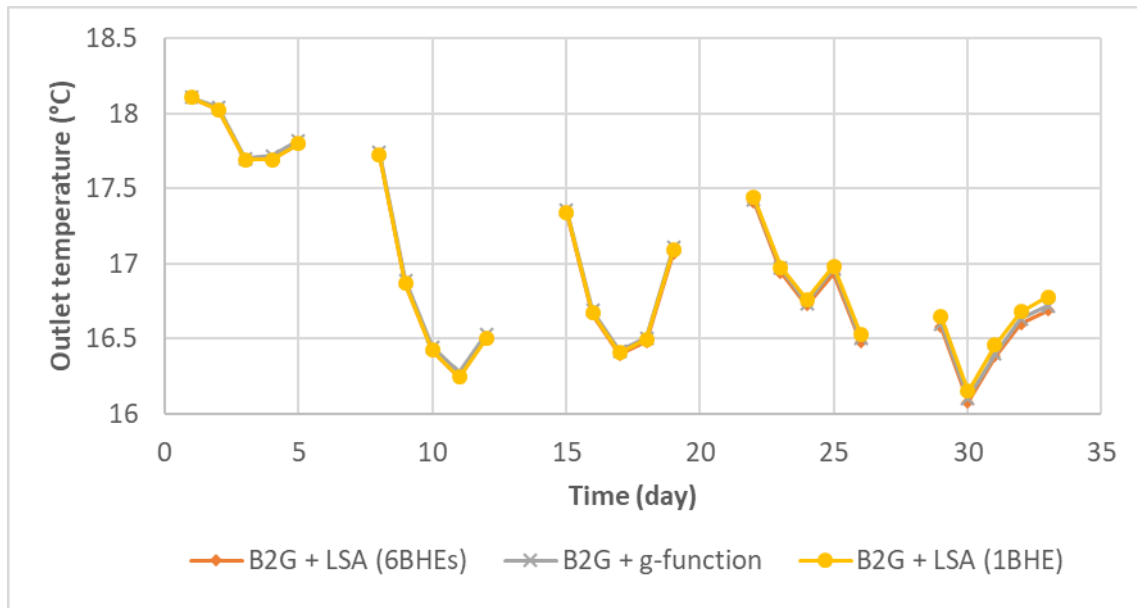


Figure 3.29. Comparison between the LSA model and g-function coupled with B2G model: BHE outlet temperature

Chapter 4

4 Modelling of the dual source heat pump system

4.1 Introduction

A complete dynamic system model that is able to reproduce the behaviour of the different components of the system and the coupling between them, is a useful tool to assist in the design and optimization of the different components and the entire system. As it is able to fairly reproduce the reality, it can act as a virtual facility, in which different control and optimization strategies can be tested without the need of testing them on site, as well as different designs and working conditions, for example, different climatic conditions. It is also possible to carry out an assessment of the system in order to find the optimal scenario among the ones tested.

In the case of GSHP and DSHP systems, it is possible to find in the literature models of these systems, following different approaches and for different purposes. A review of models of GSHP systems and specially DSHP systems in different software and especially in TRNSYS is presented in the following. In addition, a brief introduction to control strategies for this type of systems and some examples are presented.

4.1.1 Dynamic modelling of GSHP and DSHP systems

A lot of research have been carried out regarding the modelling of GSHP and DSHP systems, as they are not conventional systems and it is very important to design and operate them in an optimal manner in order to be able to compete with other conventional systems. In this background, several authors have developed models in order to assess the performance of the systems under different scenarios and find the optimal one, also understanding better how the system behave under different control strategies.

Regarding GSHP systems, several authors addressed the modelling and assessment of these systems, in this regard, TRNSYS is one of the most used simulation programs. This software allows the simulation of transient systems, and it incorporates a wide library of typically used components, modelled as a black box (called *types*), and the interconnection between components to form the entire system.

In [14], a GSHP system was modelled in TRNSYS in order to study the performance of this system applied for different building types in different climates in Europe. In [141], a hybrid ground-coupled heat pump system for heating and cooling with an electric heater for domestic hot water production was simulated using the software HVACSIM+. A GSHP system in Tunisia for heating applications with an on/off compressor was modelled in TRNSYS and the performance of the heat pump, working with CO₂ was studied [142]. The

main differences existing between air source and ground source heat pumps were studied by Safa et al. by modelling and simulating a variable capacity air source heat pump system and a horizontal ground loop GSHP system in different Canadian cities using TRNSYS [143]. A complete dynamic model in TRNSYS of a GSHP system providing heating and cooling to a departmental building in Valencia (Spain) was presented in [130], [144], where all the components were modelled and experimentally validated, including the building, fan coils, the heat pump and a dynamic BHE model.

In the case of hybrid and heat pump systems, several studies have been carried out by modelling and simulating these systems. A residential house in Tunisia was modelled in TRNSYS and coupled to a dual source heat pump using TRNSYS [145]. Standard types were used for the modelling of a CO₂ heat pump that can work with two sources: water from a tank or surface of water and the air. In [146], a dynamic model of a hybrid heat pump system (heat pump and condensing boiler) was developed in TRNSYS to study the influence of the cut-off temperature in the annual efficiency.

Regarding the modelling of DSHP systems with heat pump units that are able to work both with the air and the ground, recently research work have been carried out. Grossi et al. [147] developed a dynamic model in TRNSYS with a DSHP inverter driven and a residential building in Bologna (Italy). The heat pump used a switching temperature in order to select the air or the ground as a source. The modelling of the heat pump was developed by using a series of characteristic curves from the manufacturer and a standard U-tube BHE model was used (type 557b), which models the BHE using a fixed borehole resistance. An assessment of the system performance was carried out for the long-term and it was studied the optimal switching temperature. They concluded that this type of systems could lead to a reduction of the length of BHEs needed. Another study with a system working with a DSHP unit, able to work both with the air and the ground as a source, also using a switching temperature to select the source, was carried out in [148]. The authors developed a model via EnergyPlus software and simulated the system coupled to an office building in Padova (Italy) for eleven years, studying the performance of the system under different switching temperatures.

4.1.2 Control of systems

The main objective of heating and cooling systems, such as GSHP and DSHP systems, is to provide thermal comfort inside the conditioned spaces, always trying to reduce the energy consumption as much as possible, as well as to do it in an environmentally friendly way. In this regard, the optimization of the control of the entire system and each individual component is important in order to reduce the contribution of the different subsystems to the total energy consumption and the overall consumption. This is why the study of control and optimization strategies have been a key issue in the improvement of the efficiency of the systems. In this framework, several experimental and theoretical studies were carried out in order to develop control strategies that reduce the energy consumption of the systems but ensuring that the final objective is fulfilled (in this case, provide thermal

comfort). A review about control systems in heating and cooling applications and heat pumps can be found in [149].

The capacity control of residential heat pump heating systems was studied by Karlsson [150] by investigating the application of variable-speed capacity control to compressor, pumps and fans for optimizing the system operation. In the case of GSHP systems, the control of variable capacity heat pumps was studied by Madani [151], in the case of Swedish single-family dwellings. A model of the system was developed in TRNSYS and EES and used as a simulation tool in order to compare the seasonal performance of the systems using single or variable speed compressors. Furthermore, several control strategies for on/off compressor GSHPs were analysed by using the developed model. In [39], different control and optimization strategies were simulated using a TRNSYS model for a hybrid GSHP combined with a cooling tower in order to find the strategy that produces a lower cost under different climatic conditions. In [152], [153], the authors developed an integrated control strategy, based in part on experimental measurements, in which the speed of the compressor, circulation pumps and fan coils is varied, as well as the temperature setpoint. For this purpose, a dynamic model of the GSHP was developed.

Several studies were carried out in the optimization of the mass flow rates and the control of the circulation pumps in GSHP systems. In [154], the authors developed control strategies to predict the optimal GSHP water flow rates under partial load operation, increasing the system seasonal performance in between 20% and 40% using the experimental data from a GSHP installation in Valencia (Spain). The same installation was the object of study for developing an in-situ methodology for optimizing the frequency of the circulation pumps with a fixed capacity compressor working under variable partial load ratios [155]. Later on, this methodology was extended to the use for a multistage GSHP [156] and upgraded to ensure the thermal comfort in the conditioned spaces [157], resulting in an optimization algorithm that sets the frequency of the circulation pumps and the desired supply temperature depending on the ambient conditions and the partial load ratio. Then adapting the water temperature supply and the water mass flow rates in order to meet the thermal demand under the different ambient conditions. This strategies were later implemented in the control of the system, achieving improvement of around 33% in the efficiency of the system.

4.1.3 Approach to the dual source heat pump system modelling

Against this background, a dynamic model in TRNSYS have been developed for the DSHP plug and play system developed in the framework of the GEOTeCH project. For this purpose, a specific model of the innovative DSHP unit has been implemented in TRNSYS as a type and the specific BHE model described in chapter 3, already implemented as a TRNSYS type. The modelling of the DSHP has been carried out based on several correlations that calculate the performance of the heat pump depending on the operating variables. These correlations were previously obtained based on the experimental campaign carried out for the prototype #1 of the DSHP in the laboratory of the Institute for Energy Engineering [50]. The

description of the DSHP model and its implementation in TRNSYS is described in section 4.2.

As this system model incorporates the different components and it is capable of fairly reproducing the behaviour of the system working under different operating conditions and control strategies, it can be used as a virtual facility in order to assist in the development and testing of different optimization and control strategies before testing them experimentally. Then, it is possible to perform an energy assessment of the system in different climatic conditions and calculate the seasonal performance, analysing in which climates it would be more suitable to implement this system. Different control strategies have been implemented in the model, the main strategy relates to the selection of the optimal source/sink at each moment. In order to select the source, the temperature of the air and the ground is compared at every time step, selecting the most favourable (higher temperature for heating and lower temperature for cooling), considering a hysteresis in order to prevent the heat pump to change the operating mode very quickly. This model was previously presented in different scientific and conference papers [48], [158], [159] and it is described in detail in section 4.3, including the modelling of the different subsystems and control strategies. The assessment of the system performance under different climatic conditions is presented in section 5.1.

In order to simplify the DSHP model and be able to perform an assessment under different thermal demands, the building modelling was not included in the TRNSYS model, but the hourly thermal loads are introduced as an input and previously calculated apart in another detailed TRNSYS model of the building.

On the other hand, another TRNSYS model has been developed and adapted to the demonstration installation of Tribano (one of the demo-sites installed inside the GEOTeCH project), including a detailed model of the office building and the fan coils. Then the coupling between the heat pump and the building is fairly reproduced, considering the fan coils behaviour. This model is used for testing different control and optimization strategies, specifically, the control of the variable speed heat pump compressor based on the temperature inside the conditioned space, instead of controlling the water in the supply/return of the user circuit. In order to focus on the testing of this control strategy, it is considered that the DSHP provides only heating and cooling (not DHW) using the air as a source/sink (but not the ground). This model is detailed in section 4.4.

In this type of systems, the return temperature is usually controlled because it is simpler to implement the PID controller and the temperature sensor inside the same heat pump unit, also the inlet temperature is more constant, what is good for the compressor life. On the other hand, controlling the supply temperature is more efficient from the point of view of the user comfort, because the water entering the emission system will have a more constant temperature, maintaining the comfort inside the air-conditioned spaces. If the controlled temperature is the return temperature, the supply temperature will vary depending on the heat pump capacity at each moment. The new strategy proposed, consists in varying the compressor frequency in order to reach the desired operative temperature

in all the conditioned spaces. For this purpose, at each moment the temperature evolution in all the rooms is analysed and the worst room is selected as the controlled room in that moment, so the PID controller will set the frequency of the compressor in order to reach the comfort temperature. In order to prevent the heat pump supply temperature to reach extreme temperatures, a limit is set. This limit will be varied and analysed in a parametric analysis carried out in the model and presented in section 5.2.

4.2 Hybrid dual source heat pump model

The Dual Source Heat Pump (DSHP) described in section 2.2.3 was tested in the laboratory of the Institute of Energy Engineering in the *Universitat Politècnica de València* and modelled by the same research group. The experimental data measured in the different tests were used to obtain polynomial correlations that model the behaviour of the heat pump working in different operating modes and under different conditions. These correlations were implemented in a TRNSYS type as part of this PhD dissertation, so it is possible to use the heat pump model in a complete DSHP system in TRNSYS.

The DSHP is capable of producing heating, cooling and DHW both in summer and winter conditions. Moreover, it can work with the air or the ground as a source/sink. In total, the heat pump can operate in nine different modes. Additionally, the DSHP system includes a free-cooling heat exchanger that can be used separately from the heat pump. As a result, the DSHP system is capable of working in eleven different operating modes, as shown in Table 2.1.

Inside the DSHP TRNSYS type, the polynomial correlations obtained for the different operating modes were implemented, so the type will calculate the condenser and evaporator capacities, as well as the compressor power, depending on the operating mode and the different working conditions: compressor frequency, inlet temperature in condenser and evaporator, temperature difference in the condenser and evaporator, air temperature or fan speed.

4.2.1 Experimental tests and characterisation

An experimental test campaign was carried out at the facilities of the Institute of Energy Engineering, at the *Universitat Politècnica de València* in order to fully characterise and model the performance of the DSHP [48], [50]. For this purpose, a test bench was used to test the heat pump working in the different modes and under different operation conditions. The test bench was composed of three hydraulic loops: user, ground and DHW and a climatic chamber to assure stable conditions in all the operating modes.

The capacities of the heat pump in the different heat exchangers were measured at the water side, also the heat pump electric consumption, the fluid mass flow rates and the supply and return temperatures at each loop. Additionally, it was monitored the temperature, humidity and pressure in other points.

The main variables to characterise the heat pump performance are the condenser capacity (\dot{Q}_c), the evaporator capacity (\dot{Q}_e) and the compressor power input (\dot{W}_c), while the

independent variables are 5: the compressor frequency (f_c), inlet temperature to the evaporator (T_{ei}) and condenser (T_{ci}), and the temperature difference across the evaporator (dTe) and condenser (dTc), when the heat pump is working with the ground. When the heat pump is working with the air, the temperature difference across the evaporator (in winter mode) or condenser (in summer mode) is replaced by the fan speed (f_{fan}).

In order to characterise the performance of the unit for all the operating modes and a range of operating conditions as broad as possible, a simulation software was first employed to provide an estimation of the response surface and obtain a polynomial correlation that fits the performance of the heat pump under the different operation conditions with the minimum number of regression coefficients. For this purpose, the IMST-ART software [160] was used and 640 points were simulated. With these results, the adequate response surface was obtained using the multi-linear regression method, resulting in a polynomial expression.

After this, a test matrix of 227 points was selected to carry out the experimental tests, following the DoE methodology Central Composite Design (CCD). As an example of the DSHP performance, Figure 4.1 and Figure 4.2 show the heating capacity, compressor power input and the COP of the heat pump (considering only the compressor consumption) for M5-Winter Ground (heating using the ground as a source) and M4-Winter Air (heating using the air as a source) operating modes, respectively. The inlet temperature at the condenser is 40°C and the temperature difference across the condenser is 5K. In the M5-Winter Ground mode, the inlet temperature at the evaporator (brine temperature from the ground loop) is 0°C and the temperature difference across the evaporator is 3K, while in the M4-Winter Air mode, the inlet temperature at the evaporator is the air temperature, the dry bulb temperature was 7°C (wet bulb temperature of 6°C) and the fan speed was 50%.

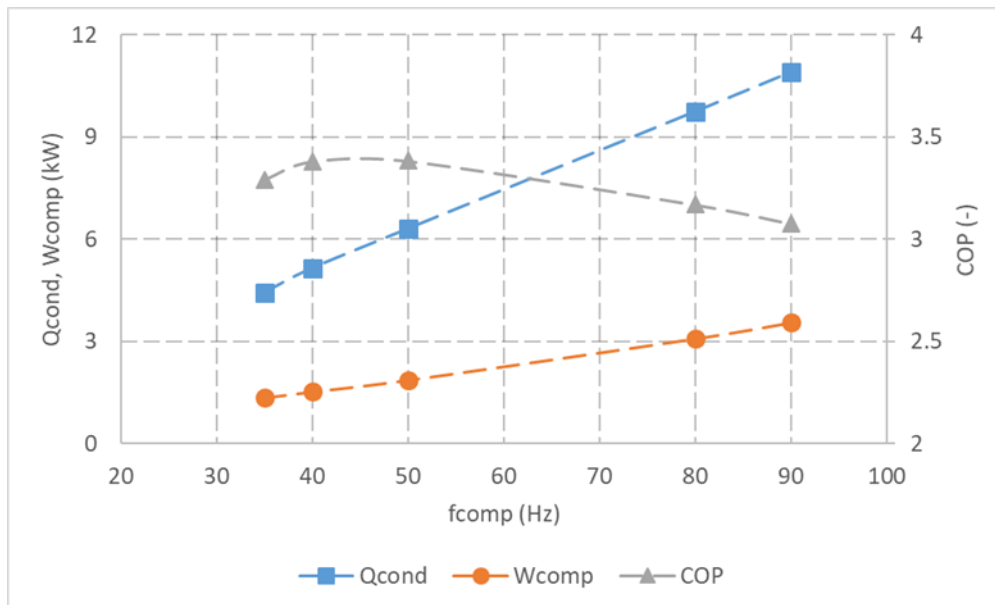


Figure 4.1. Condenser capacity, compressor power input and compressor COP in M5-Winter Ground operating mode ($T_{ci}=40^\circ\text{C}$, $dTc=5\text{ K}$, $T_{ei}=0^\circ\text{C}$, $dTe=3\text{K}$) [48]

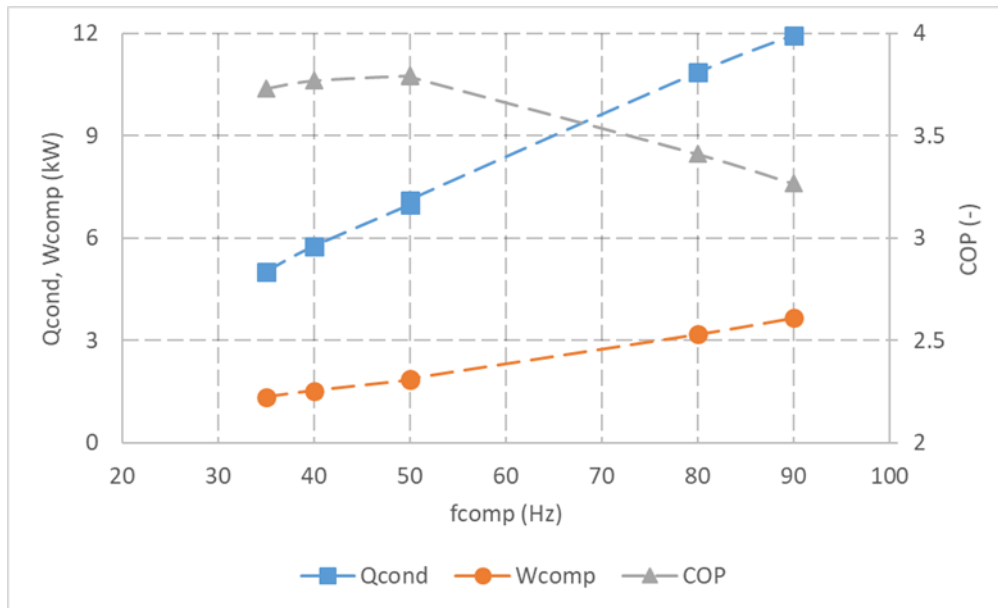


Figure 4.2. Condenser capacity, compressor power input and compressor COP in M4-Winter Air operating mode ($T_{ci}=40^{\circ}\text{C}$, $dT_c=5\text{ K}$, $T_{air}=7(6)^{\circ}\text{C}$, $f_{fan}=50\%$) [48]

The results from the experimental tests were used to adjust the polynomial correlations and obtain the regression coefficients that characterise the heat pump performance with the highest accuracy. The accuracy of the new correlations was tested, comparing the predicted performance with the experimental points, resulting in a very good agreement in all the operating modes. In Figure 4.3, it is compared the correlated and experimental compressor power input and condenser capacity for the M5-Winter Ground operating mode. The maximum deviations are lower than 3.2% for the compressor consumption and 2.6% for the condenser capacity. The maximum deviations in all the operating modes are lower than 5% [48].

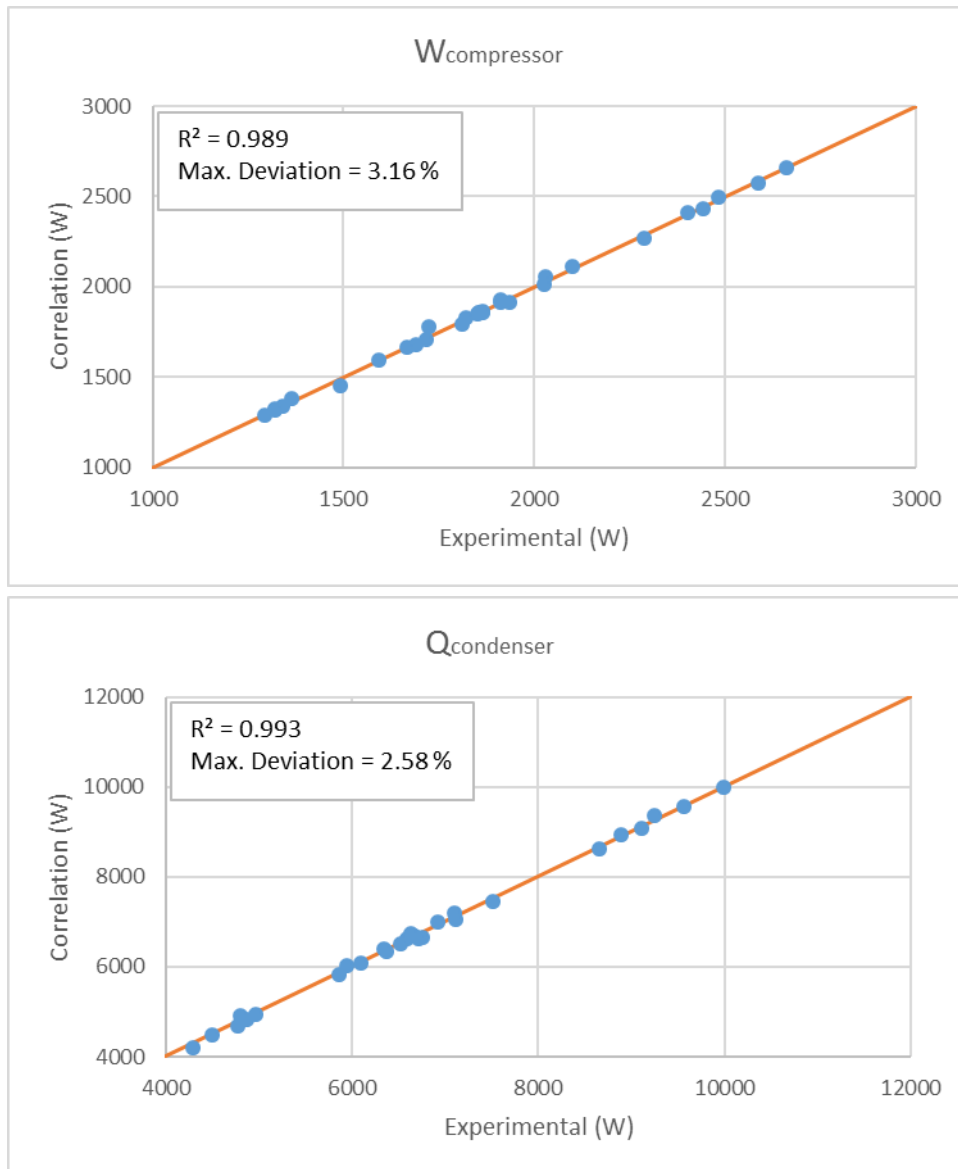


Figure 4.3. Comparison between experimental measurements and polynomial correlations for M5- Winter Ground mode: compressor consumption and condenser capacity [48]

4.2.2 Polynomial correlations for the DSHP performance calculation

With the obtained polynomial correlations it is possible to calculate the performance variables (condenser capacity (\dot{Q}_c), evaporator capacity (\dot{Q}_e) and compressor power input (\dot{W}_c), all expressed in Watts (W)) as a function of five of the independent variables:

- Compressor frequency (f_c).
- Inlet temperature to the evaporator (T_{ei}).
- Inlet temperature to the condenser (T_{ci}).
- Temperature difference across the evaporator (dTe).
- Temperature difference across the condenser (dTc).
- Fan speed (f_{fan}).

The shape, the independent variables and the coefficients of the correlations will depend on the operating mode. The coefficients of each correlation ($C_0, C_1 \dots C_{10}$) are presented in the appendix B.

4.2.2.1 Summer Air correlations

For the operating mode M1-Summer Air, the independent variables are shown in Figure 4.4, where T_a is the air temperature. The expression that correlates the evaporator capacity (heat extracted from the user loop) is presented in the equation (4.1), the expression for the compressor consumption is presented in the equation (4.2).

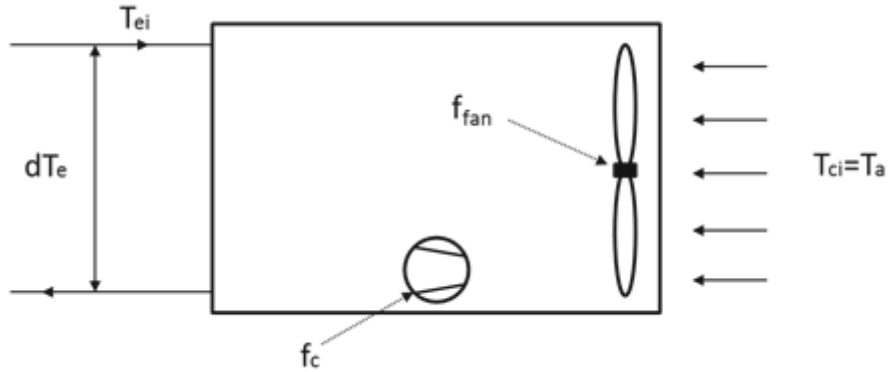


Figure 4.4. DSHP independent variables for mode M1-Summer Air [50].

$$\dot{Q}_e = f_c \cdot (C_0 + C_1 \cdot T_{ei} + C_2 \cdot T_{ci} + C_3 \cdot T_{ei} \cdot T_{ci} + C_4 \cdot T_{ei}^2 + C_5 \cdot dT_e + C_6 \cdot f_{fan} + C_7 \cdot T_{ei} \cdot dT_e + C_8 \cdot T_{ci} \cdot f_{fan}) \quad (4.1)$$

$$\dot{W}_c = f_c \cdot (C_0 + C_1 \cdot T_{ei}^2 + C_2 \cdot T_{ci}^2 + C_3 \cdot dT_e + C_4 \cdot f_{fan} + C_5 \cdot T_{ei} \cdot dT_e + C_6 \cdot f_c \cdot T_{ei} + C_7 \cdot f_c \cdot T_{ci} + C_8 \cdot f_c^2 \cdot T_{ei} \cdot T_{ci} + C_9 \cdot f_c \cdot dT_e + C_{10} \cdot \frac{1}{f_c}) \quad (4.2)$$

4.2.2.2 Winter Air and DHW Air correlation

For the M4-Winter Air and DHW Air (M6 and M7) operating modes, the independent variables are shown in Figure 4.5. The condenser capacity is calculated by the equation (4.3) and the compressor consumption by the equation (4.4). The condenser capacity corresponds to the heat provided to the user loop (Winter Air mode) or the heat provided to the DHW loop (DHW Air mode).

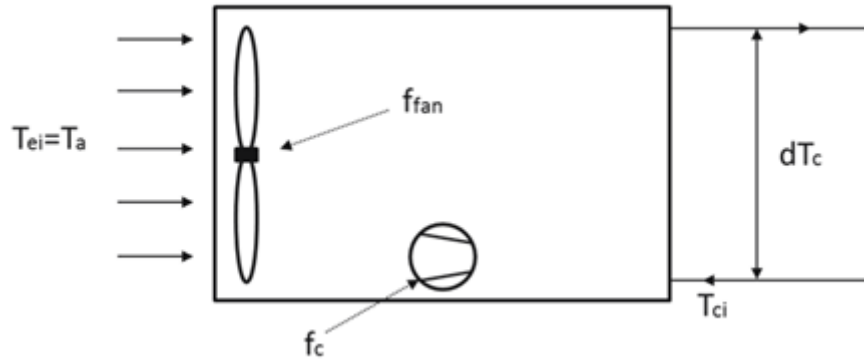


Figure 4.5. DSHP independent variables for modes M4-Winter Air, M6 and M7-DHW Air [50].

$$\dot{Q}_c = f_c \cdot (C0 + C1 \cdot Tei + C2 \cdot Tci + C3 \cdot Tei \cdot Tci + C4 \cdot Tei^2 + C5 \cdot f_{fan} + C6 \cdot dTc + C7 \cdot Tei \cdot f_{fan} + C8 \cdot Tci \cdot dTc) \quad (4.3)$$

$$\dot{W}_c = f_c \cdot (C0 + C1 \cdot Tei^2 + C2 \cdot Tci^2 + C3 \cdot f_{fan} + C4 \cdot dTc + C5 \cdot Tei \cdot f_{fan} + C6 \cdot f_c \cdot Tei + C7 \cdot f_c \cdot Tci + C8 \cdot f_c^2 \cdot Tei \cdot Tci + C9 \cdot f_c \cdot f_{fan} + C10 \cdot \frac{1}{f_c}) \quad (4.4)$$

4.2.2.3 Summer Ground, DHW User, Winter Ground and DHW Ground correlations

For the operating modes where the ground is used as a source/sink, the independent variables are shown in Figure 4.6. The condenser capacity is calculated by the equation (4.5), the evaporator capacity by the equation (4.6) and the compressor consumption by the equation (4.7). In summer mode (M2-Summer Ground), the evaporator capacity represents the heat extracted from the user loop and the condenser capacity the heat injected to the ground loop. On the other hand, in winter mode, the evaporator capacity represents the heat extracted from the ground loop and the condenser capacity, the heat injected to the user loop (M5-Winter Ground) or DHW loop (M8 and M9 DHW Ground). In the special case of M3- DHW User (Full recovery), the evaporator capacity represents the heat extracted from the user loop and the condenser capacity represents the heat injected to the DHW loop.

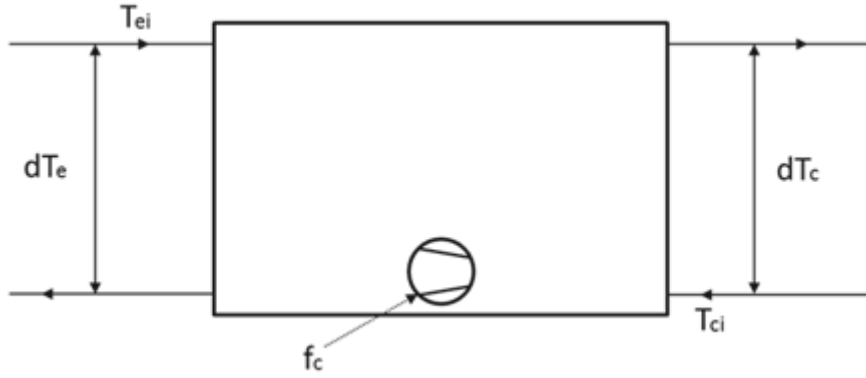


Figure 4.6. DSHP independent variables for modes M2-Summer Ground, M3 DHW-User, M5-Winter Ground, M8 and M9-DHW Ground [50].

$$\dot{Q}_c = f_c \cdot (C_0 + C_1 \cdot T_{ei} + C_2 \cdot T_{ci} + C_3 \cdot T_{ei} \cdot T_{ci} + C_4 \cdot T_{ei}^2 + C_5 \cdot dT_e + C_6 \cdot dT_c + C_7 \cdot T_{ei} \cdot dT_e + C_8 \cdot T_{ci} \cdot dT_c) \quad (4.5)$$

$$\dot{Q}_e = f_c \cdot (C_0 + C_1 \cdot T_{ei} + C_2 \cdot T_{ci} + C_3 \cdot T_{ei} \cdot T_{ci} + C_4 \cdot T_{ei}^2 + C_5 \cdot dT_e + C_6 \cdot dT_c + C_7 \cdot T_{ei} \cdot dT_e + C_8 \cdot T_{ci} \cdot dT_c) \quad (4.6)$$

$$\dot{W}_c = f_c \cdot (C_0 + C_1 \cdot T_{ei}^2 + C_2 \cdot T_{ci}^2 + C_3 \cdot dT_e + C_4 \cdot dT_c + C_5 \cdot T_{ei} \cdot dT_e + C_6 \cdot f_c \cdot T_{ei} + C_7 \cdot f_c \cdot T_{ci} + C_8 \cdot f_c^2 \cdot T_{ei} \cdot T_{ci} + C_9 \cdot f_c \cdot dT_e + C_{10} \cdot \frac{1}{f_c}) \quad (4.7)$$

As an illustrative example of the use of these correlations, Figure 4.7 shows the maps of the heat pump COP obtained from the polynomial correlations for the M5-Winter Ground mode. The $COP_{\text{compressor}}$ was calculated considering the compressor consumption only, while the COP_{global} was calculated considering also all the electric consumptions: the circulation pumps of the user and ground loops. The graphs on the left correspond to a supply temperature (T_{co}) of 45°C and the graphs on the right correspond to a supply temperature of 35°C.

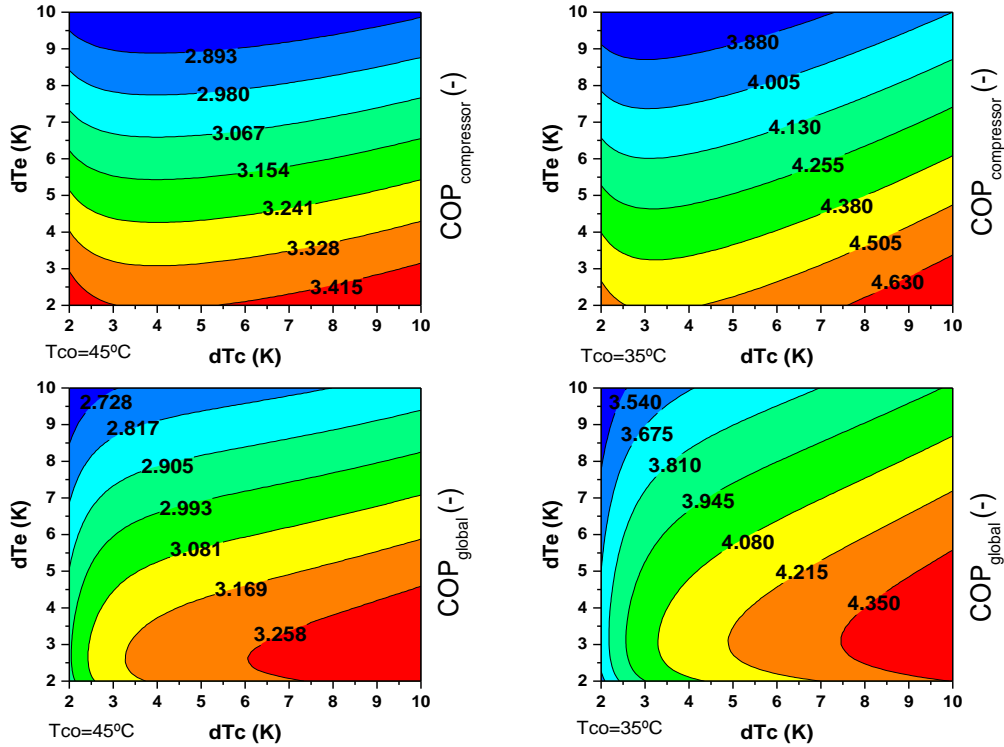


Figure 4.7. Compressor and global COP maps at different supply water temperatures ($T_{co}=45^{\circ}\text{C}$ on the left side, $T_{co}=35^{\circ}\text{C}$ on the right side) in the operating mode M5-Winter Ground, ($f_{comp} = 50 \text{ Hz}$, $T_{ei}=0^{\circ}\text{C}$) [48]

4.2.3 Fan characterization

The fan consumption was characterised based on the experimental results obtained during the test campaign. The correlation for the fan consumption is adjusted to a third-degree polynomial. As the heat pump incorporates two fans, the total fan consumption will be the consumption of 2 fans. This total fan consumption, \dot{W}_{fan} (W) is calculated according to the equation (4.8), where f_{fan} is the fan frequency (%).

$$\dot{W}_{fan} = 7.358 \cdot 10^{-4} \cdot f_{fan}^3 + 1.730 \cdot 10^{-2} \cdot f_{fan}^2 - 4.805 \cdot 10^{-2} \cdot f_{fan} \quad (4.8)$$

4.2.4 DSHP parasitic consumption

The heat pump parasitic consumption is composed of the electronics consumption (42 W) and the consumption required to energizing the solenoid valves (7.9 W each). When the heat pump is off, all valves are not energized. When the heat pump is on, there are always three solenoid valves energized. Therefore, parasitic consumption is calculated according to the equation (4.9), depending if the heat pump is on or off.

$$\dot{W}_{par,ON} = 42 + 3 \cdot 7.9 = 65.7 \text{ W} ; \quad \dot{W}_{par,OFF} = 42 \text{ W} \quad (4.9)$$

4.2.5 BPHEs pressure drop

The pressure drop in the BPHEs of the heat pump was characterised for each BPHE as a function of the mass flow rate through the corresponding loop, \dot{m} (kg/s) at a reference temperature of 25°C (298.15K). So, the reference pressure drop through one BPHE, ΔP_{ref} (Pa) is calculated according to the equation (4.10). The coefficients C1 and C2 for each BPHE are detailed in Table 4.1.

$$\Delta P_{ref} = C1 \cdot \dot{m} + C2 \cdot \dot{m}^{1.9} \quad (4.10)$$

Table 4.1. Coefficients for the calculation of the pressure drop at the BPHE of the DSHP

	User (BPHE F85)	DHW (BPHE B26)	Ground (BPHE F80AS)
C1	6.44E+03	5.55E+02	2.44E+03
C2	8.47E+04	6.38E+04	4.59E+04

In order to calculate the pressure drop at a different temperature, the pressure drop must be corrected with the real density (ρ) and dynamic viscosity (μ) of the corresponding fluid at the Average Temperature (AT) between the inlet and outlet, according to the equation (4.11). The density (ρ) and dynamic viscosity (μ) are calculated according to the equations (4.12) and (4.13), respectively. The coefficients to apply in these equations are different depending on the heat carrier fluid: water for the user and DHW loops and a mixture of propylene glycol and water for the ground loop with a 30% of propylene glycol.

$$\Delta P_{AT} = \Delta P_{ref} \cdot \left(\frac{\mu(AT)}{\mu(298.15)} \right)^{0.18} \cdot \frac{\rho(298.15)}{\rho(AT)} \quad (4.11)$$

$$\rho = C0 + C1 \cdot T + C2 \cdot T^2 + C3 \cdot T^3 \quad (4.12)$$

$$\mu = e^{C0+C1 \cdot \frac{1}{T} + C2 \cdot \frac{1}{T^2}} \quad (4.13)$$

Table 4.2. Coefficients for the calculation of the density and viscosity of the fluids

		WATER (USER, DHW)	PROPYLENE GLYCOL (Ground)
$\rho(T) \left(\frac{kg}{m^3} \right)$	C0	1.24E+01	5.40E+02
	C1	8.94E+00	4.93E+00
	C2	-2.59E-02	-1.52E-02
	C3	2.35E-05	1.36E-05
$\mu(T) (Pa \cdot s)$	C0	-7.11E+00	-2.49E+00
	C1	-2.00E+03	-5.14E+03
	C2	6.05E+05	1.22E+06

4.2.6 Free-cooling BPHE model

As explained in chapter 2, a free-cooling BPHE can be used in the DSHP system in order to provide cooling using the ground loop without the need of switching on the heat pump. This heat exchanger is external to the heat pump unit and a specific model was not selected inside the framework of the GEOTeCH project for the demo-sites. So, in order to develop a simple model that predicts the heat transfer between the ground and user loops inside the free-cooling loop, a specific BPHE model was selected and a correlation for the NTU (Number of Transfer Units) value was developed to characterise this heat transfer. This correlation have been implemented together with the DSHP correlations inside a unique TRNSYS type in order to model the behaviour of the DSHP system for all the eleven operating modes.

For the selection of the BPHE model, the SSP calculation software [161] was used, developed by SWEP, a manufacturer of BPHEs. This software incorporates the catalogue of SWEP's BPHEs and allows to select the most appropriate model depending on the required working conditions. The selected BPHE model was the B8LASW-N, with 30 plates.

The BPHE was simulated with the software for an inlet temperature of 10°C from the ground loop and 17°C from the user loop, assuming a mixture of MPG and water (30%) for the fluid in the ground loop and water in the user loop. A parametric calculation with different flow rates on the both sides was carried out, from 0.2 kg/s to 1 kg/s. A total number of 25 points were simulated and the effectiveness (ε) and the NTU values were calculated for each simulation point. A correlation was adjusted by a non-linear regression using the Solver tool in Microsoft Excel in order to minimize the difference between the simulated effectiveness and the correlated one. The resulting expression that correlates the NTU value is presented in the equation (4.14). Where A_{total} is the total area of heat exchange, N_p is the number of plates, \dot{m}_1 is the mass flow rate of the ground side (MPG 30%), \dot{m}_2 is the mass flow rate of the user side (water) and C_{min} is calculated according to the equation (4.16). The effectiveness of the heat exchanger was calculated from the NTU correlation with the expression for a counter flow heat exchanger [162], according to the equations (4.15) and (4.16).

$$NTU = \frac{A_{total} \cdot N_p}{\left[3.9637 \cdot 10^{-4} \cdot \left(\frac{\dot{m}_1}{N_p} \right)^{-0.55} + 1.3290 \cdot 10^{-4} \cdot \left(\frac{\dot{m}_2}{N_p} \right)^{-0.65} \right] \cdot C_{min}} \quad (4.14)$$

$$\varepsilon = \frac{1 - e^{-NTU \cdot (1 - C_r)}}{1 - C_r \cdot e^{-NTU \cdot (1 - C_r)}} \quad (4.15)$$

$$C_{min} = \min(\dot{m}_1 C_{p,1}, \dot{m}_2 C_{p,2}); \quad C_{max} = \max(\dot{m}_1 C_{p,1}, \dot{m}_2 C_{p,2}); \quad C_r = \frac{C_{min}}{C_{max}} \quad (4.16)$$

The effectiveness calculated from the NTU correlation was compared with the simulated by the SSP software for the specific BPHE and plotted in Figure 4.8.

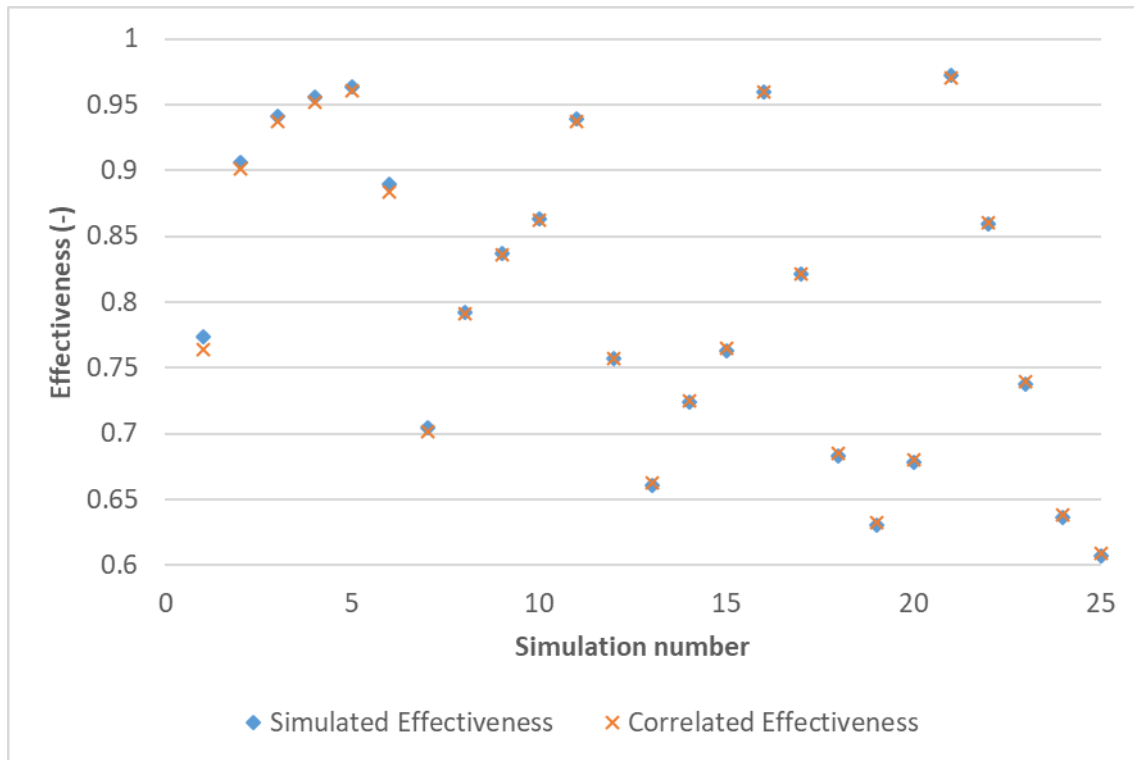


Figure 4.8. Free-cooling BPHE effectiveness correlation. Comparison with simulated results

The maximum deviation among all the simulation points was 1.2%, but the average deviation was around 0.1%.

Regarding the pressure drop in the free-cooling BPHE, the values obtained in the simulations were used to develop a correlation for the pressure drop in each side of the heat exchanger by non-linear regression. The pressure drop in the ground side ΔP_{ground} (Pa) is calculated by the equation (4.17) as a function of the ground loop mass flow rate (\dot{m}_1), and it is plotted in Figure 4.9 a), together with the values obtained in the simulation with the SSP software. The pressure drop in the user side ΔP_{user} (Pa) is calculated by the equation (4.18) as a function of the user loop mass flow rate (\dot{m}_2), and it is plotted in Figure 4.9 b).

$$\Delta P_{ground} = 11340.36 \cdot \dot{m}_1^2 \quad (4.17)$$

$$\Delta P_{user} = 11715.14 \cdot \dot{m}_2^2 \quad (4.18)$$

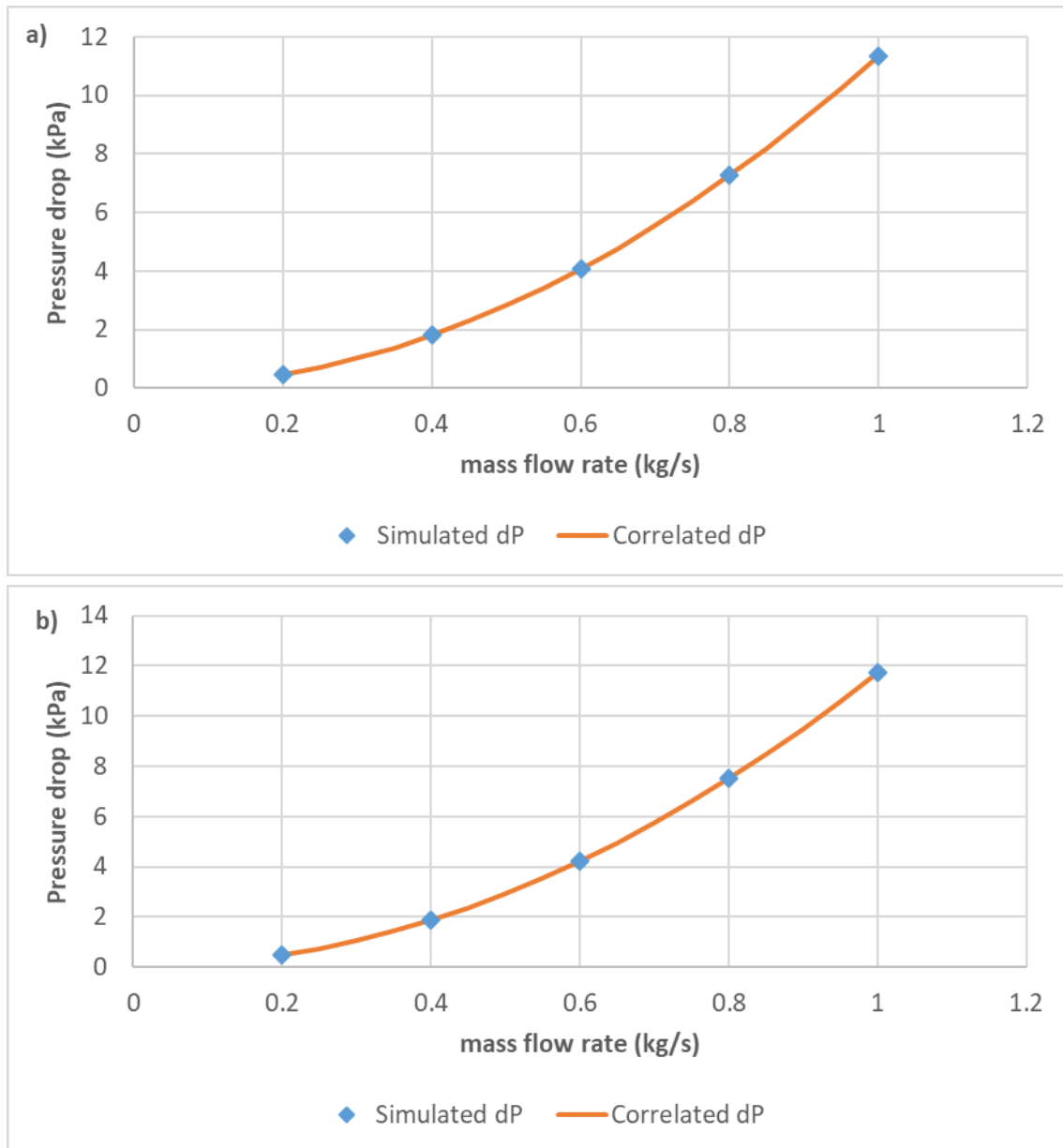


Figure 4.9. Pressure drop (dP) in each side of the free-cooling BPHE: a) ground side; b) user side

4.2.7 TRNSYS implementation of the DSHP model

A new TRNSYS type, working as a black box model for the DSHP was necessary instead of using the already available heat pump types in TRNSYS because it was desired to reproduce accurately the heat pump performance under different operating conditions, which depends not only on the source and load inlet temperatures, but also on many other variables, as was previously stated, for each of the different operating modes.

In addition, the heat pump types available in TRNSYS calculate the heat pump performance by interpolating between a fixed number of operating points when it works under conditions different from the fixed ones. Moreover, they do not consider the thermal losses in the heat pump cycle and calculate the heat transfer in the source side (ground or air) as the sum or subtraction (for cooling or heating modes, respectively) of the heat pump

capacity and the power consumption. On the other hand, the developed correlations calculate the evaporator and condenser capacities, the compressor power and other electrical losses separately, based on the experimental results.

Hence, the polynomial correlations were implemented as a TRNSYS type in which the independent variables are introduced as inputs (inlet temperature in each loop, air temperature, compressor frequency, fan frequency and temperature difference in each loop), together with the operating mode and the mass flow rate through each loop, so the capacity of each loop is calculated using the correlations and the outlet temperature of each loop is then calculated, according to the heat transfer equation (4.19). The heat capacity is calculated depending on the type of fluid (water or MPG and water mixture) according to the correlations presented in [126], already implemented in the type.

$$\dot{Q} = \dot{m} \cdot C_p \cdot (T_{out} - T_{in}) \quad (4.19)$$

The TRNSYS type is programmed in such a way that the inputs are introduced according to their hydraulic loop (user, ground or DHW) instead of the heat exchanger (condenser or evaporator). Internally, the TRNSYS type will select the corresponding correlation depending on the operating mode.

Other outputs calculated by the type are heat transfer to each loop, consumption of compressor, fan and parasitic losses, the COP of the heat pump and the pressure drops through each BPHE. The pressure drops are necessary for calculating the electric consumption of the circulation pump of each loop. This consumption is calculated outside of the heat pump type, as the pressure drop of the rest of the elements in each hydraulic circuit is needed. The code of the TRNSYS type, as well as the list of parameters, inputs and outputs is shown in the Appendix A.

The connections between the DSHP TRNSYS type and the other components in the DSHP model are shown in Figure 4.10. It is possible to see that the DSHP type receives inputs from the three hydraulic loops (mass flow rates and inlet temperatures) and the air temperature from the weather file, thereafter it will calculate the heat exchanged and the outlet temperature for each loop. Moreover, the DSHP receives signal from the controller, which will set the operating mode, the compressor frequency (depending on the supply/return temperature), the fan frequency, the desired temperature difference across the heat exchangers and the ON/OFF schedule. The electrical consumptions of the heat pump and the pressure drops will be used for calculating the energy consumption and the efficiency of the system, referred as SPFs in the figure (Seasonal Performance Factors).

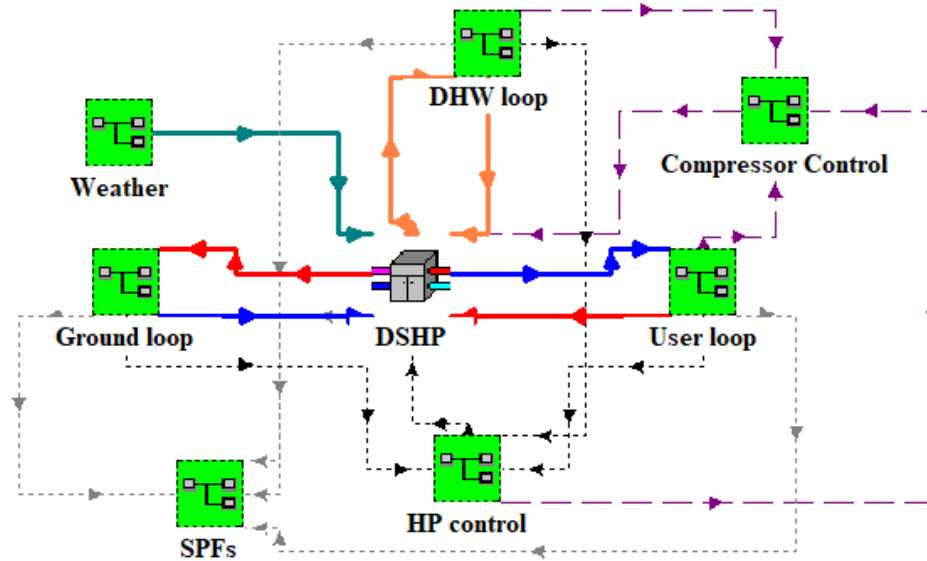


Figure 4.10. DSHP TRNSYS type connections

Despite the fact that the free-cooling loop is external to the heat pump unit, the free-cooling operation was also implemented inside the DSHP TRNSYS type, so all the eleven operating modes of the DSHP system can be simulated with only one TRNSYS type. Moreover, the ground loop and the user loop are already connected by the DSHP type, so it was simpler to implement the free-cooling BPHE correlation inside it for the modes M10-Free-cooling and M11-Free-cooling+DHW Air in order to calculate the system performance.

4.3 Integrated DSHP system modelling

A complete, detailed dynamic model of the dual source plug and play system described in chapter 2 has been developed in the TRNSYS software (TRaNsient SYstems Simulation program) [100], using the TRNSYS types developed in this PhD dissertation: the coaxial BHE dynamic model (B2G) coupled with the long term ground response model (LSA) described in chapter 3 and the DSHP black box model described in section 4.2. This software allows the simulation of transient systems by connecting the different components that model the different parts of the system. Inside the software, the components are modelled as black boxes called *types*, so the different types are interconnected and the program engine reads and processes the information flux and solves the system iteratively, determining the convergence and plotting the desired outputs. TRNSYS incorporates an extensive library of typical components (such as HVAC components, multizone building, controllers, hydronics, etc.), programmed in FORTRAN language and optionally it allows to create user types, as the one described in this PhD dissertation, being possible to couple both the user-created types with the already available in the program.

The TRNSYS system model developed in this PhD dissertation presents a modular configuration, so it is easy to replace components, modify their characteristics and operation parameters or introduce new elements. Therefore it is a very useful tool in order

to assess the performance of the system working under different conditions or operation parameters, allowing to test different optimization and control strategies without the need of implementing all of them in the real system.

It incorporates the different components of the hydraulic loops: pipes, tanks, heat exchangers, heat pump or circulation pumps. Furthermore, it incorporates different controllers (PIDs or differential controllers with hysteresis) and different operation strategies are implemented. The overall layout of the TRNSYS DSHP system model is shown in Figure 4.10. As shown in this figure, the model is organised with the DSHP as the central component and it is connected to the different parts of the system, grouped into Macros. In each macro, the different components are connected between them and with other macros. The main parts are:

- User hydraulic loop: It includes the pipes in the user circuit, a buffer tank and the control of the circulation pump. The building thermal loads are calculated apart and introduced as inputs for the system to handle.
- DHW loop: including the storage tank, the mixing valves and the DHW demand.
- Ground loop: The BHEs field is modelled as one average BHE with the B2G coaxial model and the LSA. The connecting pipes and the collector connects the BHE model with the DSHP.
- Compressor speed control: a PID controller sets the compressor frequency depending on the user circuit temperature.
- Weather: the climatological information is introduced as input with a *.tm2* weather file corresponding to the location of the system. The ambient temperature at each time step is used as the air temperature in the DSHP model.
- Heat pump control: the operation strategies are set in this macro, like the on/off schedules of the system or the selection of operating mode (selection of ground or air as a source, selection of the free-cooling mode, etc.).
- SPFs macro: the consumption of the different components is calculated here and the system efficiency is analysed by using the Seasonal Performance Factors (SPFs).

The main characteristics of the components are introduced as parameters in the different types, for example, geometric characteristics as diameters, pipes length, tank volume, roughness of the tubes, etc. Additionally, some other parameters are introduced in the Control Cards section in TRNSYS, and are considered as constants in the model. Here the main control parameters, like temperature setpoints, minimum and maximum frequency allowed in the heat pump, control deadbands, etc., but also some assumptions like assumed machinery room temperature, heat losses coefficient in the pipes, etc. are introduced. All the variables introduced here can be easily modified and could be used as variable parameters in order to make parametric analysis with the TRNEdit tool, included in TRNSYS.

The building side and emission system is modelled as an input file with the corresponding hourly thermal loads calculated apart from this model, in order to simplify

the model. It is considered that the heat pump system can be working in heating mode or cooling mode, and that two well defined seasons during the year: a summer season in which the heat pump provides cooling and a winter season in which the heat pump provides heating. So, the thermal loads will be calculated externally according to this.

The plug and play system model in TRNSYS has been developed based on the GEOTeCH design. However, some assumptions were made because no information was still available. In any case, as it is a modular model and easy to modify, it can be adapted to different installation requirements. In the following, a somewhat general description of the model and its different parts is provided with further details. It should be noted that some system and model parameters are defined depending on the specific application, thus, they cannot be fixed in the general description of the model, but they will be defined in the specific applications in chapter 5. In this chapter, the TRNSYS model of the plug and play GEOTeCH system will be simulated for different locations in Spain (Valencia, Madrid and Bilbao) and Europe (Athens, Strasbourg and Stockholm), accounting for different climatic conditions, and an assessment of the system performance will be carried out. The TRNSYS model has been roughly described previously in several works [48], [158], [159].

4.3.1 User loop

In the user loop, the water flow rate and temperature that comes from the heat pump as outputs are introduced into the buffer tank as the inlet temperature and mass flow rate. The buffer tank is connected to the supply pipe, the water temperature inside the pipe will decrease or increase through its length due to the thermal losses with the outside.

All the emission system and the coupling with the building is modelled as an ideal heat transfer in which the water in the user circuit is heated up (cooling load) or cooled down (heating load) because of the building thermal load, as detailed in section 4.3.1.3. After this, the water flows back to the heat pump through the return pipe, with the corresponding thermal losses to the environment. This outlet temperature from the return pipe is the inlet temperature in the user side of the DSHP type. The TRNSYS layout of the user loop macro is shown in Figure 4.11.

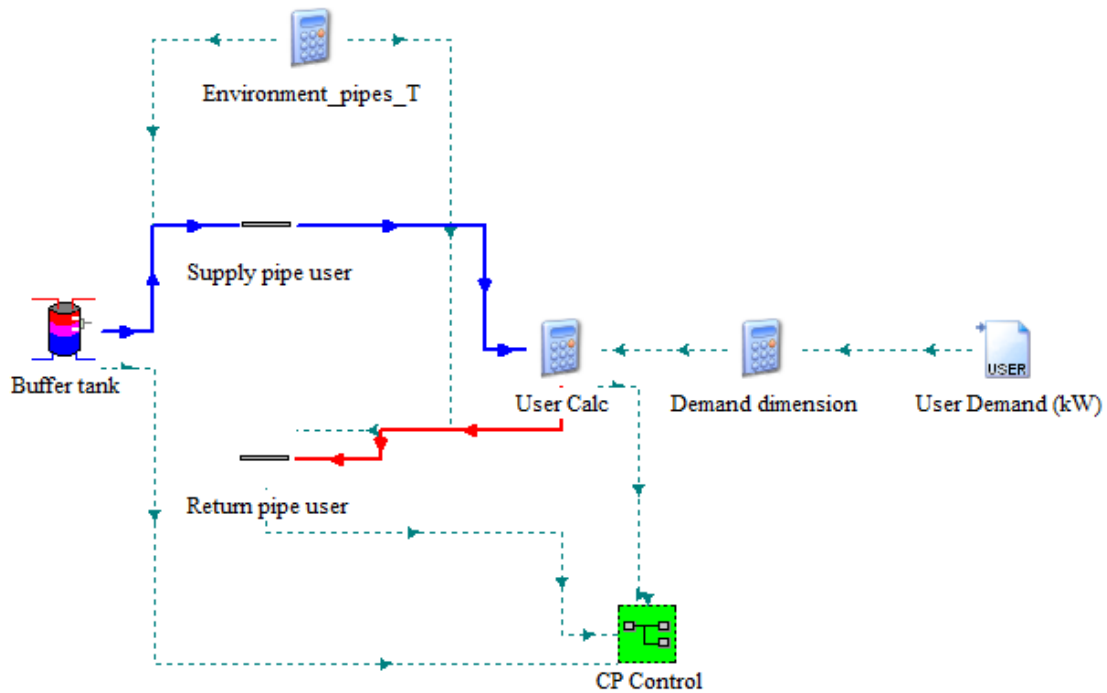


Figure 4.11. User loop macro in TRNSYS

4.3.1.1 Buffer tank sizing

The buffer tank is modelled as a stratified tank with the type 60d. It is an optional component in a system working with a variable speed heat pump, normally the hydraulic circuit provides enough inertia in order to work in safe conditions. However, from the point of view of the control of the supply temperature it is a useful component to place the sensor and prevent quick changes because of the heat pump starting or stopping. The methodology suggested here, that will be used in the DSHP modelling is based on the approach suggested by Cervera-Vázquez et al. [43]. So, the minimum volume of water will be defined by the expression presented in the equation (4.20), where $\Delta t_{min,OFF}$ is the minimum time in which the compressor should remain OFF (the suggested value is 3 minutes), ΔT_{db} is the deadband (suggested values between 3 and 5 K) and \dot{Q}_1 is the heat pump capacity at minimum speed.

$$V_{min} = \frac{\Delta t_{min,OFF}}{\rho \cdot C_p \cdot \Delta T_{db}} \cdot \dot{Q}_1 \quad (4.20)$$

On the other hand, a bigger buffer tank could be installed in order to store some thermal energy and be able to provide heating or cooling while the heat pump is off, then operating the heat pump in more optimal conditions and switch it off when the stored energy in the buffer tank is enough to handle the thermal demand.

4.3.1.2 Pipes model

For the pipes types, the model developed in [130] was used, with some improvements. This model models the heat transfer along the pipe, considering the temperature variation due to the water displacement and the thermal losses with the environment. The pipe is

divided in several nodes, following the same methodology used for the fluid nodes in the B2G model (section 3.3.2). The improvements included in the type were:

- The implementation of correlations for calculating the thermal properties of the working fluid depending if it is water or a mixture of water and MPG (30%), based on the work [126].
- Calculation of the pressure drop along the pipe, in order to calculate the electric consumption of the circulation pumps outside of the pipe type. The methodology used for calculating the pressure drop is the same than in the B2G coaxial model, described in section 3.3.3. Additionally, it is possible to define the number of elbow joints in order to consider the extra pressure drop caused by the different pipe unions. For this purpose, an extra length is calculated based on the number of simple elbows defined and the pipe diameter, according to the equation (4.21).

$$\Delta L_{extra\ per\ elbow} = 0.15871 + 0.02975 \cdot D(mm) \quad (4.21)$$

In order to characterize the pipes, it is necessary to specify the length, number of nodes, inner diameter, pipe roughness (0.0015 mm for a typical plastic pipe), number of elbow joints, the environment temperature and the thermal losses coefficient (for example 1.4 W/(m²·K)).

For the environment temperature in the pipes, it was calculated as the average temperature between the outdoor air temperature and a constant machinery room temperature of around 22°C.

4.3.1.3 Building thermal loads

In order to simplify the system model and make it faster more flexible, instead of modelling the building and the emission system inside the TRNSYS model, the hourly thermal loads are introduced as an input. For this purpose, an external building model in TRNSYS is used for calculating the cooling and heating thermal loads that the system needs to handle in order to keep the comfort inside the different rooms. The thermal loads could be calculated in another different simulation program (for example, EnergyPlus, Modelica, etc.) in which a building is modelled, as long as it provides the final hourly heating and cooling thermal loads. Thanks to this, it is easier to make an assessment of the system working in different buildings or climates, as it will be shown in the section 5.1 where an assessment of the system working in different climatic conditions is carried out for different locations in Spain and Europe.

The hourly thermal loads are introduced in absolute value as an external file. These loads have been calculated externally considering two seasons during the year: a summer season when only cooling is provided and a winter season when only heating is provided. The *season* signal is specified in the heat pump control macro, explained in section 4.3.6.1. (A value of 1 represents summer season and a value of 0 represents winter season). The summer and winter periods are estimated in the thermal loads calculation based on the heating and cooling demand during the year.

A sizing factor is included in the thermal demand, so it is possible to multiply the thermal loads by this factor, increasing or reducing the thermal demand using the same load profile. With this factor it is possible to simulate, for example, an improvement in the building envelope that would lead to a reduction in the thermal demand.

The return water temperature in the loop is calculated assuming that the water is heated up or cooled down by the thermal load, according to the equation (4.22), where *season* represents the season signal (1 for summer or 0 for winter), \dot{Q} the hourly thermal demand (W) and T_{in} the water temperature leaving the supply pipe.

$$T_{return} = season \cdot \left(T_{in} + \frac{\dot{Q}}{\dot{m} \cdot C_p} \right) + (1 - season) \cdot \left(T_{in} - \frac{\dot{Q}}{\dot{m} \cdot C_p} \right) \quad (4.22)$$

4.3.1.4 User circuit circulation pump control

The user circuit circulation pump is controlled by a PID controller that sets the mass flow rate in the user circuit in order to obtain a fixed temperature difference across the DSHP user heat exchanger. It is modelled with the type 23. The place of the sensors in order to set the temperature difference can be varied, so it is possible to fix the temperature difference between the outlet of the buffer tank and the outlet of the return pipe, for example. The temperature difference in the user circuit can be changed (usually values between 3-5 K). A schedule for the circulation pump is also provided, so there will be water circulation through the user circuit only when it is set by this schedule (normally during the working periods of the building, when heating or cooling is needed).

The constants of the PID controller are set in order to obtain a good response, i.e. the water flow is varied smoothly, but quick enough to achieve the desired temperature difference in an acceptable time. Only the proportional and integrative part of the PID are used for this controller. Figure 4.12 shows the layout in TRNSYS of the user circulation pump macro.

The values set in this model for the climatic assessment in section 5.1 are the following:

- $\Delta T_{user} = 5K$.
- PID controller constants:
 - K_p (proportional constant) = 2.
 - T_i (integral time) = 50 s.
 - T_d (derivative time): not used.

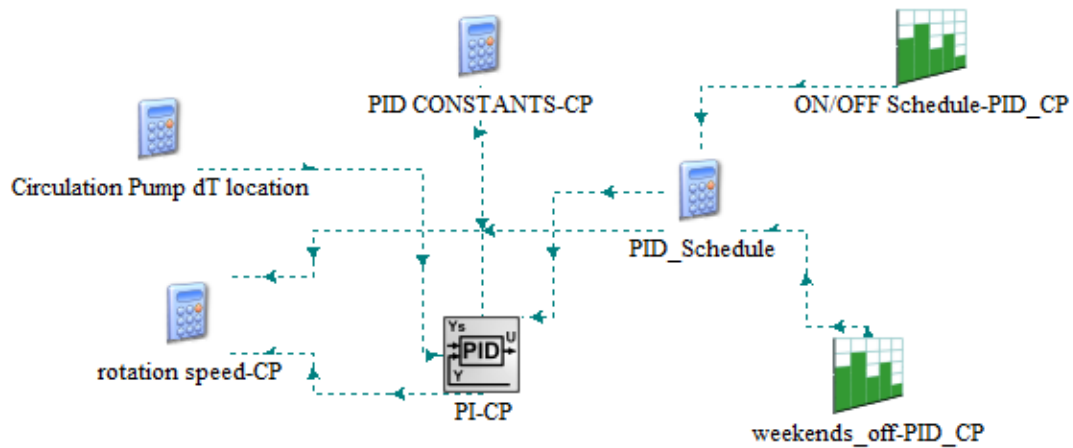


Figure 4.12. User circuit Circulation pump macro in TRNSYS

4.3.2 DHW loop

The DHW loop mainly consists of an insulated tank to store the required DHW, the mixing valves and the DHW demand. The tank incorporates an internal coil heat exchanger, so the water coming from the heat pump flows through the coil and heats up the water inside the tank. The type used for modelling the tank with the coil heat exchanger is the type 60d. The DHW demand profile is introduced as an input with an external text file, based on the profile for an office building found in the ASHRAE Handbook – HVAC applications [163] (around 7.5 l/h per person in a day). This profile determines the amount of DHW needs for each hour during the day (l/h). Therefore, the DHW tank will provide the required DHW flow at the desired temperature (for example, 45°C). The water coming from the net is assumed at an almost constant temperature (the average temperature of the location) assuming a 20% higher temperature in summer and 20% lower in winter, according to the equation (4.23).

$$T_{supply\ net} = T_{avg} \cdot (season \cdot 1.2 + (1 - season) \cdot 0.8) \quad (4.23)$$

A tempering valve (type 11b) and a mixing valve (type 11h) assures that the hot water coming from the tank is mixed with the net water when needed in order to keep the desired DHW supply temperature (for example 40°C). The TRNSYS layout is shown in Figure 4.13.

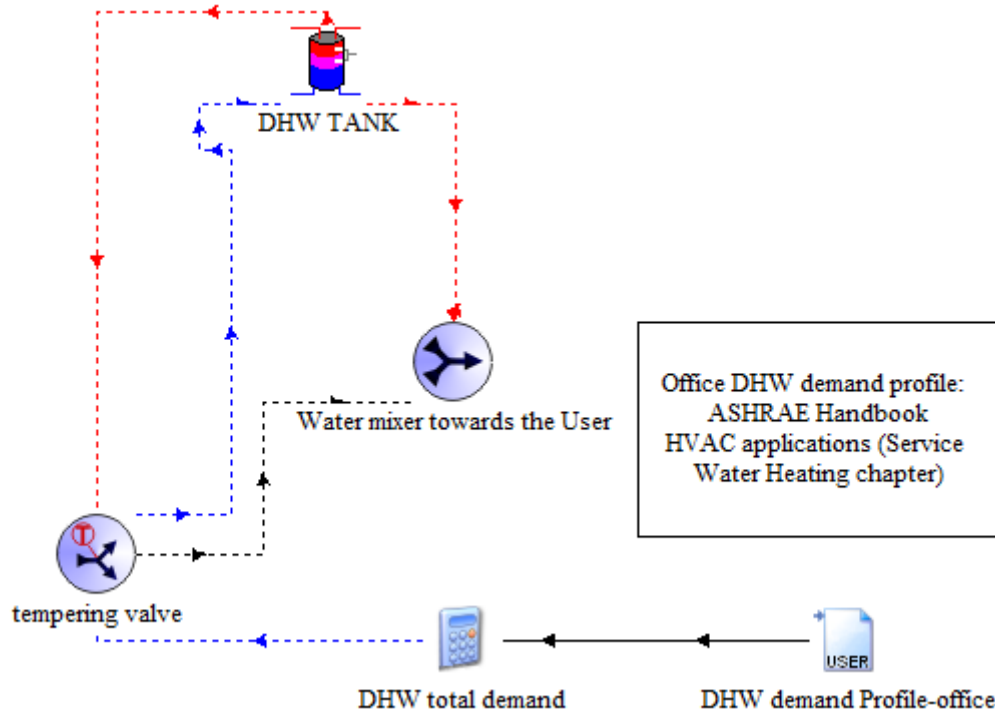


Figure 4.13. DHW loop macro in TRNSYS

4.3.3 Ground loop

The ground loop TRNSYS model consists of one distribution pipe through which the fluid flows from the heat pump to the flow diverter, where the mass flow rate is divided by the number of BHEs (it is assumed a balanced hydraulic loop in the BHEs field), the BHEs field is modelled by one average BHE model (the B2G coaxial model described in section 3.5) coupled with a long term ground model (LSA model described in section 3.7). The outlet temperature from the B2G model is used as input in the collector, where the mass flow rate is multiplied by the number of BHEs and flows back to the heat pump through a pipe. The pipes types used are the same as in the user loop and the diverter and collector are modelled with a calculator.

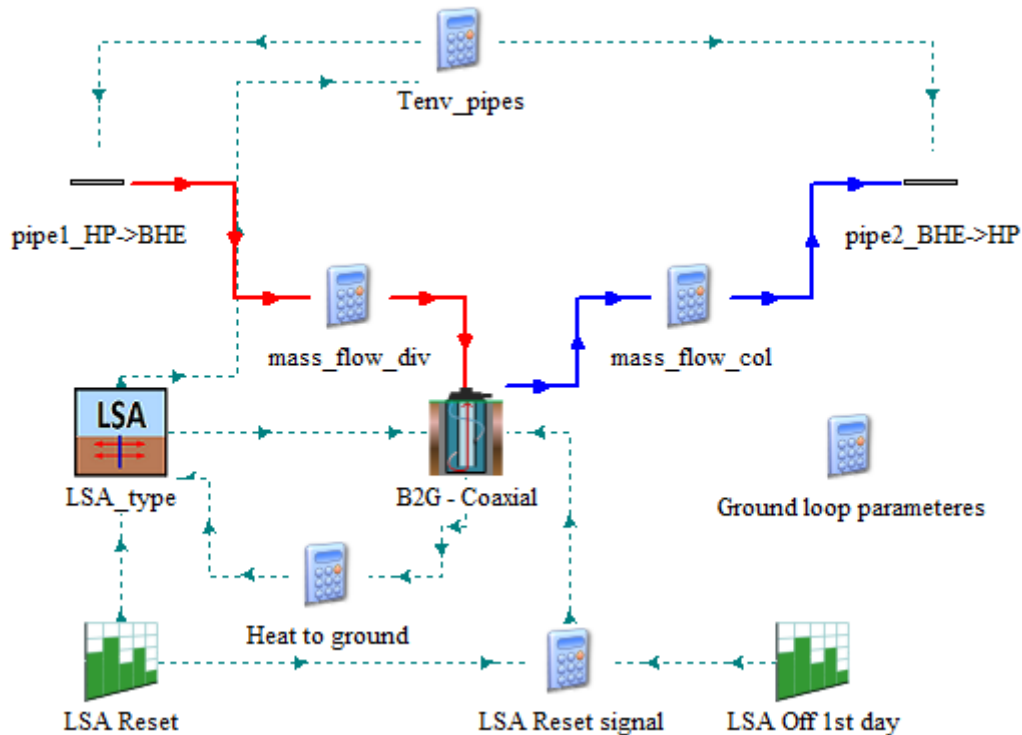


Figure 4.14. Ground loop macro in TRNSYS

The coupled BHE models work-flow is described in the following:

1. The dynamic BHE model (B2G coaxial model described in section 3.5) calculates the fluid outlet temperature during the daily operation, due to the heat transfer between the fluid flowing through the pipes and the surrounding ground (accounting for the grout capacity and thermal interaction between the fluid in the inner and outer pipe). The geometric characteristics of the BHE are introduced as parameters as well as the thermal properties of the pipes, grout and ground, the pipes roughness, the fluid used, etc.

The B2G model calculates the outlet temperature, the heat transfer with the ground and the pressure drop. The heat transfer is used as an input for the LSA model.

2. The LSA model calculates the long-term response of the ground and the interaction between BHEs in the field (as described in section 3.7) using the heat transfer from the B2G model and the field characteristics. The BHEs field distribution is introduced as an external file in order to calculate the interaction between BHEs. It is assumed that the same heat injection/extraction will take place in all the BHEs, and the LSA model will calculate the average borehole wall temperature.

During the simulation, the LSA type accumulates the heat transfer between BHE and ground and a new heat step is internally considered at a certain time during the day, given by an input signal ("LSA reset" in Figure 4.14). This signal is modelled with a forcing function (type 14h), it can take the value of 1 or 0 (an example of this signal is shown in Figure 4.15). When it changes its value, the LSA type generates a new heat step with the integrated heat transfer from the instant of the previous step.

3. When the signal changes its value from 0 to 1, then not only a new heat step is generated in the LSA type, but also the new borehole wall temperature calculated by this type is used in the B2G model as the new ground nodes temperature. This is, the B2G model resets its ground temperature, considering the long-term response and the interaction between BHEs. Normally this moment is considered at the start of the system in the morning, after the recovery period during the night when the system is usually off and the temperatures in the ground and BHE have been somewhat stabilized.

Taking a look at the Figure 4.15, the heat steps are calculated separately for the working period of the system (6h-22h) and the recovery period (22h-6h).

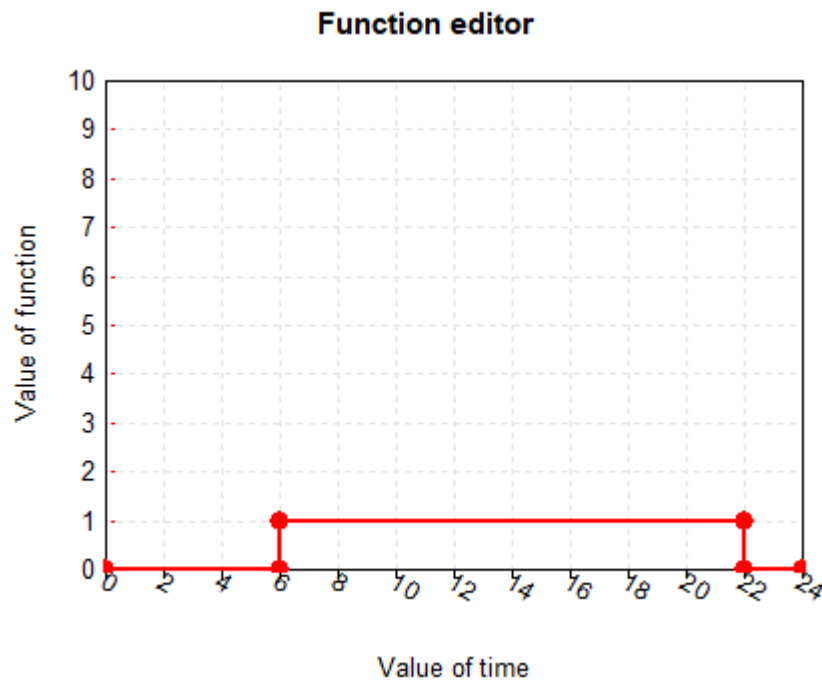


Figure 4.15. LSA reset signal

Regarding the thermal losses through the pipes, the environment temperature is calculated as a weighted average between the ground temperature (calculated by the LSA type) and the ambient temperature, since these pipes are normally buried at a shallow depth, therefore they will have a little influence from the outdoor air temperature and a higher influence from the ground temperature. It was considered that the environment temperature is a 70% of the ground temperature and a 30% of the air temperature, according to the equation (4.24).

$$T_{environment\ pipes} = (T_{ground} \cdot 0.7 + T_{outdoor\ air} \cdot 0.3) \quad (4.24)$$

Regarding the mass flow rate in the ground loop, it is calculated inside the heat pump type in order to reach the desired temperature difference across the ground BPHE, introduced as an input in the heat pump type. In this model, it is considered a value of 3K. The fluid used in the ground loop is a mixture of water and MPG (30%). The number of BHEs, depth and geometric characteristics will vary depending on the installation.

4.3.4 Weather

The ambient air temperature is introduced in the model as an input weather file (*.tm2*), including several climatic variables in hourly values for an entire year. TRNSYS incorporates a great number of weather files corresponding to different cities around the world. The type used for processing this weather file is the type 109-TMY2. The ambient air temperature is used as the outdoor air temperature for the DSHP, but also in order to calculate the thermal losses in pipes, tanks and in the source selection control.



Figure 4.16. Weather file type in TRNSYS

4.3.5 Compressor control

As was described in section 2.2.4.2, the DSHP incorporates a variable speed compressor, so the heat pump is capable of adapting its thermal capacity to the instantaneous demand. So, the compressor can vary its frequency but between a minimum and maximum frequency. In the model, these maximum and minimum frequencies are fixed as constants, for this heat pump, the recommendable minimum frequency is around 20-30 Hz, and the maximum around 70-90 Hz. This is because the heat pump efficiency decreases too much if it works below the minimum frequency or above the maximum.

In order to adapt the thermal capacity of the heat pump to the thermal demand, a desired setpoint temperature is set in the user circuit or DHW tank, and the frequency of the heat pump will increase or decrease if the actual temperature is getting away from this setpoint temperature, proportionally to the difference between the actual temperature and the setting. Moreover, when the compressor reaches the minimum frequency (20 Hz) and the thermal demand is low, the compressor cycles on/off with this minimum frequency, adapting in this manner the energy provided by the heat pump to the thermal demand.

There are two main monitored temperatures to control in the user circuit: the supply temperature at the outlet of the buffer tank or the return temperature (inlet to the heat pump). Usually the return temperature is controlled because it is simpler to implement the PID controller and the temperature sensor inside the same heat pump unit and the inlet temperature is more constant, what is good for the compressor life. On the other hand, controlling the supply temperature is more efficient from the point of view of the user comfort, because the water entering the emission system will have a more constant temperature, maintaining the comfort inside the air-conditioned spaces. If the controlled temperature is the return temperature, the supply temperature will vary depending on the instant thermal demand. In this model, the supply temperature at the outlet of the buffer tank is controlled.

In the case of the DHW loop, the controlled temperature is the temperature inside the tank, at a distance from the bottom of 1/3 of the tank height, in order to keep the water above this level at a higher temperature.

In order to set the compressor frequency, a PID controller is used (type 23), but only the proportional and integral actions are used. This controller compares the real controlled temperature with the setpoint, increasing or decreasing the compressor frequency in order to reach the desired value. Additionally, a differential controller with hysteresis (type 2b) controls the cycling of the compressor at the minimum frequency when the thermal demand is very low. For this purpose, a lower and higher limit around the temperature setpoint is set, so the compressor will cycle on/off between these limits if the thermal demand is low. Different dead bands for the higher and lower limit can be selected, but in this case, symmetric values are used.

Each time that the heat pump switches on, it starts at the minimum frequency during a defined starting time (normally 30 seconds), then only the proportional action of the PID controller is used and later on, the integral action is also taking part in the control. In order for the controller to know the status of the heat pump the previous time step, the type 93 is used as input value recall. The layout of the compressor control is shown in Figure 4.17.

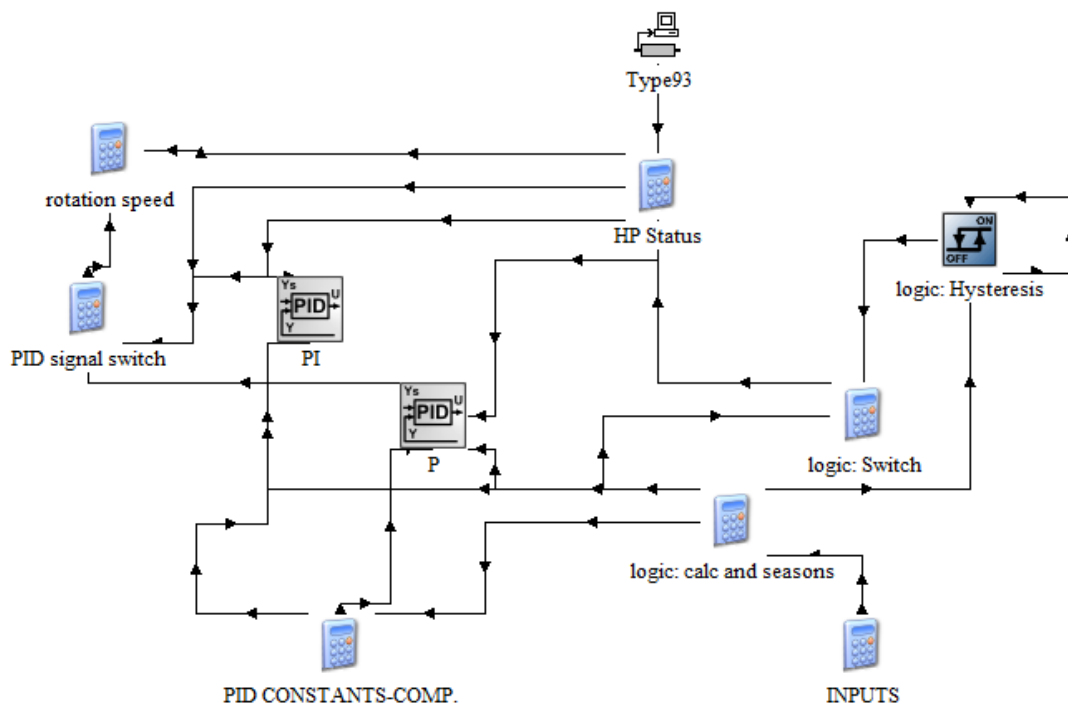


Figure 4.17. Compressor control macro in TRNSYS

The control parameter can be changed according to the desired control strategy. An example of possible control parameters is shown here:

- Minimum frequency of the compressor = 20 Hz.
- Maximum frequency of the compressor = 80 Hz.
- Supply temperature for heating = 45°C.
- Supply temperature for cooling = 12°C.

- Hysteresis ON=2K.
- Hysteresis OFF=2K.
- PID controller constants:
 - Kp (proportional constant) = 10.
 - Ti (integral time) = 180 s.
 - Td (derivative time): not used.

4.3.6 DSHP control

In this macro, the main variables used to control the heat pump operation are set. First of all, the working schedules of the system are set. So, the period during the day in which the heat pump is allowed to produce DHW and heating/cooling are defined by forcing functions (type 14h).

In this model, it has been assumed that the DHW is produced during the night and stored in the DHW tank, so during the day, the heat pump will produce only heating and cooling, using the DHW produced the previous night. The schedule for producing heating and cooling is from 6h to 22h, and the DHW is produced from 4h to 6h, just before the start of the heating/cooling in order to prevent thermal losses in the storage tank. The system is off during the weekends.

The on/off signal is also controlled here, a calculator receives the on/off signals from the deadband controllers of the compressor that set if the DHW tank is already at the desired temperature and if the temperature at the user circuit is already at the setpoint, it applies the corresponding schedules and determines if the heat pump must provide DHW or heating/cooling or remain off. This *switch* signal is also used as input in the mode selection calculator explained below. The layout of the heat pump control macro is shown in Figure 4.18.

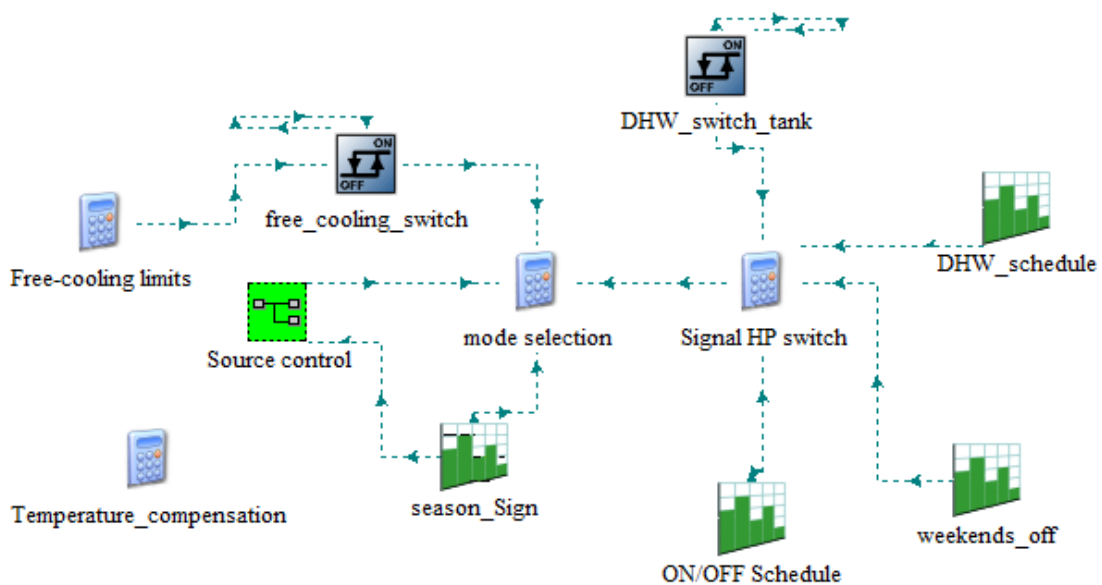


Figure 4.18. Heat Pump control macro in TRNSYS

4.3.6.1 Season signal

The season signal is defined by a forcing function and it provides a value of 0 when the system should work in heating mode (winter) and a value of 1 when the system should work in cooling mode (summer). The definition of the two seasons is made depending on the heating/cooling loads calculated with the building model, outside of the DSHP system model in TRNSYS, and should coincide with the definition of the thermal loads. An example of season signal is presented in Figure 4.19, where the summer and winter seasons are defined for a whole year in hours (8760 hours represent one year).

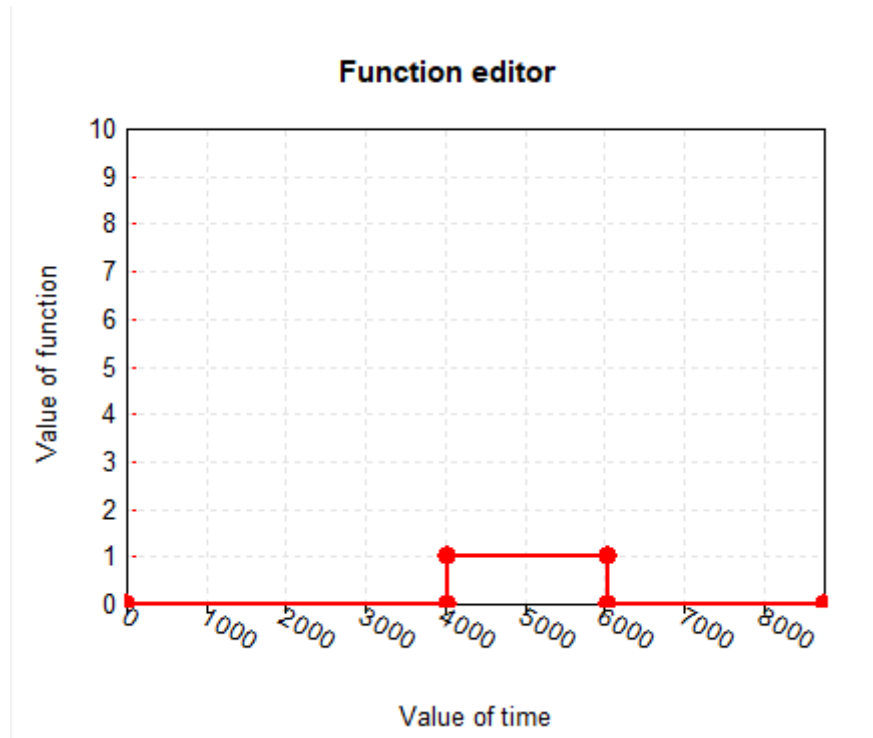


Figure 4.19. Season signal example (1=summer, 0=winter)

4.3.6.2 Source control

In order to select the most favourable source, the air temperature and the ground temperature are compared, considering a hysteresis band, following the methodology explained in section 2.2.4.1. In the TRNSYS model, the air temperature is introduced from the weather file and the ground temperature from the first ground node of the B2G coaxial model. The hysteresis used is $\pm 2\text{K}$.

In addition, the frost formation in the evaporator of the heat pump when working with the air is taken into account. A correlation based on the experimental tests was developed in order to determine when the frost starts to appear in the evaporator depending on the compressor and fan frequencies. The equation (4.25) is used in order to determine the air temperature at which the frost starts its formation, so if the air temperature is below this point, the heat pump will switch to the ground as a source.

$$T_{amb}(\text{°C}) = \left(\frac{freq_{fan}(\%)}{2.5235 \cdot freq_{compressor}(\text{Hz})^{1.0869}} \right)^{\frac{1}{0.9128}} \quad (4.25)$$

The source selection macro in TRNSYS is shown in Figure 4.20.

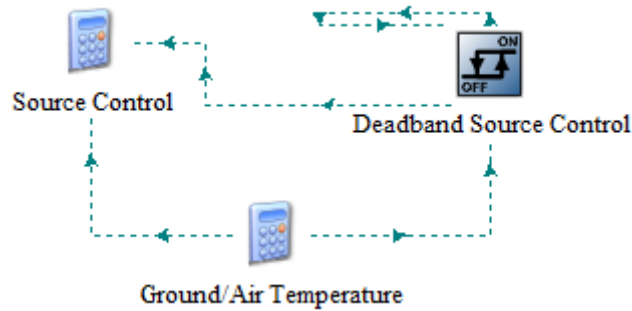


Figure 4.20. Source control macro in TRNSYS

4.3.6.3 Free-cooling control

The free-cooling mode will be selected when there is a cooling demand and the fluid temperature coming from the ground loop is lower than a determined value. In the TRNSYS model this is modelled by a differential controller with hysteresis, so when the return temperature from the ground is below the lower limit, the free-cooling mode is selected; if this temperature increases until the upper limit, then the free-cooling mode is deselected and the heat pump will provide mechanical cooling.

The values set in this model are 10°C for the lower limit and 15°C for the upper limit.

4.3.6.4 Operating mode selection

Once it is selected in the different subsystems of the control Macro described previously if the system must be on because of the schedule, if the system must work in winter or summer mode, if the heat pump must provide DHW or heating/cooling due to the schedules or if the set points are already met or not, and in the case of cooling, if it must be provided by free-cooling, the final operating mode selection is carried out. So a calculator takes all of these signals and sets the final operating mode that will be introduced in the heat pump as an input. The selection of operating mode is summarized in Figure 4.21.

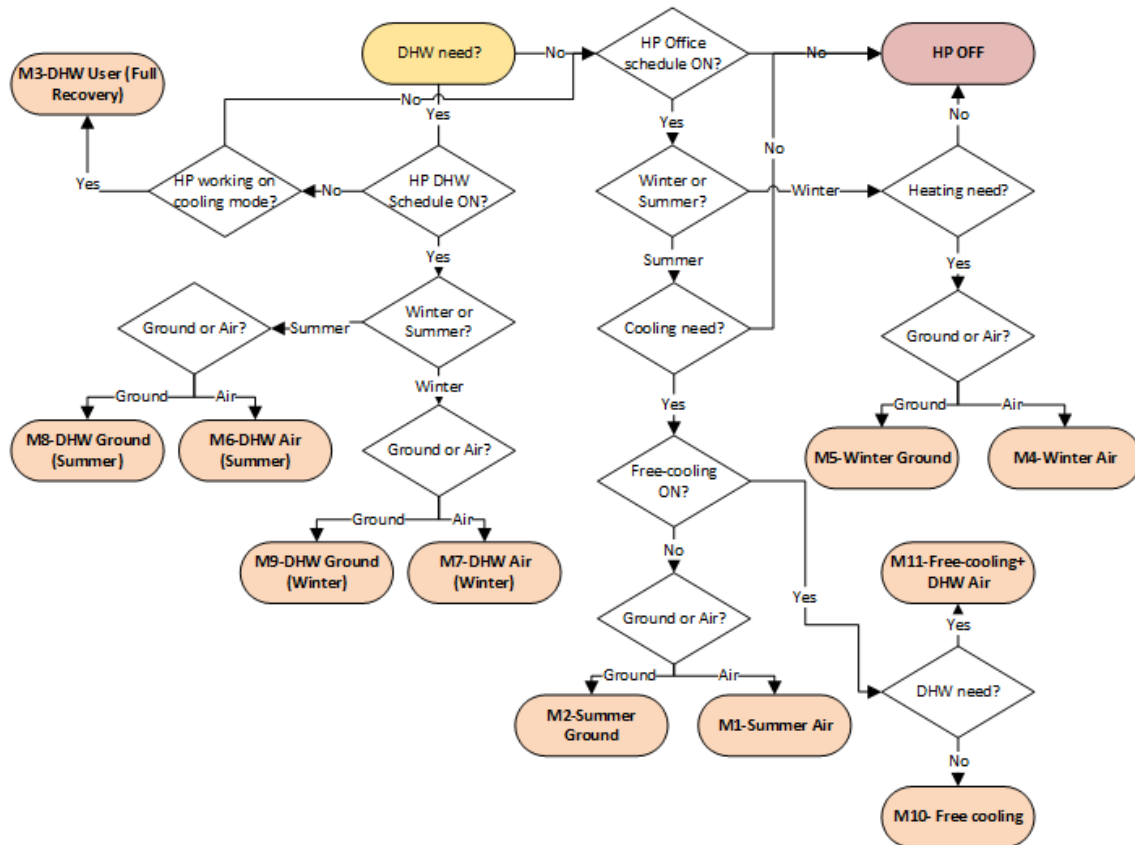


Figure 4.21. Flux diagram for the operating mode selection

4.3.6.5 Temperature compensation

In order to increase the efficiency of the system, a supply temperature compensation strategy was implemented in the model as an optimization strategy. It mainly consists in adapting the supply temperature according to the outdoor ambient temperature. So, if the heat pump is providing cooling but the outdoor temperature decreases, there will be no need to supply water as cold as before, so the supply temperature can be increased, increasing then the Coefficient Of Performance (COP) of the heat pump. On the other hand, if the outdoor temperature increases, the thermal demand will increase and the supply temperature should be lower. This optimization strategy allows taking advantage of milder outdoor ambient temperatures to improve the efficiency of the heat pump whenever it is possible. The methodology used in this model is detailed in [164].

Therefore, the supply temperature will be calculated at each simulation time step so it is possible to meet the user comfort even in the most extreme conditions (the maximum and minimum ambient temperatures for the whole year in the system location are used, so it is necessary to find these temperatures in order to apply this methodology correctly). The supply temperature (T_{SB}) will be determined based on:

- Maximum annual ambient temperature on the location ($T_{amb,max}$).
- Minimum annual ambient temperature on the location ($T_{amb,min}$).
- The desired comfort temperature (T_{room}).

- Maximum supply temperature for heating ($T_{SB)max}$).
- Minimum supply temperature for cooling ($T_{SB)min}$).

The supply temperature is calculated for each time step according to the equations (4.26) and (4.27).

$$T_{SB} = (1 + \beta) \cdot T_{room} - \beta \cdot T_{amb} \quad (4.26)$$

$$\beta \text{ (cooling)} = \frac{T_{room} - T_{SB)min}}{T_{amb)max} - T_{room}} \quad ; \quad \beta \text{ (heating)} = \frac{T_{SB)max} - T_{room}}{T_{room} - T_{amb)min}} \quad (4.27)$$

where T_{amb} is the ambient temperature. The supply temperature limits are fixed in order to avoid operating problems in the heat pump (freezing risk, very low pressure ratios in the compressor or very low COPs). In heating mode, the supply temperature limits that have been set are 35°C and 45°C; in cooling mode, the supply temperature will have a lower limit of 7°C and a higher limit of 15°C, the comfort temperature is set to 23°C.

4.3.7 Components power consumption

In order to calculate the system efficiency, it is necessary to first calculate the consumption of all the components. The consumption of the heat pump compressor, the heat pump fan and the parasitic consumption are calculated inside the heat pump type and collected inside the SPFs macro, shown in Figure 4.22.

Regarding the circulation pumps, their consumption will depend on the pressure drop inside the circuit, so the pressure drop in all the pipes in the system, the BHE, the BPHEs in the heat pump are summed up and the total pressure drop in each circuit is calculated.

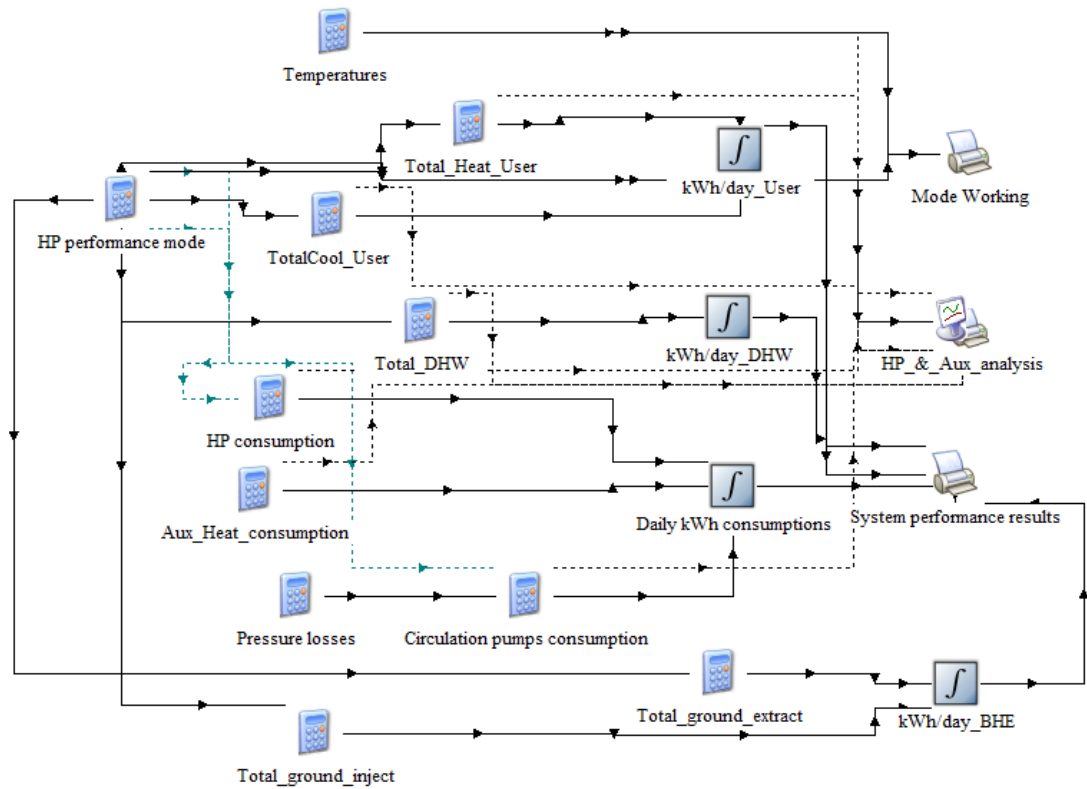


Figure 4.22. SPFs macro in TRNSYS

4.3.7.1 Circulation pumps

The same circulation pump was used for the three circuits. A correlation for the calculation of the pump electrical consumption depending on the pressure drop of the circuit and the volumetric flow rate was developed based on the experimental data obtained in the test campaign. So, the electrical consumption of one circulation pump $\dot{W}_{pump}(W)$ is calculated as a function of the pressure drop in the circuit Δp (kPa) and the volumetric flow rate \dot{V} (m^3/h), according to the equation (4.28) and the coefficients of the Table 4.3.

$$\dot{W}_{pump} = a_0 + a_1 \cdot \Delta p + a_2 \cdot \Delta p^2 + a_3 \cdot \dot{V} + a_4 \cdot \Delta p \cdot \dot{V} \quad (4.28)$$

Table 4.3. Coefficients for the calculation of the circulation pumps consumption

a0	3.9793
a1	0.7885
a2	0.0041
a3	2.2990
a4	0.2561

4.3.8 Performance assessment of the system

The efficiency of the system is calculated by using the Seasonal Performance Factors (SPFs) defined in the SEPAMO European project (SEASONAL Performance factor and MONITORING for heat pump systems in the building sector) [165]. In this project, several SPFs are defined, depending on how many components are considered for the calculation of the

system consumption. SPF1 (equation (4.29)) considers the heat provided to the user and DHW loop, as well as the heat pump consumption; SPF2 (equation (4.30)) considers also the source consumption (fan and ground circulation pump); SPF3 (equation (4.31)) also considers the backup heater consumption (not included in this model) and SPF4 (equation (4.32)) also considers the consumption of the user and DHW loop circulation pumps.

$$SPF1 = \frac{\int_0^t (\dot{Q}_{USER} + \dot{Q}_{DHW}) \cdot dt}{\int_0^t (\dot{W}_{HP}) \cdot dt} \quad (4.29)$$

$$SPF2 = \frac{\int_0^t (\dot{Q}_{USER} + \dot{Q}_{DHW}) \cdot dt}{\int_0^t (\dot{W}_{HP} + \dot{W}_{FAN} + \dot{W}_{BHE}) \cdot dt} \quad (4.30)$$

$$SPF3 = \frac{\int_0^t (\dot{Q}_{USER} + \dot{Q}_{DHW}) \cdot dt}{\int_0^t (\dot{W}_{HP} + \dot{W}_{FAN} + \dot{W}_{BHE} + \dot{W}_{BACKUP}) \cdot dt} \quad (4.31)$$

$$SPF4 = \frac{\int_0^t (\dot{Q}_{USER} + \dot{Q}_{DHW}) \cdot dt}{\int_0^t (\dot{W}_{HP} + \dot{W}_{FAN} + \dot{W}_{BHE} + \dot{W}_{BACKUP} + \dot{W}_{USER} + \dot{W}_{DHW}) \cdot dt} \quad (4.32)$$

where \dot{Q} is the useful heat in the user loop (\dot{Q}_{USER}) or DHW loop (\dot{Q}_{DHW}), and \dot{W} is the power consumption of each of the components existing in the system (heat pump \dot{W}_{HP} , fan \dot{W}_{FAN} , ground loop circulation pump \dot{W}_{BHE} , user circuit circulation pump \dot{W}_{USER} and DHW loop circulation pump \dot{W}_{DHW}), including the back-up system electrical consumption \dot{W}_{BACKUP} in case that there is any. The energy assessment will be carried out for one year of operation. So, the integration period will correspond to one year.

This values are provided by the types in TRNSYS and collected in the SPFs macro, shown in Figure 4.22. As there is no backup heater included in the model, the SPF3 will not be analysed in this system.

4.4 Tribano demo-site model: office building and heat pump control

As it was stated previously, a dynamic model of a system is a helpful tool in order to implement and test different control and optimization strategies without the need of implementing them in the real system, so it is possible to carry out a parametric analysis with different system configurations and control parameters in order to find the optimal solution, from the performance point of view.

In this regard, a dynamic model of the Tribano demo-site (described in section 2.3) has been developed in order to study a different control strategy for the heat pump compressor frequency in which the frequency will vary depending on the temperature inside the rooms directly, instead of controlling the supply temperature to the emission system. Furthermore, the addition of a buffer tank, an optimized schedule for the fan coils, the variation of the internal circuit circulation pump frequency and the use of a night mode has

also been tested inside the model, so it is possible to determine the optimal configuration and control strategy that provides comfort to the user with the lowest power consumption.

For this purpose, a complete building model has been developed as well as the coupling between the heat pump and the building, modelling the fan coils emission system. Therefore, the room temperature control strategy can be tested, as the dynamics of the whole system are well reproduced: the room temperature variation, the response of the emission system to the variation of the compressor frequency, etc. With the aim of simplifying the model and focusing on the compressor frequency control, only the air side of the DSHP has been used in the model, so the ground loop has been left aside.

The modelling of the building and the fan coils was based on a previous TRNSYS model developed in [130], where a departmental building in the *Universitat Politècnica de València*, in Valencia (Spain) was modelled together with the whole GSHP system that provided heating and cooling to the department. The office building in the Tribano demo-site was modelled based on the available information: number of fan coils per room, occupancy, schedules, construction year, building orientation, windows, adjacency and additional heat gains. The fan coils models were adapted to the ones installed in the Tribano demo-site and coupled to the building and heat pump models.

The DSHP installed in the Tribano system corresponds to the prototype #3 developed inside the GEOTeCH project, with a nominal capacity of 16 kW. Therefore, the DSHP model developed from the prototype #1 experimental data, with a nominal capacity of 8 kW, has been adapted.

With the model, it is possible to simulate the performance of the system during one year (or more) and calculate the system consumption under different configurations and control strategies. On the other hand, it is possible to calculate if the comfort was met in the different air-conditioned rooms during the occupied periods, for this purpose the European standard 15251:2007 was used [166]. It is important to mention that the controlled temperature inside the rooms as well as the temperature used to check the comfort requirements is the operative temperature, defined as the average temperature between the air in the zone and the average Mean Radiant Temperature (MRT) of the zone.

The different control strategies that can be tested inside the model are:

- Compressor frequency control. The frequency of the compressor is varied in order to meet the thermal demand of the building controlling one temperature controlling one temperature in the system:
 - Water temperature control.
 - Room temperature control.
- Internal circuit circulation pump.
 - Fixed speed.
 - Temperature difference control.
- Incorporation of a buffer tank in the supply of the internal circuit.
- Optimization of the fan coils working schedule.

- Night mode: the system operates at night only to maintain a minimum temperature setpoint during the winter (lower than the comfort setpoint during the working hours) and the system stops at night during the summer period.

The layout of the system model in TRNSYS is shown in Figure 4.23, where the different macros that define the system model are presented, as well as the constants that define the optimization strategies tested in the model.

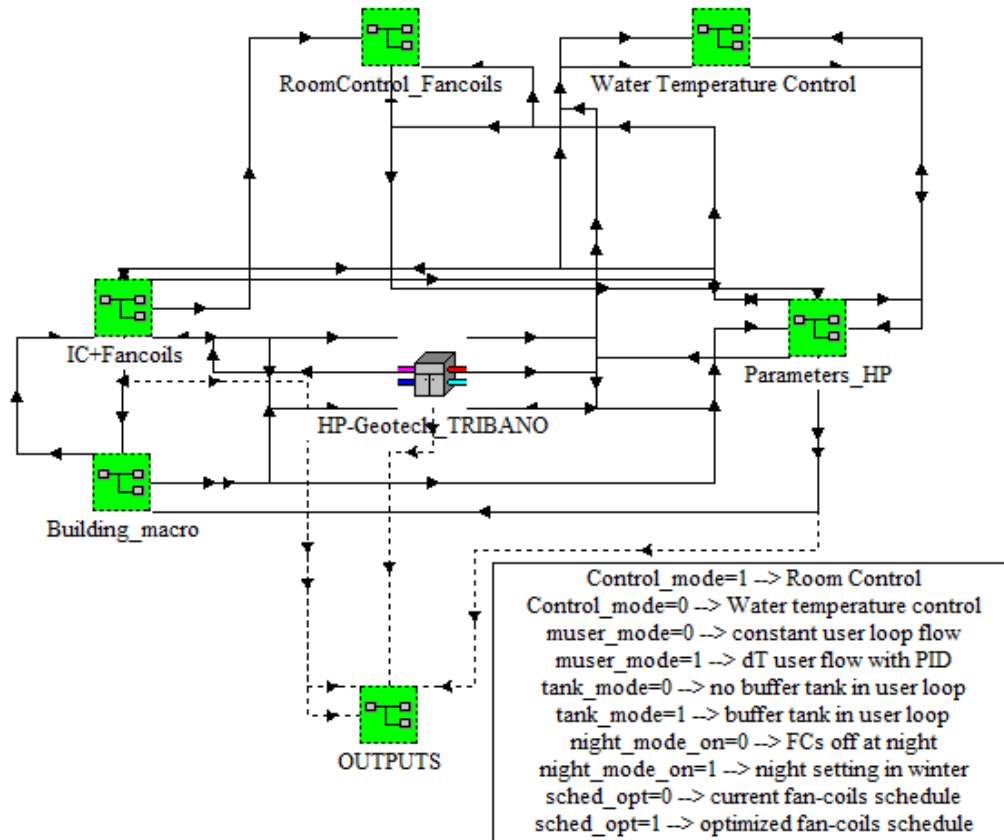


Figure 4.23. TRNSYS layout of the Tribano demo-site model

4.4.1 Heat pump model adaptation

The DSHP installed at the Tribano demo-site is quite similar to the prototype #1, from which the heat pump TRNSYS type was developed. The compressor cylinder capacity of the prototype #1 is 25 cc, while the cylinder capacity of the prototype #3 compressor is 38 cc, around a 50% bigger. So, in order to adapt the heat pump model to the Tribano heat pump, the condenser capacity, the evaporator capacity, the power input and the fan consumption is multiplied by a factor of 1.5 (a 50% higher) for a determined operating conditions. Furthermore, experimental data from the demo-site and the tests carried out with the prototype #3 by the University of Padova for the heat pump characterisation were used in order to check this scaling factor, obtaining a good agreement. Based on the experimental data from the prototype #3 tests, the parasitic losses were estimated in 82 W whenever the heat pump is on (not necessarily the compressor working).

4.4.2 Office building modelling

The office building corresponding to the air-conditioned spaces has been modelled in TRNSYS using the type 56 and the TRNBuild tool [167], based on the available data described in section 2.3.1. In this tool, the different thermal zones of a building can be modelled as one thermal node (see Figure 4.24), with the corresponding capacity of the zone (mainly the air volume) and the heat transfer with the adjacent zones and the exterior are simulated, also considering internal gains (lighting, occupancy, office equipment, etc.) air infiltrations from the outside, air coupling between zones, ventilation system, heating and cooling systems, the envelope materials and their thermal properties or the windows.

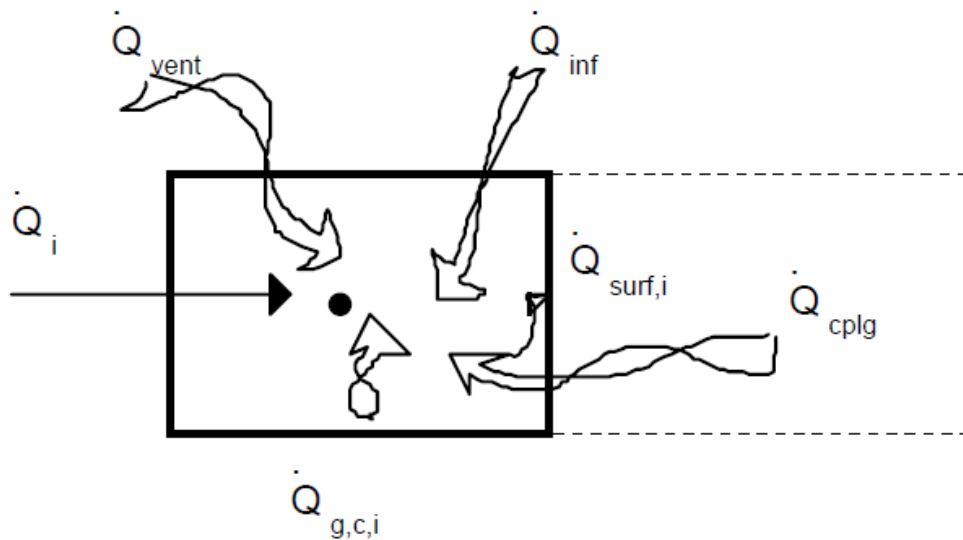


Figure 4.24. Heat balance on the zone air node [167]

The building model is used in the TRNSYS system model inside the type 56, as shown in Figure 4.25, where the building macro is presented and the main inputs to the building are detailed. A weather data file (type 109-TMY2), together with a psychometrics model (type 33e) and a sky temperature model (type 69b) are used in order to obtain the main climatic inputs to the building (solar irradiation on each surface of the building, dry and wet bulb temperatures, air humidity and sky temperature). As there is no weather file for Tribano or Padova in the TRNSYS weather library, the weather file for Venice is used (the closest Italian city available in the library). Additionally, a control for the natural ventilation (windows opening) has been defined in the macro VENTILATION_BUILDING.

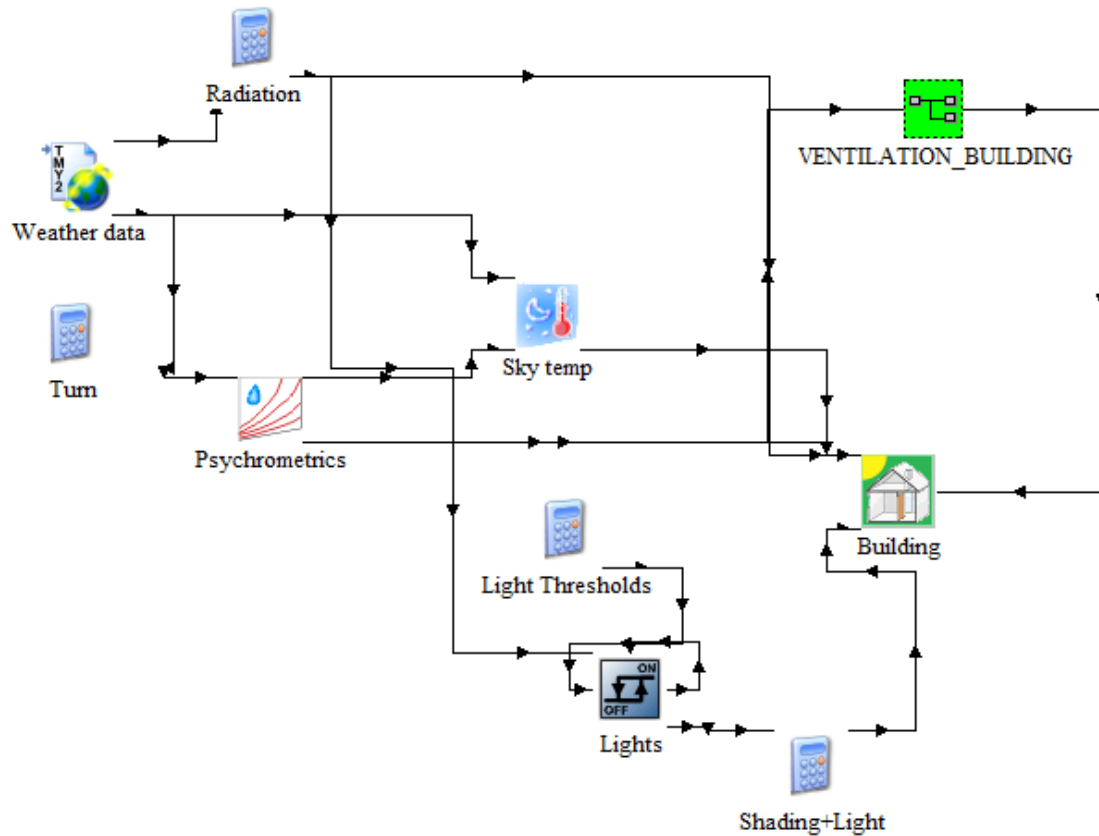


Figure 4.25. Tribano building macro in TRNSYS

The map of the building was shown in Figure 2.12. The three offices and the meeting room were modelled each one as one thermal zone, furthermore, the not air-conditioned area was also modelled as one thermal zone with no air-conditioning. Therefore, there are five thermal zones in the building model:

- Research and Development office, called RES in the model (Ricerca E Sviluppo).
- Sales office, called COMM in the model (Commerciale).
- Administration office, called AMM in the model (Amministrazione).
- Meeting room, called META in the model (Meta' Sala Incontri).
- Not air-conditioned area, called CORR (corridor).

The adjacency between zones is modelled, so there will be heat transfer between zones through the internal walls because of the temperature difference between zones. Moreover, the air flow exchange between the four conditioned zones and the corridor due to the opening of the doors is modelled as a coupling air flow of 1 kg/h. The adjacency with the production building in the zones RES and CORR is modelled as a temperature boundary, so it is supposed that the production building maintains a fixed temperature of 18°C in winter and 21°C in summer. The adjacency to the other half of the building (right side of the building) is considered as an adiabatic condition. The scheme of the thermal zones in the building is shown in Figure 4.28, with the number of fan coils (FCs), the air coupling

between zones, the temperature boundaries and other additional thermal gains explained in section 4.4.2.2.

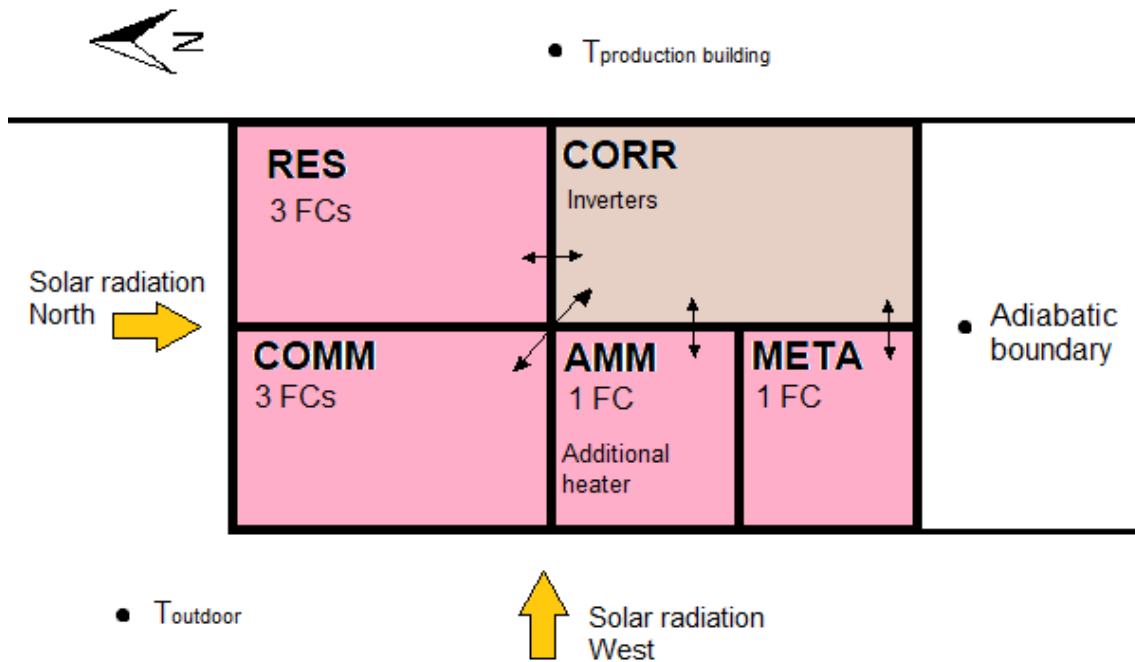


Figure 4.26. Tribano building modelling. Thermal zones scheme

The four conditioned zones (coloured in pink) are exposed to the outdoor conditions, this adjacency is modelled as a heat transfer between the outdoor air temperature and the thermal zone air due to the temperature difference, considering the U-value of the wall and windows depending on the materials and thickness of the different layers. But it is also considered the radiative heat transfer due to the solar irradiation on the exterior walls (they will be heated up because of this solar radiation and later on this heat will be rejected to the zone air), the solar radiation through the windows (the properties of the windows are considered, like the g-value), the infiltration of outdoor air inside the zones (0.6 ach) and the natural ventilation when the windows are opened.

The air-conditioned zones are located at the second floor of the office building (and top floor). It is considered that there is no heat transfer with the floor underneath and the floor is in contact with the outside, with the corresponding solar radiation on a horizontal surface and outdoor air temperature.

4.4.2.1 Building envelope

The building envelope is defined by the external walls, roof and windows. There was no information about the specific materials of which they were built, but it is known that the building was constructed in the 90's. So, in order to define the materials and global heat transfer coefficient per unit area (U-value) of the walls, roof and windows, the data collected in the TABULA European project [168] was used. In the project website, it is possible to find a webtool, with data about the construction materials used for the construction of different types of buildings, during different time spans and different countries (see Figure 4.27). So,

the construction data corresponding to an apartment block built between the years 1991 and 2005 in Italy with advanced refurbishment was used.










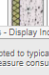
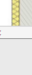
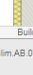


		Existing state	Usual Refurbishment	Advanced Refurbishment
Roof 2	surface area	679.1m ²	679.1 m ²	679.1m ²
	type of construction / refurbishment measure	Ceiling with reinforced brick-concrete slab, medium insulation Solaio latero-cementizio, medio livello di isolamento	add 8 cm of insulation aggiunta di 8 cm di materiale isolante	add 12 cm of insulation aggiunta di 12 cm di materiale isolante
	picture			
	U-value	0.57 W/(m ² K)	0.27 W/(m ² K)	0.21 W/(m ² K)
Wall 1	surface area	440.4m ²	440.4 m ²	440.4m ²
	type of construction / refurbishment measure	Concrete masonry (also prefabricated, 30 cm), medium insulation Muratura in calcestruzzo (anche prefabbricata, 30 cm), medio livello di isolamento	add 6 cm of insulation aggiunta di 6 cm di materiale isolante	add 9 cm of insulation aggiunta di 9 cm di materiale isolante
	picture			
	U-value	0.60 W/(m ² K)	0.32 W/(m ² K)	0.26 W/(m ² K)
Wall 2	surface area	1328.5m ²	1328.5 m ²	1328.5m ²
	type of construction / refurbishment measure	Hollow brick masonry (40 cm), medium insulation Muratura in mattoni forati (40 cm), medio livello di isolamento	add 6 cm of insulation aggiunta di 6 cm di materiale isolante	add 9 cm of insulation aggiunta di 9 cm di materiale isolante
	picture			
	U-value	0.59 W/(m ² K)	0.31 W/(m ² K)	0.25 W/(m ² K)
Wall 3	surface area	760.0m ²	760.0 m ²	760.0m ²
	type of construction / refurbishment measure	Concrete masonry (also prefabricated, 18-20 cm), medium insulation Muratura in calcestruzzo (anche prefabbricata, 18-20 cm), medio livello di isolamento	add 6 cm of insulation aggiunta di 6 cm di materiale isolante	add 10 cm of insulation aggiunta di 10 cm di materiale isolante
	picture			
	U-value	0.59 W/(m ² K)	0.31 W/(m ² K)	0.25 W/(m ² K)
Country:  In charge: Politecnico di Torino - Department of Energetics Charts - Display indicators: adapted to typical level of measure consumption Display Primary Energy on pages "Varianti": Total primary energy Assessment of Energy Carriers: European standard values Building: IT.MidClim AB 07.Gen.ReEx.001 				

Figure 4.27. TABULA Webtool [168]

The definition of the different wall types (outwall or intwall), floor and windows are introduced in the TRNBuild interface, as shown in Figure 4.28. Here, it is introduced the area of wall/floor/roof, the type of wall, the boundary condition, the area of windows in the wall, the internal or external shading in the windows and the orientation of the surface. Regarding the windows, it was considered that in the zones RES, COMM and AMM, the area of windows is around a 25% of the wall surface. In the case of the meeting room (META), the entire wall is glazed, so it was considered a windows surface of around a 95% of the wall. The blinds incorporated on the inside side of the windows of the offices are modelled with an internal shadowing factor only in summer. For the meeting room, it was considered a constant internal shadowing during the whole year (as the blinds are used the whole year) and an external shadowing factor during the summer (as an external sunshade is used when the radiation is too high). The detailed information about the walls and windows definition is presented in the Appendix C Tribano office building characteristics.

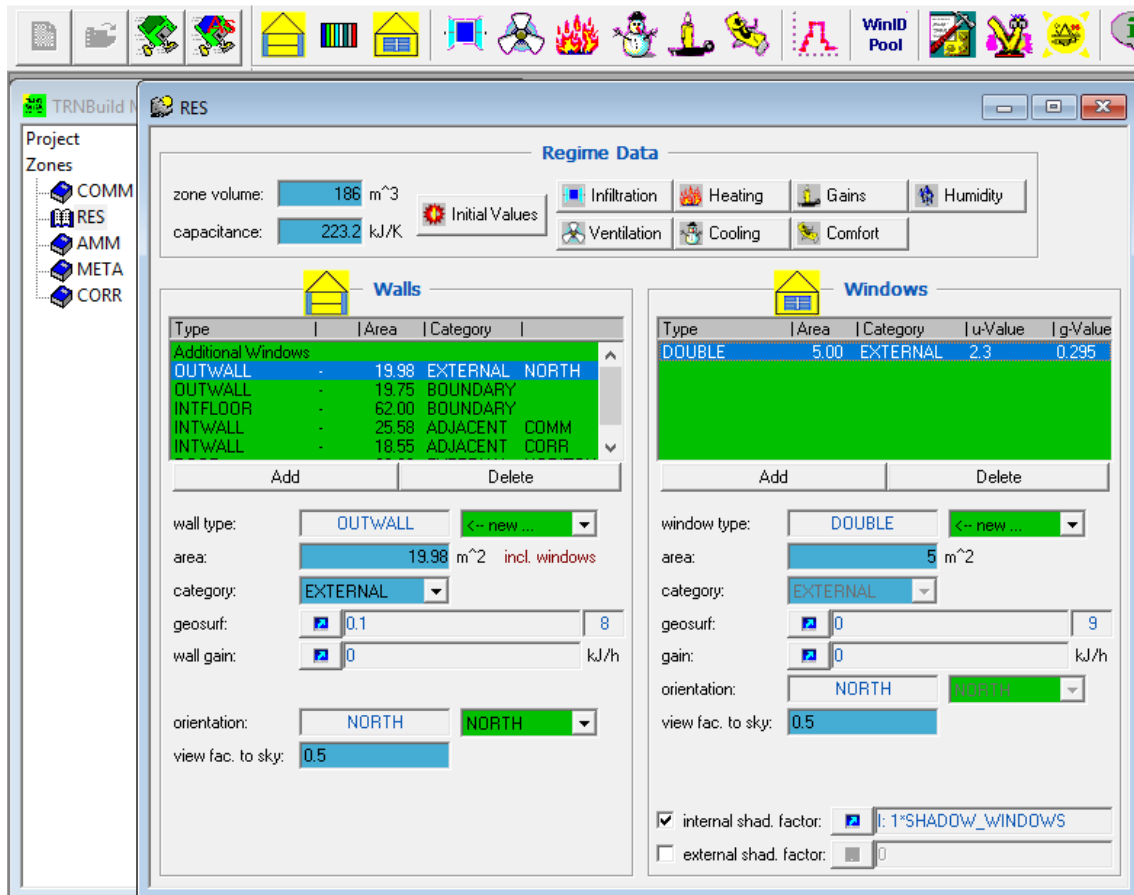


Figure 4.28. Tribano building model in TRNBuild

4.4.2.2 Internal gains

The different heat gains due to the internal loads is considered for the different thermal zones. Based on the information about the number of people and computers used in the different rooms and the working schedules (shown in Table 2.3), the internal gains were defined in each thermal zone, considering that not all the people will be inside the room the whole time, and then their computers will be off (they might be travelling, in the production building, the meeting room, etc.)

Table 4.4. Internal gains definition in TRNBuild for the thermal zones

Zone	Schedule (Monday – Friday)	Occupancy and equipment	Number of fan coils	Additional gains
RES	8 h – 18 h	5 people 5 computers	3	-
COMM	8 h – 18 h	5 people 5 computers	3	-
AMM	8 h – 18 h	3 people 3 computers	1	2 kW heater
META	9 h – 12 h	4 people 1 computer	1	-
CORR	8h – 18 h	No people 1 printer	0	Inverters 0.5 kW

Regarding the occupancy, it was considered a degree of activity corresponding to “seated, light work, typing”, included in the TRNBuild tool, following the standard ISO 7730. Except for the meeting room, where it was considered a degree of activity corresponding to “seated, very light writing”. It is considered that the entire surface of the zones is illuminated with artificial lighting during the opening hours, and the total heat gain produced is 10 W/m².

Additionally, a small electric heater of around 2 kW is used in the administration office, and some electronic inverters are placed in the corridor that are on whenever there is solar radiation (as they are used for the solar panels on the roof). It was supposed a heat rejection of 500 W due to the heat rejected by the inverters when they are working.

4.4.2.3 Natural ventilation

It is possible that, despite the heating and cooling system, the indoor temperature in a room would increase too much and the user would open the windows, generating an outdoor air flow inside the room. In order to model this phenomenon, an input signal from the corresponding room is sent to the building type, and it will consider that an air renovation of 2 ach is introduced in the zone with the outdoor conditions (temperature and humidity).

The human behaviour of opening the windows when it is too hot inside and closing the windows when the zone temperature reaches an acceptable temperature is modelled by differential controllers with hysteresis (shown in Figure 4.29). So, when the indoor temperature increases above 27°C, there will be natural ventilation, but when the temperature of the room decreases below 26°C, the natural ventilation will stop, simulating the opening/closing of the windows (always assuring that the outdoor temperature is below the indoor temperature to prevent the entrance of hot air).

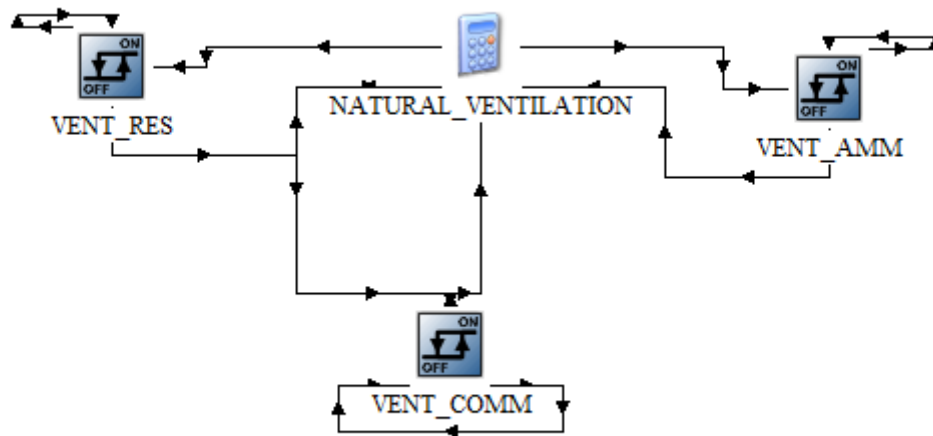


Figure 4.29. Tribano building natural ventilation control

4.4.3 Internal circuit

The circuit that connects the heat pump to the fan coils inside the building is modelled with two pipe models (same type described in section 4.3.1.2), in order to account for the supply and return pipes, and the fan coils models (explained in section 4.4.4). A buffer tank was added to the internal circuit (type 60d), just after the heat pump supply, before the supply pipe. However, the TRNSYS model was developed in such a way that it is possible to bypass this tank and test the performance of the system when using it or not. The buffer tank was sized according to the methodology explained in section 4.3.1.1, with a resulting tank volume of 60 litres. The length of pipes between the heat pump and the fan coils was assumed 25 m and 15 simple elbow joints were considered for each pipe in order to account for all the possible additional pressure drop in the pipes due to different elbows and connections. Regarding the thermal losses in the distribution pipes, the pipes are located almost entire inside the building, so a weighted average temperature between the machinery room and the outdoor temperature is used in order to set the environmental temperature used in the heat loss calculation, according to the equation (4.33).

$$T_{environment\ pipes} = (T_{machinery\ room} \cdot 0.8 + T_{outdoor\ air} \cdot 0.2) \quad (4.33)$$

The layout of the internal circuit macro is shown in Figure 4.30. The macro where the fan coils models are defined is described in section 4.4.4.

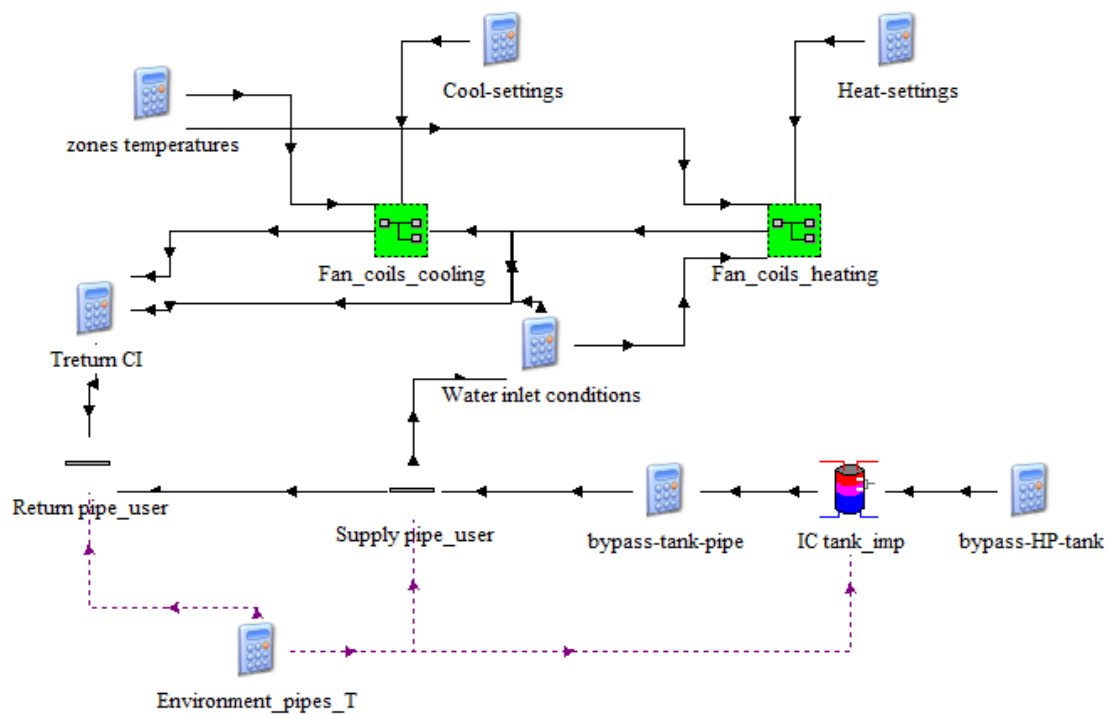


Figure 4.30. Internal circuit and fan coils macro in TRNSYS

4.4.4 Fan coils modelling

The modelling of the fan coils was developed based on the work [130], as the modelling presented in this PhD thesis was validated with experimental data, but adapting the fan coils

models to this specific application. In each thermal zone, one heat exchanger type models the behaviour of one of the fan coils in the room, the heat gain that it introduces will be multiplied by the number of fan coils in the zone. Regarding the heat exchanger type used for the fan coil, it was considered a different type for heating and cooling applications, so the heating fan coil was modelled as a simple cross flow heat exchanger with fluids unmixed (type 5e). For the cooling application, a detailed heat exchanger, including the heat exchange and dehumidification phenomenon, was used (type 52b).

As it is shown in Figure 4.30, there are different macros for the cooling fan coil models and the heating fan coil models. Inside each macro, a calculator distributes the water flow rate among the different fan coils and sets the inlet temperature of the fan coils, as it is shown in Figure 4.31. Furthermore, in this macro the outlet temperature from the fan coils is collected and the final temperature resulting due to the water mixing is calculated and will be used as the inlet temperature in the return pipe.

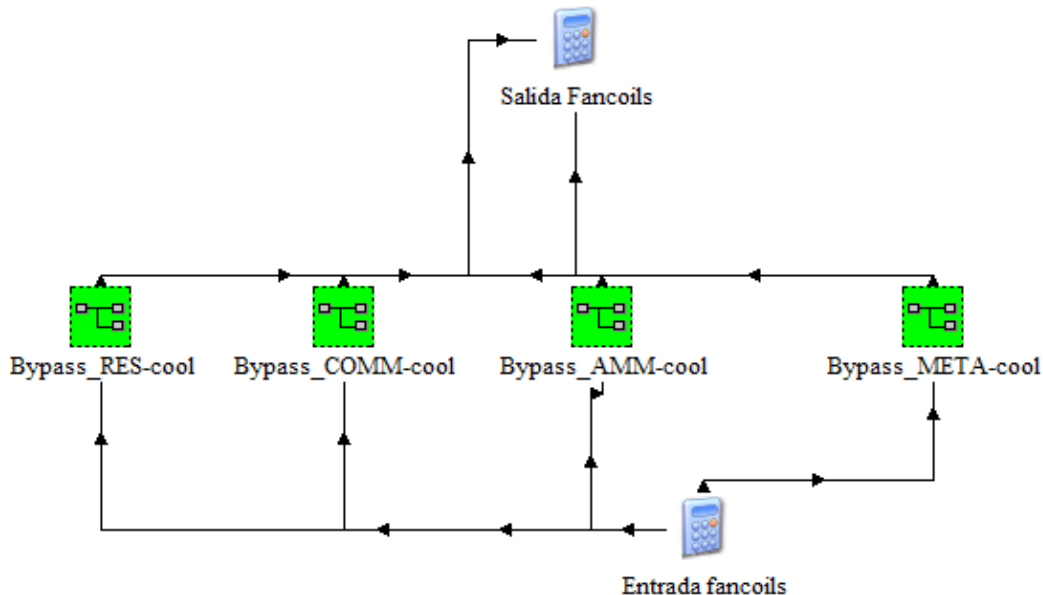


Figure 4.31. Fan coils connection in TRNSYS

4.4.4.1 Cooling fan coil model

The cooling fan coils are modelled with the type 52b. In this type, the geometric characteristics of the fan coil are introduced as parameters, so the heat transfer between the water and the room air is calculated based on these geometric characteristics and the inlet conditions of each flow (temperature and flow of water and air and air humidity). The same model used in [130] was used here, but adapting the size of the fan coil to the model installed in Tribano. The humidity ratio of the room air is calculated at the inlet and the outlet of the heat exchanger, with the types 33e and 33c, respectively, in order to calculate the humidity ratios.

A differential controller with hysteresis (type 2b) is used in order to control the operation of the fan coil, so the fan coil will switch off when the zone air temperature falls below the lower limit and it will switch on when it rises above the upper limit. A

symmetrical dead band around the setpoint temperature is used for defining these limits ($\pm 1K$).

The air flow depends on the fan speed selected in the fan coil, a new type has been developed in order to set the corresponding fan speed depending on the room air temperature and is described in section 4.4.4.3. The power consumption will also depend on the fan speed and will be calculated also inside this new type.

The heat extracted from the zone air temperature and the dehumidification are calculated and introduced as a cooling and dehumidification load in the corresponding thermal zone in the type 56 (building model), multiplied by the number of fan coils presented in the thermal zone. Furthermore, the outlet temperature of the water is calculated and used in the calculation of the return temperature.

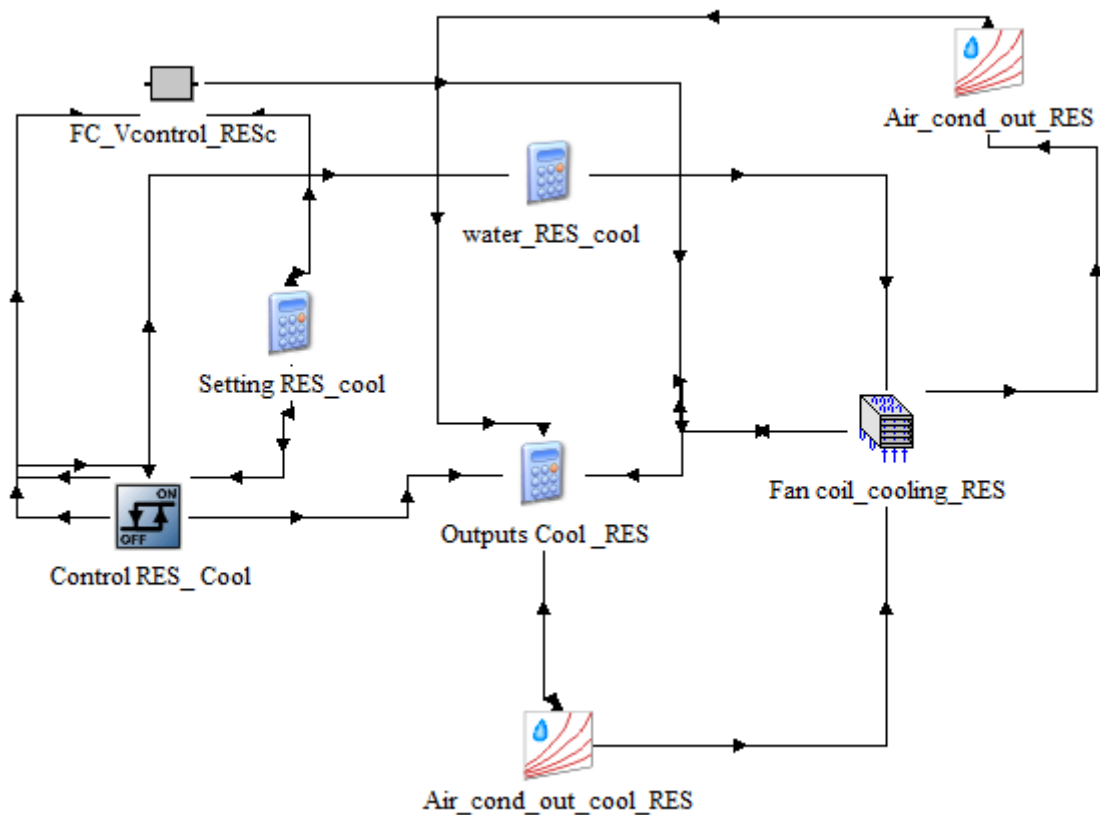


Figure 4.32. Fan coil TRNSYS modelling in cooling mode

4.4.4.2 Heating fan coil model

The heating fan coil was modelled using a simpler heat exchanger type. A cross flow heat exchanger with fluids unmixed type was used (type 5e). In this type, the overall heat transfer coefficient of the heat exchanger (UA value) is introduced as an input instead of defining its geometrical characteristics. A correlation for calculating this UA value was developed, adapting the correlation used in [130], as a function of the water mass flow rate, based on the catalogue data of the fan coil model in the manufacturer webpage (FLAT S-20 fan coil, manufactured by Galletti). This data is presented in Table 2.4 (heating capacity at

different mass flow rates and fan speeds). The expression used for calculating the overall heat transfer coefficient (in $\text{kJ}/(\text{h}\cdot\text{K})$) is presented in the equation (4.34).

$$UA_{\text{heating}} \left(\frac{\text{kJ}}{\text{h}\cdot\text{K}} \right) = (1454.55 \cdot \dot{m}_{\text{water,FC}} + 58.77) \cdot 3.6 \quad (4.34)$$

The heating fan coil macro is very similar to the cooling fan coil macro, it also incorporates a differential controller with hysteresis to control the fan coil cycling, the outlet water temperature is also calculated and the fan speed is set by the fan speed controller type depending on the zone air temperature. The main difference is that in the heating model, the humidity is not considered, the UA value is introduced as an input in the heat exchanger and calculated in the fan coil controller type and it is a heating gain the one introduced in the type 56 into the corresponding thermal zone, multiplied by the number of fan coils in the zone. This macro is shown in Figure 4.33.

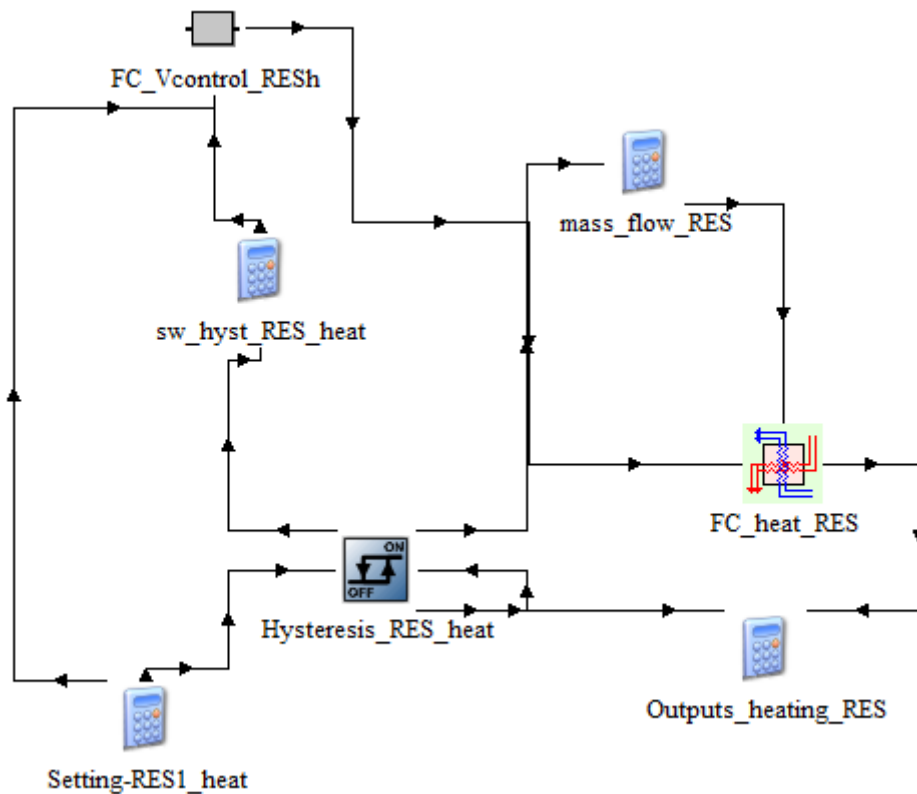


Figure 4.33. Fan coil TRNSYS modelling in heating mode

4.4.4.3 Fan coils control

A new type has been developed in order to control the fan speed in each fan coil depending on the room air temperature. In this type it is also calculated the overall heat transfer coefficient (UA value) and the power consumption of the fan coil.

The fan coil is capable of working at three different speeds, corresponding to different air flow rates, as shown in Table 2.4. The speed control type compares the actual room temperature with the desired room temperature and uses two limits in order to determine the fan speed, so the fan speed will increase if the room temperature is moving away from

the setpoint (too low in heating or too high in cooling), then improving the heat transfer to compensate the undesired room temperature. The control strategy for heating mode is explained as follows, the first and second limit will be below the setpoint:

- If the room temperature is above the setpoint, the fan speed will be the minimum (speed 1).
- If the room temperature is below the setpoint and above the first limit (T limit 1), but it was previously at speed 1, it is kept at speed 1. Otherwise, it will be set at speed 2 (medium speed).
- If the room temperature is between the first limit and the second limit (T limit 2), if the previous speed was the speed 3 (maximum speed), it is kept at speed 3. Otherwise, it is set at speed 2.
- If the room temperature is below the second limit, the fan speed will be the speed 3.

An example of this control is shown in Figure 4.34. The control strategy is analogous in cooling mode.

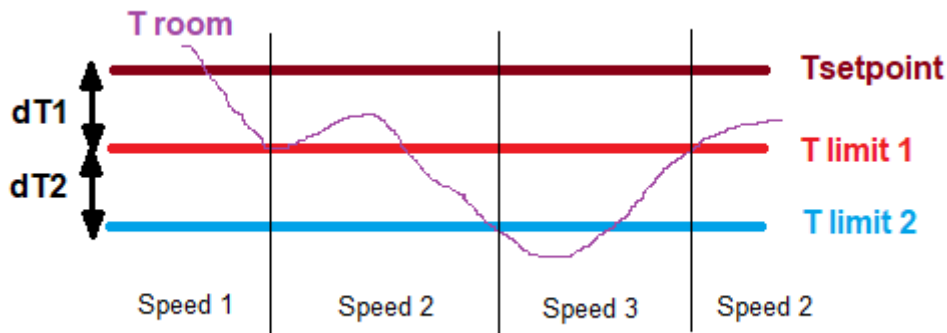


Figure 4.34. Fan speed controller for heating mode

4.4.4.4 Fan coils pressure drop

The pressure drop is calculated for one fan coil, as they are connected in parallel. A correlation has been obtained based on the catalogue data and depending on the water flow rate. The correlation is presented in the equation (4.35) and plotted in Figure 4.35.

$$dP(kPa) = 1.4103 \cdot e^{(6.8741 \cdot 10^{-3} \cdot \dot{m}_{water,FC})} \quad (4.35)$$

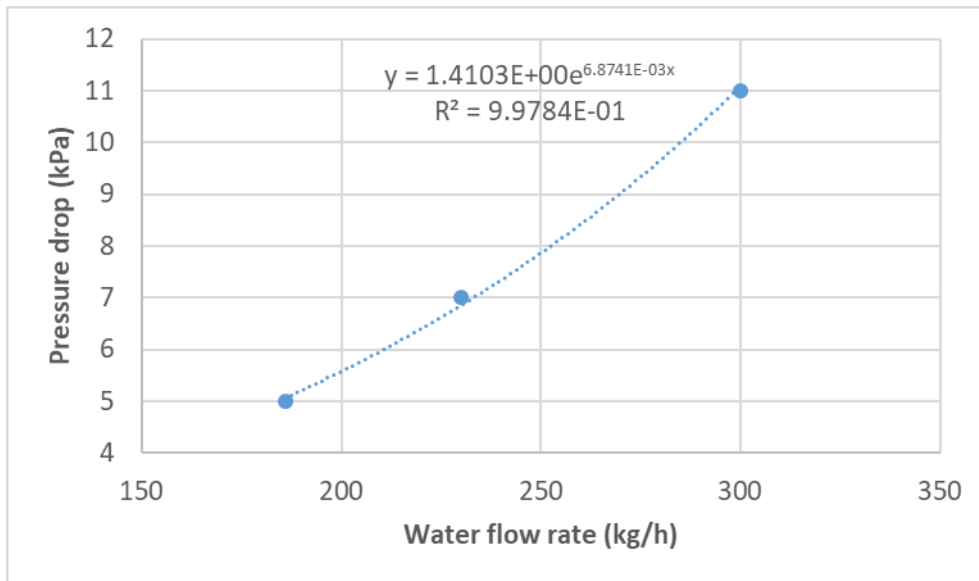


Figure 4.35. Pressure drop in the fan coils

4.4.5 Compressor control

The compressor of the heat pump can vary its frequency in order to adapt the capacity of the heat pump to the thermal demand of the building. In practice, the compressor frequency is varied with a PID controller, trying to keep a determined water temperature in the internal circuit (supply or return side). In this model, an alternative control strategy for the compressor frequency variation is proposed, in which the compressor frequency will be varied as a function of the temperature in the rooms, for this purpose, first the worst room must be selected and the compressor frequency will be varied in order to reach the desired room temperature. Both strategies can be compared in the model in order to obtain the savings of applying the new strategy in comparison with the water temperature control.

4.4.5.1 Water temperature control

The water temperature control strategy is the same explained for the plug and play system in section 4.3.5. It is possible to select the supply temperature control (after the buffer tank if there is any) or the return temperature control (inlet of the heat pump). The PID controller will compare the actual water temperature with the desired setpoint and will increase or decrease the compressor frequency in order to reach the setpoint and keep that temperature. Usually only the proportional and integral actions of the PID are used. The control parameters used in this model are:

- Minimum frequency of the compressor = 20 Hz.
- Maximum frequency of the compressor = 80 Hz.
- Hysteresis ON=1.5K.
- Hysteresis OFF=1.5K.
- PID controller constants:
 - Kp (proportional constant) = 10.

- T_i (integral time) = 300 s.
- T_d (derivative time): not used.

The setpoint temperatures can be varied easily and will be study in a parametric analysis. Furthermore, the setpoint will change depending on the controlled temperature selected (supply or return). Figure 4.36 shows the scheme of the water temperature control macro in TRNSYS.

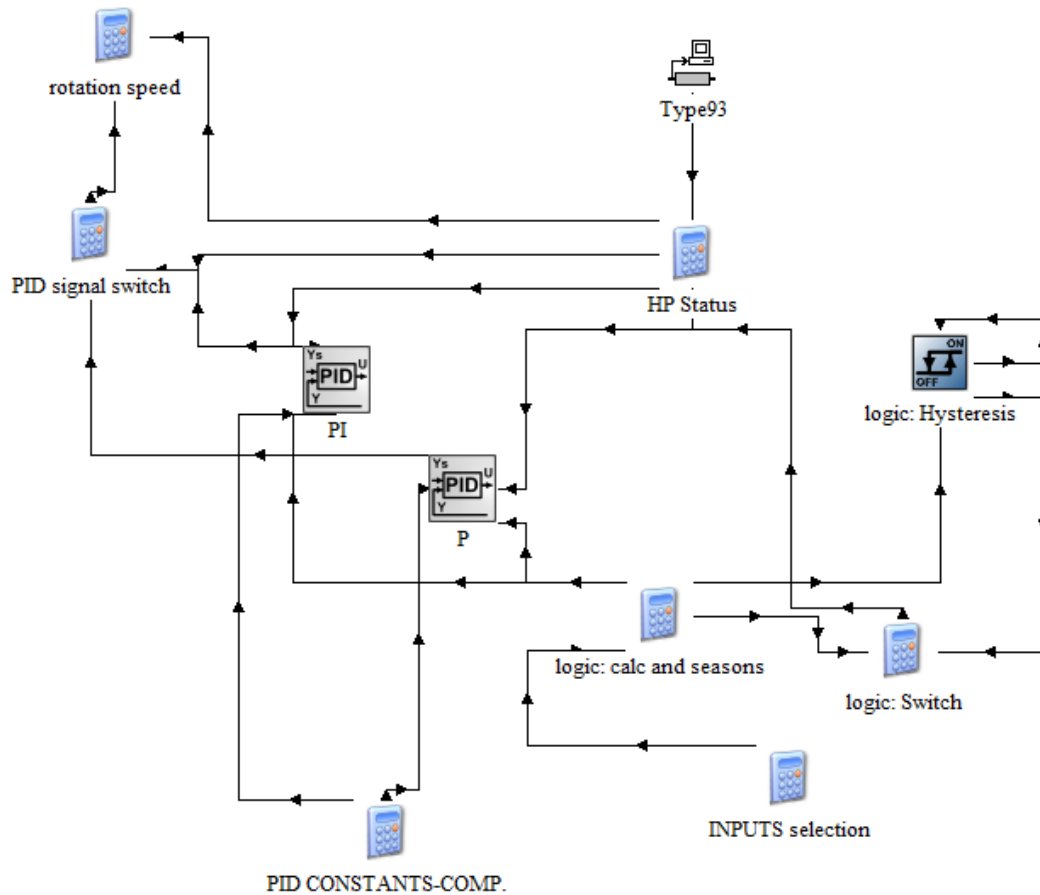


Figure 4.36. Water temperature control in TRNSYS

4.4.5.2 Room Temperature control

A new room temperature control has been developed in order to set the frequency of the compressor based on the temperature of the conditioned spaces instead of just controlling the supply temperature. This control strategy is based on the fact that, when the thermal load is not very high, there is no need of producing water at the supply temperature setpoint, but it could be produced at a reduced temperature, then increasing the efficiency of the heat pump. So the frequency of the compressor will be controlled by a PID controller, trying to maintain the room temperatures at the desired setpoint (23°C, for example), whenever the supply temperature is not too extreme, in order to prevent too extreme outlet temperatures and thus, a very low efficiency of the heat pump.

For this purpose, two PID controllers are used at the same time and the resulting frequencies calculated by each controller are compared, using the minimum frequency as the compressor frequency:

- Supply temperature PID. It will calculate the frequency of the compressor based on the supply temperature, trying to maintain this temperature at the maximum setpoint. A differential controller with hysteresis is also used, in order to make the heat pump cycle with the minimum frequency when the thermal load is low, therefore preventing the supply temperature to increase too much in heating mode and to reach a very low temperature in cooling mode.
- Room temperature PID. First, the worst room at each moment is selected based on their actual temperature and their temporal evolution. A new TRNSYS type was developed for this purpose. Then, the PID controller will calculate the compressor frequency in order to reach the desired temperature in the worst room at every moment.

A scheme of this control strategy is shown in Figure 4.37. It is important to mention that, the PID controllers will use the proportional and integral action whenever they are the PID actuating (their compressor frequency is the lowest). However, only the proportional action will be used when they are not the actuating controller. This is necessary in order to prevent the controller to accumulate the error with the integral part, when it is trying to control a temperature that it is not actually controlling in this moment, because the PID that is actuating is the other one.

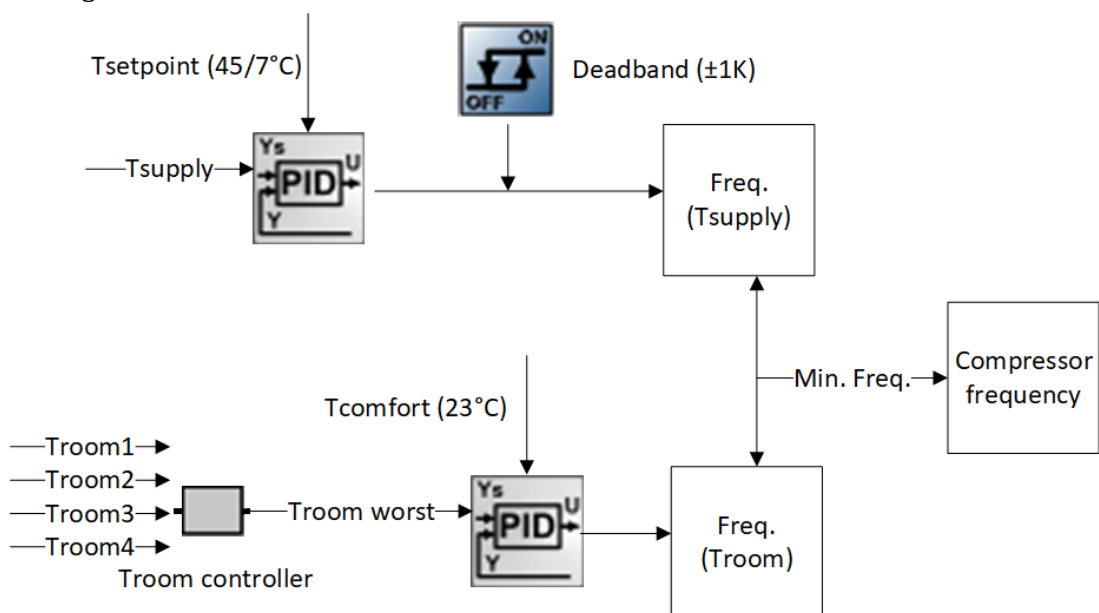


Figure 4.37. Scheme of the compressor frequency control using the room temperature approach

Worst room selection

A new type has been developed to select the worst room at each moment based on their actual temperature and the temporal evolution, the TRNSYS type code and the main parameters to introduce are presented in Appendix A. For this purpose, the inputs introduced in the type are:

- Current temperature of each zone.
- Setpoint of each zone.
- ON/OFF signal. In order to know if the fan coils of each zone are on or off. If all the fan coils are off, the controller will produce a signal in order to switch off the heat pump.
- Season signal, to know if the heat pump is working in heating or cooling mode.

The parameters introduced in the type are:

- Number of rooms to be controlled.
- Number of simulation time steps used to calculate the temporal evolution of the room temperature.
- Deadband used in the rooms' thermostat.

The type will calculate the worst room and it will produce as outputs its temperature, setpoint and a signal to send to the PID controllers in order to know if there is any fan coil working or if all of them are off, in which case the heat pump will stop.

The procedure used to select the worst temperature is described as follows:

1. The current temperature of each room is stored until the number of time steps selected. This value will be used in the following time steps in order to calculate the temperature slope in the room.
2. If all the fan coils are off, the controller will produce as output that the heat pump is off and it will end the procedure. If there is at least one fan coil operating, the controller will continue as follows.
3. The slope of the temperature evolution is calculated for each room using the number of time steps defined (n_{steps}). The equation (4.36) shows the expression used for calculating the slope of the room i at a determined time step t , where Δt is the simulation time step.

$$T_{slope_{room,i}}(t) = \frac{T_{room,i}(t) - T_{room,i}(t - n_{steps} \cdot \Delta t)}{n_{steps} \cdot \Delta t} \quad (4.36)$$

4. All the rooms temperature will be compared with their corresponding setpoint and the limit given by the deadband, if they are out of the deadband (below the limit in heating mode or above the limit in cooling mode), the room with the highest temperature difference between the room temperature and the corresponding setpoint will be selected as the worst room.
5. If all the rooms are inside the limit, the temperature slopes will be compared and the worst room will be the room with the lowest slope value in heating mode (the room where the temperature is decreasing faster) and the one with the highest value in cooling mode (the room where the temperature is increasing faster).

The entire room control macro is shown in Figure 4.38. Regarding the parameters used in the control, they are summarized here:

- Minimum frequency of the compressor = 20 Hz.
- Maximum frequency of the compressor = 80 Hz.
- PID controllers constants (both):
 - K_p (proportional constant) = 20.
 - T_i (integral time) = 300 s (when PID is actuating).
 - T_d (derivative time): not used.
- Hysteresis supply temperature= ± 1.5 K.
- Supply temperature setpoints= 45°C for heating and 7°C for cooling (changed in the parametric analysis).
- Room temperature setpoint= 23°C .
- Deadband worst room selection = 1K.
- Number of time steps (n_{steps}) = 2.

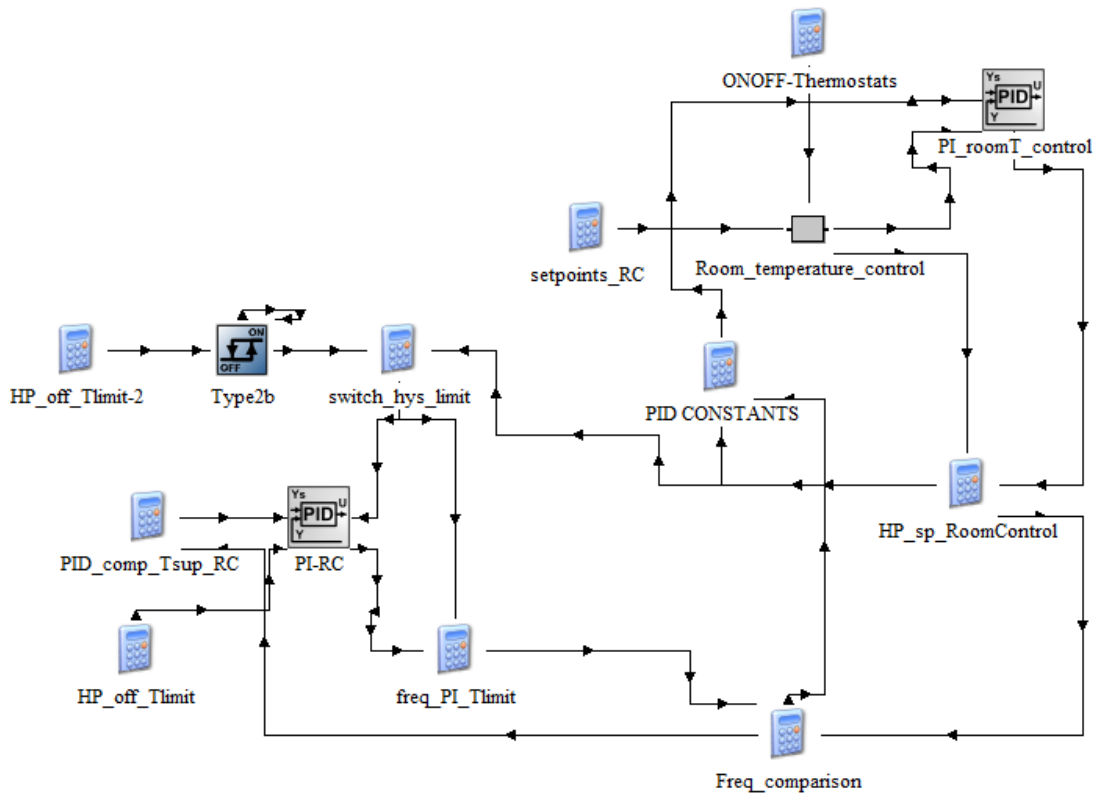


Figure 4.38. Room temperature control in TRNSYS

4.4.6 Heat pump parameters

The main parameters that define the operation and control of the system are defined inside this macro (Figure 4.39).

On one hand, the main inputs to the building are defined in the calculator INPUTS_BUILDING. First of all, the working schedules are defined using forcing functions:

- Season signal: summer season (cooling mode) from 15th May until 1st October.
- Working Schedule of the office: from 8h to 18h during the weekdays.
- Original fan coils schedule of all the rooms: from 7.5h to 20h during the weekdays.
- Optimized fan coils schedule of the offices: from 7h to 19h during the weekdays.
- Optimized fan coils schedule of the meeting room: from 7h to 13h during the weekdays.

Secondly, the shadowing factors for the offices rooms and the meeting room depending on the season:

- An internal shadowing factor of 0.8 during the summer season in the offices windows.
- An internal shadowing factor of 0.4 the whole year for the meeting room.
- An external shadowing factor of 0.6 during the summer.

Finally, other inputs defined here are:

- The temperature of the production building: 18°C in winter and 21°C in summer.
- The working signal for the inverters in the corridor: when there is solar radiation.
- The night mode setting: 15°C when it is on.

On the other hand, the heat pump control parameters are defined in the calculator HP_parameters. Here, the control parameters defined as constants in the TRNSYS model are set:

- The compressor frequency control: water temperature or room temperature.
- Mass flow rate through the internal circuit depending on the circulation pump control: fixed speed and a flow rate of 3000 kg/h or variable speed and a constant temperature difference (3 or 5 K).
- The speed of the heat pump fan: it is assumed a speed proportional to the compressor frequency: $f_{fan}(\%) = f_{compressor}(Hz) + 10$.
- The working mode of the heat pump: M1-Summer Air or M4-Winter Air.

Finally, a PID controller calculates the mass flow rate through the internal circuit in order to obtain a constant temperature difference in the circuit. This mass flow rate will be used in the model only when this operation mode is selected. The main parameters of the PID controller are:

- Minimum mass flow rate = 1000 kg/h.
- Maximum mass flow rate = 3500 kg/h.
- PID controller constants:
 - Kp (proportional constant) = 10.
 - Ti (integral time) = 50 s.

- Td (derivative time): not used.

The entire macro layout is shown in Figure 4.39.

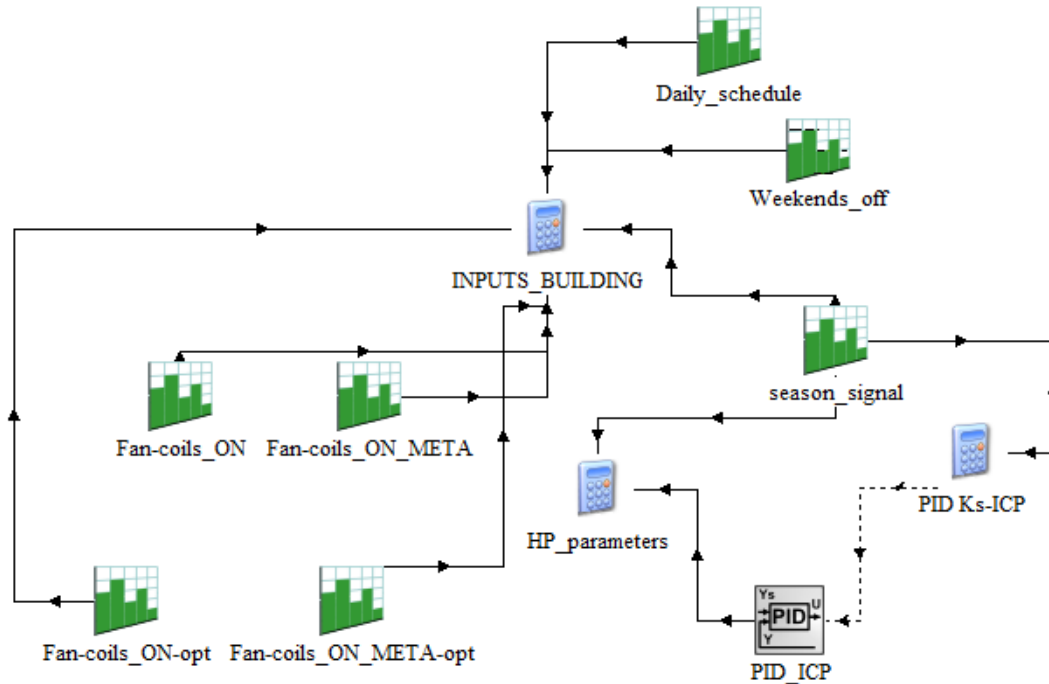


Figure 4.39. Heat pump parameters macro in TRNSYS

4.4.7 Outputs: power consumption and comfort

The main outputs calculated in order to compare the different scenarios that can be tested with the model are the energy consumption and the comfort achieved. The energy consumption will be the integration of the power input in the different components of the system:

- Heat pump, including the consumption of the compressor, the fan and the parasitic losses.
- Fan coils, the fan coils consumption depends on the fan speed and the time that is working. The sum of all the different fan coils consumption will determine the total fan coils consumption.
- Circulation pump. The internal circulation pump used in this heat pump is the same used for the prototype #1, so the correlation presented in the equation (4.28) is used to calculate the power consumption as a function of the total pressure drop in the circuit and the flow rate. The total pressure drop includes the pressure drop caused by the heat pump BPHE, the supply and return pipes and the fan coil pressure drop.

On the other hand, it is important to check that the comfort requirements were met inside the different thermal zones. For this purpose, the operative temperature at each moment inside each room is analysed and compared to the comfort requirements during the occupied periods. The European standard 15251:2007 was used [166] to define the maximum acceptable temperature in cooling and the minimum acceptable temperature in

heating for an office space. This standard defines different comfort categories (from category I to category IV, being I the most strict) and different limits for each category.

The category II defines the minimum temperature for heating in 20°C and the maximum temperature for cooling 26°C. The category III defines 19°C and 27°C, respectively. But the main comfort category used was the category II.

So, the time during which each zone presents an operative temperature out of the limits of the category II is integrated and produced as outputs:

- Heating mode: $T_{operative} < 20^{\circ}\text{C}$.
- Cooling mode: $T_{operative} > 26^{\circ}\text{C}$.

Therefore, for each thermal zone there will be an indicator of the number of hours “out of comfort”. In order to carry out a deeper analysis if needed, it was also calculated the time in which the operative temperature of each zone was between specific temperature ranges:

- Heating mode:
 - Lower than 19°C.
 - [19°C -20°C].
 - [20°C -21°C].
 - [21°C -23°C].
 - [23°C -25°C].
 - Higher than 25°C.
- Cooling mode:
 - Lower than 23°C.
 - [23°C -25°C].
 - [25°C -26°C].
 - [26°C -27°C].
 - Higher than 27°C.

The TRNSYS macro regarding the power consumption and comfort analysis is shown in Figure 4.40.

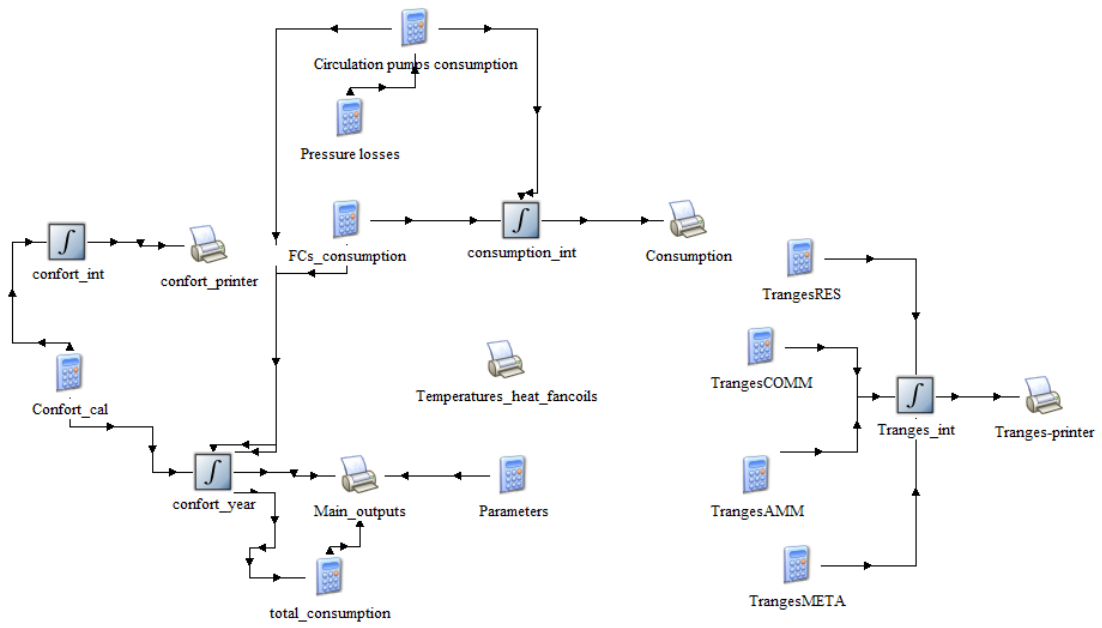


Figure 4.40. Outputs macro in TRNSYS

Chapter 5

5 Applications of the system model

The models developed in TRNSYS described in the chapter 4 were used to carry out an assessment of the system and analyse the impact of the system operation under different conditions and different optimization strategies.

The first model consists of the plug and play system developed in the GEOTeCH project, a Dual Source Heat Pump (DSHP) system capable of providing heating, cooling or DHW to an office building or small dwelling, working both with air or the ground as a source. The model is modular and includes all the main components of the system. The thermal loads of the building are introduced as an input in order to make the model simpler and easy to modify. An assessment of the system working under different climatic conditions is carried out, using three different locations in Spain and three different locations in Europe.

The second model is based on one of the demonstration installations of this plug and play system located in Tribano (Italy). A detailed model of the office building was developed and coupled with the DSHP system model, considering the fan coils as emission system. An optimization strategy for the compressor frequency was proposed and tested with the model in order to estimate the possible savings of implementing this optimization strategy. The strategy consists of using the temperature of the conditioned spaces as the controlled temperature in order to set the compressor frequency. In addition, some other conventional optimization strategies were also tested with the model.

Some examples of the system operation simulated by the models for some of the scenarios simulated in the assessments are shown in the end of each section: section 5.1.3. DSHP system operation and 5.2.2. Tribano system operation.

5.1 Assessment of the DSHP system in different climates

The model of the DSHP system described in section 4.3 was used in order to simulate the performance of the system working under different climatic conditions. For this purpose, it is necessary to modify some parameters and inputs in the model:

- The weather file of the specific city, used to set the outdoor air temperature. They are extracted from the weather database Meteonorm [169].
- The thermal loads, introduced as an input in the user loop. One building model will be used and adapted to the different locations in order to calculate the thermal loads that will be introduced as an input.

- The seasons definition (winter / summer) used for setting the heating or cooling period. This definition will depend on the thermal loads calculation, according to the heating / cooling demand during the year.
- Maximum, minimum and average air temperature for the equations used in the temperature compensation strategy. These temperatures will be calculated from the weather file of each location.
- Ground properties of the location: the thermal conductivity and volumetric heat capacity. These values were defined based on the work carried out in the framework of the GEOTeCH project, presented in [170] considering the thickness of sediment layers and the thermal properties of sediments and bedrock.
- Undisturbed ground temperature, calculated as the average ambient air temperature in the location. Since the BHE is short, no geothermal gradient has been considered.

Regarding the thermal loads, it was used a complete building model previously developed in TRNSYS and validated with experimental data as a part of a GSHP system model of an existing installation [130], [144]. The building corresponds to the Applied Thermodynamics department, in the *Universitat Politècnica de València*, in València (Spain), and was built in the 70's. It consists of nine offices, a computer room, a printer room and one corridor, with a total of 250 m² air-conditioned area, located at the second floor of the building. This building was air-conditioned by a GSHP system with a nominal capacity of around 17 kW in heating and 14.7 kW in cooling and a BHE field of six 50 m deep U-tube BHEs. The existing GSHP system was built in the framework of the GeoCool European project [19] and refurbished and optimized in the framework of the Ground-Med project [20]. The building model incorporates all the information regarding walls and windows materials, occupancy and other internal gains, etc.

The thermal demand of the building will be influenced by the climate conditions, but also by the construction typology, that will depend on the location of the building and its age. Therefore, the building model has been adapted to the different locations in which the DSHP system will be analysed, so the air-conditioned area has been adapted to the DSHP capacity (the previous building was air-conditioned by an around 16 kW heat pump in Valencia and the new DSHP has a nominal capacity of around 8 kW) and the façade of the building was adapted to the different locations. The building was modelled following an analogous method than the one explained in section 4.4.2 and a one year simulation was carried out with the corresponding weather conditions in order to obtain the hourly thermal loads during one year.

The walls and windows properties (layers materials, insulation thickness, etc.) were adapted to the construction typology of each specific location. For this purpose, the information gathered in the building typology data base from the IEE European Project TABULA (Typology Approach for Building Stock Energy Assessment) [168] was used. It incorporates a webtool (<http://webtool.building-typology.eu>) where the typical walls and windows properties are defined depending on the type of building, location and year of

construction for 13 European countries. In this webpage a brief description of the type of wall/roof/window is found and the corresponding global heat transfer coefficient (U-value).

Three cities in Spain and Europe were selected that were representative of different climates:

- Locations in Spain:
 - Valencia (Mediterranean climate).
 - Madrid (Continental climate).
 - Bilbao (Atlantic climate).
- Locations in Europe:
 - Athens (Warmer climate).
 - Strasbourg (Average climate).
 - Stockholm (Colder climate).

5.1.1 Assessment for different locations in Spain

The assessment of the DSHP system in different location in Spain was previously presented in the congress CYTEF 2018 [158].

In order to calculate the thermal loads for the DSHP system operating in the three representatives cities in Spain, the building model was simulated in the different cities with the corresponding weather files. The weather file introduces the dry and wet bulb temperatures, solar radiation and sun position and humidity for each hour of the year. This data is used as an input in the building for calculating the heat transfer between the building and the environment.

The building model was kept as the original model, with no modifications in the façade, as only one typology is defined in the TABULA database for the entire Spanish country. However, the final thermal load was scaled, considering a 50% of the hourly load, as the nominal capacity of the DSHP is 8 kW and the GSHP installed for the real building has a nominal capacity of around 17 kW. This adaptation of the thermal load is analogous as considering half the surface of the building to air-condition (125 m² instead of 250 m²). A one year simulation of the building under the weather conditions of each city was carried out in order to keep the comfort temperature inside the building during the conditioning hours: from 7h to 22h (23 °C for heating and cooling). The resulting thermal loads for the three cities in Spain are shown in Figure 5.1.

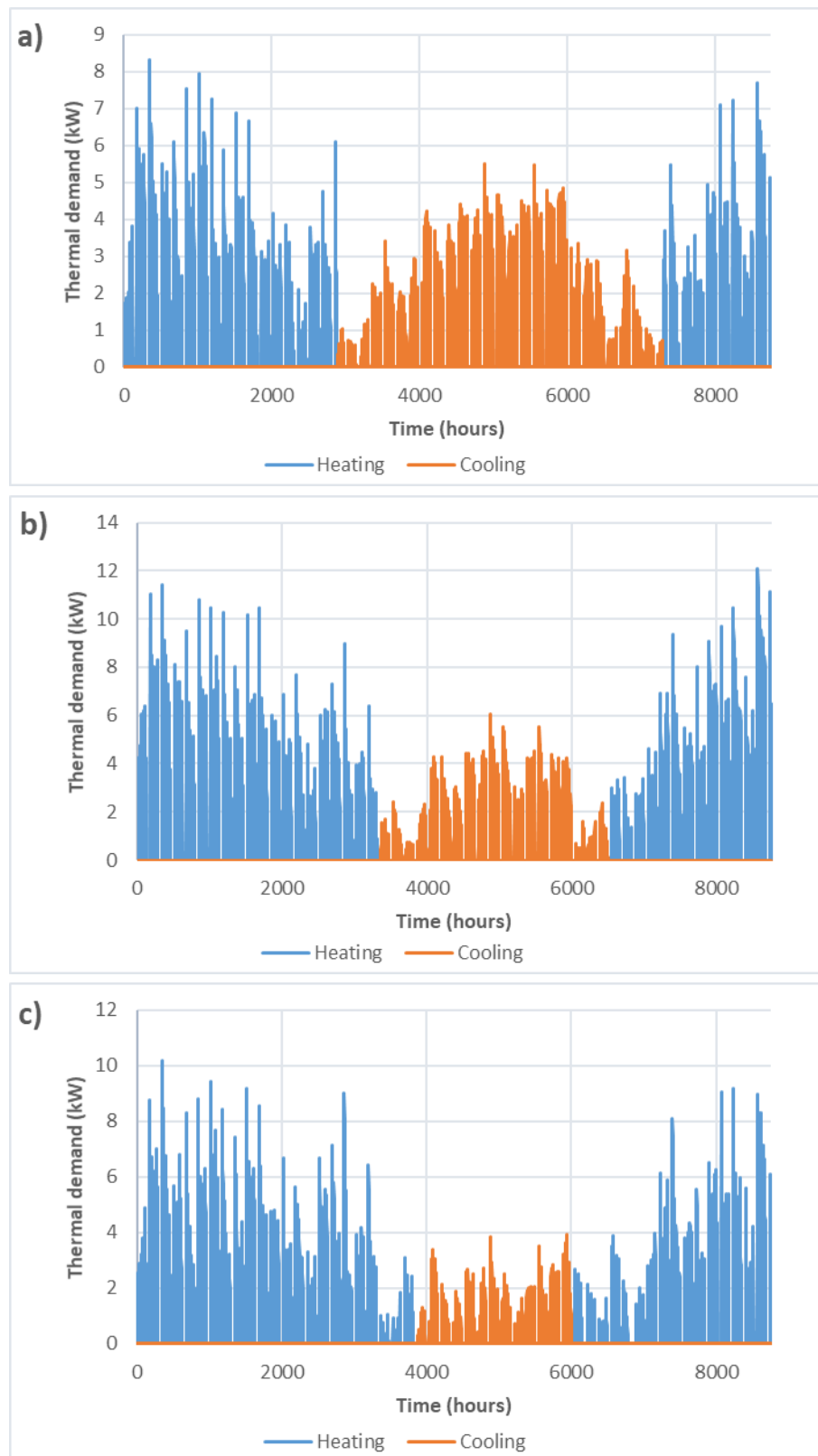


Figure 5.1. Thermal loads in different locations in Spain: a) Valencia; b) Madrid; c) Bilbao

It is important to mention that the definition of the system seasons has been estimated considering the cooling and heating loads. So, among the period in which there is a transition from heating loads to cooling loads, a day was selected to switch the heat pump working mode from heating to cooling and analogously from cooling to heating. As the

climate is different in each city, the seasons will be defined differently, according to the thermal loads calculated for each location. The main inputs that are different in each location are the ones concerning the thermal loads, climate conditions and ground properties and are summarized in Table 5.1.

Table 5.1. Main inputs for the different locations in Spain

Location	Valencia	Madrid	Bilbao
Peak heating (kW)	8.3	12.1	10.2
Peak cooling (kW)	5.5	6.1	3.9
Heating demand (kWh)	4243	8926	7615
Cooling demand (kWh)	3923	2972	1304
Yearly thermal demand (kWh)	8166	11898	8920
Summer period	01/05-1/11	21/05-01/10	11/06-10/09
Max. ambient temperature (°C)	34	37	34
Min. ambient temperature (°C)	-1	-6	-3
Average ambient temperature (°C)	17.3	13.9	14.1
Soil conductivity (W/(m·K))	2.1	3.3	3.5
Soil volumetric capacity (kJ/(m ³ ·K))	3200	2194	1200

The main components of the system and the control parameters are kept the same for all the three locations, in order to provide a fair comparison:

- Schedules: air conditioning from 6h to 22h, DHW production from 4h to 6h.
- Occupancy of the building, based on the real schedule of the professors that work in the offices.
- DHW demand: profile corresponding to an office of five people (equivalent to the occupancy of those five offices considered for the calculation of the thermal demand of the building).
- BHEs field: Four coaxial BHEs in a rectangular distribution and a separation of 3 m between BHEs. The geometry of the pipes and borehole that was used in the models is the same than the GEOTHEX BHE described in Table 3.6, but with a depth of 50 m and without the spiral rib. The working fluid used in the ground loop is water.
- Dual Source Heat pump: prototype #1 (nominal capacity 8 kW).
- Buffer tank size: 55 litres.
- DHW tank: 300 litres.

A simulation of the DSHP system operation in each city was carried out. The simulation time was one year (8760 h), and the time step was 1 minute.

5.1.1.1 Results of the assessment in Spain

The energy provided by the heat pump in each operation mode for each city is plotted in Figure 5.2 and the total energy provided by the system is shown in Table 5.2 divided in air-conditioning (operating modes M1-M5) and DHW (operating modes M6-M9). The total energy provided by the system for the air-conditioning of the building is around a 5% higher than the total energy demand shown in Table 5.1 for all the three cities. The main reason of

this difference is thermal losses with the environment in the different components of the system (buffer tank and pipes).

The DHW produced by the full-recovery mode (M3) was not considered in Table 5.2. This energy was not taken into account because it is a “free energy” produced by the heat pump as a consequence of producing cooling with the DHW loop as a condenser.

Table 5.2. Total energy provided by the heat pump for the three cities in Spain

Location	Valencia	Madrid	Bilbao
Air-conditioning (kWh)	8603	12397	9426
DHW (kWh)	487	554	601

The DHW demand is quite lower than the energy needed for air-conditioning. Furthermore, the DHW energy production is higher in colder cities, probably due to the higher thermal losses and the lower water temperature from the net due to a longer winter. But also, the cities with a lower DHW energy produced by the heat pump coincide with the ones with a higher production of DHW in Full-recovery mode.

Most of the energy provided by the heat pump is in the mode M5-Winter Ground, especially in Madrid and Bilbao, where the heating need is higher. The second operating mode most used is M2-Summer Ground and the third one is M4-Winter Air (more than 90% of the total energy provided by the heat pump in the three cities is in these three operating modes). In the case or Bilbao, the M4-Winter Air mode is more used than M2-Summer Ground, due to the low cooling demand.

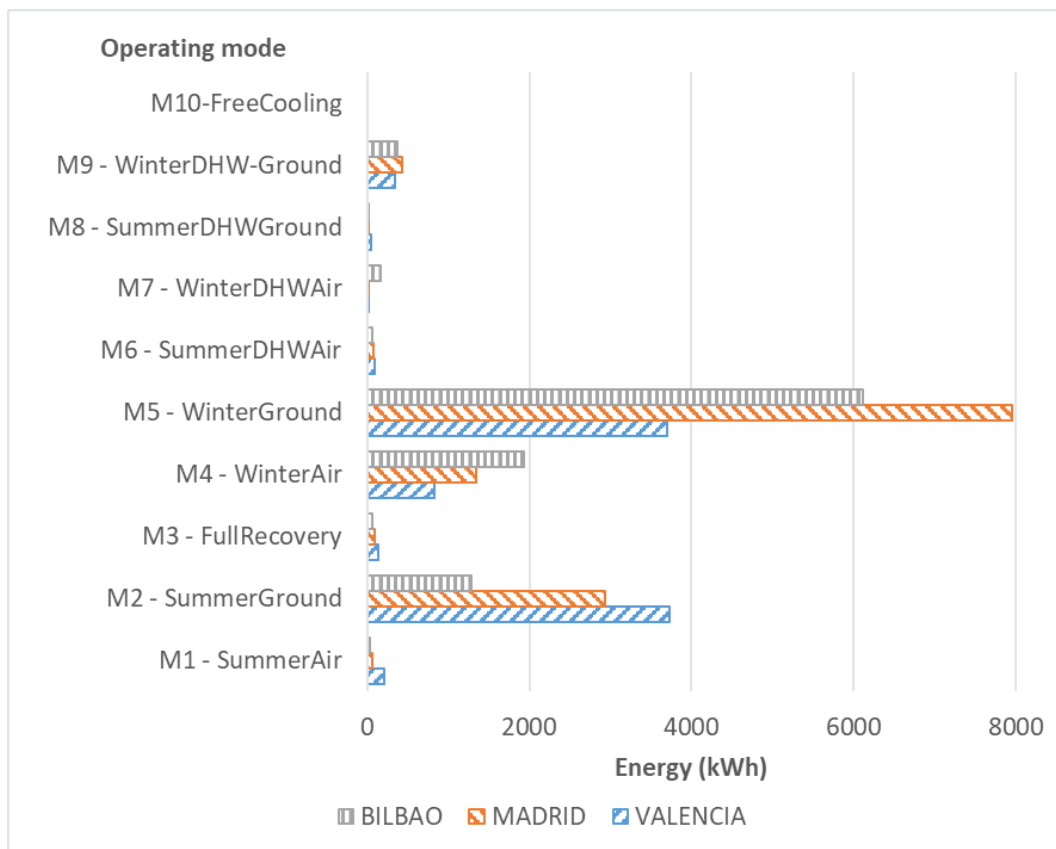


Figure 5.2. Thermal energy provided by the heat pump in the different working modes for the three cities in Spain

Focusing on the heating demand, Madrid is the location where more heating energy was produced using the ground (around 7960 kWh), followed by Bilbao (around 6100 kWh) and Valencia (around 3700 kWh). On the other hand, the location where more heating was produced using the air was Bilbao (around 1940 kWh), then Madrid (around 1350 kWh) and Valencia (around 830 kWh). Regarding the cooling demand, Valencia is the location with a higher amount of energy was produced for cooling purposes, both using the ground and the air, followed by Madrid.

The share of operating modes in each location shows how useful is working with a dual source heat pump instead of an air-source or ground-source. This share for each city is presented in Figure 5.3.

Valencia is the location with a higher balance of use of the ground as a source/sink for air-conditioning. The percentage of energy provided by the heat pump (41%) is the same for heating (M5) than for cooling (M2). While in the other locations, this use is more unbalanced (61% heating and 23% cooling in Madrid, 61% heating and 13% cooling in Bilbao).

Regarding the use of the air as a source/sink, it is not used very often for cooling (2% in Valencia, 1% in Madrid and almost 0% in Bilbao), but it is for heating production (9% in Valencia, 10% in Madrid and 19% in Bilbao). So, Bilbao is the location where the air is used in a higher rate and then, it is more useful to have a dual source heat pump.

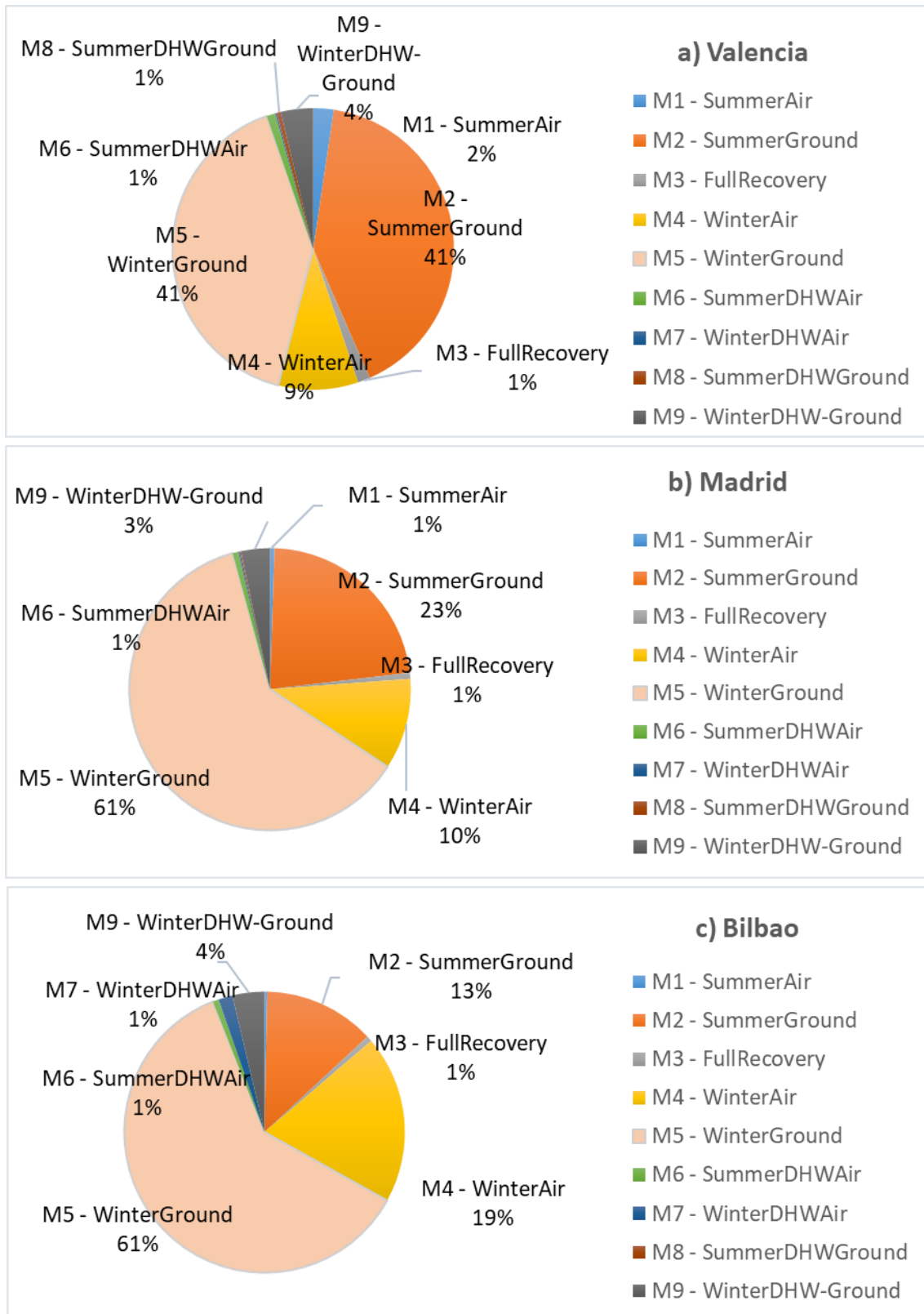


Figure 5.3. Share of the thermal energy produced by the heat pump in the three Spanish cities

Getting back the issue of the heat balance in the ground, in Table 5.3 it is shown the heat extracted and injected to the ground during the whole year simulation. It is possible to see that only in Valencia there is some thermal balance (at the end of the year the heat injected

is around 500 kWh higher than the heat extracted), therefore the ground temperature would not vary very much. On the other hand, the ground is quite unbalanced in Madrid and Bilbao, where the heat extracted is quite higher, so the ground temperature would decrease over the years.

Table 5.3. Heat extraction and injection in the ground for the three cities in Spain

Location	Valencia	Madrid	Bilbao
Extraction (kWh)	-3572	7201	5567
Injection (kWh)	4088	3173	1384
Balance (kWh)	516	-4028	-4183

Another conclusion from this performance assessment is that, as it could be seen, there is no free-cooling in any of the locations. This happened because the ground temperature in summer is too high and it is not enough to handle the cooling load (it was higher than 15°C during the summer periods). The free-cooling starts if the return temperature from the ground is lower than 10°C and there is a cooling demand. This conclusion can also be extracted from Table 5.4, where the maximum, minimum and average return temperatures of the water from the ground loop are shown. The average temperature in the three cities is above 10°C.

Table 5.4. Return temperature from the ground loop in the three cities in Spain

Location	Valencia	Madrid	Bilbao
Maximum temperature (°C)	26.1	21.9	20.4
Minimum temperature (°C)	8.8	4.3	4.7
Average temperature (°C)	17.0	12.5	12.3

Regarding the efficiency of the system, the SPFs according to the SEPEMO definition are shown in Figure 5.4, as it was described in section 4.3.8.

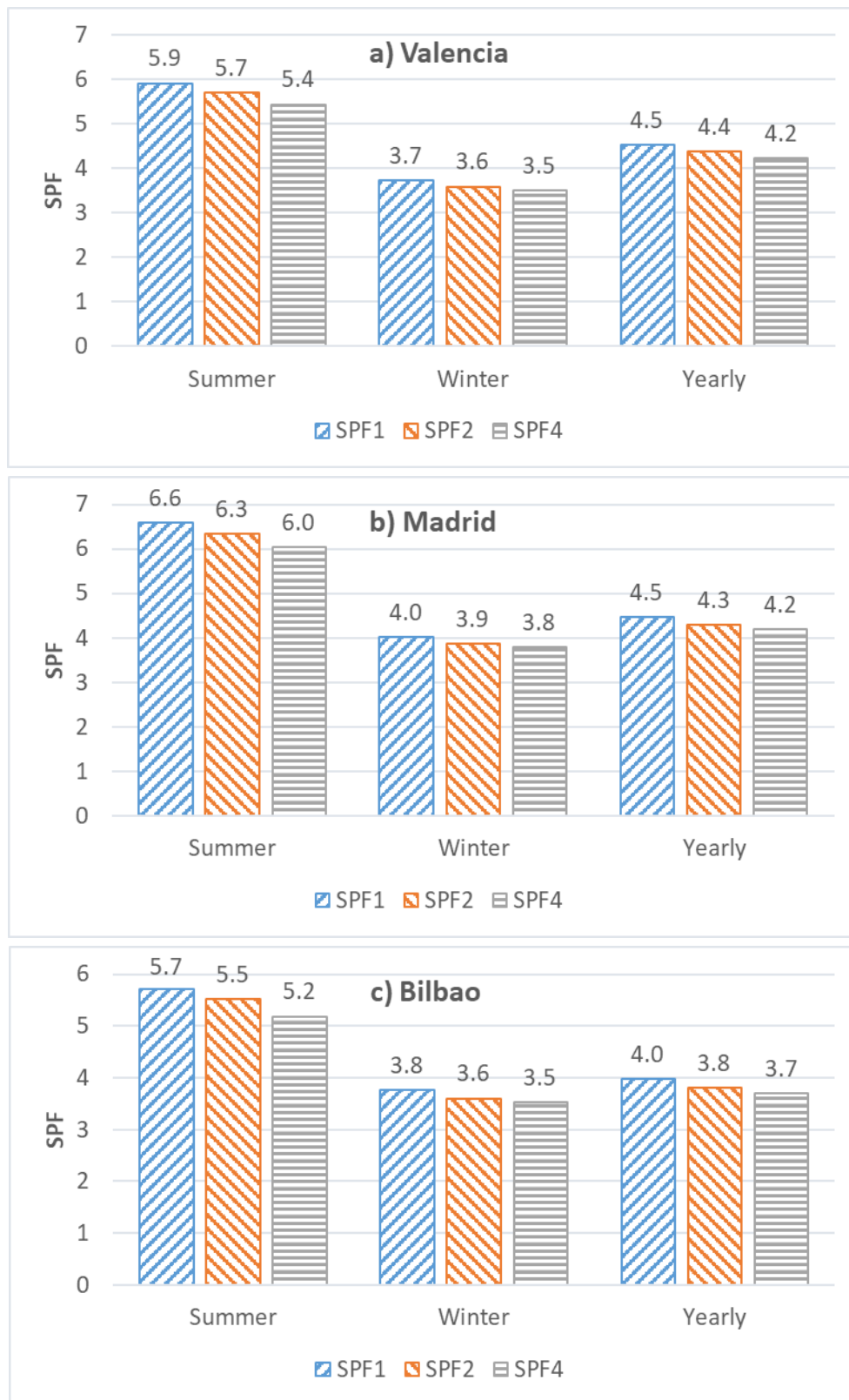


Figure 5.4. Seasonal Performance Factors obtained for the three cities in Spain

Taking a look at the SPF1, SPF2 and SPF4 of the three cities, it seems that the parasitic consumption of the different components in the system are relatively small in comparison with the heat pump consumption, as the values of SPF2 and SPF4 are just slightly lower than

the SPF1 and SPF2 values, respectively. Furthermore, the values for summer are quite higher than the values for winter, this is because the heat pump presents a higher COP working in summer than in winter and because the operating conditions are more favourable in summer (temperature difference between source and load).

Considering the summer and winter SPFs, Madrid is the location with the highest efficiency (a SPF4 of 6.0 for summer and 3.8 for winter). However, the yearly SPFs are approximately equal to the ones in Valencia (with a SPF4 of 4.2). This is due to the fact that the summer SPFs are higher than the values for winter and the summer is longer in Valencia. As the summer is longer, the SPF for summer will have a greater influence in the yearly SPF.

A summary of the SPF4 values for the three cities is shown in Figure 5.5 in order to provide a comparison easier.

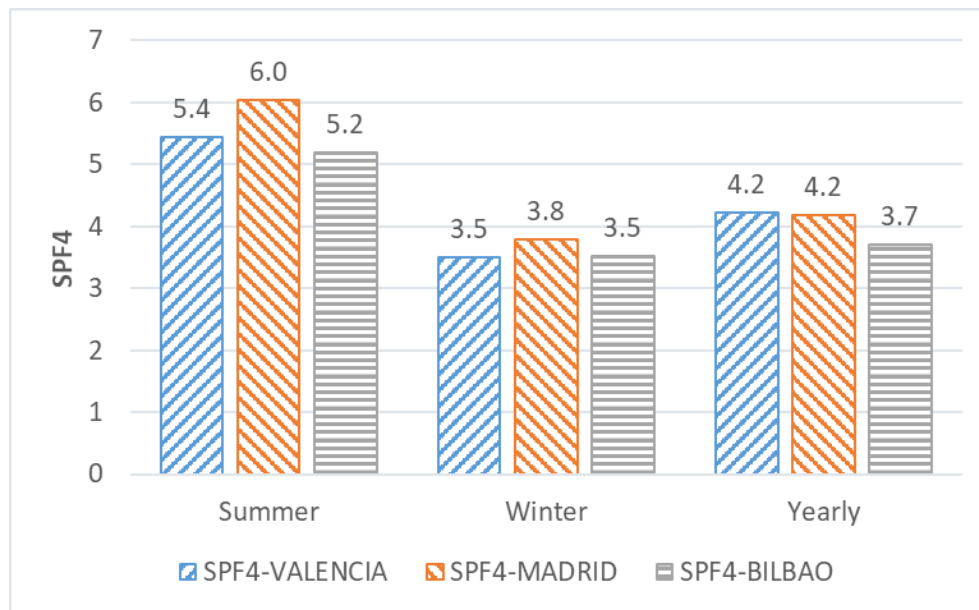


Figure 5.5. System Seasonal Performance Factor 4 (SPF4) for the three locations in Spain

The difference in the SPF values between the three locations is influenced by the air temperature, but mostly by the temperature of the water coming from the ground loop, as the ground is the most used source/sink. The return temperature from the ground loop was shown in Table 5.4.

One reason why Madrid presents the highest SPF4 value for summer could be that the return temperature from the ground is the lowest and Madrid presents the highest use of the ground (92% of the energy in summer is provided in mode M2-SummerGround). In winter, the SPF4 values in the three cities are rather similar (3.5 for Valencia and Bilbao and 3.8 for Madrid). Another reason why Madrid could present the most efficient performance is that its thermal demand is higher, therefore, the compressor would work at higher frequencies closer to the nominal frequency where the compressor presents the highest efficiency. Furthermore, a low thermal demand increases the time in which the compressor would cycle on/off, reducing the global seasonal performance factor because of the starts/stops and the compressor working at very low frequencies. Thus, as the thermal demand is higher in Madrid, the time in which the compressor is cycling would be lower.

5.1.2 Assessment for different locations in Europe

The assessment of the DSHP system operating in different cities in Europe was previously presented in the II Research Track conference organised by the International Ground Source Heat Pump Association (IGSHPA) [159]. The methodology used in this assessment is analogous to the one followed previously in section 5.1.1, so in this section it was described in a lower degree of detail.

In the case of the cities in Europe, the European regulation EU Reg. 811/2013 [171] for energy labelling of space heaters was followed. This regulation defines three cities as representative for each type of climate: Athens for warmer climate, Strasbourg for average and Helsinki for colder. However, no data about the façade typology in Finland was found in the TABULA database. So, as Stockholm presents a similar climate (the maximum, minimum and average temperatures in Helsinki are 24°C, -21°C and 4.7°C, respectively, while in the case of Stockholm, they are 28°C, -20°C and 5.3°C) and Sweden is a neighbouring country to Finland, Stockholm was selected as the representative city for colder climates in this analysis.

So, the construction typologies and U-values for buildings constructed in the 70's in the three countries (Greece, France and Sweden) were taken from the TABULA database, corresponding to a wall type Wall1 (existing state) and a window type Window 1 (usual refurbishment), as the real windows in the department were improved. The corresponding U-values are shown in Table 5.5.

Table 5.5. U-value extracted from the TABULA database for each representative city in Europe

Location	Athens	Strasbourg	Stockholm
U-value envelope (W/m ² K)	2.2	0.78	0.41
U-value windows (W/m ² K)	3.2	1.4	0.9

The walls in the model of the building for each city were adapted to each typology, so the walls layers were modified accordingly in order to obtain the defined U-value, the windows surface was maintained the same. Furthermore, the thermal loads were adapted, considering a 30% of the conditioned surface (75 m²), this is, considering the 30% of the value of the hourly heat loads calculated for the entire building, in order to adapt the peak to the capacity of the heat pump. The building adapted to each city was simulated for an entire year under the corresponding weather conditions, in order to reach the thermal comfort inside the conditioned spaces (23°C). The resulting thermal loads obtained for the three European cities are shown in Figure 5.6.

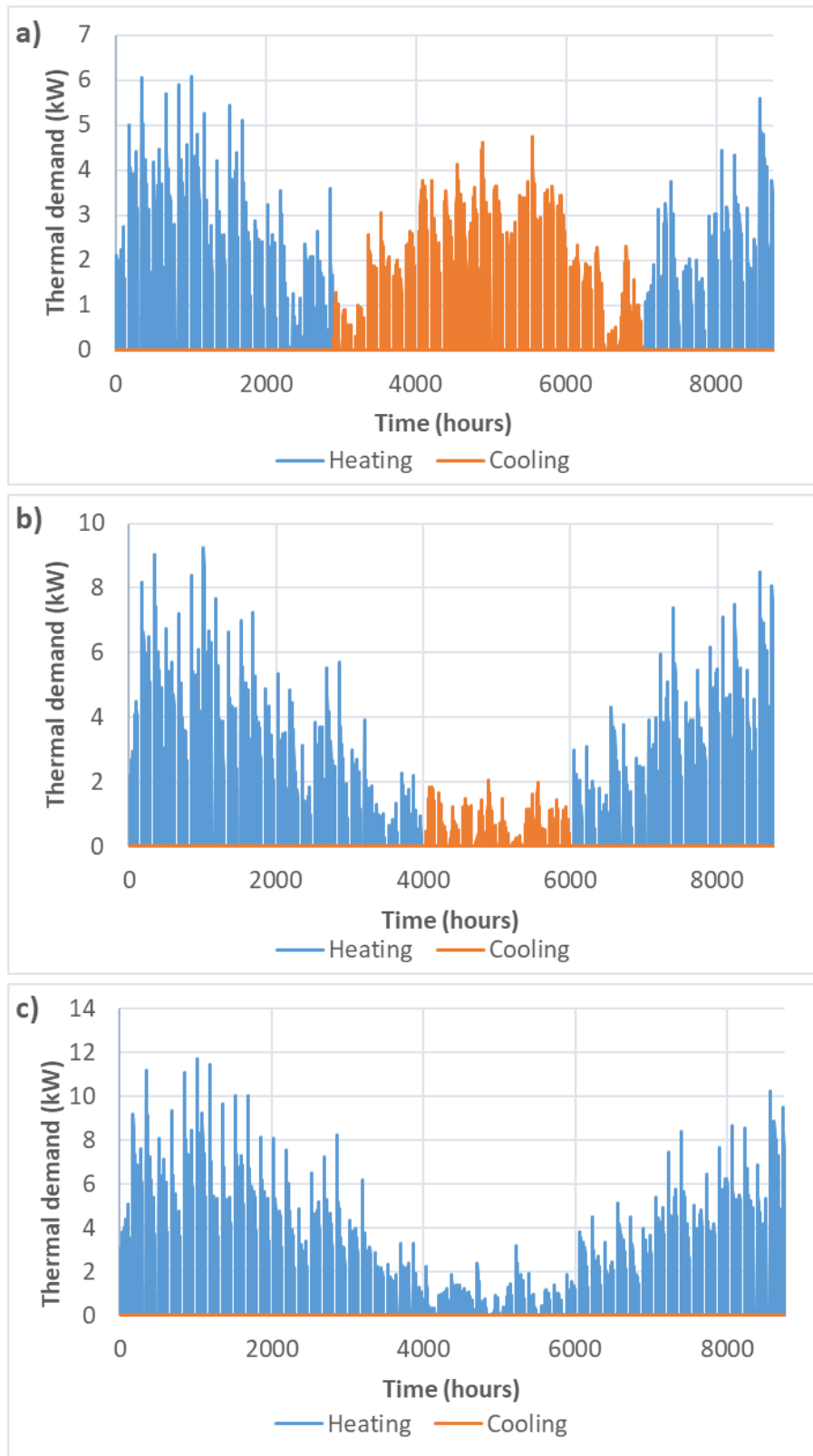


Figure 5.6. Thermal loads in the three cities in Europe: a) Athens; b) Strasbourg; c) Stockholm

It can be seen that in Stockholm there is no summer period, as it is a very cold city. The peak loads, together with the seasonal and yearly thermal demand are shown in Table 5.6. In this table, the main inputs for each city are also shown, including the maximum, minimum

and average ambient temperature and the ground properties, which will influence in the ground loop performance.

Table 5.6. Main inputs for the different locations in Europe

Location	Athens	Strasbourg	Stockholm
Peak heating (kW)	6.1	9.2	11.7
Peak cooling (kW)	4.8	2.1	0
Heating demand (kWh)	3565	7766	11491
Cooling demand (kWh)	3262	514	0
Yearly demand (kWh)	6827	8280	11491
Summer period	02/05 - 22/10	18/06 - 10/09	-
Max. ambient temperature (°C)	38	32	28
Min. ambient temperature (°C)	0	-11	-20
Average ambient temperature (°C)	17.6	9.8	5.3
Soil conductivity (W/(m·K))	3.75	1	3.75
Soil volumetric capacity (kJ/(m ³ ·K))	1250	1250	1250

The main components of the system and the control parameters are kept the same for all the three locations, in order to provide a fair comparison, and are kept quite similar to the ones in the assessment of the Spanish cities:

- Schedules: air conditioning from 6h to 22h, DHW production from 4h to 6h.
- Occupancy of the building, based on the real schedule of the professors that work in the offices.
- DHW demand: profile corresponding to an office of five people (equivalent to the occupancy of those five offices considered for the calculation of the thermal demand of the building).
- BHEs field: Four coaxial BHEs in a rectangular distribution and a separation of 3 m between BHEs. The geometry of the pipes and borehole that was used in the models is the same than the GEOTHEX BHE described in Table 3.6, but with a depth of 50 m and without the spiral rib. The working fluid used in the ground loop is a mixture of water and MPG (30%).
- Dual Source Heat pump: prototype #1 (nominal capacity 8 kW).
- Buffer tank size: 150 litres, in order to provide some heating and cooling storage, according to the GEOTeCH demo-site of Amsterdam.
- DHW tank: 300 litres.

Moreover, the main parameters of the system that will vary from one location to the other are the thermal load profile, the heating (winter) and cooling (summer) period, the ambient temperature and the ground thermal properties, due to differences in the climatological and geological conditions of the locations. A simulation of the DSHP system operation in each city was carried out for one year (8760 h) and a time step of 1 minute.

5.1.2.1 Results of the assessment in Europe

The energy produced by the heat pump in each operation mode for the different cities is plotted in Figure 5.7 and the total energy for the entire year is shown in Table 5.7, divided in air-conditioning (heating and cooling: operating modes M1-M5 and M10) and DHW (operating modes M6-M9). The total energy produced by the heat pump for heating and cooling plus the free-cooling is around a 7% higher than the total thermal demand shown in Table 5.6, due to the thermal losses in the pipes and buffer tank. Regarding the energy produced for DHW purposes, it is higher in colder locations because the water coming from the net has a lower temperature, then it is necessary more energy in order to heat it up until the required temperature.

Table 5.7. Total energy provided by the heat pump for the three cities in Spain

Location	Athens	Strasbourg	Stockholm
Air-conditioning (kWh)	7344	8913	12243
DHW (kWh)	488	634	772

Most of the energy is produced in M5-Winter Ground for all the locations, then, the second most used operating mode is M4-Winter Air (for Stockholm and Strasbourg) and the third mode with a higher contribution is M2-Summer Ground (only in Athens). The free-cooling mode is used only in Strasbourg, and the modes M3-Full Recovery and M1-Summer Air are only used in Athens, but in a very low proportion.

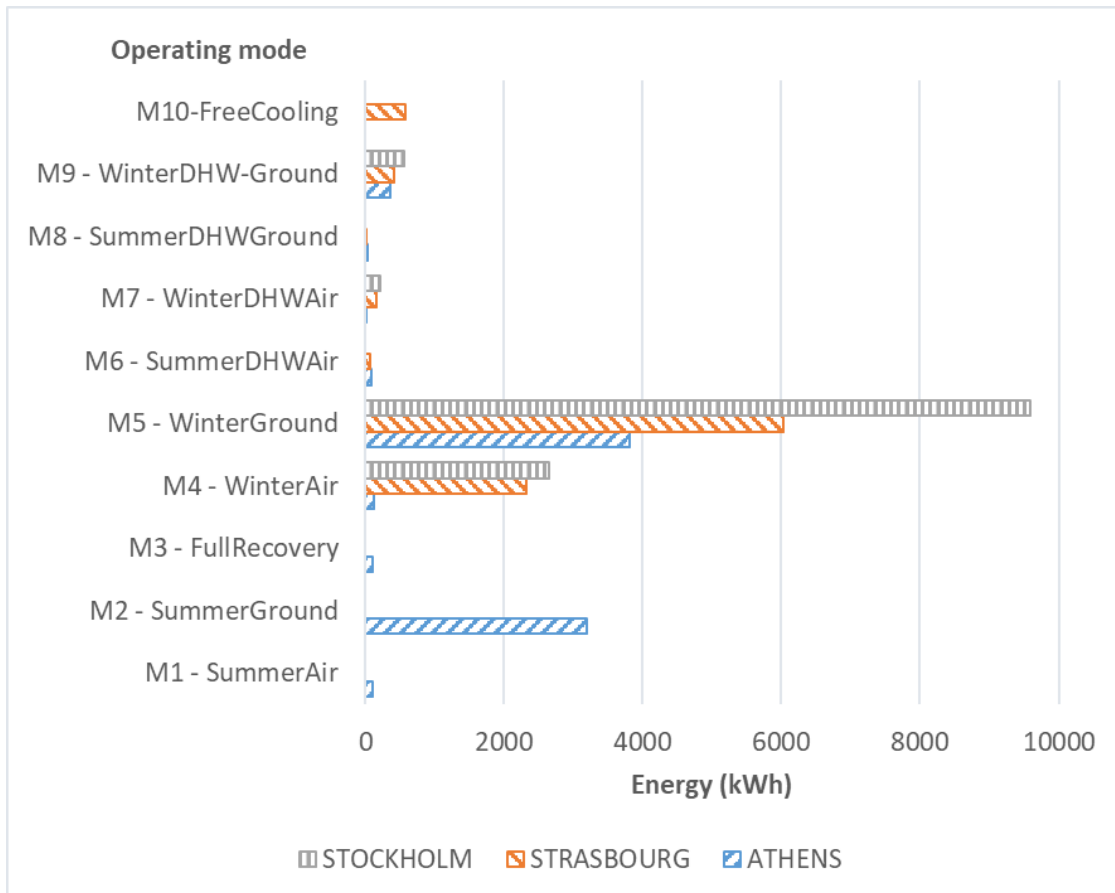


Figure 5.7 Thermal energy produced by the heat pump in the different working modes for the three cities in Europe

The share of energy produced by the heat pump for the different cities is shown in Figure 5.8.

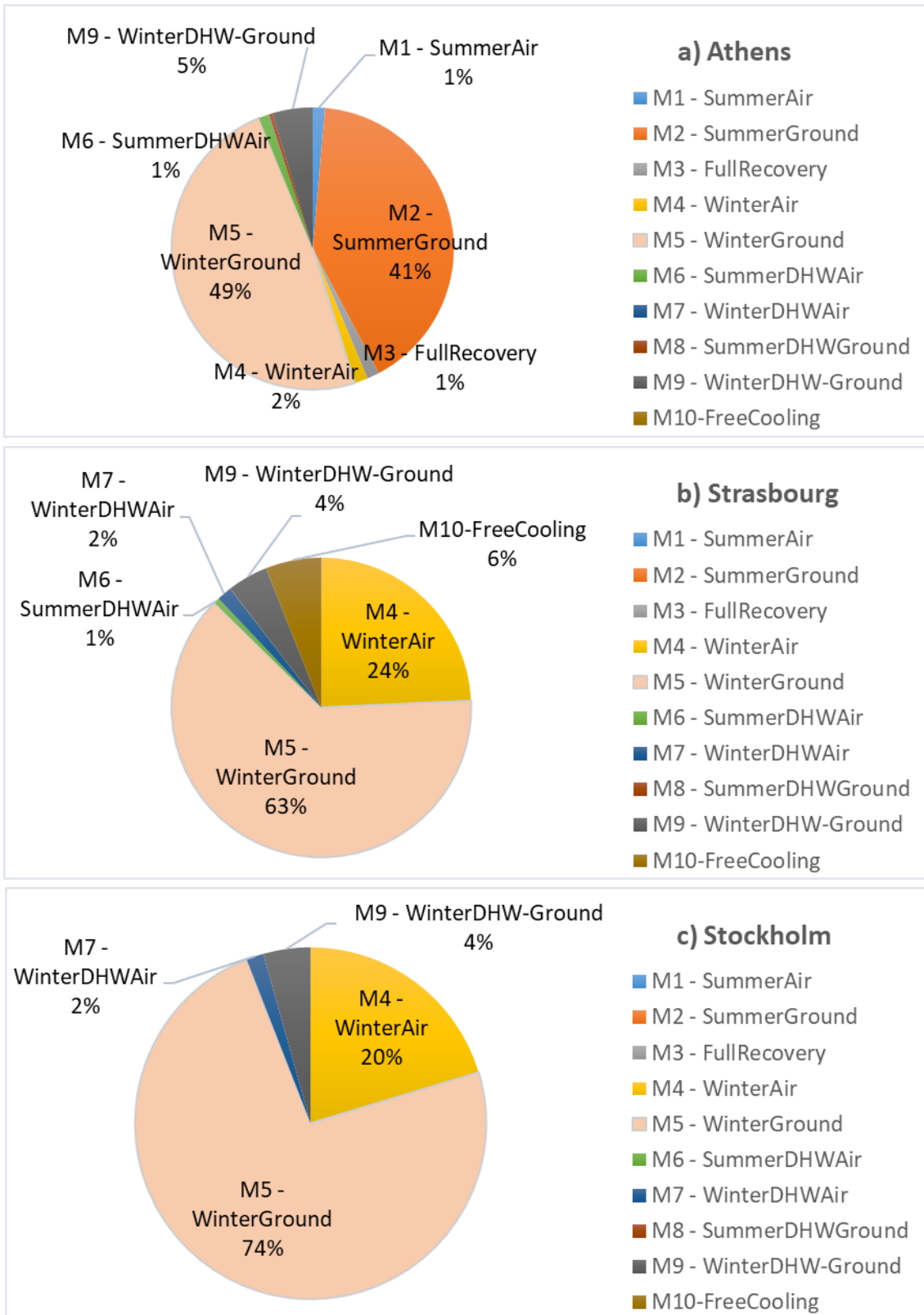


Figure 5.8. Share of thermal energy produced by the heat pump for the three European cities

In Athens, the most used source/sink is the ground (around a 95% of the total energy). This happens because of the warm climate, which makes the ground the most favourable source/sink for producing heating/cooling, as the ground temperature is closer to the comfort temperature (the average return temperature from the ground is 17.8°C, as shown in Table 5.9) than the air temperature.

Regarding Strasbourg, it presents a very low cooling demand (as it has a mild summer), and it is met by free-cooling (6% of the total), as the water coming from the ground loop is quite cold (the average return temperature is 6.6°C). The air is used to produce a 27% of the total energy, presenting the most balanced rate (air/ground) of the three cities.

In the case of Stockholm, all the energy produced by the heat pump is used to provide heating and DHW, and the air is used a 22%, being the ground the most used source.

The heat extracted and injected in the ground for the three cities is shown in Table 5.8, as well as the heat balance. It is possible to see that only Athens presents a thermal balance in the ground, so its temperature will not vary practically. On the other hand, the heat extracted in Strasbourg and Stockholm is much higher than the heat injected (mainly due to the long winters and short or inexistent summer). Therefore, the ground temperature will increase over the years.

Table 5.8. Heat extraction and injection in the ground for the three cities in Spain

Location	Athens	Strasbourg	Stockholm
Extraction (kWh)	3690	5257	8257
Injection (kWh)	3515	575	0
Balance (kWh)	-176	-4682	-8257

The Table 5.9 presents the return temperature from the ground loop in each of the Spanish cities. It reached values below zero, this is why a mixture of water and MPG was used. It is also possible to see the influence of the ground properties in the return temperature, as the minimum temperature is lower in Strasbourg (-4.4°C) than in Stockholm (-3.8°C), despite the colder climate in Stockholm. This happens because the ground thermal conductivity in Strasbourg is very low (1 W/(m·K)), so the local ground temperature would decrease to a higher degree due to a lower effectiveness in the heat transfer between the BHE and the ground.

Table 5.9. Return temperature from the ground loop in the three cities in Spain

Location	Athens	Strasbourg	Stockholm
Maximum temperature (°C)	25.1	15.1	10.6
Minimum temperature (°C)	10.3	-4.4	-3.8
Average temperature (°C)	17.8	6.6	3.5

The system Seasonal Performance Factors (SPF4), are shown in Figure 5.9 for the three cities. Athens presents the higher efficiency both in summer and winter, this is due to the

fact that it uses mostly the ground and that the return temperature from the ground is closer to the comfort temperature than in the other cities.

In Athens, the SPF4 for summer is almost a 50% higher than the one in winter, this is because the DSHP presents a better performance in cooling mode and more favourable working conditions in summer, as was previously stated in the work [48], where the SPF4 for the DSHP system working in Amsterdam presented a value around 40% higher than the winter value. Regarding the summer season in Strasbourg, the cooling demand is handled by the use of free-cooling (what would suggest a higher SPF value), but in the summer SPF, the performance of the heat pump producing DHW is also considered, leading to a lower SPF4 in the summer season.

The SPF4 in winter is slightly higher in Athens, due to the use of the ground and a higher return temperature. In Strasbourg and Stockholm is similar, as they use the operation modes M4 and M5 in a similar rate and the return temperature from the ground is also similar. Nevertheless, as in Stockholm the ground is used in a higher percentage, the final SPF4 is slightly higher.

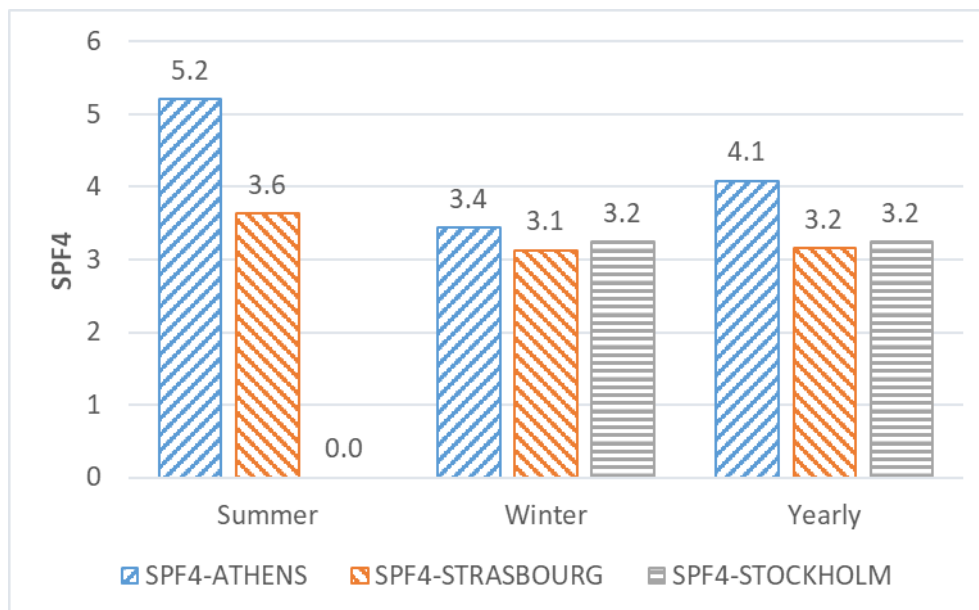


Figure 5.9. System Seasonal Performance Factor (SPF4) for the three cities in Europe

As it happened with the assessment in Spain, the length of the summer and winter seasons influences in the yearly SPF. The longer the winter, the higher influence the winter SPF has in the yearly SPF and, due to the worse performance of the heat for heating in comparison with cooling, the lower the yearly SPF would be. So the SPF4 will be lower in heating dominated areas. Therefore, as Athens is the city with the longest summer, the yearly SPF4 will be the largest.

Focusing on the dual source concept, it is not recommended to use a DSHP system in warmer places like Athens or Valencia, because the heat pump will work with a higher efficiency using the ground, and the air mode will not be practically used. On the other hands, the air is used in a higher rate in colder places like Strasbourg, Stockholm or Bilbao

(more than 20%), therefore the use of a DSHP would mean a reduction in the BHEs size, reducing the investment cost.

Finally, the SPF values obtained are lower than the ones expected from a standard GSHP system existing in the market. The main reason for this is that the DSHP developed in the GEOTeCH project is still a prototype that works with the refrigerant R32, and the compressors available at the time of its construction were not optimized yet, leading to a low performance of the unit. It is expected that, once the components have been improved for this refrigerant, the final unit would achieve efficiencies comparable to the ones in the market.

5.1.3 DSHP system operation

In order to illustrate the operation of the system in the simulations with the TRNSYS model, some representative periods during the year were chosen.

In Figure 5.10, the source selection control and the change of operating mode can be observed during one week of the system operating in Bilbao. Bilbao was selected because it is one of the locations with a higher use of the air for heating, not only the ground. At the start of the day, the DHW mode is selected (M9 Winter-DHW Ground), as the ground temperature is above the air temperature. Later on, when the heating mode starts, the mode M5-Winter ground is selected, as the ground is still hotter than the air (considering a hysteresis of ± 2 K). The days where the air temperature rises 2K above the ground temperature, then the heat pump changes to M4-Winter Air. If the air temperature decreases 2K below the ground temperature, it changes to M5 again.

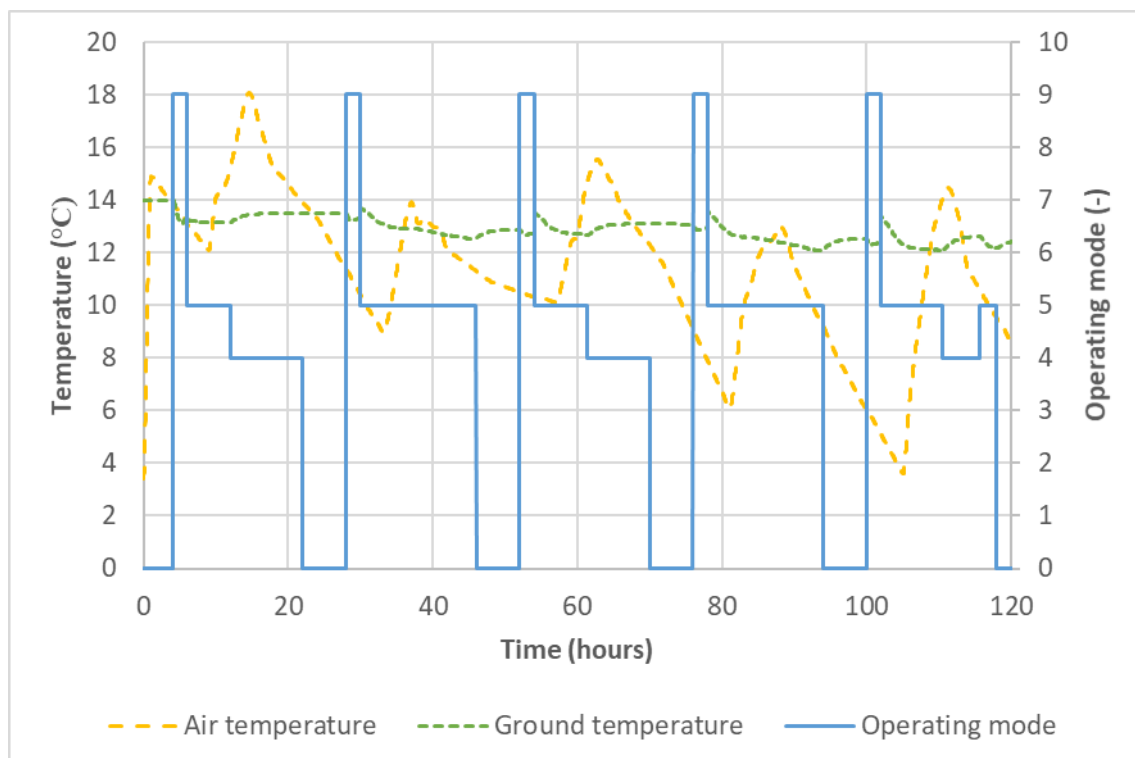


Figure 5.10. Change of working mode during one week in winter for Bilbao

Regarding the operation in winter, a ten hours period at the beginning of the day for the DSHP system working in Valencia was selected (hour 77 corresponds to 5 a.m.). Figure 5.11 shows the operation of the system during this period. In Figure 5.11a), the inlet and outlet temperature at the heat pump, the user and the ground circuits are presented, as well as the outlet temperature of the buffer tank and the calculated supply temperature with the temperature compensation algorithm described in section 4.3.6.5. It is possible to see that the required supply temperature at the start of the day is higher than that in the middle of the day (as the air temperature would be higher in the middle of the day and it is not necessary to supply the water so hot).

In Figure 5.11b), the compressor frequency and the temperature difference at the internal circuit are shown. It is possible to see that at the start of the day (hour 78), the frequency of the compressor increases sharply, due to the start of the system and the high demand at the start of the day; the rest of the day, the compressor is cycling at the minimum frequency (20 Hz). It is also possible to see that the temperature difference in the internal circuit is kept around 5 K whenever the heat pump is on, thanks to the PID controlling the mass flow rate in the user circuit.

Moreover, the outlet temperature from the heat pump and the buffer tank follows the dynamic evolution of the desired supply temperature, but it is cycling around this temperature, as the thermal demand is low and the heat pump is cycling during this period.

In Figure 5.12, a representative period for summer was selected in the middle of a day for the system working in Valencia. Analogously as in Figure 5.11, the desired supply temperature decreases in the middle of the day, because the temperature is hotter during this time. The supply temperature from the buffer tank follows this variation of the desired supply temperature.

In Figure 5.12b), it is also plotted the supply temperature from the DHW tank, the operating mode and the switch of the heat pump (0 means off, 1 means on). The desired temperature at the DHW tank 45°C (at 1/3 of the tank height from the bottom), with a hysteresis of $\pm 2\text{K}$, then, when this temperature decreases below the lower limit, the system requires DHW. Normally, out of the DHW period (4h-6h), it is not possible to produce DHW, but in cooling mode, when there is a need of DHW, the mode M3-Full Recovery is selected, and the heat pump produces cooling using the DHW loop as condenser, then heating up the DHW tank. This change can be observed twice in the graph.

In conclusion, the plug and play system model developed in TRNSYS is able to reproduce the dynamics of the different components of the system and the coupling between them. It is possible to predict the behaviour of the whole system and calculate its efficiency working under different conditions and then, evaluate the advantages and disadvantages of this type of system in the different scenarios and find in which one the system reaches the best performance.

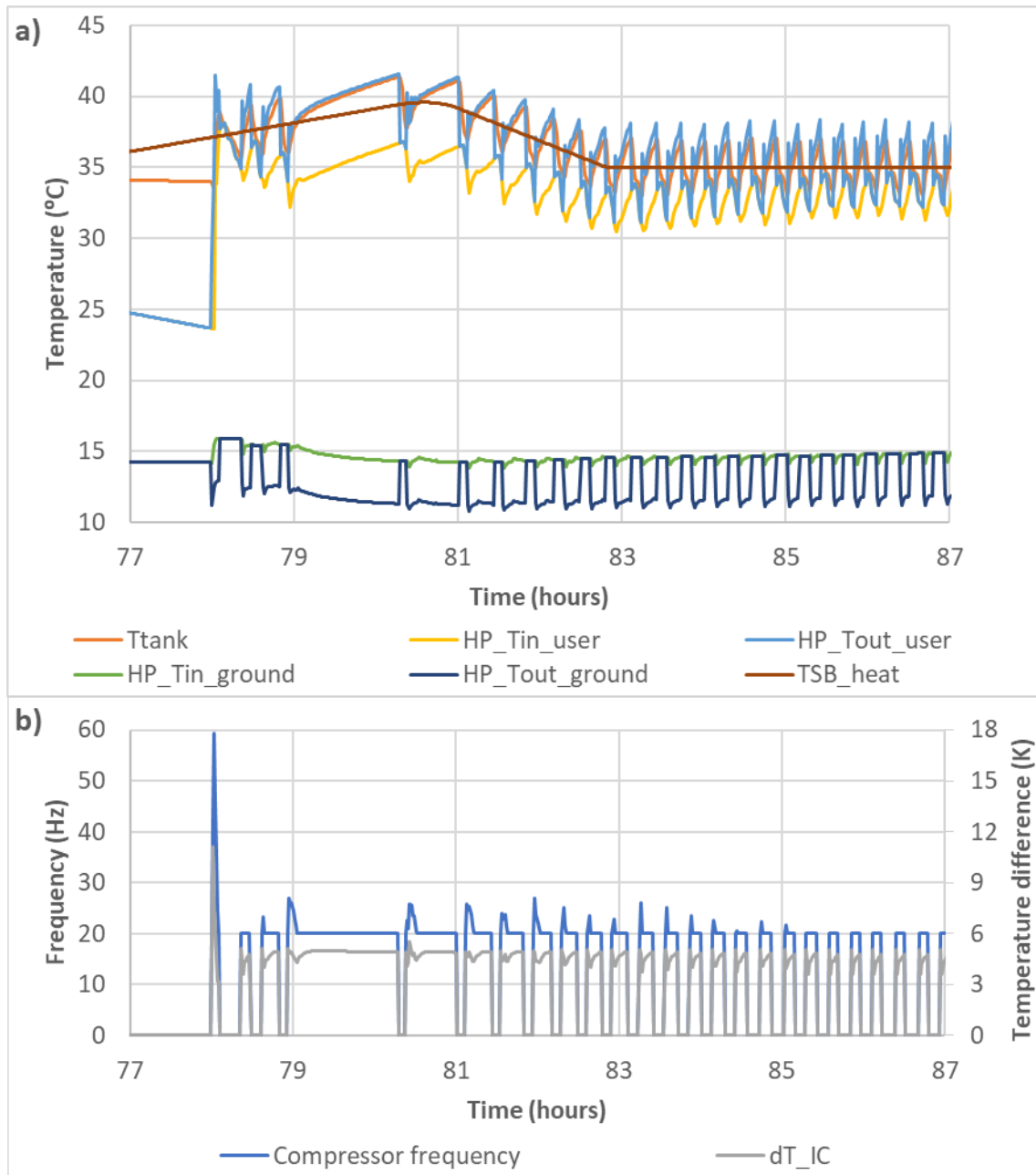


Figure 5.11. Winter day in Valencia: a) temperatures in the heat pump, buffer tank and supply set point; b) compressor frequency and temperature difference in the internal circuit

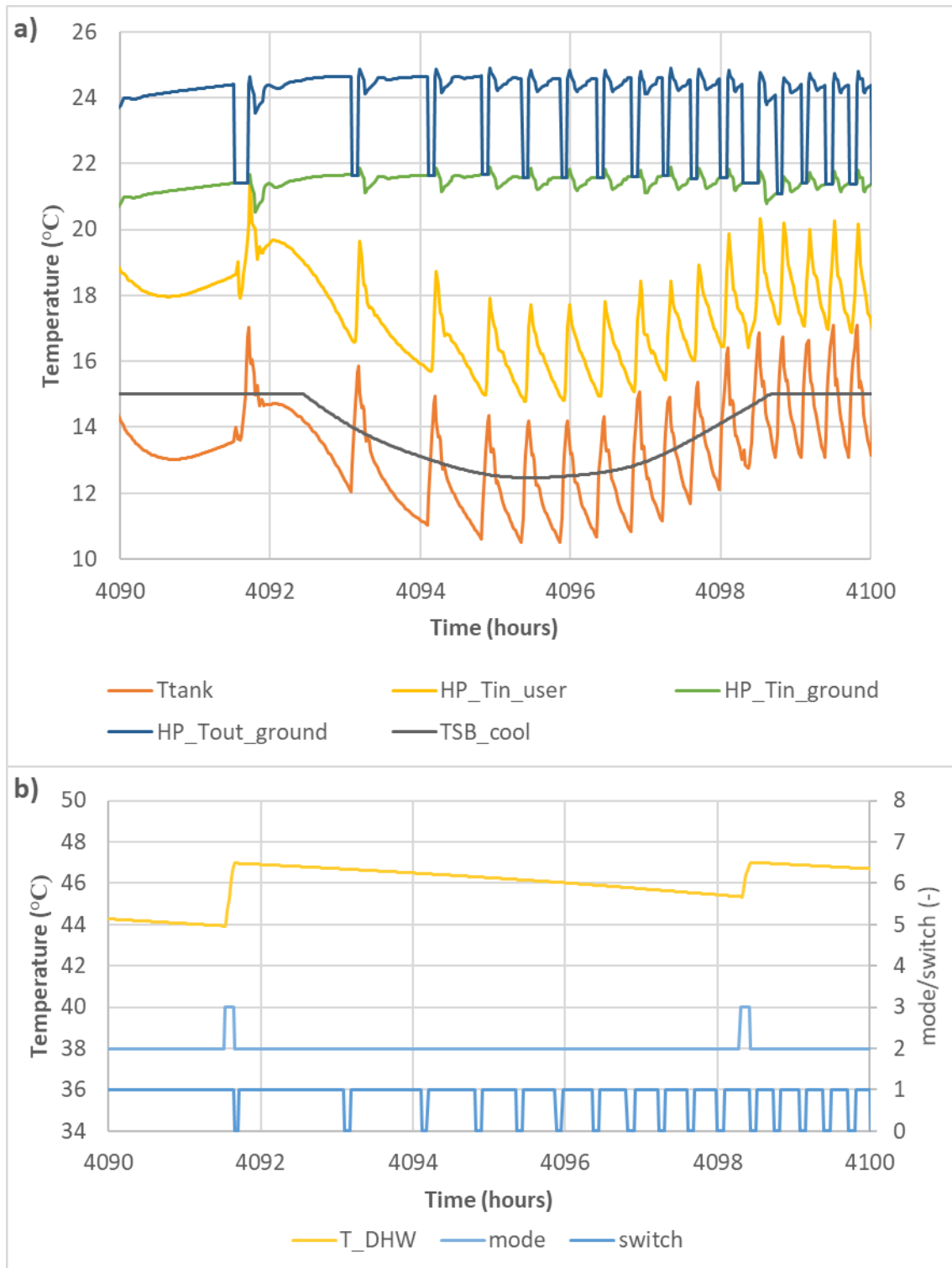


Figure 5.12. Summer day in Valencia: a) temperatures in the heat pump, buffer tank and supply set point; b) Temperature from DHW tank, operating mode and heat pump switch

5.2 Room temperature control

The model of the Tribano demo-site in TRNSYS described in section 4.4, which incorporates the model of the building, the coupling with the fan coils and the heat pump model adapted to the Tribano heat pump, was used in order to test the effectiveness of several control and optimization strategies, especially the room temperature control strategy implemented in the model. This strategy mainly consists of controlling the compressor frequency with the operative temperature of the different zones, finding firstly the most unfavourable room, and using its temperature to set the frequency of the compressor by using a PID controller. Neither the ground loop nor the DHW loop were incorporated in this model in order to simplify it and to focus on the room temperature control strategy, therefore the heat pump will work only in the operating modes M1-Summer Air and M4-Winter Air.

5.2.1 Parametric analysis

Different control and optimization strategies have been tested in the model, with different temperature setpoints. The strategies tested were:

- Compressor frequency control
 - Water temperature control.
 - Return temperature 45°C/12°C (heating/cooling).
 - Supply temperature 50°C/7°C.
 - Room temperature control with limits in the supply temperature:
 - Supply temperature limits in heating: 40°C, 45°C and 50°C.
 - Supply temperature limits in cooling: 7°C, 10°C and 12°C.
- Setting in the rooms of 23°C during all the year.
- Internal circuit circulation pump.
 - Fixed speed: 3000 kg/h in the internal circuit.
 - Temperature difference (dT) control, with two different dTs:
 - dT=3K.
 - dT=5K.
- Buffer tank
 - No buffer tank.
 - Incorporation of a buffer tank in the supply of the internal circuit (60 litres).
- Fan coils schedule:
 - Original schedule: 7.5h-20h.
 - Optimization of the fan coils working schedule:
 - Offices: 7h-19h.

- Meeting room: 7h-13h.
- Night mode:
 - Fan coils off at night (out of the fan coils schedule).
 - Night mode: in winter, at times out of the fan coils schedule, the system works to provide a minimum setting of 15°C in the conditioned spaces.

The original operation of the system in Tribano was controlling the compressor frequency with the return temperature in the internal circuit, with setpoints of 45°C in heating and 12°C in cooling. There is no buffer tank, the circulation pump operates at a fixed speed (around 3000 kg/h of water flow rate) and there is no optimization in the fan coils schedules nor a night mode implemented. In all the simulations, the heat pump is maintained on during the whole day, as it is in the real demo-site.

A combination of the different strategies was established and a parametric analysis was carried out, with a total of 178 simulations for a whole year operation and a simulation time step of 1 minute. The main results obtained in each simulation are the total power consumption during the year and the number of hours “out of comfort” in each thermal zone. As explained in section 4.4.7, it is considered “out of comfort” in a zone when the internal operative temperature is lower than 20°C in heating or higher than 26°C in cooling (category II of European standard 15251:2007[166]).

The temperature difference control for the circulation pump was only simulated with the buffer tank, because the temperature just at the outlet of the heat pump presents very sharp changes due to the start/stop of the compressor, and then it is not easily implementable in the reality. On the other hand, the use of a buffer tank makes the temperature changes smoother and easier to control.

The entire matrix with the 178 simulations is presented in the Appendix D, where the scenario number and the control strategies simulated are presented. The different scenarios have been numbered according to the energy savings presented in comparison with the base case (the first scenario is the one with higher energy savings). However, the fulfilment of the comfort requirements was not considered in this numbering, therefore the higher energy savings does not always implies the better scenario, as the number of hours out of comfort could be too high. In addition, the final results for each simulation are also shown: total energy consumption of the system as a percentage of the original system operation (6.69 MWh), and number of hours “out of comfort” in each thermal zone. A legend of colours was used in order to select the optimal simulations, the values coloured in green are better than the ones in yellow or red, progressively. In order to select the optimal configurations, it was selected that combination with a lower energy consumption in which the comfort is met during most of the time.

As a first approach in the study of different control and optimization strategies, some results of the system working only with the water temperature control (not the room control temperature control) is shown in Table 5.10. Except the first scenario (the original one), the rest of the scenarios had the buffer tank incorporated, the night mode control was

not applied in these simulations. The base scenario is the number 157, with the original operating conditions. In all the scenarios, the comfort requirements were fulfilled.

Table 5.10. First results of the system working under the water temperature control (base scenario underlined)

n	User pump control	Buffer tank	Setpoints heating / cooling	Optimized fan coil schedule	Electrical consumption (MWh) and savings (%)
<u>157</u>	<u>Constant speed</u>	<u>No</u>	<u>45 °C / 12 °C</u> <u>Return temperature</u>	<u>No</u>	<u>6.69</u>
177	Constant speed	Yes	50 °C / 7 °C Supply temperature	No	7.57 (-13%)
172	Constant speed	Yes	50 °C / 7 °C Supply temperature	Yes	7.26 (-8%)
146	$\Delta T = 3 \text{ K}$	Yes	50 °C / 7 °C Supply temperature	No	6.37 (5%)
132	$\Delta T = 5 \text{ K}$	Yes	50 °C / 7 °C Supply temperature	No	6.21 (7%)
120	$\Delta T = 3 \text{ K}$	Yes	50 °C / 7 °C Supply temperature	Yes	6.04 (10%)
103	$\Delta T = 5 \text{ K}$	Yes	50 °C / 7 °C Supply temperature	Yes	5.88 (12%)

From these first studies, it can be extracted that varying the user pump speed in order to achieve a constant ΔT in the user loop would produce some energy savings: between 5%-7% compared to the base scenario, but 18%-20% in comparison with the same operating parameters and constant circulation pump speed. In addition, optimizing the fan coil schedule would produce some additional energy savings (around 5% higher than only with the ΔT user pump control).

Once analysed the savings produced only with the application of the circulation pump control strategy and the optimization of the fan coils schedule, it is analysed the best results obtained with the system working only with the water temperature control (not the room control temperature control) and the rest of control strategies (circulation pump variable speed, fan coils schedule optimization and night mode), but also changing the setpoint for the supply water temperature. These results are shown in Table 5.11. Except the base scenario (the original one), the rest of the scenarios had the buffer tank incorporated. The comfort requirements were fulfilled in all of the scenarios shown in this table.

Table 5.11. Best results of the system working under the water temperature control. The base scenario is underlined

n	User pump control	Buffer tank	Setpoints heating / cooling	Optimized fan coil schedule	Night mode	Electrical consumption (MWh) and savings (%)
<u>157</u>	<u>Constant speed</u>	<u>No</u>	<u>45 °C / 12 °C (return)</u>	<u>No</u>	<u>No</u>	<u>6.69</u>
42	$\Delta T = 3 \text{ K}$	Yes	40 °C / 10 °C (supply)	Yes	Yes	4.99/25.4%
61	$\Delta T = 3 \text{ K}$	Yes	40 °C / 10 °C (supply)	No	Yes	5.21/22.2%
65	$\Delta T = 3 \text{ K}$	Yes	40 °C / 7 °C (supply)	Yes	Yes	5.26/21.4%
80	$\Delta T = 3 \text{ K}$	Yes	45 °C / 10 °C (supply)	Yes	Yes	5.47/18.3%
81	$\Delta T = 3 \text{ K}$	Yes	40 °C / 7 °C (supply)	No	Yes	5.48/18.2%
87	$\Delta T = 5 \text{ K}$	Yes	45 °C / 7 °C (supply)	Yes	Yes	5.48/16.5%

As a conclusion of these studies, varying the user pump speed in order to achieve a constant temperature difference in the user loop, together with the night mode application and reducing the supply temperature in heating and increasing it in cooling produce some energy savings (between 16% and 25% in comparison with the base scenario). The optimum temperature difference would be 3K. Furthermore, the optimal temperature setpoints would be between 40°C -45°C for heating and 7°C-10°C for cooling.

After this, the best scenarios working with the room temperature control (apart from the other control strategies and parameters) are analysed. The results from the best scenarios are gathered in Table 5.12, with the supply temperature limits used, the temperature difference used in the circulation pump control, if the system is using the optimization of the schedule of the fan coils, the savings in the consumption as a percentage of the original configuration and the number of hours during the whole year “out of comfort” in the different thermal zones: Research and Development office (RES), Sales office (COMM), Administration office (AMM) and Meeting room (META). All the scenarios incorporated the night mode control strategy. The comfort requirements considered for the calculation of the number of hours out of control are the category II from the standard 15251:2007, as explained in section 4.4.7

Table 5.12. Results from the best scenarios for the parametric analysis for comfort category II: supply temperature limits, temperature difference for the circulation pump control, savings with respect to original scenario and hours out of comfort

n	Tlimit heating (°C)	Tlimit cooling (°C)	dT (K)	Opt. fan coil schedule	Savings	RES (h)	COMM (h)	AMM (h)	META (h)
12	40	10	3	Yes	30.7%	0.42	2.00	8.75	11.52
23	40	7	3	Yes	28.5%	0.42	0.53	0.03	11.52
28	40	10	3	No	27.6%	1.20	2.73	3.68	7.33
35	45	10	3	Yes	26.9%	0.17	1.70	8.73	1.95
38	45	7	5	Yes	26.0%	0.23	0.33	0.30	11.12
40	40	7	3	No	25.7%	1.22	1.48	0.15	7.32
46	45	7	3	Yes	24.7%	0.17	0.23	0.02	1.95

It is possible to see in Table 5.12 that in some zones the number of hours out of control is somewhat higher, but if a slightly less restricted comfort requirements are considered (category III in standard 15251:2007 - 19°C in heating and 27°C in summer), the number of hours out of comfort is practically zero, as shown in Table 5.13. Therefore, during the hours out of comfort shown in Table 5.12 the actual temperature is just slightly out of the original comfort requirements (category II of standard 15251:2007).

Table 5.13. Results from the best scenarios for the parametric analysis for comfort category III: supply temperature limits, temperature difference for the circulation pump control, savings with respect to original scenario and hours out of comfort

n	Tlimit heating (°C)	Tlimit cooling (°C)	dT (K)	Opt. fan coil schedule	Savings	RES (h)	COMM (h)	AMM (h)	META (h)
12	40	10	3	Yes	30.7%	0.05	0.08	0.00	1.42
23	40	7	3	Yes	28.5%	0.05	0.08	0.00	1.42
28	40	10	3	No	27.6%	0.25	0.32	0.02	1.28
35	45	10	3	Yes	26.9%	0.02	0.02	0.00	0.10
38	45	7	5	Yes	26.0%	0.02	0.05	0.00	0.85
40	40	7	3	No	25.7%	0.25	0.33	0.02	1.28
46	45	7	3	Yes	24.7%	0.02	0.02	0.00	0.10

Considering the best scenarios, the highest savings are obtained with a temperature difference of 3K for the circulation pump control, generally. The less strict the limits (higher limit in heating and lower in cooling), produce a higher consumption, but also a slightly reduction in the number of hours out of comfort. Apparently, the limit for heating could be set to 40°C (the lower value tested) and still obtaining a reasonable comfort. However, in the case of cooling, the scenarios in which the limit was set to 12°C produce a rather high number of hours out of comfort, therefore it should be set to 10°C the maximum.

The power consumption during the entire year for each component of the system is shown in Table 5.14, where the consumption of the different components is shown for the original scenario (number 1). The consumption of the components for the best solutions obtained are also shown, with the percentage with respect to the original scenario.

Table 5.14. Power consumption of each component: total consumption (kWh) and percentage with respect to the base scenario (underlined).

	Compressor	Fan	Parasitic losses	Fan coils	Circulation pump
<u>157</u>	<u>3888 kWh</u>	<u>443 kWh</u>	<u>718 kWh</u>	<u>164 kWh</u>	<u>1479 kWh</u>
12	3168 (-18%)	303 (-32%)	718 (0%)	186 (+13%)	264 (-82%)
23	3283 (-16%)	333 (-25%)	718 (0%)	177 (+8%)	274 (-81%)
28	3330 (-14%)	312 (-30%)	718 (0%)	214 (+30%)	271 (-82%)
35	3393 (-13%)	337 (-24%)	718 (0%)	173 (+5%)	270 (-82%)
38	3511 (-10%)	359 (-19%)	718 (0%)	170 (3%)	196 (-87%)
40	3431 (-12%)	341 (-23%)	718 (0%)	204 (+24%)	280 (-81%)
46	3508 (-10%)	368 (-17%)	718 (0%)	164 (0%)	279 (-81%)

It is possible to see that the highest savings are obtained in the circulation pump (more than 1 MWh), because there is no need of keeping circulating a such a high mass flow rate; so, with the temperature difference the mass flow rate will decrease and therefore, the power consumption of the circulation pump. The main effect of the room temperature control is shown in the compressor consumption. It is the second component with higher energy savings (in absolute values, not in percentage with the original scenario), in the scenario 12, savings of around 700 kWh are achieved. As the fan speed is set proportionally to the compressor frequency, the higher the compressor savings, the higher the fan savings, but in absolute value, the savings in the fan are relatively small compared to the circulation pump or the compressor. The parasitic losses in the heat pump are the same in all the scenarios because the heat pump is kept on every day for the entire day. Regarding the fan coils consumption, the difference between scenarios is quite small, the consumption is even slightly higher in some scenarios due to the fact that the fan coils might be working during the night in winter because of the night mode. On the original case, only the heat pump was working during the night, but the fan coils were off. A higher energy consumption of the fan coils is observed in the scenarios where the fan coils schedule has not been optimized.

As a conclusion, the scenario number 12 would be the best option (40°C/10°C as supply temperature limits and dT of 3 K in the circulation pump control), as it is the scenario with the highest energy savings that meets the comfort requirements, although not strictly. If it is demanded to meet stricter comfort requirements, then the scenario number 46 would be the best option, with supply temperature limits of 45°C/7°C and a dT of 3K or 5K).

Comparing these savings with the ones obtained with the system operating under the water temperature control but implementing the rest of optimization strategies (Table 5.11), it is possible to see that the room temperature control produces higher energy

savings (around 25%-31% in the best cases with room temperature control against 16%-25% in the best cases of the system working with the water temperature control). It can be observed that using the room temperature control implies extra savings of around 5% in comparison with the supply water temperature control but maintaining the rest of optimization strategies. However, the highest savings are obtained by controlling the circulation pump speed with a fixed temperature difference instead of constant speed.

5.2.2 Tribano system operation

The system operation has been illustrated by selecting some representative days for heating and cooling operation. The scenario number 45 has been selected for this purpose, so the following parameters are set in the model:

- Room temperature control for the compressor frequency.
 - Supply temperature limit of 40°C for heating.
 - Supply temperature limit of 10°C for cooling.
- Circulation pump controlled by temperature difference of 3K.
- Buffer tank installed.
- Night mode enabled.
- Optimized schedule for the fan coil operation.

The main variables taking part in the system operation have been plotted for three representative days.

A representative day for heating mode (12th March) is shown in Figure 5.13. The supply and return temperature in the internal circuit, together with the four zones operative temperatures are plotted in Figure 5.13 a). The supply temperature plotted is the outlet temperature from the buffer tank (the one controlled for the temperature limit and temperature difference in the internal circuit). In Figure 5.13 b), the outdoor temperature and the compressor frequency are plotted.

The daily operation of the system working in heating mode, shown in Figure 5.13, is the following:

1. 0:00-7:00 (1680-1687h). At the start of the day, it is possible to see the night mode operation of the system, with the heat pump cycling at a low frequency in order to keep the temperature in the zones around 15°C.
2. 07:00-08:00 (1687h-1688h). When the operation of the fan coils starts at 7h, the heat pump frequency is set very high, as the temperature in the zones is quite low compared to the comfort temperature (23°C).
3. 08:00-13:00 (1688h-1693h). When the office schedule starts at 8h and the people enters the building, the temperature in the offices increases due to the internal gains in the rooms. The compressor frequency is adapted in order to keep the temperature in the rooms around 23°C and the supply temperature below the limit (40°C), as it can be seen along the day.

4. 13:00-18:00 (1693h-1698h). After 13h, the fan coils in the meeting room (META) are switched off, and then the temperature setpoint for this room is no longer 23°C, but 15°C (due to the night mode), so it will decrease naturally until it reaches 15°C. In the rest of the zones, the temperature is kept around 23°C, commuting the worst room according to their temperature evolution. The heat pump will cycle, as the thermal demand is not very high, so when the temperature in some room reaches the lower limit (22°C), the heat pump will start, and it will stop when the room reaches the upper limit (24°C).
5. 18:00-19:00 (1698h-1699h). The working schedule ends, so the room temperatures decreases suddenly until 19:00, when the fan coils are switched off.
6. 19:00-24:00 (1699h-1704h). The system works in night mode, so the heat pump and the fan coils will be off until one room reaches the night mode temperature (15°C).

A representative day for cooling mode in spring is shown in Figure 5.14 (5th June). The variables plotted are the same as in Figure 5.13. The operation during the day is analogous to the heating day, but in cooling mode there is no night mode, so the system stops during the night. As it is a day in spring, the ambient temperatures are quite mild (between 12°C and 24°C), so the thermal load is not very high. It is possible to see how the system is capable of working with room temperatures below 24°C easily, with a supply temperature above the limit (10°C). Here the advantage of having the room control temperature is demonstrated, as it is possible to keep the comfort inside the rooms with a milder supply temperature, then consuming less energy in the heat pump. During this day, the heat pump never stops in the operating hours.

Another representative day for cooling mode (10th July) with more extreme temperatures (between 19°C and 28°C) was selected and plotted in Figure 5.15. Here it can be seen that the supply temperature is kept all the time at the minimum temperature (10°C) and still, the desired indoor temperature of 23°C is not met in all the rooms (in the administration office (AMM) the room temperature reaches 25°C, what is still considered comfort). In this figure is also possible to see very clear the sharp changes in the indoor temperatures due to the schedule of the internal gains (occupancy and fan coils switching on/off), as explained above.

In conclusion, the model developed for the Tribano demo-site is able of reproducing the dynamics of the system and its different components and allows the estimation of the performance for an entire year. A new control strategy for the compressor frequency has been developed in order to control the temperature inside the rooms instead of controlling the supply temperature, therefore being able to reduce the supply temperature when the temperature inside the rooms is already inside the comfort levels.

A parametric analysis was carried out to find out which combination of parameters and control strategies is able to reach the thermal comfort inside the rooms with the lowest energy consumption.

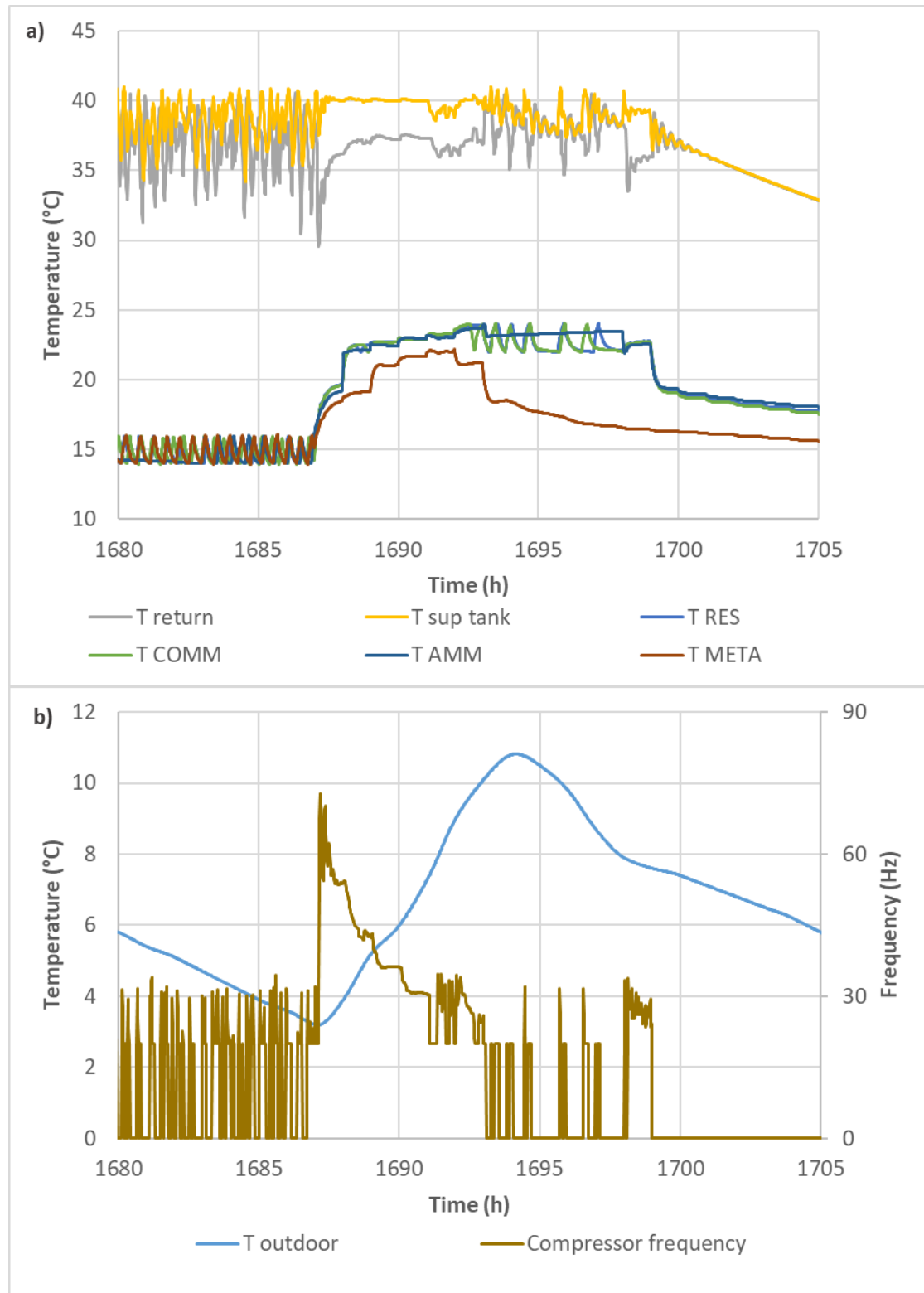


Figure 5.13. Operation of the system for a heating day (12th March): a) supply and return and operative temperature in the zones; b) outdoor temperature and compressor frequency

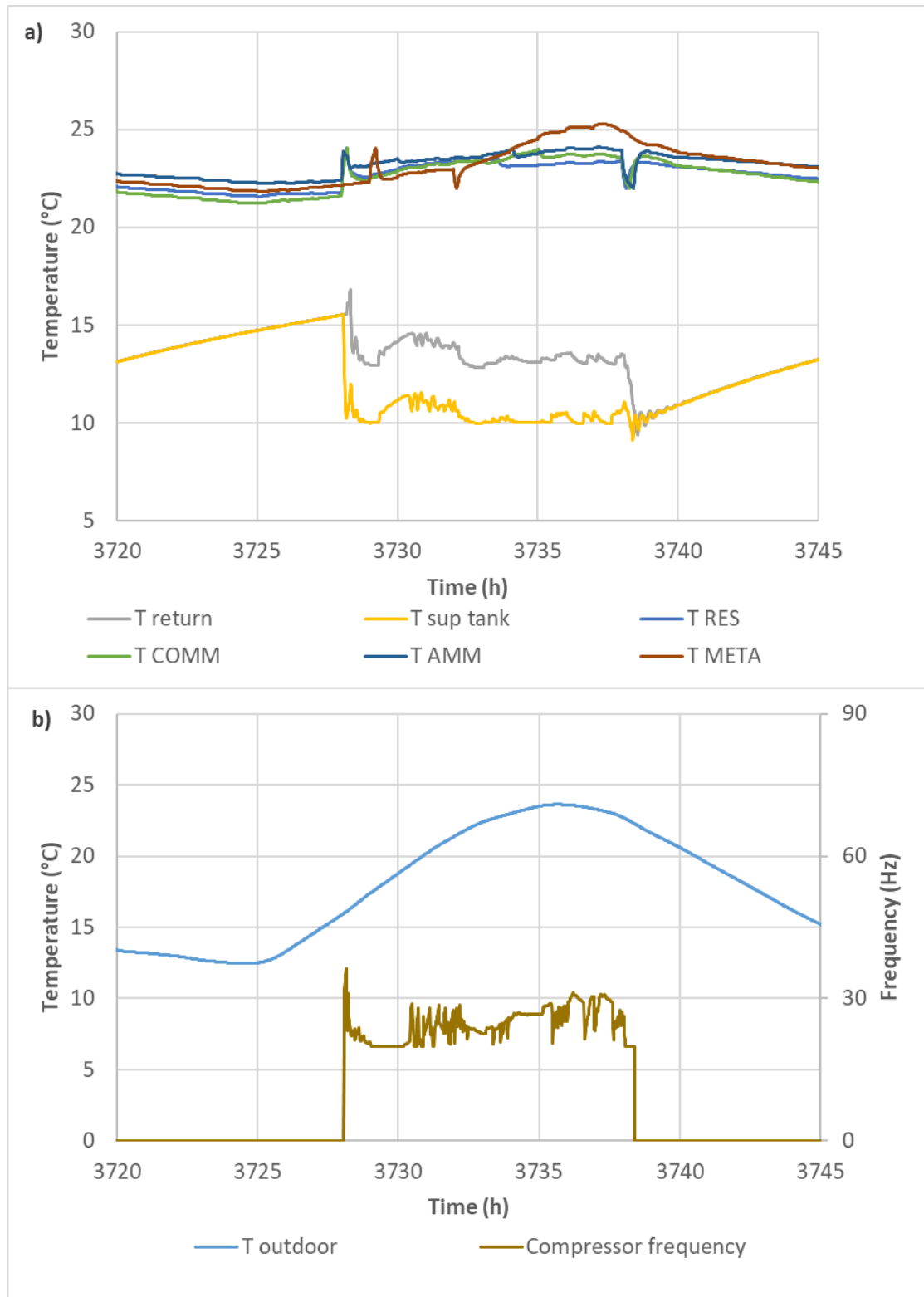


Figure 5.14. Operation of the system for a cooling day in spring (5th June): a) supply and return and operative temperature in the zones; b) outdoor temperature and compressor frequency

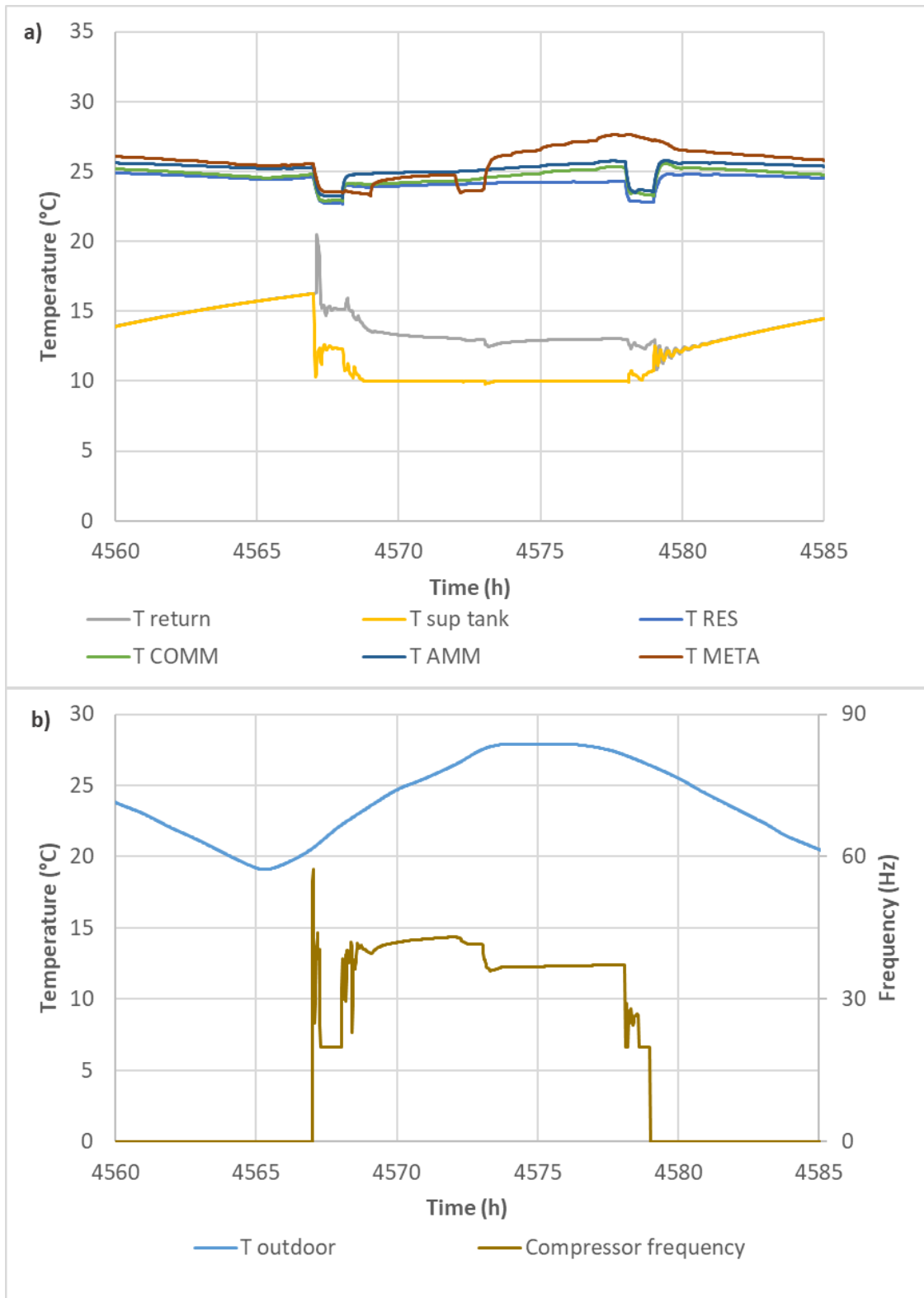


Figure 5.15. Operation of the system for a cooling day in summer (10th July): a) supply and return and operative temperature in the zones; b) outdoor temperature and compressor frequency

Chapter 6

6 Conclusions

In this PhD dissertation, first a dynamic model of a new coaxial helical Borehole Heat Exchanger (BHE) was developed, able to reproduce the dynamic response of the BHE, especially in terms of the fluid temperature evolution. This BHE model has been used to model a complete Dual Source Heat Pump (DSHP) system, providing a useful tool to assist in the design and optimization of the different components, carry out an energy assessment under different conditions and also test different control strategies in order to optimize the performance of the system. Both the modelling of the BHE and DSHP system was carried out in the TRNSYS software. The DSHP system was designed and developed in the framework of the European project GEOTeCH, including the innovative coaxial helical BHE and the DSHP.

The new BHE presents a coaxial configuration with an insulated inner pipe in order to reduce the thermal losses between the inner and outer pipe and a spiral rib attached to the inner tube, so the fluid follows a helical path through the outer pipe with some fluid leaking through the gap between the rib and the outer pipe wall.

The DSHP is a prototype with variable speed compressor, able to handle the necessities of heating, cooling and Domestic Hot Water (DHW) in small-scale buildings like offices and small dwellings. It is capable of working using the air or the ground as a source/sink, depending on which is more favourable at each moment. Furthermore, the system incorporates a free-cooling heat exchanger in order to meet the cooling necessities of the building when the water coming from the ground loop is cold enough. As a result, it is a complex system, able to work in eleven operating modes, depending on the final use (air-conditioning or DHW production), the season (winter or summer), the source/sink (air or ground) and other additional modes. The entire system and its main components has been described in more detail in chapter 2, as well as one of the demonstration facilities installed in Tribano (Italy), which is used as a reference in the modelling of the system.

Regarding the BHE modelling, a new dynamic model, able to reproduce the short term behaviour of the coaxial BHE with a low computational time was developed (B2G model) and implemented in TRNSYS. However, it is necessary to also model the long-term response of the ground and the thermal interaction between BHEs inside a field. So, a ground response model has also been developed (LSA model) for this purpose. The modelling of the coaxial BHE and the long-term response of the ground was described in chapter 3.

The new dynamic BHE model has been developed based on the B2G model, developed previously by the same research group for a U-tube configuration [119]. The U-tube B2G

model has been adapted to standard coaxial configurations, but also including the effect of the helical path through the outer tube. For this purpose, the thermal network has been adapted and improved, including new features: the vertical thermal conduction in the grout and ground, the option of considering layered soils with different thermal properties at different depths and three ground nodes instead of only one. So, it was also necessary to calculate the position of the ground nodes that reproduces with the highest accuracy the ground thermal response.

In order to calculate the optimal location of the ground nodes, a new methodology has been developed, obtaining polynomial correlations that were implemented inside the B2G coaxial model, so it automatically calculates the ground nodes position depending on the thermo-physical properties of the ground, the BHE geometry and the operating conditions of the system (heat injection period during a day). The new methodology consists in comparing the ground temperatures calculated by the B2G model, adapted to a constant heat flux on the borehole wall surface, and the Infinite Cylindrical Source model, in order to find the location of the ground nodes that minimizes the difference between them. For this purpose, an optimization algorithm in MATLAB® was used. A parametric study was carried out for a wide range of values of the different influencing variables allowing the determination of the polynomial correlations that finally were implemented in the B2G model.

The new B2G coaxial model has been validated with experimental data from different BHEs, with different geometries and ground properties. The coaxial helical BHE has been simulated with the B2G model using experimental data from a TRT, the influence of the spiral rib was analysed, assuming that the leaking of the fluid through the gap between the rib and the wall would generate a higher turbulence and then, increase the convective heat transfer. The results showed a quite small influence of this phenomenon, due to the fact that other factors influence to a greater extent in the borehole thermal resistance, for example the ground and grout thermal properties. The B2G coaxial model has also been validated against experimental data for standard coaxial BHE configurations. For this purpose, a Distributed Thermal Response Test (DTRT) was used, analysing both the simulated outlet temperature and the vertical temperature profile of the fluid inside the pipes, but also monitored data from the demo-site in Tribano was used to validate the model with real operation data. The results showed a good agreement between the experimental and simulated results in all the studies, demonstrating that the B2G coaxial model is able to reproduce the short-term response of a BHE, focused on the temperature evolution of the fluid inside the pipes, with an automated calculation of the amount of ground necessary for accurately reproducing the ground thermal response.

The long-term response of the ground was calculated in previous works with the U-tube B2G model by using a *g-function* previously calculated for a specific BHE configuration. In order to avoid the necessity of calculating previously a *g-function* for each configuration, a model based on the Infinite Line Source and adapted from an already existing tool for calculating the thermal interference between BHEs systems [138] was implemented in

TRNSYS, together with a load aggregation algorithm to reduce its simulation time. It was denominated LSA (Line Source Approach) model. This model is able to calculate the ground temperature response due to the injection of variable heat loads to the ground by the different BHEs in a field, considering the thermal interaction between them. In order to obtain a complete model of the BHEs field in TRNSYS, the LSA calculates the initial ground temperature periodically (usually each 24 hours), and the B2G model uses it as the initial ground temperature for the calculation of the dynamic evolution of the fluid temperature. In this manner, a complete ground model is obtained, able to reproduce both the dynamic behaviour of the BHE in terms of the fluid temperature and the long-term response of the ground, both with a low computational cost and avoiding relying on previously generated long-term models.

Concerning the DSHP system, in order to reproduce the behaviour of the entire system, a complete model in TRNSYS has been developed, in which each component of the system has been considered and coupled with the rest of the components. For this purpose, it was necessary to previously develop the detailed model of the coaxial helical BHE, but also to model the DSHP, as they are innovative components developed in the framework of the GEOTeCH project. The DSHP model was developed previously based on the data obtained from an experimental campaign [50] and, in this PhD dissertation, it was implemented in TRNSYS, together with a model of the free-cooling heat exchanger.

The resulting DSHP system model presents a modular configuration, easy to modify in order to adapt it to different installations and test different control parameters and optimization strategies. A complete control strategy is implemented inside the model to select among the eleven operating modes in which the system can work, selecting the optimal source/sink (ground or air) and setting the compressor frequency in order to meet the thermal demand. The optimal source/sink was selected comparing the ground and air temperatures using the more favourable (the hotter for heating and the colder for cooling). The model of the system has been detailed in chapter 4, where an extensive description of the different parts and the models used can be found.

The system model has been adapted to two configurations in order to carry out different assessments and testing of optimization strategies. The first one corresponds to the complete DSHP system, as defined by the GEOTeCH project, but the building is modelled by means of an input file with the corresponding thermal loads, resulting from simulating the building separately, in this manner this model can be applied to any building and location. For the second one, the Tribano demo-site was used as a reference, so the office building air-conditioned by the GEOTeCH system was modelled in detail and coupled to the heat pump system, considering the fan coils used as the emission system. A new strategy for the control of the compressor frequency was implemented in this model, based on setting this frequency by controlling the indoor temperature of the conditioned spaces directly, instead of controlling the temperature of the water supply to the emission system. In order to simplify this model and focus on the new control strategy, only the production of heating and cooling working with the air as a source/sink was included, not the ground loop nor the

DHW production. Finally, these two adaptations of the TRNSYS model were applied to two different studies, described in chapter 5.

The first study consists in the assessment of the DSHP system in different locations in Spain (Valencia, Madrid and Bilbao) and Europe (Athens, Strasbourg and Stockholm). For this purpose, the model of an existing departmental building in València (Spain) was adapted to the different locations and simulated for a one year period. So, the corresponding thermal loads were calculated and introduced in the TRNSYS model of the DSHP system as an input and a one year simulation was carried out. It was concluded that the DSHP presents a better performance during the summer period than the winter period, due to the fact that the heat pump presents higher COP values when working in cooling mode than in heating mode, additionally, the system works under more favourable conditions in summer than in winter. Therefore, in cooling dominated locations, the yearly performance will be better, mainly because the heat pump presents a better performance in cooling mode. Regarding the dual source concept, it was concluded that it is not recommended for cooling dominated areas (like Valencia or Athens), as the ground is the more favourable source/sink during the entire year, and the system will not practically select the air. On the other hand, it could be an attractive alternative compared to standard ground source heat pumps in average and cold climates (Bilbao, Strasbourg or Stockholm), because the air is selected in a higher rate in colder places, so it is possible to meet the thermal necessities of the building with a lower heat injection/extraction in the ground. Therefore the required BHE field would be smaller and so the total investment cost.

In the second study, the model of the Tribano demo-site was used. A parametric study was carried out, in which different control strategies and parameters were tested, mainly the control of the compressor frequency depending on the rooms temperatures. The rest of the optimization strategies were: controlling the circulation pump speed at the internal circuit by means of controlling the temperature difference in the circuit; using a buffer tank; optimizing the fan coils schedule and using a night mode. The main control parameter was the supply temperature limit that is allowed in heating and cooling. As a result, implementing all the optimization strategies except the room temperature control leads to a reduction of around 12% in the energy consumption. But a reduction of around a 30% could be achieved by implementing all the optimization strategies (including the room temperature control) and setting adequately the temperature limits in the supply temperature.

6.1 Future research

Despite the satisfactory results obtained with the models developed in this PhD thesis and the assessments carried out based on them, there is still room for some improvements in the different parts addressed:

1. Coaxial helical BHE model.

The B2G coaxial helical model could be improved by modelling in a higher detail the effect of the spiral rib attached to the inner tube in the heat transfer with the ground. In

order to do this, some correlations could be extracted from CFD simulations or from experimental tests, comparing the same BHE geometry, with and without the helical rib. In addition, the real pressure drop that results in the coaxial helical BHE could be correlated from some experimental tests in different BHE geometries in which some variables would be changed: mass flow rate, type of fluid and working temperatures. From these experimental tests and the monitoring of the pressure drop, a correlation could be obtained and implemented inside the TRNSYS type, depending on the BHE geometry (diameters and rib height), pipes material, mass flow rate, type of fluid and temperature. For the moment, the pressure drop is calculated for a standard coaxial BHE.

2. B2G model and its applications.

First, all the new features included in the coaxial B2G model could be introduced in the previous U-tube B2G model: different ground layers and vertical conduction in the grout and ground (already implemented and presented in [172]), three ground nodes and implementation of the correlations for calculating the optimal position (as they don't depend on the internal BHE configuration but only on the borehole diameter), the calculation of the pressure drop and the coupling with the LSA model instead of the g -function model.

Regarding the applications of the B2G model, it was previously addressed its use as a tool to assist in the estimation of the ground thermal properties and the calculation of the borehole resistance based on the values of the internal thermal resistances calculated inside the B2G model, as was studied in [173] for a U-tube configuration, where the B2G model was used in order to estimate the ground thermal properties using the data from the first time period of heat injection in a Thermal Response Test (TRT), leading to a reduction in the necessary time for this type of tests and improving its economic feasibility. This application could be further studied and improved by carrying out various experimental tests in different locations, with different ground properties, BHE configurations and geometries. The utility of the B2G model as a tool to estimate the ground thermal properties would be validated comparing the experimental results with the simulated ones in a great number of field tests.

In this regard, the reduction of the TRT time for the estimation of the ground thermal properties was also addressed by Pasquier [174], in this case using the time derivative of the temperature.

3. Long-term BHE field model

The LSA model implemented in TRNSYS was adapted from the tool developed by Witte [138] and based on an algebraic approximation of the Infinite Line Source model (ILS). It provided good results when compared to the g -function model, which had been previously used in the coupling with the B2G model. A more deep study could be done by comparing this approximation to other approximations of the ILS, like the one provided by Ingersoll et al. [61] and Abramovitz and Stegun [63]. The aggregation method used could also be compared with other aggregation methods, like the one developed by Bernier et al. [114].

4. Energy optimization control strategies implementation on site.

The room temperature control described in section 4.4 for controlling the compressor frequency could be implemented in one of the demo-sites installed in the framework of the GEOTeCH project, then checking the savings calculated in section 5.2. The rest of optimization strategies and control parameters could also be tested on site.

References

- [1] European Parliament and Council of the European Union, "Directive 2009/28/EC of the European Parliament and of the Council of 23 April 2009 on the promotion of the use of energy from renewable sources and amending and subsequently repealing repealing Directives 2001/77/EC and 2003/30/EC," *Off. J. Eur. Union*, vol. 52, no. L 140, pp. 16–62, 2009.
- [2] European Parliament and Council of the European Union, "Decision no 406/2009 of the European Parliament and of the Council of 23 April 2009 on the effort of Member States to reduce their greenhouse gas emissions to meet the Community's greenhouse gas emission reduction commitments up to 2020," *Off. J. Eur. Union*, vol. 52, no. L 140, pp. 136–148, 2009.
- [3] European Commission, "Europe 2020 - A strategy for smart, sustainable and inclusive growth," 2010.
- [4] European Commission, "HORIZON 2020 - Secure, Clean and Efficient Energy." [Online]. Available: <http://ec.europa.eu/programmes/horizon2020/en/h2020-section/secure-clean-and-efficient-energy>. [Accessed: 18-Jan-2019].
- [5] European Commission, "2030 climate & energy framework." [Online]. Available: https://ec.europa.eu/clima/policies/strategies/2030_en. [Accessed: 04-Apr-2019].
- [6] European Commission, *A policy framework for climate and energy in the period from 2020 to 2030*, no. COM(2014) 15 final. 2014.
- [7] European Commission, *A Clean Planet for all - A European strategic long-term vision for a prosperous, modern, competitive and climate neutral economy*, vol. COM(2018)7. 2018.
- [8] United Nations, "Sustainable Development Goals - 7 Affordable and clean energy." [Online]. Available: <https://www.un.org/sustainabledevelopment/energy/>. [Accessed: 04-Apr-2019].
- [9] IEA, "Technology Roadmap: Energy-Efficient Buildings: Heating and Cooling Equipment. Technical report," Paris, France, 2011.
- [10] International Energy Agency, *Energy Efficiency 2017*. IEA, 2017.
- [11] European Technology Platform on Renewable Heating and Cooling. Secretariat of the RHC-Platform, "Strategic Research and Innovation Agenda for Renewable Heating & Cooling," Brussels, 2013.
- [12] S. J. Rees, *Advances in Ground-Source Heat Pump Systems*. Woodhead Publishing, 2016.
- [13] A. D. Carvalho, P. Moura, G. C. Vaz, and A. T. De Almeida, "Ground source heat pumps as high efficient solutions for building space conditioning and for integration in smart grids," *Energy Convers. Manag.*, vol. 103, pp. 991–1007, 2015.
- [14] M. Rivoire, A. Casasso, B. Piga, and R. Sethi, "Assessment of Energetic, Economic and Environmental Performance of Ground-Coupled Heat Pumps," *Energies*, vol. 11, no. 1941, 2018.
- [15] J. F. Urchueguía, M. Zacarés, J. M. Corberán, Á. Montero, J. Martos, and H. Witte, "Comparison between the energy performance of a ground coupled water to water heat pump system and an air to water heat pump system for heating and cooling in typical conditions of the European Mediterranean coast," *Energy Convers. Manag.*, vol. 49, no. 10, pp. 2917–2923, Oct. 2008.
- [16] J. S. Jeon, S. R. Lee, and M. J. Kim, "A modified mathematical model for spiral coil-type horizontal ground heat exchangers," *Energy*, vol. 152, no. June, pp. 732–743, 2018.
- [17] P. Bayer, D. Saner, S. Bolay, L. Rybach, and P. Blum, "Greenhouse gas emission savings of ground source heat pump systems in Europe: A review," *Renew. Sustain. Energy*

- Rev.*, vol. 16, no. 2, pp. 1256–1267, Feb. 2012.
- [18] V. Somogyi, V. Sebestyén, and G. Nagy, “Scientific achievements and regulation of shallow geothermal systems in six European countries – A review,” 2016.
- [19] European Commission, “GeoCool ‘Geothermal Heat Pump for Cooling and Heating along European coastal Areas’ (EU 5th Framework Programme, NNE5-2001-00847),” 2003. [Online]. Available: http://cordis.europa.eu/project/rcn/86940_en.html. [Accessed: 28-Feb-2018].
- [20] European Commission, “GROUND-MED ‘Advanced ground source heat pump systems for heating and cooling in Mediterranean climate’ (TREN/FP7EN/218895),” 2009. [Online]. Available: <http://groundmed.eu/>. [Accessed: 21-Apr-2019].
- [21] G. Florides and S. Kalogirou, “Ground heat exchangers—A review of systems, models and applications,” *Renew. Energy*, vol. 32, no. 15, pp. 2461–2478, Dec. 2007.
- [22] L. Aresti, P. Christodoulides, and G. Florides, “A review of the design aspects of ground heat exchangers,” *Renew. Sustain. Energy Rev.*, vol. 92, pp. 757–773, Sep. 2018.
- [23] S. J. Rees, “Horizontal and compact ground heat exchangers,” in *Advances in Ground-Source Heat Pump Systems*, S. J. Rees, Ed. Woodhead Publishing, 2016, pp. 117–156.
- [24] D. T. Gordon, “Analytical and Experimental Study on Coaxial Borehole Heat Exchangers,” University of Windsor, 2017.
- [25] D. Gordon, T. Bolisetti, D. S. K. Ting, and S. Reitsma, “A physical and semi-analytical comparison between coaxial BHE designs considering various piping materials,” *Energy*, vol. 141, pp. 1610–1621, 2017.
- [26] T. Kurevija, M. Macenić, and K. Strpić, “Steady-State Heat Rejection Rates for a Coaxial Borehole Heat Exchanger During Passive and Active Cooling Determined With the Novel Step Thermal Response Test Method,” *Rud. Zb.*, vol. 33, no. 2, pp. 61–71, 2018.
- [27] J. Acuña, “Distributed thermal response tests – New insights on U-pipe and Coaxial heat exchangers in groundwater-filled boreholes,” KTH, 2013.
- [28] S. Focaccia and F. Tinti, “An innovative Borehole Heat Exchanger configuration with improved heat transfer,” *Geothermics*, vol. 48, pp. 93–100, Oct. 2013.
- [29] R. M. Lazzarin, “Dual source heat pump systems: Operation and performance,” *Energy Build.*, vol. 52, pp. 77–85, 2012.
- [30] K. Bakirci, O. Ozyurt, K. Comakli, and O. Comakli, “Energy analysis of a solar-ground source heat pump system with vertical closed-loop for heating applications,” *Energy*, vol. 36, no. 5, pp. 3224–3232, 2011.
- [31] L. I. Lubis, M. Kanoglu, I. Dincer, and M. A. Rosen, “Thermodynamic analysis of a hybrid geothermal heat pump system,” *Geothermics*, vol. 40, no. 3, pp. 233–238, Sep. 2011.
- [32] W. Liu, G. Chen, B. Yan, Z. Zhou, H. Du, and J. Zuo, “Hourly operation strategy of a CCHP system with GSHP and thermal energy storage (TES) under variable loads: A case study,” *Energy Build.*, vol. 93, pp. 143–153, Apr. 2015.
- [33] G. B. M. A. Litjens, E. Worrell, and W. G. J. H. M. van Sark, “Lowering greenhouse gas emissions in the built environment by combining ground source heat pumps, photovoltaics and battery storage,” *Energy Build.*, vol. 180, pp. 51–71, Dec. 2018.
- [34] N. Pardo, Á. Montero, J. Martos, and J. F. Urchueguía, “Optimization of hybrid – ground coupled and air source – heat pump systems in combination with thermal storage,” *Appl. Therm. Eng.*, vol. 30, no. 8–9, pp. 1073–1077, Jun. 2010.
- [35] Y. Kim, J. Lee, and S. Jeon, “Hybrid ground source heat pumps systems,” in *Advances in Ground-Source Heat Pump Systems*, S. J. Rees, Ed. Woodhead Publishing, 2016, pp. 331–357.
- [36] J. M. Corberan, “New trends and developments in ground-source heat pumps,” in *Advances in Ground-Source Heat Pump Systems*, S. J. Rees, Ed. Woodhead Publishing, 2016, pp. 359–385.
- [37] H. Wang, B. Bai, G. Feng, L. Yu, X. Liu, and Y. Luo, “Simulation and Analysis of Air-soil Dual Source Heat Pump Energy Consumption in Cold Regions,” *Procedia Eng.*, vol.

- 121, pp. 1397–1405, Jan. 2015.
- [38] Y. Nam, R. Ooka, and Y. Shiba, “Development of dual-source hybrid heat pump system using groundwater and air,” *Energy Build.*, vol. 42, no. 6, pp. 909–916, Jun. 2010.
- [39] C. Yavuzturk and J. D. Spitler, “Comparative study of operating and control strategies for hybrid ground-source heat pump systems using a short time step simulation model,” *ASHRAE Trans.*, vol. 106, 2000.
- [40] European Commission, “Geothermal Technology for Economic Cooling and Heating (H2020-LCE-2014-2, GEOTeCH-656889),” 2015. [Online]. Available: <http://www.geotech-project.eu/>. [Accessed: 20-Jan-2019].
- [41] GEOTHEX BV, “GEOTHEX.” [Online]. Available: <http://www.geothex.nl/>. [Accessed: 21-Apr-2019].
- [42] Geothermal Technology for Economic Cooling and Heating (H2020-LCE-2014-2 GEOTeCH-656889), “Deliverable D4.6 Global system model of plug & play installations. WP4 Plug and Play Geothermal System Development,” 2016.
- [43] J. Cervera-Vázquez, C. Montagud-Montalvá, and J. M. Corberán, “Sizing of the buffer tank in chilled water distribution air-conditioning systems,” *Sci. Technol. Built Environ.*, vol. 22, no. 3, pp. 290–298, 2016.
- [44] CEN, “EN 1717 Protection against pollution of potable water in water installations and general requirements of devices to prevent pollution by backflow,” Brussels, 2000.
- [45] X. Masip, A. Cazorla-Marin, J. Marchante, J. M. Corberán, and C. Montagud, “Energy and techno-economic assessment of the effect of the coupling between an air source heat pump and the storage tank for sanitary hot water production,” *Appl. Therm. Eng.*, vol. 159, p. 113853, 2019.
- [46] H. J. L. Witte, “The GEOTHEX geothermal heat exchanger, characterisation of a novel high efficiency heat exchanger design,” in *The 12th International conference on Energy Storage (Innstock 2012)*, 2012.
- [47] HiRef S.p.A., “HiRef.” [Online]. Available: <https://hiref.it/en>. [Accessed: 25-Jan-2019].
- [48] J. M. Corberán, A. Cazorla-Marín, J. Marchante-Avellaneda, and C. Montagud, “Dual source heat pump, a high efficiency and cost-effective alternative for heating, cooling and DHW production,” *Int. J. Low-Carbon Technol.*, vol. 13, no. 2, pp. 161–176, 2018.
- [49] J. Marchante-Avellaneda, J. M. Corberán, A. Cazorla-Marin, and C. Montagud, “Diseño de una bomba de calor de 8 kW con foco de calor dual: aerotermia y geotermia,” in *IX Congreso Ibérico y VII Congreso Iberoamericano de Ciencias y Técnicas del Frío - CYTEF2018*, 2018, p. 1193.
- [50] J. Marchante-avellaneda, J. M. Corberán, A. Cazorla-Marin, and C. Montagud, “Initial Test Campaign of an Innovative Dual Source Heat Pump,” in *IX Congreso Ibérico y VII Congreso Iberoamericano de Ciencias y Técnicas del Frío - CYTEF2018*, 2018, p. 1205.
- [51] F. Tinti *et al.*, “Ground temperature monitoring for a coaxial geothermal heat exchangers field: practical aspects and main issues from the first year of measurements,” *Mining-Geology-Petroleum Eng. Bull.*, vol. 33, no. 5, pp. 47–57, 2018.
- [52] D. Pomarè Montin, “Relazione geologico-idrogeologica. Impianto di Geoscambio a circuito chiuso. Comune di Tribano ‘Hydro-geological study. Closed-lopp geothermal Plant. Municipality of Tribano,’” Santo Stefano di Cadore (BL), 2017.
- [53] Ente Nazionale Italiano di Unificazione (UNI), “UNI 11466:2012 Sistemi geotermici a pompa di calore. Requisiti per il dimensionamento e la progettazione. ‘Heat pump geothermal systems: Design and sizing requirements,’” Milano, 2012.
- [54] S. Javed, P. Fahlén, and J. Claesson, “Vertical ground heat exchangers: a review of heat flow models,” in *Effstock*, 2009.
- [55] C. Zhang, Y. Wang, Y. Liu, X. Kong, and Q. Wang, “Computational methods for ground thermal response of multiple borehole heat exchangers: A review,” *Renew. Energy*, vol. 127, pp. 461–473, Nov. 2018.

- [56] H. Yang, P. Cui, and Z. Fang, "Vertical-borehole ground-coupled heat pumps: A review of models and systems," *Appl. Energy*, vol. 87, pp. 16–27, 2010.
- [57] M. Li and A. C. K. Lai, "Review of analytical models for heat transfer by vertical ground heat exchangers (GHEs): A perspective of time and space scales," *Appl. Energy*, vol. 151, pp. 178–191, 2015.
- [58] H. S. Carslaw and J. C. Jaeger, *Conduction of heat in solids*, Second ed. New York, NY, USA: Oxford University Press, 1959.
- [59] R. Al-Khoury, *Computational Modeling of Shallow Geothermal Systems*. CRC Press, 2012.
- [60] W. T. Kelvin, *Mathematical and physical papers*. London, UK: Cambridge University Press, 1882.
- [61] L. R. Ingersoll and H. J. Plass, "Theory of the ground pipe heat source for the heat pump," *Heating, Pip. Air Cond.*, vol. 20, no. 7, pp. 119–122, 1948.
- [62] S. Morchio and M. Fossa, "Thermal Modeling of Deep Borehole heat exchangers for geothermal applications in densely populated urban areas," *Therm. Sci. Eng. Prog.*, p. 100363, Jun. 2019.
- [63] M. Abramowitz and I. Stegun, *Handbook of Mathematical Functions*. National Bureau of Standards, 1964.
- [64] L. R. Ingersoll, O. J. Zobel, and A. C. Ingersoll, *Heat conduction with engineering, geological and other applications*. New York, NY, USA: McGraw-Hill, 1954.
- [65] D. P. Hart and R. Couvillion, *Earth-Coupled Heat Transfer*. Dublin, OH: National Water Well Association, 1986.
- [66] S. P. Kavanaugh, "Simulation and experimental verification of vertical ground coupled heat pump systems," Oklahoma State University, 1985.
- [67] P. Eskilson, "Thermal Analysis of Heat Extraction Boreholes," University of Lund, 1987.
- [68] M. Philippe, M. Bernier, and D. Marchio, "Validity ranges of three analytical solutions to heat transfer in the vicinity of single boreholes," *Geothermics*, vol. 38, no. 4, pp. 407–413, 2009.
- [69] L. Lamarche, "Short-term behavior of classical analytic solutions for the design of ground-source heat pumps," *Renew. Energy*, vol. 57, pp. 171–180, 2013.
- [70] P. Conti, "Dimensionless Maps for the Validity of Analytical Ground Heat Transfer Models for GSHP Applications," *Energies*, vol. 9, no. 11, p. 890, Oct. 2016.
- [71] C. Yavuzturk, "Modeling of vertical ground loop heat exchangers for ground source heat pump systems," Oklahoma State University, 1999.
- [72] H. Y. Zeng, N. R. Diao, and Z. H. Fang, "A finite line-source model for boreholes in geothermal heat exchangers," *Heat Transf. - Asian Res.*, vol. 31, no. 7, pp. 558–567, 2002.
- [73] L. Lamarche and B. Beauchamp, "A new contribution to the finite line-source model for geothermal boreholes," *Energy Build.*, vol. 39, no. 2, pp. 188–198, Feb. 2007.
- [74] M. Cimmino, M. Bernier, and F. Adams, "A contribution towards the determination of g-functions using the finite line source," *Appl. Therm. Eng.*, vol. 51, no. 1–2, pp. 401–412, Mar. 2013.
- [75] M. Cimmino and M. Bernier, "A semi-analytical method to generate g-functions for geothermal bore fields," *Int. J. Heat Mass Transf.*, vol. 70, pp. 641–650, Mar. 2014.
- [76] Y.-L. Nian and W.-L. Cheng, "Analytical g-function for vertical geothermal boreholes with effect of borehole heat capacity," *Appl. Therm. Eng.*, vol. 140, pp. 733–744, Jul. 2018.
- [77] J. Acuña, M. Fossa, P. Monzó, and B. Palm, "Numerically generated g-functions for ground coupled heat pump applications," in *Proceedings of the 2012 COMSOL Conference*, 2012, pp. 1–6.
- [78] P. Monzó, P. Mogensen, J. Acuña, F. Ruiz-Calvo, and C. Montagud, "A novel numerical approach for imposing a temperature boundary condition at the borehole wall in borehole fields," *Geothermics*, vol. 56, pp. 35–44, 2015.

- [79] P. Eskilson and J. Claesson, "Simulation model for thermally interacting heat extraction boreholes," *Numer. Heat Transf.*, vol. 13, no. 2, pp. 149–165, Mar. 1988.
- [80] N. K. Muraya, "Numerical modeling of the transient thermal interference of vertical U-tube heat exchangers," Texas A&M University, 1994.
- [81] R. Al-Khoury and P. G. Bonnier, "Efficient finite element formulation for geothermal heating systems. Part II: transient," *Int. J. Numer. Methods Eng.*, vol. 67, no. 5, pp. 725–745, 2006.
- [82] R. Al-Khoury, P. G. Bonnier, and R. B. J. Brinkgreve, "Efficient finite element formulation for geothermal heating systems. Part I: steady state," *Int. J. Numer. Methods Eng.*, vol. 63, no. 7, pp. 988–1013, 2005.
- [83] H.-J. G. Diersch, D. Bauer, W. Heidemann, W. Rühak, and P. Schätzl, "Finite element modeling of borehole heat exchanger systems: Part 2. Numerical simulation," *Comput. Geosci.*, vol. 37, no. 8, pp. 1136–1147, Aug. 2011.
- [84] H.-J. G. Diersch, D. Bauer, W. Heidemann, W. Rühak, and P. Schätzl, "Finite element modeling of borehole heat exchanger systems: Part 1. Fundamentals," *Comput. Geosci.*, vol. 37, no. 8, pp. 1122–1135, Aug. 2011.
- [85] W. Yang, M. Shi, G. Liu, and Z. Chen, "A two-region simulation model of vertical U-tube ground heat exchanger and its experimental verification," *Appl. Energy*, vol. 86, no. 10, pp. 2005–2012, 2009.
- [86] M. De Carli, M. Tonon, A. Zarrella, and R. Zecchin, "A computational capacity resistance model (CaRM) for vertical ground-coupled heat exchangers," *Renew. Energy*, vol. 35, no. 7, pp. 1537–1550, Jul. 2010.
- [87] A. Zarrella, M. Scarpa, and M. De Carli, "Short time step analysis of vertical ground-coupled heat exchangers: The approach of CaRM," *Renew. Energy*, vol. 36, no. 9, pp. 2357–2367, Sep. 2011.
- [88] D. Bauer, W. Heidemann, H. Müller-Steinhagen, and H.-J. G. Diersch, "Thermal resistance and capacity models for borehole heat exchangers," *Int. J. Energy Res.*, vol. 35, no. 4, pp. 312–320, Mar. 2011.
- [89] D. Bauer, W. Heidemann, and H.-J. G. Diersch, "Transient 3D analysis of borehole heat exchanger modeling," *Geothermics*, vol. 40, no. 4, pp. 250–260, Dec. 2011.
- [90] P. Pasquier and D. Marcotte, "Short-term simulation of ground heat exchanger with an improved TRCM," *Renew. Energy*, vol. 46, pp. 92–99, Oct. 2012.
- [91] L. Lamarche, S. Kajl, and B. Beauchamp, "A review of methods to evaluate borehole thermal resistances in geothermal heat-pump systems," *Geothermics*, vol. 39, no. 2, pp. 187–200, Jun. 2010.
- [92] M. Li and A. C. K. Lai, "New temperature response functions (G functions) for pile and borehole ground heat exchangers based on composite-medium line-source theory," *Energy*, vol. 38, no. 1, pp. 255–263, Feb. 2012.
- [93] S. Javed and P. E. J. Claesson, "New analytical and numerical solutions for the short-term analysis of vertical ground heat exchangers," *ASHRAE Trans.*, vol. 117, no. 1, pp. 3–12, 2011.
- [94] S. L. Do and J. S. Haberl, "A review of ground coupled heat pump models used in whole-building computer simulation programs," in *Proceedings of the 17th Symposium for Improving Building Systems in Hot and Humid Climates*, 2010.
- [95] J. D. Spitler, "GLHEPRO – A DESIGN TOOL FOR COMMERCIAL BUILDING GROUND LOOP HEAT EXCHANGERS," in *Proceedings of the Fourth International Heat Pumps in Cold Climates Conference*, 2000, pp. 17–18.
- [96] T. Blomberg, J. Claesson, P. Eskilson, G. Hellström, and B. Sanner, "EED - Earth Energy Designer." 2016.
- [97] Department Of Energy, "EnergyPlus." 1998.
- [98] Modelica Association, "Modelica." 1996.
- [99] D. Picard and L. Helsen, "Advanced hybrid model for borefield heat exchanger performance evaluation, an implementation in Modelica," in *10th International Modelica Conference*, 2014.

- [100] S. A. Klein, W. A. Beckman, and J. A. Duffie, "TRNSYS: A Transient System Simulation Program." Solar Energy Laboratory, University of Wisconsin, Madison, USA, 2007.
- [101] S. A. Klein, W. A. Beckman, and J. A. Duffie, "TRNSYS - a transient simulation program," in *ASHRAE Transactions* 82, 1976.
- [102] P. Pärish, O. Mercker, P. Oberdorfer, E. Bertram, R. Tepe, and G. Rockendorf, "Short-term experiments with borehole heat exchangers and model validation in TRNSYS," *Renew. Energy*, vol. 74, pp. 471–477, 2015.
- [103] P. Eskilson, *Superposition borehole model. Manual for computer code*. Lund, Sweden: Department of Mathematical Physics, Lund Institute of Technology, 1986.
- [104] D. Pahud, A. Fromentin, and J.-C. Hadorn, "The Superposition Borehole Model for TRNSYS (TRNSBM)." LASEN-DGC-EPFL, Lausanne, 1996.
- [105] D. Pahud, "The Superposition Borehole Model for TRNSYS 16 or 17 (TRNSBM)." Scuola universitaria professionale della Svizzera italiana, pp. 1–16, 2012.
- [106] G. Hellström, "Duct ground heat storage model. Manual for computer code." Department of Mathematical Physics, University of Lund, 1989.
- [107] G. Hellström, "Ground Heat Storage. Thermal Analyses of Duct Storage Systems," University of Lund, 1991.
- [108] D. Pahud and G. Hellström, "The new duct ground heat model for TRNSYS," in *Eurotherm Seminar n°49, Physical models for Thermal Energy Stores*, 1996, pp. 127–136.
- [109] D. Pahud, G. Hellström, and L. Mazzarella, "Duct ground heat storage model for TRNSYS (TRNVDST). User manual." LASEN-DGC-EPFL, Laussane, Switzerland, 1997.
- [110] A. Huber and O. Schuler, "Berechnungsmodul für Erdwärmesonden," Bern, 1997.
- [111] M. Wetter and A. Huber, "Vertical Borehole Heat Exchanger. EWS model. TRNSYS type 451." Zentralschweizerisches Technikum Luzern, Luzern, 1997.
- [112] M. N. Özisik, *Heat Conduction*, 2nd editio. New York, NY: John Wiley & Sons, Inc, 1993.
- [113] C. Yavuzturk and J. D. Spitler, "A Short Time Step Response Factor Model for Vertical Ground Loop Heat Exchangers Cenk Yavuzturk," *ASHRAE Trans.*, vol. 105, no. 2, pp. 475–485, 1999.
- [114] M. A. Bernier, P. Pinel, R. Labib, and R. Paillot, "A Multiple Load Aggregation Algorithm for Annual Hourly Simulations of GCHP Systems," *HVAC&R Res.*, vol. 10, no. 4, pp. 471–487, Oct. 2004.
- [115] F. Ruiz-Calvo, M. De Rosa, P. Monzó, C. Montagud, and J. M. Corberán, "Coupling short-term (B2G model) and long-term (g-function) models for ground source heat exchanger simulation in TRNSYS. Application in a real installation," *Appl. Therm. Eng.*, vol. 102, pp. 720–732, Jun. 2016.
- [116] M. Fossa and D. Rolando, "Improved Ashrae method for BHE field design at 10 year horizon," *Energy Build.*, vol. 116, pp. 114–121, Mar. 2016.
- [117] M. A. Bernier, "Closed-loop ground-coupled heat pump systems," *ASHRAE J.*, vol. 48, no. 9, pp. 12-18+20+22+24, 2006.
- [118] M. Fossa, "The temperature penalty approach to the design of borehole heat exchangers for heat pump applications," *Energy Build.*, vol. 43, no. 6, pp. 1473–1479, Jun. 2011.
- [119] F. Ruiz-Calvo, M. De Rosa, J. Acuña, J. M. Corberán, and C. Montagud, "Experimental validation of a short-term Borehole-to-Ground (B2G) dynamic model," *Appl. Energy*, vol. 140, pp. 210–223, Feb. 2015.
- [120] M. De Rosa, F. Ruiz-Calvo, J. M. Corberán, C. Montagud, and L. A. Tagliafico, "A novel TRNSYS type for short-term borehole heat exchanger simulation: B2G model," *Energy Convers. Manag.*, vol. 100, pp. 347–357, 2015.
- [121] A. Cazorla-Marin, C. Montagud, J. M. Corberán, and J. Acuña, "Modeling of a coaxial Borehole Heat Exchanger and experimental validation," in *10º Congreso Internacional Ingeniería Termodinámica 10CNIT*, 2017, pp. 162–163.
- [122] A. Cazorla-Marin, C. Montagud, and J. M. Corberán, "Adaptation of the B2G dynamic model to new borehole heat exchanger coaxial configurations," in *IX Congreso*

- Ibérico y VII Congreso Iberoamericano de Ciencias y Técnicas del Frío - CYTEF2018*, 2018, p. 1186.
- [123] A. Cazorla-marín, F. Ruiz-calvo, H. Witte, C. Montagud, and J. M. Corberán, “An Innovative Co-Axial Spiral Borehole Heat Exchanger Dynamic Model,” in *European Geothermal Congress 2016*, 2016, p. T-UTES-127.
- [124] A. Cazorla-Marin, C. Montagud, H. Witte, R. Hylkema, and J. Corberan, “Modelling and Experimental Validation of a Novel Co-axial Spiral Borehole Heat Exchanger,” in *IGSHPA Research Conference Proceedings*, 2017, pp. 212–220.
- [125] A. Cazorla-Marín, C. Montagud, J. M. Corberán, F. Tinti, and S. Focaccia, “Upgrade of the B2G dynamic geothermal heat exchanger model: optimal location of the ground nodes,” in *IGSHPA Research Track 2018*, 2018, pp. 20–28.
- [126] Å. Melinder, *Properties of Secondary Working Fluids for Indirect Systems*. Paris, France: International Institute of Refrigeration, IIR, 2010.
- [127] V. Gnielinski, “G1 Heat Transfer in Pipe flow,” in *VDI Heat Atlas*, Second Edi., VDI-Gesellschaft Verfahrenstechnik und Chemieingenieurwesen, Ed. Düsseldorf: Springer-Verlag Berlin Heidelberg, 2010.
- [128] V. Gnielinski, “G2 Heat Transfer in Concentric Annular and Parallel Plate Ducts,” in *VDI Heat Atlas*, Second Edi., VDI-Gesellschaft Verfahrenstechnik und Chemieingenieurwesen, Ed. Düsseldorf: Springer-Verlag Berlin Heidelberg, 2010.
- [129] P. Lax and B. Wendroff, “Systems of conservation laws,” *Commun. Pure Appl. Math.*, vol. 13, pp. 217–237, 1960.
- [130] F. Ruiz-Calvo, “Análisis y modelado de una instalación geotérmica para climatización de un conjunto de oficinas,” Universitat Politècnica de València, 2015.
- [131] S. W. Churchill, “Friction factor equation spans all fluid-flow regimes,” *Chem. Eng.*, vol. 84, no. 24, pp. 91–92, 1977.
- [132] F. M. White, *Fluid mechanics*, Sixth edit. McGraw-Hill, 2008.
- [133] MathWorks, *Global Optimization Toolbox - User's Guide - MATLAB*. 2017.
- [134] J. Acuña and B. Palm, “Distributed thermal response tests on pipe-in-pipe borehole heat exchangers,” *Appl. Energy*, vol. 109, pp. 312–320, Sep. 2013.
- [135] R. A. Beier, J. Acuña, P. Mogensen, and B. Palm, “Transient heat transfer in a coaxial borehole heat exchanger,” *Geothermics*, vol. 51, pp. 470–482, Jul. 2014.
- [136] Groenholland BV, “Groenholland Geo Energy Systems.” [Online]. Available: <http://www.groenholland.com/en/>. [Accessed: 13-Mar-2019].
- [137] H. J. L. Witte, “Methode voor het bepalen van interferentie tussen kleine gesloten bodemenergiesystemen. Rapport GHNL 011103,” 2011.
- [138] H. J. L. Witte, “A Novel Tool for Assessing Negative Temperature Interactions between Neighbouring Borehole Heat Exchanger Systems A Novel Tool for Assessing Negative Temperature Interactions between Neighbouring Borehole Heat Exchanger Systems,” in *14th International Conference on Energy Storage*, 2018.
- [139] A. Cazorla-Marín, F. Ruiz-Calvo, C. Montagud, and J. M. Corberán, “Nuevo modelo dinámico de un intercambiador enterrado en TRNSYS: adaptación del modelo B2G a largos periodos de simulación,” in *CYTEF2016 - PROCEEDINGS. Advances in Refrigeration Sciences and Technologies - VIII*, 2016.
- [140] F. Ruiz-Calvo and C. Montagud, “Reference data sets for validating GSHP system models and analyzing performance parameters based on a five-year operation period,” *Geothermics*, vol. 51, pp. 417–428, 2014.
- [141] P. Cui, H. Yang, J. D. Spitler, and Z. Fang, “Simulation of hybrid ground-coupled heat pump with domestic hot water heating systems using HVACSIM+,” *Energy Build.*, vol. 40, no. 9, pp. 1731–1736, Jan. 2008.
- [142] R. Chargui, H. Sammouda, and A. Farhat, “Geothermal heat pump in heating mode: Modeling and simulation on TRNSYS,” *Int. J. Refrig.*, vol. 35, no. 7, pp. 1824–1832, Nov. 2012.
- [143] A. A. Safa, A. S. Fung, and R. Kumar, “Comparative thermal performances of a ground source heat pump and a variable capacity air source heat pump systems for

- sustainable houses," *Appl. Therm. Eng.*, vol. 81, pp. 279–287, Apr. 2015.
- [144] F. Ruiz-Calvo, C. Montagud, A. Cazorla-Marín, and J. M. Corberán, "Development and Experimental Validation of a TRNSYS Dynamic Tool for Design and Energy Optimization of Ground Source Heat Pump Systems," *Energies*, vol. 10, p. 1510, 2017.
- [145] R. Chargui and H. Sammouda, "Modeling of a residential house coupled with a dual source heat pump using TRNSYS software," *Energy Convers. Manag.*, vol. 81, pp. 384–399, 2014.
- [146] G. Bagarella, R. Lazzarin, and M. Noro, "Annual simulation, energy and economic analysis of hybrid heat pump systems for residential buildings," *Appl. Therm. Eng.*, vol. 99, pp. 485–494, Apr. 2016.
- [147] I. Grossi, M. Dongellini, A. Piazzzi, and G. L. Morini, "Dynamic modelling and energy performance analysis of an innovative dual-source heat pump system," *Appl. Therm. Eng.*, vol. 142, pp. 745–759, Sep. 2018.
- [148] A. Zarrella *et al.*, "A double source heat pump: a case study," in *IGSHPA Research Track 2018*, 2018, pp. 390–398.
- [149] G. F. Hundy, A. R. Trott, and T. C. Welch, "Control Systems," in *Refrigeration, Air Conditioning and Heat Pumps*, 5th ed., Butterworth-Heinemann, 2016, pp. 409–419.
- [150] F. Karlsson, "Capacity Control of Residential Heat Pump Heating Systems," Chalmers University of Technology, 2007.
- [151] H. Madani, "Capacity-controlled Ground Source Heat Pump Systems for Swedish single-family dwellings," KTH Royal Institute of Technology, 2012.
- [152] D. Del Col, M. Azzolin, G. Benassi, and M. Mantovan, "Experimental Analysis of Optimal Operation Mode of a Ground Source Heat Pump System," *Energy Procedia*, vol. 45, pp. 1354–1363, Jan. 2014.
- [153] D. Del Col, M. Azzolin, G. Benassi, and M. Mantovan, "Energy efficiency in a ground source heat pump with variable speed drives," *Energy Build.*, vol. 91, pp. 105–114, Mar. 2015.
- [154] K. C. Edwards and D. P. Finn, "Generalised water flow rate control strategy for optimal part load operation of ground source heat pump systems," *Appl. Energy*, vol. 150, pp. 50–60, 2015.
- [155] C. Montagud, J. M. Corberán, and Á. Montero, "In situ optimization methodology for the water circulation pumps frequency of ground source heat pump systems," *Energy Build.*, vol. 68, pp. 42–53, 2014.
- [156] J. Cervera-Vázquez, C. Montagud, and J. M. Corberán, "In situ optimization methodology for the water circulation pumps frequency of ground source heat pump systems: Analysis for multistage heat pump units," *Energy Build.*, vol. 88, pp. 238–247, 2015.
- [157] J. Cervera-Vázquez, C. Montagud, and J. M. Corberán, "In situ optimization methodology for ground source heat pump systems: Upgrade to ensure user comfort," *Energy Build.*, vol. 109, pp. 195–208, 2015.
- [158] A. Cazorla-Marín, C. Montagud, J. M. Corberán, and J. Marchante, "TRNSYS modelling and energy assessment of a dual source heat pump system," in *IX Congreso Ibérico y VII Congreso Iberoamericano de Ciencias y Técnicas del Frío - CYTEF2018*, 2018, p. 1185.
- [159] A. Cazorla-Marín, C. Montagud, J. M. Corberán, and J. Marchante-Avellaneda, "Seasonal performance assessment of a Dual Source Heat Pump system for heating, cooling and domestic hot water production," in *IGSHPA Research Track 2018*, 2018, pp. 180–188.
- [160] J. M. Corberan, J. González, P. Montes, and R. Blasco, "'ART' A computer code to assist the design of refrigeration and A/C equipment," *International Refrigeration and Air Conditioning Conference*. p. 570, 2002.
- [161] SWEPE, "SSP calculation software." 2016.
- [162] T. L. Bergman, A. S. Lavine, F. P. Incropera, and D. P. DeWitt, "Heat Exchangers," in *Fundamentals of heat and mass transfer*, 11th ed., USA: John Wiley & Sons, Inc, 2011,

- pp. 705–765.
- [163] American Society of Heating Refrigeration and Air-conditioning Engineers (ASHRAE), “Service Water Heating,” in *ASHRAE Handbook - HVAC Applications*, Atlanta, GA: ASHRAE, 2015.
 - [164] J. Cervera Vázquez, “Control and energy optimization of ground source heat pump systems for heating and cooling in buildings,” Universitat Politècnica de València, 2016.
 - [165] SEPEMO-Build, “SEasonal PErformance factor and MOnitoring for Heat Pump Systems in the Building Sector. (IEE/08/776/SI2.529222),” 2012. [Online]. Available: <http://sepemo.ehpa.org/>. [Accessed: 23-Feb-2018].
 - [166] CEN, “EN 15251 Indoor environmental input parameters for design and assessment of energy performance of buildings- addressing indoor air quality, thermal environment, lighting and acoustics,” Brussels, 2007.
 - [167] TRANSSOLAR Energietechnik GmbH, “Multizone Building modeling with Type56 and TRNBuild,” in *TRNSYS 16 - A TRaNsient SYstem Simulation program, User manual*, Solar Energy Laboratory, University of Wisconsin-Madison, 2007.
 - [168] IEE, “TABULA “Typology Approach for Building Stock Energy Assessment,”” 2009. [Online]. Available: <http://episcope.eu/iee-project/tabula/>. [Accessed: 28-Feb-2018].
 - [169] Meteotest, “Meteonorm,” 1981. [Online]. Available: <https://meteonorm.com/>. [Accessed: 21-Apr-2019].
 - [170] F. Tinti, S. Kasmaee, M. Elkarmoty, S. Bonduà, and V. Bortolotti, “Suitability Evaluation of Specific Shallow Geothermal Technologies Using a GIS-Based Multi Criteria Decision Analysis Implementing the Analytic Hierarchic Process,” *Energies*, vol. 11, no. 2, pp. 457–478, 2018.
 - [171] European Commission, *Comission delegated regulation (EU) No 811/2013*. 2013.
 - [172] A. Cazorla-marín, C. Montagud, Á. Montero, J. Martos, and J. M. Corberán, “Influence of Different Ground Thermal Properties in a Borehole Heat Exchanger ’ s Performance Using the B2G Dynamic Model,” in *IGSHPA Research Conference Proceedings*, 2017, pp. 192–200.
 - [173] A. Cazorla-marín, F. Ruiz-calvo, Á. Montero, J. Martos, C. Montagud, and J. M. Corberán, “Estimating Ground Thermal Properties of a Borehole Heat Exchanger using the B2G Dynamic Model,” in *European Geothermal Congress 2016*, 2016, p. T-UTES-129.
 - [174] P. Pasquier, “Interpretation of the first hours of a thermal response test using the time derivative of the temperature,” *Appl. Energy*, vol. 213, no. January, pp. 56–75, 2018.

Publications

Publications in peer-reviewed journals

1. J. M. Corberán, [A. Cazorla-Marín](#), J. Marchante-Avellaneda, and C. Montagud, “Dual source heat pump, a high efficiency and cost-effective alternative for heating, cooling and DHW production,” *Int. J. Low-Carbon Technol.*, vol. 13, no. 2, pp. 161–176, 2018.
2. F. Ruiz-Calvo, C. Montagud, [A. Cazorla-Marín](#), and J. M. Corberán, “Development and Experimental Validation of a TRNSYS Dynamic Tool for Design and Energy Optimization of Ground Source Heat Pump Systems,” *Energies*, vol. 10, p. 1510, 2017.

Publications in conference proceedings

1. [A. Cazorla-Marín](#), C. Montagud, J. M. Corberán, F. Tinti, and S. Focaccia, “Upgrade of the B2G dynamic geothermal heat exchanger model: optimal location of the ground nodes,” in *IGSHPA Research Track 2018*, 2018, pp. 20–28.
2. [A. Cazorla-Marín](#), C. Montagud, J. M. Corberán, and J. Marchante-Avellaneda, “Seasonal performance assessment of a Dual Source Heat Pump system for heating , cooling and domestic hot water production,” in *IGSHPA Research Track 2018*, 2018, pp. 180–188.
3. [A. Cazorla-Marín](#), C. Montagud, and J. M. Corberán, “Adaptation of the B2G dynamic model to new borehole heat exchanger coaxial configurations,” in *IX Congreso Ibérico y VII Congreso Iberoamericano de Ciencias y Técnicas del Frío - CYTEF2018*, 2018, p. 1186.
4. [A. Cazorla-Marín](#), C. Montagud, J. M. Corberán, and J. Marchante, “TRNSYS modelling and energy assessment of a dual source heat pump system,” in *IX Congreso Ibérico y VII Congreso Iberoamericano de Ciencias y Técnicas del Frío - CYTEF2018*, 2018, p. 1185.
5. H. Witte; [A. Cazorla-Marín](#); J. M. Corberán. (2018). “An efficient borehole heat exchanger model for the analysis of transient thermal response: comparison with some existing models,” in *14th International Conference on Energy Storage (EnerSTOCK2018)*, 2018.
6. [A. Cazorla-Marín](#), C. Montagud, J. M. Corberán, and J. Acuña, “Modeling of a coaxial Borehole Heat Exchanger and experimental validation,” in *10º Congreso Internacional Ingeniería Termodinámica 10CNIT*, 2017, pp. 162–163.
7. J. M. Corberán, [A. Cazorla-Marín](#), J. Marchante-Avellaneda, C. Montagud, X. Masip, “Modelling and energy analysis of a dual source heat pump system in an office building,” in *16th International Conference on Sustainable Energy Technologies (SET 2017)*, 2017.
8. [A. Cazorla-Marín](#), C. Montagud, H. Witte, R. Hylkema, and J. Corberan, “Modelling and Experimental Validation of a Novel Co-axial Spiral Borehole Heat Exchanger,” in *IGSHPA Research Conference Proceedings*, 2017, pp. 212–220.

9. A. Cazorla-marín, C. Montagud, Á. Montero, J. Martos, and J. M. Corberán, "Influence of Different Ground Thermal Properties in a Borehole Heat Exchanger ' s Performance Using the B2G Dynamic Model," in *IGSHPA Research Conference Proceedings*, 2017, pp. 192–200.

10. J. Cervera-Vázquez, C. Montagud, J. M. Corberán; A. Cazorla-Marín, "Optimal control and operation of a GSHP system for heating and cooling in an office building," in *IGSHPA Research Conference Proceedings*, 2017, pp. 160–168.

11. C. Montagud, A. Cazorla-Marín, J. M. Corberán, "Análisis experimental de once años de funcionamiento de una instalación de bomba de calor geotérmica en un edificio de oficinas en la Universidad Politécnica de Valencia," in *V Congreso de Energía Geotérmica en la Edificación y la Industria (GeoEner 2017)*, 2017, pp 67-76.

12. A. Cazorla-marín, F. Ruiz-calvo, Á. Montero, J. Martos, C. Montagud, and J. M. Corberán, "Estimating Ground Thermal Properties of a Borehole Heat Exchanger using the B2G Dynamic Model," in *European Geothermal Congress 2016*, 2016, p. T-UTES-129.

13. A. Cazorla-marín, F. Ruiz-calvo, H. Witte, C. Montagud, and J. M. Corberán, "An Innovative Co-Axial Spiral Borehole Heat Exchanger Dynamic Model," in *European Geothermal Congress 2016*, 2016, p. T-UTES-127.

14. A. Cazorla-Marín, F. Ruiz-Calvo, C. Montagud, J. M. Corberán, "Nuevo Modelo Dinámico de Un Intercambiador Enterrado en Trnsys: Adaptación del Modelo B2G a Largos Periodos de Simulación," in *VIII Congreso Ibérico y VI Congreso Iberoamericano de Ciencias y Técnicas del Frío (CYTEF 2016)*, 2016.

Appendixes

A. Computer Codes of the TRNSYS types

A.1. Coaxial B2G model

A.1.1. Parameters, inputs and outputs of the B2G coaxial TRNSYS type

Table A. 1. Parameters of the B2G coaxial TRNSYS type

n	Model Parameters	Units	Min.	Max.
1	Number of vertical nodes	-	0	400
2	BHE depth	m	0	Inf.
3	Inner diameter of inner pipe	m	0	Inf.
4	Outer diameter of inner pipe	m	0	Inf.
5	Inner diameter of outer pipe	m	0	Inf.
6	Outer diameter of outer pipe	m	0	Inf.
7	Borehole diameter	m	0	Inf.
8	Inner pipe conductivity	W/(m·K)	0	Inf.
9	Outer pipe conductivity	W/(m·K)	0	Inf.
10	Initial temperature	°C	-Inf.	Inf.
11	Monopropylene glycol percentage	%	0	100
12	Logical unit input file 1	-	40	60
13	Inner tube roughness	mm	0	Inf.
14	Outer tube roughness	mm	0	Inf.
15	Logical unit input file 2	-	40	60
16	Spiral rib angle	degrees	-90	90
17	Number of ribs	-	0	Inf.
18	Convection enhancement factor	-	0	Inf.

Table A. 2. Inputs of the B2G coaxial TRNSYS type

n	Model Inputs	Units	Min.	Max.
1	Inlet temperature	°C	-Inf	Inf.
2	Flow rate	kg/hr	0	Inf.
3	Reset temperature	°C	-Inf	Inf.
4	Ground conductivity	W/(m·K)	0	Inf.
5	Ground volumetric capacity	kJ/(m ³ ·K)	0	Inf.
6	Heat injection period	hr	0	Inf.
7	Borehole radius	m	0	Inf.
8	Reset signal	-	0	1
9	Sense of fluid	-	-1	1

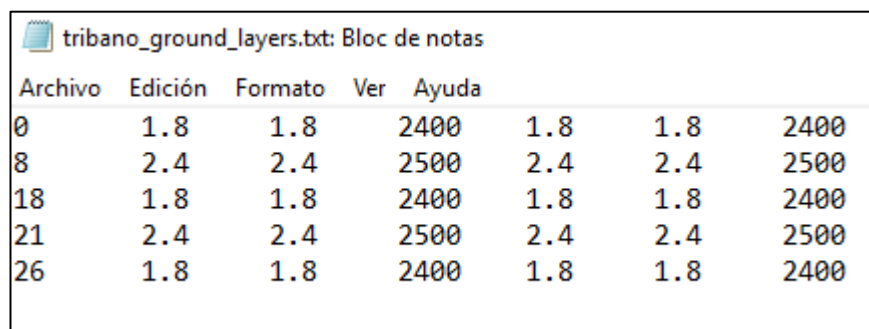
Table A. 3. Outputs of the B2G coaxial TRNSYS type

n	Model Outputs	Units	Min.	Max.
1	Outlet temperature	°C	-Inf	120
2	Flow rate	kg/hr	0	Inf.
3	Grout temperature	°C	-Inf	Inf.
4	Ground node 1 temperature	°C	-Inf	Inf.
5	Ground node 2 temperature	°C	-Inf	Inf.
6	Reynolds number inner pipe	-	0	Inf.
7	Reynolds number outer pipe	-	0	Inf.
8	Pressure drop inner pipe	Pa	0	Inf.
9	Pressure drop outer pipe	Pa	0	Inf.
10	Number of ground layers	-	0	Inf.
11	Heat transfer to fluid	kJ/hr	0	Inf.

A.1.2. External files B2G coaxial TRNSYS type

Two external files are necessary in the B2G coaxial TRNSYS type as text files (.txt):

- Definition of the ground layers and their thermal properties. The values are introduced in this order, separated by tabulations:
 - Top depth of the ground layer (m).
 - Radial thermal conductivity of the grout (W/(m·K)).
 - Vertical thermal conductivity of the grout (W/(m·K)).
 - Grout thermal volumetric capacity (kJ/(m³·K)).
 - Radial thermal conductivity of the ground (W/(m·K)).
 - Vertical thermal conductivity of the ground (W/(m·K)).
 - Ground thermal volumetric capacity (kJ/(m³·K)).



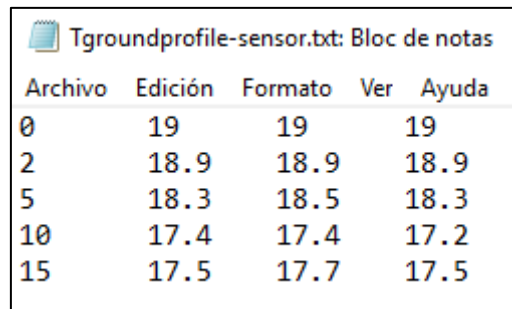
tribano_ground_layers.txt: Bloc de notas

Archivo	Edición	Formato	Ver	Ayuda
0	1.8	1.8	2400	1.8 1.8 2400
8	2.4	2.4	2500	2.4 2.4 2500
18	1.8	1.8	2400	1.8 1.8 2400
21	2.4	2.4	2500	2.4 2.4 2500
26	1.8	1.8	2400	1.8 1.8 2400

Figure A. 1. External file 1: definition of the ground layers thermal properties

- Definition of the ground nodes initial temperatures at different depths. The values are introduced in this order, separated by tabulations:
 - Top depth of the ground layer (m).

- Initial temperature of ground node 1 (°C).
- Initial temperature of ground node 2 (°C).
- Initial temperature of the undisturbed ground node (°C).



Archivo	Edición	Formato	Ver	Ayuda
0	19	19	19	
2	18.9	18.9	18.9	
5	18.3	18.5	18.3	
10	17.4	17.4	17.2	
15	17.5	17.7	17.5	

Figure A. 2. External file 2: definition of the initial ground nodes temperatures

A.1.3. B2G coaxial FROTRAN code

```

SUBROUTINE TYPE428 (TIME,XIN,OUT,T,DTDT,PAR,INFO,ICNTRL,*)
C*****
C Object: B2G - Coaxial-spiral
C Simulation Studio Model: B2G - Coaxial-spiral
C
C Author: IIE
C Editor:
C Date:December 21, 2015
C (Comments and routine interface generated by TRNSYS Studio)
C*****
C TRNSYS access functions (allow to access TIME etc.)
  USE TrnsysConstants
  USE TrnsysFunctions
C-----
C   REQUIRED BY THE MULTI-DLL VERSION OF TRNSYS
  !DEC$ATTRIBUTES DLLEXPORT :: TYPE428           !SET THE CORRECT
TYPE NUMBER HERE
C-----
C TRNSYS DECLARATIONS
  IMPLICIT NONE !REQUIRES THE USER TO DEFINE ALL VARIABLES BEFORE USING THEM
DOUBLE PRECISION XIN !THE ARRAY FROM WHICH THE INPUTS TO THIS TYPE WILL BE RETRIEVED
DOUBLE PRECISION OUT !THE ARRAY WHICH WILL BE USED TO STORE THE OUTPUTS FROM THIS
TYPE
DOUBLE PRECISION TIME !THE CURRENT SIMULATION TIME - YOU MAY USE THIS VARIABLE BUT DO
NOT SET IT!
DOUBLE PRECISION PAR !THE ARRAY FROM WHICH THE PARAMETERS FOR THIS TYPE WILL BE
RETRIEVED
DOUBLE PRECISION STORED !THE STORAGE ARRAY FOR HOLDING VARIABLES FROM TIMESTEP TO
TIMESTEP
DOUBLE PRECISION T !AN ARRAY CONTAINING THE RESULTS FROM THE DIFFERENTIAL
EQUATION SOLVER
DOUBLE PRECISION DTDT !AN ARRAY CONTAINING THE DERIVATIVES TO BE PASSED TO THE
DIFF.EQ. SOLVER
INTEGER*4 INFO(15) !THE INFO ARRAY STORES AND PASSES VALUABLE INFORMATION
TO AND FROM THIS TYPE
INTEGER*4 NP,NI,NOUT,ND !VARIABLES FOR THE MAXIMUM NUMBER OF
PARAMETERS,INPUTS,OUTPUTS AND DERIVATIVES
INTEGER*4 NPAR,NIN,NDER !VARIABLES FOR THE CORRECT NUMBER OF
PARAMETERS,INPUTS,OUTPUTS AND DERIVATIVES
INTEGER*4 IUNIT,IType !THE UNIT NUMBER AND TYPE NUMBER FOR THIS COMPONENT
INTEGER*4 ICNTRL!AN ARRAY FOR HOLDING VALUES OF CONTROL FUNCTIONS WITH THE NEW SOLVER
INTEGER*4 NSTORED!THE NUMBER OF VARIABLES THAT WILL BE PASSED INTO AND OUT OF STORAGE
CHARACTER*3 OCHECK!AN ARRAY TO BE FILLED WITH THE CORRECT VARIABLE TYPES FOR THE
OUTPUTS

```

```

CHARACTER*3 YCHECK!AN ARRAY TO BE FILLED WITH THE CORRECT VARIABLE TYPES FOR THE
INPUTS
C-----
C   USER DECLARATIONS - SET THE MAXIMUM NUMBER OF PARAMETERS (NP), INPUTS (NI),
C   OUTPUTS (NOUT), AND DERIVATIVES (ND) THAT MAY BE SUPPLIED FOR THIS TYPE
   PARAMETER (NP=18,NI=9,NOUT=11,ND=0)
   integer MAXPOINTS
   PARAMETER (MAXPOINTS=500)
C-----
C   REQUIRED TRNSYS DIMENSIONS
   DIMENSION XIN(NI),OUT(NOUT),PAR(NP),YCHECK(NI),OCHECK(NOUT),
   1  STORED(MAXPOINTS*10+1),T(ND),DTDT(ND)
   INTEGER NITEMS
C-----
C   ADD DECLARATIONS AND DEFINITIONS FOR THE USER-VARIABLES HERE
   double precision time0,delt
   double precision Tc(MAXPOINTS), Tcini(MAXPOINTS)
   double precision Te(MAXPOINTS), Teini(MAXPOINTS)
   double precision Tb(MAXPOINTS), Tbini(MAXPOINTS)
   double precision Tg1(MAXPOINTS), Tg1ini(MAXPOINTS)
   double precision Tg2(MAXPOINTS), Tg2ini(MAXPOINTS)
   double precision Tug(MAXPOINTS), Tugini(MAXPOINTS)
   double precision Tci(MAXPOINTS)
   double precision Tei(MAXPOINTS)
   double precision Teo(MAXPOINTS)
   double precision Tgr(MAXPOINTS)
   double precision Tbw(MAXPOINTS)
   double precision qeb(MAXPOINTS)
   double precision qbg1(MAXPOINTS)
C   OUTPUTS
   DOUBLE PRECISION Tout
C   PARAMETERS
   integer N !nodes
   DOUBLE PRECISION L !length
   DOUBLE PRECISION Dci !central inner diameter
   DOUBLE PRECISION Dco !central outer diameter
   DOUBLE PRECISION Dei !external inner diameter
   DOUBLE PRECISION Deo
   DOUBLE PRECISION D_b
   DOUBLE PRECISION alpha !spiral angle
   integer ribs !spiral ribs
   DOUBLE PRECISION Tinit !initial temperature
   double precision x !percentage of propylene glycol
   double precision b !h convección annulus-bh
C   INPUTS
   DOUBLE PRECISION Tin !inlet temperature
   DOUBLE PRECISION flow !flow rate
   DOUBLE PRECISION Tres !reset temperature
   DOUBLE PRECISION D_1,D_2,D_3
   integer res,res1 !reset
   integer sense !sense=1: from annulus to inner; sense=-1: opposite sense
   double precision UAvg2,UAvg1,UAvb !vertical conduction resistance between nodes
in the ground
   double precision UAab_e,UAbg_e,UAgg_e !axial conduction in the end of the bhe
   double precision hconvc,Nu,Nu2,Pr,mu,k,Re,efe,ro_c,cp_c !inner
   double precision Deq,Seq,hconvec,hconveb,ro_e,cp_e, Leq !annulus
   double precision xm,ym,y !propylene glycol and water mixture
   double precision dx,dt,vc,ve,dt_ac,dTin !B2G
   integer i
   DOUBLE PRECISION UAci_ei,UAeo_gr,UAb1,UAb2,UAbg,UAgg
   double precision UAconv_c,UAconv_ec,UAconv_eb
   double precision UAce,UAb1,UAbg1
   DOUBLE PRECISION Cb !borehole_capacity
   DOUBLE PRECISION Cg1,Cg2 !ground_capacity
   DOUBLE PRECISION k_p_c,k_p_e,R_b,D_1_m,D_2_m,D_x
   DOUBLE PRECISION Reo,Rb_e,R_1_e,R_2_e

```

```

double precision Rb_e_m,R_1_e_m,R_2_e_m
double precision k_b_m,k_g_m,pl
double precision UAsurf_g1,UAsurf_g2,UAsurf_b
double precision UAext_b,UAext_g1,UAext_g2
double precision Ts_b,Ts_g1,Ts_g2,Tsini_b,Tsini_g1,Tsini_g2
double precision Teff_b,Teff_g1,Teff_g2
double precision Teffini_b,Teffini_g1,Teffini_g2
double precision hsurf_b,hsurf_g1,hsurf_g2
double precision Tdb,Tsky,radiat,Twb
double precision absorptance, emissivity
double precision UAg_u,UAg_u_e,R_3_e
integer lu_file,xtmp,ytmp,ztmp,itmp,jtmp,ktmp,ltmp,nl,layer
DOUBLE PRECISION, allocatable :: z,k_b_r,k_b_v,c_b,k_g_r,k_g_v,c_g
DIMENSION z(:),k_b_r(:),k_b_v(:),c_b(:),k_g_r(:),k_g_v(:),c_g(:)
double precision a_D
double precision Nu1,fg,k1,Re2,Nu3,Nulam,Nuturb
double precision sup_e,sup_c,m_e,C_c,C_e
double precision deltaP_ann,deltaP_in,f_D,v,zeta
double precision rough_in,rough_ann
double precision Tb_av, Tg1_av,Tg2_av
double precision k_pen,c_pen,t_pen,rb_pen,Fob
C-----INITIAL TEMPERATURE-----
DOUBLE PRECISION, allocatable :: z2,T0_g1,T0_g2,T0_ug
DIMENSION z2(:),T0_g1(:),T0_g2(:), T0_ug(:)
integer lu_file2, xtmp2,ytmp2,nl2,i2,ztmp2, wtmp2
C-----
double precision, parameter :: pi=3.14159265358979323
double precision, parameter :: Boltz=5.67*10**(-8)
real, parameter :: g=9.81

C GET GLOBAL TRNSYS SIMULATION VARIABLES
TIME0=getSimulationStartTime()
DELT=getSimulationTimeStep()
C-----
C READ IN THE VALUES OF THE PARAMETERS IN SEQUENTIAL ORDER
N=PAR(1)
L=PAR(2)
Dci=PAR(3)
Dco=PAR(4)
Dei=PAR(5)
Deo=PAR(6)
D_b=PAR(7)
k_p_c=PAR(8)
k_p_e=PAR(9)
Tinit=PAR(10)
x=PAR(11)
lu_file=JFIX(PAR(12)+0.1)
rough_in=PAR(13)
rough_ann=PAR(14)
lu_file2=JFIX(PAR(15)+0.1)
alpha=PAR(16)/180*pi
ribs=PAR(17)
b=PAR(18)
C-----
C RETRIEVE THE CURRENT VALUES OF THE INPUTS TO THIS MODEL FROM THE XIN ARRAY IN
SEQUENTIAL ORDER
Tin=XIN(1)
flow=XIN(2)
Tres=XIN(3)
k_pen=XIN(4)
c_pen=XIN(5)
t_pen=XIN(6)
rb_pen=XIN(7)
res=XIN(8)
sense=XIN(9)

```

```

        IUNIT=INFO(1)
        ITYPE=INFO(2)
C-----
C  SET THE VERSION INFORMATION FOR TRNSYS
C  IF(INFO(7).EQ.-2) THEN
        INFO(12)=16
        OPEN (unit=15,
& File = 'D:\Tc.txt',status = 'unknown')
        OPEN (unit=13,
& File = 'D:\Te.txt',status = 'unknown')
        OPEN (unit=11,
& File = 'D:\Tb.txt',status = 'unknown')
        OPEN (unit=7,
& File = 'D:\Tg1.txt',status = 'unknown')
        OPEN (unit=5,
& File = 'D:\Tg2.txt',status = 'unknown')
        RETURN 1
    ENDIF
C-----
C  DO ALL THE VERY LAST CALL OF THE SIMULATION MANIPULATIONS HERE
C  IF (INFO(8).EQ.-1) THEN
        CLOSE (15)
        CLOSE (13)
        CLOSE (11)
        CLOSE (7)
        CLOSE (5)
        CLOSE (lu_file)
        close(lu_file2)
        deallocate (z)
        deallocate (k_b_r)
        deallocate (k_b_v)
        deallocate (c_b)
        deallocate (k_g_r)
        deallocate (k_g_v)
        deallocate (c_g)
        deallocate (z2)
        deallocate (T0_g1)
        deallocate (T0_g2)
        deallocate (T0_ug)
        RETURN 1
    ENDIF
C-----
C  PERFORM ANY 'AFTER-ITERATION' MANIPULATIONS THAT ARE REQUIRED HERE
C  e.g. save variables to storage array for the next timestep
C  IF (INFO(13).GT.0) THEN
        NITEMS=N*12+12+7*OUT(10)+1
        CALL getStorageVars(STORED,NITEMS,INFO)
        STORED(12*N+1)=STORED(12*N+7)
        STORED(12*N+2)=STORED(12*N+8)
        STORED(12*N+3)=STORED(12*N+9)
        STORED(12*N+4)=STORED(12*N+10)
        STORED(12*N+5)=STORED(12*N+11)
        STORED(12*N+6)=STORED(12*N+12)
        DO i=1,N
            STORED(i)=STORED(6*N+i)
            STORED(N+i)=STORED(7*N+i)
            STORED(2*N+i)=STORED(8*N+i)
            STORED(3*N+i)=STORED(9*N+i)
            STORED(4*N+i)=STORED(10*N+i)
            STORED(5*N+i)=STORED(11*N+i)
            WRITE(15,100,advance='no') STORED(i)
            WRITE(13,100,advance='no') STORED(N+i)
            WRITE(11,100,advance='no') STORED(2*N+i)
            WRITE(7,100,advance='no') STORED(3*N+i)
            WRITE(5,100,advance='no') STORED(4*N+i)
        ENDDO
    ENDIF

```

```

        STORED(NITEMS)=res
        WRITE(15,110)
        WRITE(13,110)
        WRITE(11,110)
        WRITE(7,110)
        WRITE(5,110)

        CALL setStorageVars(STORED,NITEMS,INFO)

        RETURN 1
    ENDIF
100  format(f9.6,1x)
110  format(i3)
120  format(f7.5)
C-----
C   DO ALL THE VERY FIRST CALL OF THE SIMULATION MANIPULATIONS HERE
    IF (INFO(7).EQ.-1) THEN
C       SET SOME INFO ARRAY VARIABLES TO TELL THE TRNSYS ENGINE HOW THIS TYPE IS TO
WORK
        INFO(6)=NOUT
        INFO(9)=1
        INFO(10)=0 !STORAGE FOR VERSION 16 HAS BEEN CHANGED
C       IN SOME CASES, THE NUMBER OF VARIABLES MAY DEPEND ON THE VALUE OF PARAMETERS
TO THIS MODEL....
        NIN=NI
        NPAR=NP
        NDER=ND
C       CALL THE TYPE CHECK SUBROUTINE TO COMPARE WHAT THIS COMPONENT REQUIRES TO
WHAT IS SUPPLIED IN
C       THE TRNSYS INPUT FILE
        CALL TYPECK(1,INFO,NIN,NPAR,NDER)
C       SET THE NUMBER OF STORAGE SPOTS NEEDED FOR THIS COMPONENT
        n1=0
        rewind(lu_file)
        do while (.not.eof(lu_file))
            read (lu_file, *) xtmp, ytmp, ztmp, itmp, jtmp, ktmp,ltmp
            n1 = n1 + 1
        end do

        rewind(lu_file)
        n1=n1+1
        allocate (z(n1))
        allocate (k_b_r(n1))
        allocate (k_b_v(n1))
        allocate (c_b(n1))
        allocate (k_g_r(n1))
        allocate (k_g_v(n1))
        allocate (c_g(n1))

        do i=1, (n1-1)

            read(lu_file, *) z(i),k_b_r(i),k_b_v(i),c_b(i),k_g_r(i),
            k_g_v(i),c_g(i)
        end do
        if (z(n1-1).gt.L) then
            z(n1)=z(n1-1)
        else
            z(n1)=L+10
        endif
C-----Initial Temperature-----
        n12=0
        rewind(lu_file2)
        do while (.not.eof(lu_file2))
            read (lu_file2, *) xtmp2, ytmp2, ztmp2, wtmp2
            n12 = n12 + 1
        end do

```

```

rewind(lu_file2)
n12=n12+1
allocate (z2(n12))
allocate (T0_g1(n12))
allocate (T0_g2(n12))
allocate (T0_ug(n12))

do i=1, (n12-1)
  read(lu_file2, *) z2(i),T0_g1(i), T0_g2(i),T0_ug(i)
end do

if (z2(n12-1).gt.L) then
  z2(n12)=z2(n12-1)
else
  z2(n12)=L+10
endif
C-----
OUT(10)=n1
NITEMS=N*12+12+7*n1+1
CALL setStorageSize(NITEMS,INFO)

DO i=1,n1
  STORED(12*N+12+i)=z(i)
  STORED(12*N+12+n1+i)=k_b_r(i)
  STORED(12*N+12+2*n1+i)=k_b_v(i)
  STORED(12*N+12+3*n1+i)=c_b(i)
  STORED(12*N+12+4*n1+i)=k_g_r(i)
  STORED(12*N+12+5*n1+i)=k_g_v(i)
  STORED(12*N+12+6*n1+i)=c_g(i)
ENDDO
C-----INITIAL TEMPERATURE-----
dx=L/(N-1)

DO i=1,N
  do i2=1,n12-1
    if (((i-1)*dx .ge. z2(i2)) .and.
    ((i-1)*dx .lt. z2(i2+1))) then
      STORED(3*N+i)=T0_g1(i2)
      STORED(4*N+i)=T0_g2(i2)
      STORED(5*N+i)=T0_ug(i2)
    endif
  enddo
enddo

C-----
CALL setStorageVars(STORED,NITEMS,INFO)
C RETURN TO THE CALLING PROGRAM
RETURN 1
ENDIF
C-----
C DO ALL OF THE INITIAL TIMESTEP MANIPULATIONS HERE - THERE ARE NO ITERATIONS AT
THE INITIAL TIME
IF (TIME .LT. (getSimulationStartTime() +
getSimulationTimeStep()/2.D0)) THEN
C SET THE UNIT NUMBER FOR FUTURE CALLS
IUNIT=INFO(1)
ITYPE=INFO(2)
C PERFORM ANY REQUIRED CALCULATIONS TO SET THE INITIAL VALUES OF THE OUTPUTS
HERE
Tout=Tinit
OUT(1)=Tout
OUT(2)=flow
OUT(3)=Tout
OUT(4)=Tout
OUT(5)=Tout

```



```

C      PERFORM ANY REQUIRED CALCULATIONS TO SET THE INITIAL STORAGE VARIABLES HERE
      NITEMS=N*12+12+7*n1+1
      DO i=1,3*N      !Tcini, Teini, Tbini
        STORED(i)=Tinit
      ENDDO
      STORED(N*12+1)=Tinit
      STORED(N*12+2)=Tinit
      STORED(N*12+3)=Tinit
      STORED(N*12+4)=Tdb
      STORED(N*12+5)=Tdb
      STORED(N*12+6)=Tdb
      STORED(NITEMS)=1

C      PUT THE STORED ARRAY IN THE GLOBAL STORED ARRAY
      CALL setStorageVars(STORED,NITEMS,INFO)
C      RETURN TO THE CALLING PROGRAM
      RETURN 1
    ENDIF

-----
C      *** ITS AN ITERATIVE CALL TO THIS COMPONENT ***
-----

      n1=OUT(10)
      NITEMS=N*12+12+7*n1+1
      CALL getStorageVars(STORED,NITEMS,INFO)
      DO i=1,N
        Tcini(i)=STORED(i)
        Teini(i)=STORED(N+i)
        Tbini(i)=STORED(2*N+i)
        Tg1ini(i)=STORED(3*N+i)
        Tg2ini(i)=STORED(4*N+i)
        Tugini(i)=STORED(5*N+i)
      ENDDO
      Tsini_b=STORED(12*N+1)
      Tsini_g1=STORED(12*N+2)
      Tsini_g2=STORED(12*N+3)
      Teffini_b=STORED(12*N+4)
      Teffini_g1=STORED(12*N+5)
      Teffini_g2=STORED(12*N+6)
      DO i=1,n1
        z(i)=STORED(12*N+12+i)
        k_b_r(i)=STORED(12*N+12+n1+i)
        k_b_v(i)=STORED(12*N+12+2*n1+i)
        c_b(i)=STORED(12*N+12+3*n1+i)
        k_g_r(i)=STORED(12*N+12+4*n1+i)
        k_g_v(i)=STORED(12*N+12+5*n1+i)
        c_g(i)=STORED(12*N+12+6*n1+i)
      ENDDO
      res1=STORED(NITEMS)

      if(res.gt.res1)then
        DO i=1,N
          Tg1(i)=Tres
          Tg1ini(i)=Tres
          Tg2(i)=Tres
          Tg2ini(i)=Tres
          Tugini(i)=Tres
          Tug(i)=Tres
          Tb(i)=Tres
          Tbini(i)=Tres
          Tc(i)=Tres
          Te(i)=Tres
          Tcini(i)=Tres
          Teini(i)=Tres
        ENDDO
        if (sense .gt.0) then
          Tcini(1)=Tres

```

```

else
    Teini(1)=Tres
endif
Tsini_b=Tres
Ts_b=Tres
Tsini_g1=Tres
Ts_g1=Tres
Tsini_g2=Tres
Ts_g2=Tres
endif
C-----
C *** PERFORM ALL THE CALCULATION HERE FOR THIS MODEL. ***
C-----
C          ADD YOUR COMPONENT EQUATIONS HERE; BASICALLY THE EQUATIONS THAT WILL
CALCULATE THE OUTPUTS BASED ON THE PARAMETERS AND THE INPUTS. REFER TO CHAPTER 3 OF
THE TRNSYS VOLUME 1 MANUAL FOR DETAILED INFORMATION ON WRITING TRNSYS COMPONENTS.
C *****GEOMETRIC PARAMETERS*****
sup_e=pi/4*(Dei*Dei-Dco*Dco)
sup_c=pi/4*Dci*Dci
dx=L/(N-1)
C *****
m_e=flow/3600
C *****
C * Convective heat transfer coefficient *
C *****
C Water and Propylene glycol mixture (0%<=X<=60% ; Tfreeze<y<100°C)
xm=30.7031
ym=32.7083
C FLUID PROPERTIES EXTERNAL
y=(Teini(1)+Teini(N))/2

mu=exp(6.837e-1-3.045e-2*(y-ym)+2.525e-4*(y-ym)**2-1.399e-6*(y-ym)
**3+3.328e-2*(x-xm)-3.984e-4*(x-xm)*(y-ym)+4.332e-6*(x-xm)*
(y-ym)**2-1.860e-8*(x-xm)*(y-ym)**3+5.453e-5*(x-xm)**2-8.600e-8*
(x-xm)**2*(y-ym)-1.593e-8*(x-xm)**2*(y-ym)**2-4.465e-11*(x-xm)**2*
(y-ym)**3-3.900e-6*(x-xm)**3+1.054e-7*(x-xm)**3*(y-ym)-1.589e-9*
(x-xm)**3*(y-ym)**2-1.587e-8*(x-xm)**4+4.475e-10*(x-xm)**4*
(y-ym)+3.564e-9*(x-xm)**5)/1000 !Pa·s

k=4.513e-1+7.955e-4*(y-ym)+3.482e-8*(y-ym)**2-5.966e-9*(y-ym)
**3-4.795e-3*(x-xm)-1.678e-5*(x-xm)*(y-ym)+8.941e-8*(x-xm)*
(y-ym)**2+1.493e-10*(x-xm)*(y-ym)**3+2.076e-5*(x-xm)**2+1.563e-7*
(x-xm)**2*(y-ym)-4.615e-9*(x-xm)**2*(y-ym)**2+9.897e-12*(x-xm)**2
*(y-ym)**3-9.083e-8*(x-xm)**3-2.518e-9*(x-xm)**3*(y-ym)+6.543e-11*
(x-xm)**3*(y-ym)**2-5.952e-10*(x-xm)**4-3.605e-11*(x-xm)**4*(y-ym)
+2.104e-11*(x-xm)**5 !W/(m·K)

cp_e=(3.882e3+2.699e0*(y-ym)-1.659e-3*(y-ym)**2-1.032e-5*(y-ym)
**3-1.304e1*(x-xm)+5.070e-2*(x-xm)*(y-ym)-4.752e-5*(x-xm)*(y-ym)
**2+1.522e-6*(x-xm)*(y-ym)**3-1.598e-1*(x-xm)**2+9.534e-5*(x-xm)
**2*(y-ym)+1.167e-5*(x-xm)**2*(y-ym)**2-4.870e-8*(x-xm)**2*(y-ym)
**3+3.539e-4*(x-xm)**3+3.102e-5*(x-xm)**3*(y-ym)-2.950e-7*(x-xm)
**3*(y-ym)**2+5.000e-5*(x-xm)**4-7.135e-7*(x-xm)**4*(y-ym)-
4.959e-7*(x-xm)**5)/1000 !kJ/(kg·K)

ro_e=1.018e3-5.406e-1*(y-ym)-2.666e-3*(y-ym)**2+1.347e-5*(y-ym)
**3+7.604e-1*(x-xm)-9.450e-3*(x-xm)*(y-ym)+5.541e-5*(x-xm)*(y-ym)
**2-1.343e-7*(x-xm)*(y-ym)**3-2.498e-3*(x-xm)**2+2.700e-5*(x-xm)
**2*(y-ym)-4.018e-7*(x-xm)**2*(y-ym)**2+3.376e-9*(x-xm)**2*(y-ym)
**3-1.550e-4*(x-xm)**3+2.829e-6*(x-xm)**3*(y-ym)-7.175e-9*(x-xm)
**3*(y-ym)**2-1.131e-6*(x-xm)**4-2.221e-8*(x-xm)**4*(y-ym)+
2.342e-8*(x-xm)**5 !kg/m^3

Pr=mu*cp_e*1000/k
C-----ANNULUS-----
C SPIRAL

```

```

IF (vanes.gt.0) then
  Seq=pi/vanes*sin(alpha)*(Dei+Dco)/2*(Dei-Dco)/2
  Deq=4*Seq/(pi/vanes*sin(alpha)*(Dei+Dco)+(Dei-Dco))
  Leq=L/sin(alpha)
  Re=flow/(3600*vanes)*Deq/(Seq*mu)
if (flow .lt. 200) then
  hconvec = 50
else
  if (Re .lt. 2300) then
    Nu2=1.615*(Re*Pr*Deq/Leq)**(1.0/3)
    Nu=(49.371+(Nu2-0.7)**3)**(1.0/3)
  else
    if(Re .gt. 10000) then
      efe=(1.8*log10(Re)-1.5)**(-2.0)
      Nu=(efe/8)*Re*Pr/(1+12.7*(efe/8)**0.5*(Pr**(2.0/3)-1))*
        (1+(Deq/Leq)**(2.0/3))
    else
      Nu2=1.615*(2300*Pr*Deq/Leq)**(1.0/3)
      Nu=((0.0308/8)*10000*Pr/(1+12.7*(0.0308/8)**0.5*
        (Pr**(2.0/3)-1))*(1+(Deq/Leq)**(2.0/3)))-
        (49.371+(Nu2-0.7)**3.0)**(1.0/3)/(10000-2300)
      *(Re-2300)+(49.371+(Nu2-0.7)**3)**(1.0/3)
    endif
  endif
  hconvec=Nu*k/Deq
  hconvec=b*hconvec!enhancement coefficient
endif

ELSE
C COAXIAL STANDARD
Leq=L
a_D=Dco/Dei
Deq=Dei-Dco
Re=m_e*4/(pi*mu*(Dei+Dco))
v=m_e/(ro_e*sup_e)
zeta=(((Dei/2)-(Dco/2))**2*((Dei/2)**2-(Dco/2)**2))/
  (((Dei/2)**4-(Dco/2)**4-((Dei/2)**2-(Dco/2)**2)**2/(log(Dei/Dco)))

if (Re .lt. 10) then
  hconvec = 50
else
  if (Re .lt. 2300) then !laminar flow
    Nu1=3.66+1.2*a_D**0.5
    fg=1.615*(1+0.14*a_D**(1.0/3))
    Nu2=fg*(Re*Pr*Deq/Leq)**(1.0/3)
    Nu3=(2/(1+22*Pr))**(1.0/6)*(Re*Pr*Deq/Leq)**0.5
    Nu=(Nu1**3+Nu2**3+Nu3**3)**(1.0/3)
  else
    if(Re .gt. 10000) then
      Re2=Re*((1+a_D**2)*log(a_D)+(1-a_D**2))/
        ((1-a_D**2)*log(a_D))
      efe=(1.8*log10(Re2)-1.5)**(-2.0)
      k1=1.07+900/Re-0.63/(1+10*Pr)
      Nu=(efe/8)*Re*Pr/(k1+12.7*(efe/8)**0.5*(Pr**(2.0/3)-1))
        *(1+(Deq/Leq)**(2.0/3))*(0.9-0.15*a_D**0.6)
    else
      Nu1=3.66+1.2*a_D**0.5
      fg=1.615*(1+0.14*a_D**(1.0/3))
      Nu2=fg*(2300*Pr*Deq/Leq)**(1.0/3)
      Nu3=(2/(1+22*Pr))**(1.0/6)*(2300*Pr*Deq/Leq)**0.5
      Nu1am=(Nu1**3+Nu2**3+Nu3**3)**(1.0/3)

      Re2=10000*((1+a_D**2)*log(a_D)+(1-a_D**2))/
        ((1-a_D**2)*log(a_D))
      efe=(1.8*log10(Re2)-1.5)**(-2.0)

```

```

        k1=1.07+900/10000-0.63/(1+10*Pr)
        Nuturb=(efe/8)*10000*Pr/(k1+12.7*(efe/8)**0.5*
        (Pr**(2.0/3)-1))*(1+(Deq/Leq)**(2.0/3))*
        (0.9-0.15*a_D**0.6)
        Nu=(10000-Re)/7700.0*Nulam+(Re-2300)/7700.0*Nuturb
    endif
endif
hconveb=Nu*k/Deq
hconvec=hconveb

f_D=8*((8/Re*zeta)**12+((2.457*log(((7/Re*zeta)**0.9
+0.27*rough_ann/Deq*zeta)**(-1))))**16
+(37530/Re*zeta)**16)**(-1.5))**(1.0/12)

deltaP_ann=f_D*Leq*v*v*ro_e/(Deq*2)
out(9)=deltaP_ann
endif

ENDIF
out(7)=Re

```

C FLUID PROPERTIES CENTRAL

```

y=(Tcini(1)+Tcini(N))/2
mu=exp(6.837e-1-3.045e-2*(y-ym)+2.525e-4*(y-ym)**2-1.399e-6*(y-ym)
**3+3.328e-2*(x-xm)-3.984e-4*(x-xm)*(y-ym)+4.332e-6*(x-xm)*
(y-ym)**2-1.860e-8*(x-xm)*(y-ym)**3+5.453e-5*(x-xm)**2-8.600e-8*
(x-xm)**2*(y-ym)-1.593e-8*(x-xm)**2*(y-ym)**2-4.465e-11*(x-xm)**2*
(y-ym)**3-3.900e-6*(x-xm)**3+1.054e-7*(x-xm)**3*(y-ym)-1.589e-9*
(x-xm)**3*(y-ym)**2-1.587e-8*(x-xm)**4+4.475e-10*(x-xm)**4*
(y-ym)+3.564e-9*(x-xm)**5)/1000

k=4.513e-1+7.955e-4*(y-ym)+3.482e-8*(y-ym)**2-5.966e-9*(y-ym)
**3-4.795e-3*(x-xm)-1.678e-5*(x-xm)*(y-ym)+8.941e-8*(x-xm)*
(y-ym)**2+1.493e-10*(x-xm)*(y-ym)**3+2.076e-5*(x-xm)**2+1.563e-7*
(x-xm)**2*(y-ym)-4.615e-9*(x-xm)**2*(y-ym)**2+9.897e-12*(x-xm)**2
*(y-ym)**3-9.083e-8*(x-xm)**3-2.518e-9*(x-xm)**3*(y-ym)+6.543e-11*
(x-xm)**3*(y-ym)**2-5.952e-10*(x-xm)**4-3.605e-11*(x-xm)**4*(y-ym)
+2.104e-11*(x-xm)**5

cp_c=(3.882e3+2.699e0*(y-ym)-1.659e-3*(y-ym)**2-1.032e-5*(y-ym)
**3-1.304e1*(x-xm)+5.070e-2*(x-xm)*(y-ym)-4.752e-5*(x-xm)*(y-ym)
**2+1.522e-6*(x-xm)*(y-ym)**3-1.598e-1*(x-xm)**2+9.534e-5*(x-xm)
**2*(y-ym)+1.167e-5*(x-xm)**2*(y-ym)**2-4.870e-8*(x-xm)**2*(y-ym)
**3+3.539e-4*(x-xm)**3+3.102e-5*(x-xm)**3*(y-ym)-2.950e-7*(x-xm)
**3*(y-ym)**2+5.000e-5*(x-xm)**4-7.135e-7*(x-xm)**4*(y-ym)-
4.959e-7*(x-xm)**5)/1000

ro_c=1.018e3-5.406e-1*(y-ym)-2.666e-3*(y-ym)**2+1.347e-5*(y-ym)
**3+7.604e-1*(x-xm)-9.450e-3*(x-xm)*(y-ym)+5.541e-5*(x-xm)*(y-ym)
**2-1.343e-7*(x-xm)*(y-ym)**3-2.498e-3*(x-xm)**2+2.700e-5*(x-xm)
**2*(y-ym)-4.018e-7*(x-xm)**2*(y-ym)**2+3.376e-9*(x-xm)**2*(y-ym)
**3-1.550e-4*(x-xm)**3+2.829e-6*(x-xm)**3*(y-ym)-7.175e-9*(x-xm)
**3*(y-ym)**2-1.131e-6*(x-xm)**4-2.221e-8*(x-xm)**4*(y-ym)+
2.342e-8*(x-xm)**5

Pr=mu*cp_c*1000/k
Re=m_e*4/(pi*Dci*mu)
v=m_e/(ro_c*sup_c)
if (Re .lt. 10) then
    hconvc = 50
else
    if (Re .lt. 2300) then
        Nu2=1.615*(Re*Pr*Dci/L)**(1.0/3)
        Nu=(49.371+(Nu2-0.7)**3)**(1.0/3)
    else
        if(Re .gt. 10000) then

```

```

        efe=(1.8*log10(Re)-1.5)**(-2.0)
        Nu=(efe/8)*Re*Pr/(1+12.7*(efe/8)**0.5*(Pr**(2.0/3)-1))*
        (1+(Dci/L)**(2.0/3))
    else
        Nu2=1.615*(2300*Pr*Dci/L)**(1.0/3)
        Nu=((0.0308/8)*1000*Pr/(1+12.7*(0.0308/8)**0.5*
        (Pr**(2.0/3)-1))*(1+(Dci/L)**(2.0/3)))-
        (49.371+(Nu2-0.7)**3.0)**(1.0/3))/(1000-2300)
        *(Re-2300)+(49.371+(Nu2-0.7)**3)**(1.0/3)
    endif
endif
hconvc=Nu*k/Dci
endif
f_D=8*((8/Re)**12+((2.457*log(((7/Re)**0.9+0.27*rough_in/Dci)
**(-1)))**16+(37530/Re)**16)**(-1.5))**(1.0/12)

deltaP_in=f_D*L*v*v*ro_c/(Dci*2)
out(8)=deltaP_in
OUT(6)=Re
C *****
C * Calculation *
C *****
C-----Resistances between nodes-----
Fob=k_pen/c_pen/1000.0*t_pen*3600.0/(rb_pen**2.0)
D_1=(0.976793695+0.611235719*Fob**0.420103213)*rb_pen*2
D_2=(0.926304847+1.416714074*Fob**0.451363605)*rb_pen*2
D_3=(0.767002847+2.312548693*Fob**0.466673669)*rb_pen*2
R_b=D_b/2
D_1_m=0.5*(D_1+D_b)
D_2_m=0.5*(D_2+D_1)
D_x=(D_b+Deo)/2
Reo=Deo/2
C_e=ro_e*cp_e*1000*sup_e*dx
C_c=ro_c*cp_c*1000*sup_c*dx
UAconv_eb=hconvec*pi*Dei*dx
UAconv_c=hconvc*pi*Dci*dx
UAci_ei=(2*pi*k_p_c*dx)/log(Dco/Dci)
UAconv_ec=hconvec*pi*Dco*dx
UAeo_gr=(2*pi*k_p_e*dx)/log(Deo/Dei)
UAce=1/(1/UAconv_c+1/UAci_ei+1/UAconv_ec)
C Thermal network
if(flow .le. 0) flow=0
vc=sense*m_e/(ro_c*sup_c)
ve=sense*m_e/(ro_e*sup_e)
dt=min(abs(dx/vc*0.99),abs(dx/ve*0.99))
DELT=DELT*3600
if(DELT .LT. dt) then
dt=DELT
endif
dt_ac=0
if (sense .gt.0) then
dTin=(Tin-Teini(1))/DELT
else
dTin=(Tin-Tcini(1))/DELT
endif
do while(dt_ac .LT. DELT)
layer=1
C-----Thermal resistances calculation in each layer-----
UAb1=(2*pi*k_b_r(layer)*dx)/log(D_x/Deo)
UAb2=(2*pi*k_b_r(layer)*dx)/log(D_b/D_x)
UAbg=(2*pi*k_g_r(layer)*dx)/log(D_1_m/D_b)
UAgg=(2*pi*k_g_r(layer)*dx)/log(D_2_m/D_1_m)
UAgu=(2*pi*k_g_r(layer)*dx)/log(D_3/D_2_m)
Cg1=pi/4*(D_1**2-D_b**2)*dx*c_g(layer)*1000
Cg2=pi/4*(D_2**2-D_1**2)*dx*c_g(layer)*1000
Cb=pi/4*(D_b**2-Deo**2)*c_b(layer)*dx*1000

```

C Vertical conduction resistance in the ground

```

UAvg2=pi/4*(D_2**2-D_1**2)*k_g_v(layer)/dx
UAvg1=pi/4*(D_1**2-D_b**2)*k_g_v(layer)/dx
UAvb=pi/4*(D_b**2-Deo**2)*k_b_v(layer)/dx

```

```

C-----
UAeb=1/(1/UAconv_eb+1/UAeo_gr+1/UAAb1)
UAbg1=1/(1/UAb2+1/UAbg)
if (sense .gt.0) then
  Te(1)=dTin*dt+Teini(1)
  Tc(1)=Tcini(1)-vc*dt/dx*(Tcini(1)-Tcini(2))
  -UAce/C_c*dt*(Tcini(1)-Teini(1))
else
  Tc(1)=dTin*dt+Tcini(1)
  Te(1)=Teini(1)+ve*dt/dx*(Teini(1)-Teini(2))-dt/C_e*(UAce*
  (Teini(1)-Tcini(1))+UAeb*(Teini(1)-Tbini(1)))
endif
Tb(1)=Tbini(1)+dt/Cb*(UAeb*(Teini(1)-Tbini(1))
-UAbg1*(Tbini(1)-Tg1ini(1))+UAvb*
(Tbini(2)-Tbini(1)))

Tg1(1)=Tg1ini(1)+dt/Cg1*(UAbg1*(Tbini(1)-Tg1ini(1))+
-UAgg*(Tg1ini(1)-Tg2ini(1))+UAvg1*
(Tg1ini(2)-Tg1ini(1)))

Tg2(1)=Tg2ini(1)+dt/Cg2*(UAgg*(Tg1ini(1)-Tg2ini(1))
+UAvg2*(Tg2ini(2)-Tg2ini(1))+UAgv*(Tugini(1)-Tg2ini(1)))

Tug(1)=Tugini(1)
qeb(1)=UAeb*(Tb(1)-Te(1))/dx
qbg1(1)=UAbg1*(Tg1(1)-Tb(1))/dx

Tci(1)=(Te(1)*1/((1/UAci_ei)+(1/UAconv_ec))+Tc(1)*UAconv_c)/
(UAconv_c+1/((1/UAci_ei)+(1/UAconv_ec)))
Tei(1)=(Tc(1)*1/((1/UAci_ei)+(1/UAconv_c))+Te(1)*UAconv_ec)/
(UAconv_ec+1/((1/UAci_ei)+(1/UAconv_c)))

Teo(1)=(Tb(1)*1/((1/UAb1)+(1/UAeo_gr))+Te(1)*UAconv_eb)/
(UAconv_eb+1/((1/UAb1)+(1/UAeo_gr)))
Tgr(1)=(Te(1)*1/((1/UAconv_eb)+(1/UAeo_gr))+Tb(1)*UAb1)/
(UAb1+1/((1/UAconv_eb)+(1/UAeo_gr)))

Tbw(1)=(Tb(1)*UAb2+Tg1(1)*UAbg)/
(UAb2+UAbg)

DO i=2,(N-1)

```

```

  if ((i*dx).gt.(z(layer+1))) then

```

```

    layer=layer+1
    pl=(i*dx-z(layer))/dx

```

C -----Thermal resistances calculation in each layer-----

```

  UAb1=(2*pi*(pl*k_b_r(layer)+(1-pl)*k_b_r(layer-1))*dx)
  /log(D_x/Deo)
  UAb2=(2*pi*(pl*k_b_r(layer)+(1-pl)*k_b_r(layer-1))*dx)
  /log(D_b/D_x)
  UAbg=(2*pi*(pl*k_g_r(layer)+(1-pl)*k_g_r(layer-1))*dx)
  /log(D_1_m/D_b)
  UAgg=(2*pi*(pl*k_g_r(layer)+(1-pl)*k_g_r(layer-1))*dx)
  /log(D_2_m/D_1_m)
  UAgv=(2*pi*(pl*k_g_r(layer)+(1-pl)*k_g_r(layer-1))*dx)
  /log(D_3/D_2_m)

  Cg1=pi/4*(D_1**2-D_b**2)*dx*(pl*c_g(layer)+(1-pl)*
  c_g(layer-1))*1000
  Cg2=pi/4*(D_2**2-D_1**2)*dx*(pl*c_g(layer)+(1-pl)*
  c_g(layer-1))*1000
  Cb=pi/4*(D_b**2-Deo**2)*(pl*c_b(layer)+(1-pl)*

```

```

.      c_b(layer-1))*dx*1000
C      Vertical conduction resistance in the ground
      UAvg2=pi/4*(D_2**2-D_1**2)*
.      (p1*k_g_v(layer)+(1-p1)*k_g_v(layer-1))/dx
      UAvg1=pi/4*(D_1**2-D_b**2)*
.      (p1*k_g_v(layer)+(1-p1)*k_g_v(layer-1))/dx
      UAvb=pi/4*(D_b**2-Deo**2)*
.      (p1*k_b_v(layer)+(1-p1)*k_b_v(layer-1))/dx
C      -----
      else
C      -----Thermal resistances calculation in each layer-----
      UAb1=(2*pi*k_b_r(layer)*dx)/log(D_x/Deo)
      UAb2=(2*pi*k_b_r(layer)*dx)/log(D_b/D_x)
      UAbg=(2*pi*k_g_r(layer)*dx)/log(D_1_m/D_b)
      UAgg=(2*pi*k_g_r(layer)*dx)/log(D_2_m/D_1_m)
      UAgu=(2*pi*k_g_r(layer)*dx)/log(D_3/D_2_m)
      Cg1=pi/4*(D_1**2-D_b**2)*dx*c_g(layer)*1000
      Cg2=pi/4*(D_2**2-D_1**2)*dx*c_g(layer)*1000
      Cb=pi/4*(D_b**2-Deo**2)*c_b(layer)*dx*1000
C      Vertical conduction resistance in the ground
      UAvg2=pi/4*(D_2**2-D_1**2)*k_g_v(layer)/dx
      UAvg1=pi/4*(D_1**2-D_b**2)*k_g_v(layer)/dx
      UAvb=pi/4*(D_b**2-Deo**2)*k_b_v(layer)/dx
C      -----
      endif

      UAeb=1/(1/UAconv_eb+1/UAeo_gr+1/UAb1)
      UAbg=1/(1/UAb2+1/UAbg)

      Tc(i)=Tcini(i)+dt*vc/(2*dx)*((Tcini(i+1)-Tcini(i-1))
.      +vc*dt/dx*(Tcini(i+1)-2*Tcini(i)+Tcini(i-1)))
      -UAce/C_c*dt*(Tcini(i)-Teini(i))

      Te(i)=Teini(i)-dt*ve/(2*dx)*((Teini(i+1)-Teini(i-1))
.      -ve*dt/dx*(Teini(i+1)-2*Teini(i)+Teini(i-1)))-dt/C_e*(UAce*
.      (Teini(i)-Tcini(i))+UAeb*(Teini(i)-Tbini(i)))

      Tb(i)=Tbini(i)+dt/Cb*(UAeb*
.      (Teini(i)-Tbini(i))-UAbg1*(Tbini(i)-Tg1ini(i))+UAvb*
.      (Tbini(i-1)-Tbini(i))+UAvb*(Tbini(i+1)-Tbini(i)))

      Tg1(i)=Tg1ini(i)+dt/Cg1*(UAbg1*(Tbini(i)-Tg1ini(i))-UAgg*
.      (Tg1ini(i)-Tg2ini(i))+UAvg1*
.      (Tg1ini(i-1)-Tg1ini(i))+UAvg1*(Tg1ini(i+1)-Tg1ini(i)))

      Tg2(i)=Tg2ini(i)+dt/Cg2*(UAgg*(Tg1ini(i)-Tg2ini(i))+UAvg2*
.      (Tg2ini(i-1)-Tg2ini(i))+UAvg2*(Tg2ini(i+1)-Tg2ini(i))
.      +UAgu*(Tugini(i)-Tg2ini(i)))

      Tug(i)=Tugini(i)

      qeb(i)=UAeb*(Tb(i)-Te(i))/dx
      qbg1(i)=UAbg1*(Tg1(i)-Tb(i))/dx

      Tci(i)=(Te(i)*1/((1/UAci_ei)+(1/UAconv_ec))+Tc(i)*UAconv_c)/
.      (UAconv_c+1/((1/UAci_ei)+(1/UAconv_ec)))

      Tei(i)=(Tc(i)*1/((1/UAci_ei)+(1/UAconv_c))+Te(i)*UAconv_ec)/
.      (UAconv_ec+1/((1/UAci_ei)+(1/UAconv_c)))

      Teo(i)=(Tb(i)*1/((1/UAb1)+(1/UAeo_gr))+Te(i)*UAconv_eb)/
.      (UAconv_eb+1/((1/UAb1)+(1/UAeo_gr)))

      Tgr(i)=(Te(i)*1/((1/UAconv_eb)+(1/UAeo_gr))+Tb(i)*UAb1)/
.      (UAb1+1/((1/UAconv_eb)+(1/UAeo_gr)))

```

```

        Tbw(i)=(Tb(i)*UAb2+Tg1(i)*UAbg)/
        (UAb2+UAbg)
    .
ENDDO
    if ((N*dx).gt.(z(layer+1))) then
        layer=layer+1
    endif
C-----Thermal resistances calculation in each layer-----
    Cg1=pi/4*(D_1**2-D_b**2)*dx*c_g(layer)*1000
    Cg2=pi/4*(D_2**2-D_1**2)*dx*c_g(layer)*1000
    Cb=pi/4*(D_b**2-Deo**2)*c_b(layer)*dx*1000
C    Vertical conduction resistance in the ground
    UAvg2=pi/4*(D_2**2-D_1**2)*k_g_v(layer)/dx
    UAvg1=pi/4*(D_1**2-D_b**2)*k_g_v(layer)/dx
    UAvb=pi/4*(D_b**2-Deo**2)*k_b_v(layer)/dx
C-----Axial conduction in the end-----
    Rb_e=(0.375*(D_b**2-Deo**2)*dx+Reo**3)**(1.0/3)
    R_1_e=(0.375*(D_1**2-D_b**2)*dx+Rb_e**3)**(1.0/3)
    R_2_e=(0.375*(D_2**2-D_1**2)*dx+R_1_e**3)**(1.0/3)
    R_3_e=(0.375*(D_3**2-D_2**2)*dx+R_1_e**3)**(1.0/3)
    Rb_e_m=0.5*(Rb_e+Reo)
    R_1_e_m=0.5*(R_1_e+Rb_e)
    R_2_e_m=0.5*(R_2_e+R_1_e)
    k_b_m=(k_b_r(layer)+k_b_v(layer))/2
    k_g_m=(k_g_r(layer)+k_g_v(layer))/2
    UAab_e=2*pi/(1/(Reo**2*hconvb)+((1/Reo-1/Rb_e_m)/k_b_m))
    UAbg_e=2*pi/(((1/Rb_e_m-1/Rb_e)/k_b_m)+
    .((1/Rb_e-1/R_1_e_m)/k_g_m))
    UAgg_e=2*pi*k_g_m/(1/R_1_e_m-1/R_2_e_m)
    UAg_u_e=2*pi*k_g_m/(1/R_2_e_m-1/R_3_e)
C-----
C -----in node N no heat transfer between inner&annulus -----
    Tc(N)=Tcini(N)+dt*vc/(2*dx)*((Teini(N)-Tcini(N-1))
    .+vc*dt/dx*(Teini(N)-2*Tcini(N)+Tcini(N-1)))
    .-UAce/(ro_c*(cp_c*1000)*pi*(Dci*Dci)/4*dx)*
    .dt*(Tcini(N)-Teini(N))
    .
    Te(N)=Teini(N)-dt*ve/(2*dx)*((Tcini(N)-Teini(N-1))
    .-ve*dt/dx*(Tcini(N)-2*Teini(N)+Teini(N-1)))
    .-UAce/(ro_e*(cp_e*1000)*pi*(Dei*Dei-Dco*Dco)/4*dx)*
    .dt*(Teini(N)-Tcini(N))
    .-UAeb*dt/(ro_e*(cp_e*1000)*pi*(Dei*Dei-Dco*Dco)/4*dx)*
    .(Teini(N)-Tbini(N))
    .
    Tb(N)=Tbini(N)+dt/Cb*(UAab_e*(Teini(N)-Tbini(N))
    .-UAbg_e*(Tbini(N)-Tg1ini(N))+UAvb*(Tbini(N-1)-Tbini(N)))
    .
    Tg1(N)=Tg1ini(N)+dt/Cg1*(UAbg_e*(Tbini(N)-Tg1ini(N))-UAgg_e*
    .(Tg1ini(N)-Tg2ini(N))+UAvg1*(Tg1ini(N-1)-Tg1ini(N)))
    .
    Tg2(N)=Tg2ini(N)+dt/Cg2*(UAgg_e*(Tg1ini(N)-Tg2ini(N))+UAvg2*
    .(Tg2ini(N-1)-Tg2ini(N))+UAg_u_e*(Tugini(N)-Tg2ini(N)))
    .
    Tug(N)=Tugini(N)
        qeb(N)=UAeb*(Tb(N)-Te(N))/dx
        qbg1(N)=UAbg1*(Tg1(N)-Tb(N))/dx
C-----
    DO i=1,N
        Tcini(i)=Tc(i)
        Teini(i)=Te(i)
        Tbini(i)=Tb(i)
        Tg1ini(i)=Tg1(i)
        Tg2ini(i)=Tg2(i)
        Tugini(i)=Tug(i)
    ENDDO
    Tsini_b=Ts_b

```



```

Tsini_g1=Ts_g1
Tsini_g2=Ts_g2
Teffini_b=Teff_b
Teffini_g1=Teff_g1
Teffini_g2=Teff_g2
dt_ac=dt_ac+dt
  if(dt .GT. (DELT-dt_ac)) then
    dt=DELT-dt_ac
  endif
enddo
if (sense .gt.0) then
  Tout=Tc(1)
else
  Tout=Te(1)
endif
C-----
C  SET THE STORAGE ARRAY AT THE END OF THIS ITERATION IF NECESSARY
NITEMS=N*12+12+7*n1+1
DO i=1,N
  STORED(6*N+i)=Tc(i)
  STORED(7*N+i)=Te(i)
  STORED(8*N+i)=Tb(i)
  STORED(9*N+i)=Tg1(i)
  STORED(10*N+i)=Tg2(i)
  STORED(11*N+i)=Tug(i)
ENDDO
STORED(12*N+7)=Ts_b
STORED(12*N+8)=Ts_g1
STORED(12*N+9)=Ts_g2
STORED(12*N+10)=Teff_b
STORED(12*N+11)=Teff_g1
STORED(12*N+12)=Teff_g2

CALL setStorageVars(STORED,NITEMS,INFO)
C-----
C  SET THE OUTPUTS FROM THIS MODEL IN SEQUENTIAL ORDER AND GET OUT
C      outlet temperature
C          OUT(1)=Tout
C      outlet flow rate
C          OUT(2)=flow
C          OUT(3)=sum(Tb)/N
C          OUT(4)=sum(Tg1)/N
C          OUT(5)=sum(Tg2)/N
C          OUT(11)=-flow*(cp_c+cp_e)*0.5*(Tout-Tin) !kJ/hr
C-----
C  EVERYTHING IS DONE - RETURN FROM THIS SUBROUTINE AND MOVE ON
RETURN 1
END
C-----

```

A.2. Dual Source Heat Pump (DSHP) model

A.2.1. Parameters, inputs and outputs of the DSHP TRNSYS type

Table A. 4. Parameters of the DSHP TRNSYS type

n	Model Parameters	Units	Min.	Max.
1	Minimum frequency	1/S	0	120
2	Starting time period	s	0	Inf.
3	Parasitic losses	W	0	Inf.
4	Scale factor evaporator	-	0	Inf.
5	Scale factor condenser	-	0	Inf.
6	Scale factor compressor consumption	-	0	Inf.
7	Scale factor fan consumption	-	0	Inf.

Table A. 5. Inputs of the DSHP TRNSYS type

n	Model Inputs	Units	Min.	Max.
1	Inlet temperature user	°C	-Inf	Inf.
2	Flow rate user	kg/hr	0	Inf.
3	Inlet temperature ground	°C	-Inf	Inf.
4	Flow rate ground	kg/hr	0	Inf.
5	Inlet temperature DHW	°C	-Inf	Inf.
6	Flow rate DHW	kg/hr	0	Inf.
7	Ambient temperature	°C	-Inf	Inf.
8	Compressor frequency	1/S	0	Inf.
9	Working mode	-	0	11
10	Switch	-	0	1
11	Fan speed	% (base 100)	0	Inf.
12	dT user	delta°C	0	Inf.
13	dT ground	delta°C	0	Inf.
14	dT DHW	delta°C	0	Inf.
15	schedule	-	0	1

Table A. 6. Outputs of the DSHP TRNSYS type

n	Model Outputs	Units	Min.	Max.
1	Outlet temperature user	°C	-Inf	120
2	Flow rate user	kg/hr	0	Inf.
3	Outlet temperature ground	°C	-Inf	Inf.
4	Flow rate ground	kg/hr	0	Inf.
5	Outlet temperature DHW	°C	-Inf	Inf.
6	Flow rate DHW	kg/hr	0	Inf.
7	Heat transfer to user	W	0	Inf.
8	Heat transfer to user	W	0	Inf.
9	Heat transfer to user	W	0	Inf.

n	Model Outputs	Units	Min.	Max.
10	Heat transfer to user	W	0	Inf.
11	Compressor consumption	W	0	Inf.
12	COP	-	0	Inf.
13	switch	-	0	1
14	Compressor frequency	1/S	0	Inf.
15	Starting time	-	0	1
16	Pressure drop user	Pa	0	Inf.
17	Pressure drop ground	Pa	0	Inf.
18	Pressure drop DHW	Pa	0	Inf.
19	Working mode	-	0	11
20	Fan consumption	W	0	Inf.
21	Parasitic losses	W	0	Inf.
22	Fan speed	% (base 100)	0	Inf.

A.2.2. DSHP FROTRAN code

```

SUBROUTINE TYPE427 (TIME,XIN,OUT,T,DTDT,PAR,INFO,ICNTRL,*)
C*****
C TRNSYS access functions (allow to access TIME etc.)
  USE TrnsysConstants
  USE TrnsysFunctions
C-----
C   REQUIRED BY THE MULTI-DLL VERSION OF TRNSYS
  !DEC$ATTRIBUTES DLLEXPORT :: TYPE427 !SET THE CORRECT TYPE NUMBER HERE
C-----
C TRNSYS DECLARATIONS
IMPLICIT NONE !REQUIRES THE USER TO DEFINE ALL VARIABLES BEFORE USING THEM
DOUBLE PRECISION XIN !THE ARRAY FROM WHICH THE INPUTS TO THIS TYPE WILL BE RETRIEVED
DOUBLE PRECISION OUT !THE ARRAY WHICH WILL BE USED TO STORE THE OUTPUTS FROM THIS
TYPE
DOUBLE PRECISION TIME !THE CURRENT SIMULATION TIME - YOU MAY USE THIS VARIABLE BUT DO
NOT SET IT!
DOUBLE PRECISION PAR !THE ARRAY FROM WHICH THE PARAMETERS FOR THIS TYPE WILL BE
RETRIEVED
DOUBLE PRECISION STORED !THE STORAGE ARRAY FOR HOLDING VARIABLES FROM TIMESTEP TO
TIMESTEP
DOUBLE PRECISION T !AN ARRAY CONTAINING THE RESULTS FROM THE DIFFERENTIAL
EQUATION SOLVER
DOUBLE PRECISION DTDT !AN ARRAY CONTAINING THE DERIVATIVES TO BE PASSED TO THE
DIFF.EQ. SOLVER
INTEGER*4 INFO(15) !THE INFO ARRAY STORES AND PASSES VALUABLE INFORMATION TO AND
FROM THIS TYPE
INTEGER*4 NP,NI,NOUT,ND !VARIABLES FOR THE MAXIMUM NUMBER OF
PARAMETERS,INPUTS,OUTPUTS AND DERIVATIVES
INTEGER*4 NPAR,NIN,NDER !VARIABLES FOR THE CORRECT NUMBER OF
PARAMETERS,INPUTS,OUTPUTS AND DERIVATIVES
INTEGER*4 IUNIT,ITYPE !THE UNIT NUMBER AND TYPE NUMBER FOR THIS COMPONENT
INTEGER*4 ICNTRL !AN ARRAY FOR HOLDING VALUES OF CONTROL FUNCTIONS WITH THE NEW SOLVER
INTEGER*4 NSTORED !THE NUMBER OF VARIABLES THAT WILL BE PASSED INTO AND OUT OF STORAGE
CHARACTER*3 OCHECK !AN ARRAY TO BE FILLED WITH THE CORRECT VARIABLE TYPES FOR THE
OUTPUTS
CHARACTER*3 YCHECK !AN ARRAY TO BE FILLED WITH THE CORRECT VARIABLE TYPES FOR THE
INPUTS
C-----
C USER DECLARATIONS - SET THE MAXIMUM NUMBER OF PARAMETERS (NP), INPUTS (NI),
OUTPUTS (NOUT), AND DERIVATIVES (ND) THAT MAY BE SUPPLIED FOR THIS TYPE
PARAMETER (NP=7,NI=15,NOUT=22,ND=0,NSTORED=6)

```

```

C-----
C   REQUIRED TRNSYS DIMENSIONS
C   DIMENSION XIN(NI),OUT(NOUT),PAR(NP),YCHECK(NI),OCHECK(NOUT),
C   I STORED(NSTORED),T(ND),DTDT(ND)
C   INTEGER NITEMS
C-----
C   ADD DECLARATIONS AND DEFINITIONS FOR THE USER-VARIABLES HERE
C   PARAMETERS
C   DOUBLE PRECISION Cp_user,Cp_gr,Cp_DHW,min_freq,length_start
C   double precision effHX,DHW_freq
C   double precision HP_losses, kev,kcond,kcomp,kfan
C   INPUTS
C   double precision Tin_user,m_user,Tin_gr,m_gr,Tin_DHW,m_DHW
C   double precision Tamb,Freq, dT_DHW,dT_user,dT_gr,fan_Freq
C   integer mode,switch,schedule
C   OUTPUTS
C   double precision Tout_user,Tout_gr,Tout_DHW
C   double precision Q_user,Q_gr,Q_air,Q_DHW,POWER,COP
C   double precision dP_user, dP_gr,dP_DHW,fan_power
C   integer starting
C   VARIABLES
C   double precision C0,C1,C2,C3,C4,C5,C6,C7,C8,C9,C10
C   double precision aux,time_start,Tgr_K,Tair_K,Tin_user_K,Tin_DHW_K
C   double precision qHX,m_max,Cmin,Cr,NTU,Atot,Npl !Free-cooling HX
C   double precision Tw_K,Tgl_K,Tdhw_K,T_K,m_min, Tgrini
C   double precision Tei, Tci,dTe,dTc,f_fan,fc
C   integer switch1
C-----
C   READ IN THE VALUES OF THE PARAMETERS IN SEQUENTIAL ORDER
C   min_freq=PAR(1)
C   length_start=PAR(2)
C   HP_losses=PAR(3)
C   kev=PAR(4)
C   kcond=PAR(5)
C   kcomp=PAR(6)
C   kfan=PAR(7)
C-----
C   RETRIEVE THE CURRENT VALUES OF THE INPUTS TO THIS MODEL FROM THE XIN ARRAY IN
C   SEQUENTIAL ORDER
C   Tin_user=XIN(1)
C   m_user=XIN(2)
C   Tin_gr=XIN(3)
C   m_gr=XIN(4)
C   Tin_DHW=XIN(5)
C   m_DHW=XIN(6)
C   Tamb=XIN(7)
C   Freq=XIN(8)
C   mode=XIN(9)
C   switch=XIN(10)
C   fan_Freq=XIN(11)
C   dT_user=XIN(12)
C   dT_gr=XIN(13)
C   dT_DHW=XIN(14)
C   schedule=XIN(15)
C   IUNIT=INFO(1)
C   ITYPE=INFO(2)
C-----
C   SET THE VERSION INFORMATION FOR TRNSYS
C   IF(INFO(7).EQ.-2) THEN
C   INFO(12)=16
C   RETURN 1
C   ENDIF
C-----
C   DO ALL THE VERY LAST CALL OF THE SIMULATION MANIPULATIONS HERE
C   IF (INFO(8).EQ.-1) THEN
C   RETURN 1

```

```

ENDIF
C-----
C PERFORM ANY 'AFTER-ITERATION' MANIPULATIONS THAT ARE REQUIRED HERE
C e.g. save variables to storage array for the next timestep
IF (INFO(13).GT.0) THEN
    NITEMS=6
    CALL getStorageVars(STORED,NITEMS,INFO)
    STORED(1)=STORED(3)
    STORED(2)=STORED(4)
    STORED(5)=STORED(6)
    CALL setStorageVars(STORED,NITEMS,INFO)
    RETURN 1
ENDIF
C-----
C DO ALL THE VERY FIRST CALL OF THE SIMULATION MANIPULATIONS HERE
IF (INFO(7).EQ.-1) THEN
C SET SOME INFO ARRAY VARIABLES TO TELL THE TRNSYS ENGINE HOW THIS TYPE IS TO
WORK
    INFO(6)=NOUT
    INFO(9)=1
    INFO(10)=0 !STORAGE FOR VERSION 16 HAS BEEN CHANGED
C SET THE REQUIRED NUMBER OF INPUTS, PARAMETERS AND DERIVATIVES THAT THE USER
SHOULD SUPPLY IN THE INPUT FILE. IN SOME CASES, THE NUMBER OF VARIABLES MAY DEPEND ON
THE VALUE OF PARAMETERS TO THIS MODEL....
    NIN=NI
    NPAR=NP
    NDER=ND
C CALL THE TYPE CHECK SUBROUTINE TO COMPARE WHAT THIS COMPONENT REQUIRES TO
WHAT IS SUPPLIED IN THE TRNSYS INPUT FILE
    CALL TYPECK(1,INFO,NIN,NPAR,NDER)
C SET THE NUMBER OF STORAGE SPOTS NEEDED FOR THIS COMPONENT
    NITEMS=6
    CALL setStorageSize(NITEMS,INFO)
C RETURN TO THE CALLING PROGRAM
    RETURN 1
ENDIF
C-----
C DO ALL OF THE INITIAL TIMESTEP MANIPULATIONS HERE - THERE ARE NO ITERATIONS AT
THE INITIAL TIME
IF (TIME .LT. (getSimulationStartTime() +
getSimulationTimeStep()/2.D0)) THEN
C SET THE UNIT NUMBER FOR FUTURE CALLS
    IUNIT=INFO(1)
    ITYPE=INFO(2)
C PERFORM ANY REQUIRED CALCULATIONS TO SET THE INITIAL STORAGE VARIABLES HERE
    NITEMS=6
    STORED(1)=0
    STORED(2)=-1
C PUT THE STORED ARRAY IN THE GLOBAL STORED ARRAY
    CALL setStorageVars(STORED,NITEMS,INFO)
C RETURN TO THE CALLING PROGRAM
    RETURN 1
ENDIF
C-----
C RETRIEVE THE VALUES IN THE STORAGE ARRAY FOR THIS ITERATION
NITEMS=6
CALL getStorageVars(STORED,NITEMS,INFO)
switch1=STORED(1)
time_start=STORED(2)
Tgrini=STORED(5)
if (switch.gt.switch1) then !!If the HP has just switched on --> reset the
starting time
    time_start=TIME
endif
C-----
m_max=5000

```

```

m_min=1500
Tgr_K=Tin_gr+273.15
Tair_K=Tamb+273.15
Tin_user_K=Tin_user+273.15
Tin_DHW_K=Tin_DHW+273.15
T_K=Tin_user_K
Cp_user=-1.03024E-04*T_K**3+1.13872E-01*T_K**2
.   -4.10435E+01*T_K+9.02811E+03
T_K=Tgr_K
Cp_gr=2.70720E+00*T_K+3.06317E+03
T_K=Tin_DHW+273.15
Cp_DHW=-1.03024E-04*T_K**3+1.13872E-01*T_K**2
.   -4.10435E+01*T_K+9.02811E+03
if (TIME.lt. (time_start+length_start/3600.0)) then !!If the HP is at the
starting time --> x seconds of working at minimum frequency
    starting=1
    Freq=min_freq
else
    starting=0
endif
if (schedule .eq. 0) then
    Q_user=0
    Q_gr=0
    Q_air=0
    Q_DHW=0
    Tout_user=Tin_user
    Tout_gr=Tin_gr
    Tout_DHW=Tin_DHW
    m_gr=0
    m_DHW=0
    Freq=0
    fan_Freq=0
    HP_losses=0
    COP = 0
    POWER = 0
    mode=0
    fan_power=0
    switch=0
else
C   if((switch .eq. 0) .or. (Freq .eq. 0)) then
        HP OFF
        switch=0
        Freq=0
        Q_user=0
        Q_gr=0
        Q_air=0
        Q_DHW=0
        Tout_user=Tin_user
        Tout_gr=Tin_gr
        Tout_DHW=Tin_DHW
        m_gr=0
        m_DHW=0
        Freq=0
        fan_Freq=0
        COP = 0
        POWER = 0
        fan_power=0
C   else
        HP ON
        SELECT CASE (mode)
        CASE (1) !SUMMER AIR (COOLING)
            Tei=Tin_user_K
            Tci=Tair_K
            dTe=dT_user
            f_fan=fan_freq
            fc=Freq

```

```

!Qev
  C0=5548.6639
  C1=-53.3148098
  C2=11.2676959
  C3=-0.04349628
  C4=0.12469434
  C5=39.9725529
  C6=1.69743716
  C7=-0.14938109
  C8=-0.00488309
Q_user=kev*fc*(C0+C1*Tei+C2*Tci+C3*Tei*Tci+C4*Tei**2+
C5*dTe+C6*f_fan+C7*Tei*dTe+C8*Tci*f_fan)
!COMP. POWER
  C0=-127.154822
  C1=0.00017563
  C2=0.00141202
  C3=2.79421619
  C4=-0.12269678
  C5=-0.00983765
  C6=0.00221971
  C7=-0.00059527
  C8=-1.9351E-08
  C9=-0.00094419
  C10=269.484162
POWER=kcomp*fc*(C0+C1*Tei**2+C2*Tci**2+C3*dTe+C4*f_fan+
C5*Tei*dTe+C6*fc*Tei+C7*fc*Tci+C8*fc**2*Tei*Tci+C9*fc*dTe
+C10*1/fc)
!Qcond
Q_air=Q_user+POWER
! FAN POWER
if (f_fan .gt. 90) then
  fan_power=kfan*672.2
else
  fan_power=kfan*(7.358e-4*f_fan**3+1.730e-2*f_fan**2-
4.805e-2*f_fan)
endif
Q_gr=0
Tout_gr=Tin_gr
m_gr=0
Q_DHW=0
Tout_DHW=Tin_DHW
m_DHW=0
Tout_user=Tin_user-Q_user/(Cp_user*m_user/3600)
CASE (2) !SUMMER GROUND (COOLING)
Tei=Tin_user_K
Tci=Tgr_K
dTe=dT_user
dTc=dT_gr
fc=Freq
!Qcond
  C0=-8701.32225
  C1=-28.1788217
  C2=80.4529982
  C3=-0.28374801
  C4=0.20985578
  C5=228.144306
  C6=-21.2900539
  C7=-0.79871579
  C8=0.06672825
Q_gr=kcond*fc*(C0+C1*Tei+C2*Tci+C3*Tei*Tci+C4*Tei**2+
C5*dTe+C6*dTc+C7*Tei*dTe+C8*Tci*dTc)
!Qev
  C0=-12952.3711
  C1=-28.5363323
  C2=108.876445
  C3=-0.38290305

```

```

C4=0.26260222
C5=289.161125
C6=-13.7202485
C7=-1.00802611
C8=0.03562726
Q_user=kev*fc*(C0+C1*Tei+C2*Tci+C3*Tei*Tci+C4*Tei**2+
C5*dTe+C6*dTc+C7*Tei*dTe+C8*Tci*dTc)
!COMP. POWER
C0=-92.5722913
C1=-0.00019242
C2=0.001223
C3=3.18377725
C4=0.46441926
C5=-0.0106542
C6=0.00339573
C7=-0.00143112
C8=-3.9954E-08
C9=-0.00108513
C10=273.077521

```

```

POWER=kcomp*fc*(C0+C1*Tei**2+C2*Tci**2+C3*dTe+C4*dTc+
C5*Tei*dTe+C6*fc*Tei+C7*fc*Tci+C8*fc**2*Tei*Tci+C9*fc*dTe
+C10*1/fc)
Q_air=0
Q_DHW=0
Tout_DHW=Tin_DHW
m_DHW=0
m_gr=Q_gr/(Cp_gr*dT_gr)*3600
Tout_user=Tin_user-Q_user/(Cp_user*m_user/3600)
Tout_gr=Tin_gr+Q_gr/(Cp_gr*m_gr/3600)
fan_freq=0
fan_power=0

```

CASE (3) !SUMER DHW-USER (Full Recovery - COOLING+DHW)

```

fc=Freq
Tei=Tin_user_K
Tci=Tin_DHW_K
dTe=dT_user
dTc=dT_DHW
!Qcond
C0=4727.74445
C1=-39.3932294
C2=0.39800223
C3=0.00433805
C4=0.07567215
C5=36.599223
C6=1.80988368
C7=-0.13748364
C8=-0.00088536
Q_DHW=kcond*fc*(C0+C1*Tei+C2*Tci+C3*Tei*Tci+C4*Tei**2+
C5*dTe+C6*dTc+C7*Tei*dTe+C8*Tci*dTc)

```

```

!Qev
C0=9218.75393
C1=-56.2904214
C2=-5.57459472
C3=-0.00015899
C4=0.10798941
C5=69.4645259
C6=-4.98338564
C7=-0.25004541
C8=-0.00122863

```

```

Q_user=kev*fc*(C0+C1*Tei+C2*Tci+C3*Tei*Tci+C4*Tei**2+
C5*dTe+C6*dTc+C7*Tei*dTe+C8*Tci*dTc)
!COMP. POWER
C0=-93.740434
C1=-1.477E-05
C2=0.00097976

```



```

C3=1.48684805
C4=0.36001636
C5=-0.00575447
C6=0.00319351
C7=-0.00067524
C8=-4.4724E-08
C9=0.00228534
C10=671.574371
POWER=kcomp*fc*(C0+C1*Tei**2+C2*Tci**2+C3*dTe+C4*dTc+
C5*Tei*dTe+C6*fc*Tei+C7*fc*Tci+C8*fc**2*Tei*Tci+C9*fc*dTe
+C10*1/fc)
Q_gr=0
Tout_gr=Tin_gr
m_gr=0
Q_air=0
fan_Freq=0
fan_power=0
Tout_user=Tin_user-Q_user/(Cp_user*m_user/3600)
m_DHW=Q_DHW/(Cp_DHW*dT_DHW)*3600
Tout_DHW=Tin_DHW+Q_DHW/(Cp_DHW*m_DHW/3600)
if (m_DHW .gt. m_max)then
    m_DHW=m_max
    Tout_DHW=Tin_DHW+Q_DHW/(Cp_DHW*m_DHW/3600)
endif
CASE (4) !WINTER AIR (HEATING)
Tei=Tair_K
Tci=Tin_user_K
f_fan=fan_Freq
dTc=dT_user
fc=Freq
!Qcond
C0=-3184.66564
C1=21.5650334
C2=0.14743705
C3=-0.00211118
C4=-0.03289009
C5=-7.01442131
C6=6.11162847
C7=0.02563198
C8=-0.02267399
Q_user=kcond*fc*(C0+C1*Tei+C2*Tci+C3*Tei*Tci+C4*Tei**2+
C5*f_fan+C6*dTc+C7*Tei*f_fan+C8*Tci*dTc)
!COMP POWER
C0=-131.573666
C1=-0.00028592
C2=0.00158399
C3=-0.11897733
C4=0.54428239
C5=0.00038065
C6=0.00462744
C7=-0.00231015
C8=-3.5512E-08
C9=0.00036949
C10=626.321039
POWER=kcomp*fc*(C0+C1*Tei**2+C2*Tci**2+C3*f_fan+C4*dTc+
C5*Tei*f_fan+C6*fc*Tei+C7*fc*Tci+C8*fc**2*Tei*Tci+
C9*fc*f_fan+C10*1/fc)
!Qev
Q_air=Q_user-POWER
! FAN POWER
if (f_fan .gt. 90) then
    fan_power=kfan*672.2
else
    fan_power=kfan*(7.358e-4*f_fan**3+1.730e-2*f_fan**2-
4.805e-2*f_fan)
endif

```

```

Q_gr=0
Tout_gr=Tin_gr
m_gr=0
Q_DHW=0
Tout_DHW=Tin_DHW
m_DHW=0
Tout_user=Tin_user+Q_user/(Cp_user*m_user/3600)
CASE (5) !WINTER GROUND (HEATING)
Tei=Tgr_K
Tci=Tin_user_K
dTc=dT_user
dTe=dT_gr
fc=Freq
!Qcond
C0=315.387102
C1=-14.1541646
C2=8.12306753
C3=-0.0306254
C4=0.05042289
C5=10.759983
C6=12.8758674
C7=-0.05094912
C8=-0.04422034
Q_user=kcond*fc*(C0+C1*Tei+C2*Tci+C3*Tei*Tci+C4*Tei**2+
C5*dTe+C6*dTc+C7*Tei*dTe+C8*Tci*dTc)
!Qev
C0=1123.47243
C1=-20.7506509
C2=9.25294529
C3=-0.03737603
C4=0.06634914
C5=24.0514959
C6=4.52841435
C7=-0.09822107
C8=-0.01735806
Q_gr=kev*fc*(C0+C1*Tei+C2*Tci+C3*Tei*Tci+C4*Tei**2+
C5*dTe+C6*dTc+C7*Tei*dTe+C8*Tci*dTc)
!COMP POWER
C0=-155.533465
C1=-0.00026428
C2=0.00154132
C3=-2.20033112
C4=0.51940823
C5=0.00778063
C6=0.0060652
C7=-0.00214945
C8=-6.1216E-08
C9=-0.00147175
C10=1122.14039
POWER=kcomp*fc*(C0+C1*Tei**2+C2*Tci**2+C3*dTe+C4*dTc+
C5*Tei*dTe+C6*fc*Tei+C7*fc*Tci+C8*fc**2*Tei*Tci+C9*fc*dTe
+C10*1/fc)
Q_air=0
fan_freq=0
fan_power=0
Q_DHW=0
Tout_DHW=Tin_DHW
m_DHW=0
m_gr=Q_gr/(Cp_gr*dT_gr)*3600
Tout_user=Tin_user+Q_user/(Cp_user*m_user/3600)
Tout_gr=Tin_gr-Q_gr/(Cp_gr*m_gr/3600)
CASE (6) !SUMER DHW-AIR (DHW)
Tei=Tair_K
Tci=Tin_DHW_K
dTc=dT_DHW
f_fan=fan_Freq

```

```

fc=Freq
!Qcond
C0=734.4058104
C1=-8.649674612
C2=1.556511335
C3=-0.007570794
C4=0.025449101
C5=0.220642432
C6=-1.499539531
C7=0
C8=0.002444384
Q_DHW=kcond*fc*(C0+C1*Tei+C2*Tci+C3*Tei*Tci+C4*Tei**2+
C5*f_fan+C6*dTc+C7*Tei*f_fan+C8*Tci*dTc)
!COMP. POWER
C0=-157.15495
C1=-2.5307E-05
C2=0.00163157
C3=0.0541014
C4=0.73631621
C5=-0.00031869
C6=0.00317458
C7=-0.00087445
C8=-4.4816E-08
C9=0.0009091
C10=634.525025
POWER=kcomp*fc*(C0+C1*Tei**2+C2*Tci**2+C3*f_fan+C4*dTc+
C5*Tei*f_fan+C6*fc*Tei+C7*fc*Tci+C8*fc**2*Tei*Tci+
C9*fc*f_fan+C10*1/fc)
!Qev
Q_air=Q_DHW-POWER
! FAN POWER
if (f_fan .gt. 90) then
    fan_power=kfan*672.2
else
    fan_power=kfan*(7.358e-4*f_fan**3+1.730e-2*f_fan**2-
4.805e-2*f_fan)
endif
Q_gr=0
Tout_gr=Tin_gr
m_gr=0
Q_user=0
Tout_user=Tin_user
m_DHW=Q_DHW/(Cp_DHW*dT_DHW)*3600
Tout_DHW=Tin_DHW+Q_DHW/(Cp_DHW*m_DHW/3600)
if (m_DHW .gt. m_max)then
    m_DHW=m_max
    Tout_DHW=Tin_DHW+Q_DHW/(Cp_DHW*m_DHW/3600)
endif
CASE (7) !WINTER DHW-AIR (DHW)
Tei=Tair_K
Tci=Tin_DHW_K
dTc=dT_DHW
f_fan=fan_Freq
fc=Freq
!Qcond
C0=734.4058104
C1=-8.649674612
C2=1.556511335
C3=-0.007570794
C4=0.025449101
C5=0.220642432
C6=-1.499539531
C7=0
C8=0.002444384
Q_DHW=kcond*fc*(C0+C1*Tei+C2*Tci+C3*Tei*Tci+C4*Tei**2+
C5*f_fan+C6*dTc+C7*Tei*f_fan+C8*Tci*dTc)

```

```

!COMP. POWER
  C0=-157.15495
  C1=-2.5307E-05
  C2=0.00163157
  C3=0.0541014
  C4=0.73631621
  C5=-0.00031869
  C6=0.00317458
  C7=-0.00087445
  C8=-4.4816E-08
  C9=0.0009091
  C10=634.525025
POWER=kcomp*fc*(C0+C1*Tei**2+C2*Tci**2+C3*f_fan+C4*dTc+
C5*Tei*f_fan+C6*fc*Tei+C7*fc*Tci+C8*fc**2*Tei*Tci+
C9*fc*f_fan+C10*1/fc)
!Qev
Q_air=Q_DHW-POWER
! FAN POWER
if (f_fan .gt. 90) then
  fan_power=kfan*672.2
else
  fan_power=kfan*(7.358e-4*f_fan**3+1.730e-2*f_fan**2-
4.805e-2*f_fan)
endif
Q_gr=0
Tout_gr=Tin_gr
m_gr=0
Q_user=0
Tout_user=Tin_user
m_DHW=Q_DHW/(Cp_DHW*dT_DHW)*3600
Tout_DHW=Tin_DHW+dT_DHW
if (m_DHW .gt. m_max)then
  m_DHW=m_max
  Tout_DHW=Tin_DHW+Q_DHW/(Cp_DHW*m_DHW/3600)
endif
CASE (8) !SUMMER DHW-GROUND (DHW)
  Tei=Tgr_K
  Tci=Tin_DHW_K
  dTc=dT_DHW
  dTe=dT_gr
  fc=Freq
!Qcond
  C0=2689.3674
  C1=-23.4978132
  C2=1.63008872
  C3=-0.00744301
  C4=0.05344864
  C5=4.16211926
  C6=0.25645894
  C7=-0.02701497
  C8=-0.0029536
Q_DHW=kcond*fc*(C0+C1*Tei+C2*Tci+C3*Tei*Tci+C4*Tei**2+
C5*dTe+C6*dTc+C7*Tei*dTe+C8*Tci*dTc)
!Qev
  C0=3517.35977
  C1=-28.2962942
  C2=1.00105911
  C3=-0.00781375
  C4=0.06259549
  C5=23.2901146
  C6=-0.76934081
  C7=-0.09410266
  C8=-0.00059915
Q_gr=kev*fc*(C0+C1*Tei+C2*Tci+C3*Tei*Tci+C4*Tei**2+
C5*dTe+C6*dTc+C7*Tei*dTe+C8*Tci*dTc)
! COMP.POWER

```

```

C0=-186.6261
C1=-0.00012253
C2=0.00170356
C3=-1.16197193
C4=0.69160847
C5=0.00232537
C6=0.00629516
C7=-0.00200257
C8=-7.6661E-08
C9=0.00602601
C10=1251.15513
POWER=kcomp*fc*(C0+C1*Tei**2+C2*Tci**2+C3*dTe+C4*dTc+
C5*Tei*dTe+C6*fc*Tei+C7*fc*Tci+C8*fc**2*Tei*Tci+C9*fc*dTe
+C10*1/fc)
Q_air=0
fan_freq=0
fan_power=0
m_gr=Q_gr/(Cp_gr*dT_gr)*3600
Tout_gr=Tin_gr-Q_gr/(Cp_gr*m_gr/3600)
Q_user=0
Tout_user=Tin_user
m_DHW=Q_DHW/(Cp_DHW*dT_DHW)*3600
Tout_DHW=Tin_DHW+Q_DHW/(Cp_DHW*m_DHW/3600)
if (m_DHW .gt. m_max)then
    m_DHW=m_max
    Tout_DHW=Tin_DHW+Q_DHW/(Cp_DHW*m_DHW/3600)
endif
CASE (9) !WINTER DHW-GROUND (DHW)
    Tei=Tgr_K
    Tci=Tin_DHW_K
    dTc=dT_DHW
    dTe=dT_gr
    fc=Freq
    !Qcond
        C0=2689.3674
        C1=-23.4978132
        C2=1.63008872
        C3=-0.00744301
        C4=0.05344864
        C5=4.16211926
        C6=0.25645894
        C7=-0.02701497
        C8=-0.0029536
    Q_DHW=kcond*fc*(C0+C1*Tei+C2*Tci+C3*Tei*Tci+C4*Tei**2+
C5*dTe+C6*dTc+C7*Tei*dTe+C8*Tci*dTc)
    !Qev
        C0=3517.35977
        C1=-28.2962942
        C2=1.00105911
        C3=-0.00781375
        C4=0.06259549
        C5=23.2901146
        C6=-0.76934081
        C7=-0.09410266
        C8=-0.00059915
    Q_gr=kev*fc*(C0+C1*Tei+C2*Tci+C3*Tei*Tci+C4*Tei**2+
C5*dTe+C6*dTc+C7*Tei*dTe+C8*Tci*dTc)
    ! COMP.POWER
        C0=-186.6261
        C1=-0.00012253
        C2=0.00170356
        C3=-1.16197193
        C4=0.69160847
        C5=0.00232537
        C6=0.00629516
        C7=-0.00200257

```

```

C8=-7.6661E-08
C9=0.00602601
C10=1251.15513
POWER=kcomp*fc*(C0+C1*Tei**2+C2*Tci**2+C3*dTe+C4*dTc+
C5*Tei*dTe+C6*fc*Tei+C7*fc*Tci+C8*fc**2*Tei*Tci+C9*fc*dTe
+C10*1/fc)
Q_air=0
fan_Freq=0
fan_power=0
m_gr=Q_gr/(Cp_gr*dT_gr)*3600
Tout_gr=Tin_gr-Q_gr/(Cp_gr*m_gr/3600)
Q_user=0
Tout_user=Tin_user
m_DHW=Q_DHW/(Cp_DHW*dT_DHW)*3600
Tout_DHW=Tin_DHW+Q_DHW/(Cp_DHW*m_DHW/3600)
if (m_DHW .gt. m_max)then
    m_DHW=m_max
    Tout_DHW=Tin_DHW+Q_DHW/(Cp_DHW*m_DHW/3600)
endif
CASE(10)    !FREE-COOLING (COOLING)
Atot=0.708
Npl=kev*30
if (m_gr .le. 0) m_gr=2200  !To avoid m_gr=0 in the calculation of
Cmin,NTU...
Cmin=min(m_user/3600*Cp_user,m_gr/3600*Cp_gr)
Cr=Cmin/max(m_user/3600*Cp_user,m_gr/3600*Cp_gr)
NTU=Atot*Npl/((0.396371*(m_gr/3600/Npl)**(-0.55)+
0.132902*(m_user/3600/Npl)**(-0.65))*Cmin/1000)
effHX=(1-exp(-NTU*(1-Cr)))/(1-Cr*exp(-NTU*(1-Cr)))

qHX=effHX*Cmin*(Tin_user-Tin_gr)
Tout_user=Tin_user-qHX/(m_user/3600*Cp_user)
m_gr=qHX/(Cp_gr*dT_gr)*3600
if (m_gr .lt. 100) m_gr=100  !!minimum flow rate
Tout_gr=Tin_gr+qHX/(m_gr/3600*Cp_gr)
Q_user=qHx
Q_gr=m_gr/3600*Cp_gr*(Tout_gr-Tin_gr)
Q_air=0
Q_DHW=0
Tout_DHW=Tin_DHW
m_DHW=0
POWER=0
COP=0
Freq=0
fan_Freq=0
fan_power=0
CASE(11)    !FREE-COOLING + DHW-AIR (COOLING + DHW)
!FREE-COOLING
Atot=0.708
Npl=kev*30
if (m_gr .le. 0) m_gr=2200  !To avoid m_gr=0 in the calculation of
Cmin,NTU...
Cmin=min(m_user/3600*Cp_user,m_gr/3600*Cp_gr)
Cr=Cmin/max(m_user/3600*Cp_user,m_gr/3600*Cp_gr)
NTU=Atot*Npl/((0.396371*(m_gr/3600/Npl)**(-0.55)+
0.132902*(m_user/3600/Npl)**(-0.65))*Cmin)
effHX=(1-exp(-NTU*(1-Cr)))/(1-Cr*exp(-NTU*(1-Cr)))
qHX=effHX*Cmin*(Tin_user-Tin_gr)
Tout_user=Tin_user-qHX/(m_user/3600*Cp_user)
m_gr=qHX/(Cp_gr*dT_gr)*3600
if (m_gr .lt. 100) m_gr=100  !!minimum flow rate
Tout_gr=Tin_gr+qHX/(m_gr/3600*Cp_gr)
Q_user=qHx
Q_gr=m_gr/3600*Cp_gr*(Tout_gr-Tin_gr)
!SUMMER DHW-AIR
Tei=Tair_K

```

```

Tci=Tin_DHW_K
dTc=dT_DHW
f_fan=fan_Freq
fc=Freq
!Qcond
C0=1220.1326
C1=-10.4855873
C2=1.70128747
C3=-0.00805672
C4=0.02599301
C5=-9.47217618
C6=-1.49271298
C7=0.03340391
C8=0.00243155
Q_DHW=kcond*fc*(C0+C1*Tei+C2*Tci+C3*Tei*Tci+C4*Tei**2+
C5*f_fan+C6*dTc+C7*Tei*f_fan+C8*Tci*dTc)
!COMP. POWER
C0=-157.15495
C1=-2.5307E-05
C2=0.00163157
C3=0.0541014
C4=0.73631621
C5=-0.00031869
C6=0.00317458
C7=-0.00087445
C8=-4.4816E-08
C9=0.0009091
C10=634.525025
POWER=kcomp*fc*(C0+C1*Tei**2+C2*Tci**2+C3*f_fan+C4*dTc+
C5*Tei*f_fan+C6*fc*Tei+C7*fc*Tci+C8*fc**2*Tei*Tci+
C9*fc*f_fan+C10*1/fc)
!Qev
Q_air=Q_DHW-POWER
! FAN POWER
if (f_fan .gt. 90) then
    fan_power=kfan*672.2
else
    fan_power=kfan*(7.358e-4*f_fan**3+1.730e-2*f_fan**2-
4.805e-2*f_fan)
endif
m_DHW=Q_DHW/(Cp_DHW*dT_DHW)*3600
Tout_DHW=Tin_DHW+Q_DHW/(Cp_DHW*m_DHW/3600)
if (m_DHW .gt. m_max)then
    m_DHW=m_max
    Tout_DHW=Tin_DHW+Q_DHW/(Cp_DHW*m_DHW/3600)
endif
CASE DEFAULT
Q_user=0
Q_gr=0
Q_air=0
Q_DHW=0
Tout_user=Tin_user
Tout_gr=Tin_gr
Tout_DHW=Tin_DHW
m_gr=0
m_DHW=0
Freq=0
switch=0
fan_Freq=0
COP = 0
POWER = 0
fan_power=0
END SELECT
COP = max(0.0, ((Q_user+Q_DHW)/(POWER+HP_losses+fan_power
+0.0000000001)))
endif

```

```

endif !schedule
C -----dP HEs-----
Tw_K=(Tin_user+Tout_user)/2+273.15
Tgl_K=(Tin_gr+Tout_gr)/2+273.15
Tdhw_K=(Tin_DHW+Tout_DHW)/2+273.15

dP_user=(6440.307372*m_user/3600+84726.7797762*(m_user/3600)**1.9)
.*(exp(-7.1143-2000.3/Tw_K+604550/Tw_K**2)/0.00089469538)**0.18*
.996.7081883/(12.36+8.944*Tw_K-0.02592*Tw_K**2+0.00002346*Tw_K**3)

dP_gr=(2440.7344482826*m_gr/3600+45916.157422236*(m_gr/3600)**1.9)
.*(exp(-2.4901-5142.2/Tgl_K+1221300/Tgl_K**2)/0.00249604995849732)
.**0.18*1021.77434344/(539.5+4.928*Tgl_K-0.01515*Tgl_K**2+
.0.00001357*Tgl_K**3)

dP_DHW=(555.14808585*m_DHW/3600+63817.818321689*(m_DHW/3600)**1.9)
.*(exp(-7.1143-2000.3/Tdhw_K+604550/Tdhw_K**2)/0.00089469538)**0.18
.996.7081883/(12.36+8.944*Tdhw_K-0.02592*Tdhw_K**2+0.00002346*
.Tdhw_K**3)
if ((mode .eq. 10) .or. (mode .eq. 11)) then
    dP_user=11715.13964*(m_user/3600.0)**2.000299848
    dP_gr=11340.35869*(m_user/3600.0)**2.000169156
endif
C -----
C SET THE STORAGE ARRAY AT THE END OF THIS ITERATION IF NECESSARY
NITEMS=6
STORED(3)=switch
STORED(4)=time_start
STORED(6)=Tout_gr
CALL setStorageVars(STORED,NITEMS,INFO)
C -----
C SET THE OUTPUTS FROM THIS MODEL IN SEQUENTIAL ORDER AND GET OUT
OUT(1)=Tout_user
OUT(2)=m_user
OUT(3)=Tout_gr
OUT(4)=m_gr
OUT(5)=Tout_DHW
OUT(6)=m_DHW
OUT(7)=Q_user
OUT(8)=Q_gr
OUT(9)=Q_air
OUT(10)=Q_DHW
OUT(11)=POWER
OUT(12)=COP
OUT(13)=switch
OUT(14)=Freq
OUT(15)=starting
OUT(16)=dP_user
OUT(17)=dP_gr
OUT(18)=dP_DHW
OUT(19)=mode
OUT(20)=fan_power
OUT(21)=HP_losses
out(22)=fan_Freq
C -----
C EVERYTHING IS DONE - RETURN FROM THIS SUBROUTINE AND MOVE ON
RETURN 1
END
C -----

```


A.3. Line Source Approach (LSA) model

A.3.1. Parameters, inputs and outputs of the LSA TRNSYS type

Table A. 7. Parameters of the LSA TRNSYS type

n	Model Parameters	Units	Min	Max.
1	Number of BHEs	-	0	Inf.
2	Depth	m	0	Inf.
3	Borehole diameter	m	0	Inf.
4	Undisturbed ground temperature	°C	-Inf.	Inf.
5	Soil thermal conductivity	W/(m·K)	0	Inf.
6	Soil volumetric capacity	kJ/(m ³ ·K)	0	Inf.
7	Time interval	-	0	Inf.
8	k	-	0	Inf.
9	m	-	0	Inf.
10	Logic unit input file	-	0	Inf.

Table A. 8. Inputs of the LSA TRNSYS type

n	Model Inputs	Units	Min	Max.
1	Heat transfer to ground	W	-Inf.	Inf.
2	step	-	0	1

Table A. 9. Outputs of the LSA TRNSYS type

n	Model Outputs	Units	Min	Max.
1	Ground temperature	°C	-Inf.	Inf.

A.3.2. External file LSA TRNSYS type

The distribution of the BHEs in the field is introduced using a text file (.dat) with the coordinates of each BHE (in meters).

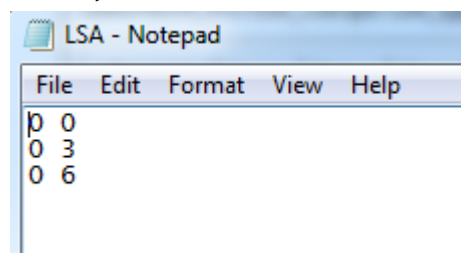


Figure A. 3. External file with the BHEs coordinates in the field (x, y)

A.3.3. LSA FORTRAN code

The subroutines “lsa_hc_atdist” and “read_data02” have not been included in this code of the LSA type, as they have been used from a previous program [138].

The lsa_hc_atdist subroutine calculates the ground temperature increase at a defined distance from the center of the borehole, considering the ground properties, the heat injection step and the duration of it. The Hart and Couvillon algebraic approach of the

infinite line source is used, as explained in section 3.7. The `read_data02` subroutine reads the input file and saves the position of the different BHEs.

```

SUBROUTINE TYPE446 (TIME,XIN,OUT,T,DTDT,PAR,INFO,ICNTRL,*)
!C*****
!C Object: LSA
!C Simulation Studio Model: LSA
!C Author: D. P. Hart and R. Couvillon, HJL Witte (adaptation to Fortran Code), IIE
(adaptation to TRNSYS proforma)
!C Editor:
!C Date:      February 02, 2017 last modified: February 02, 2017
!C
!C (Comments and routine interface generated by TRNSYS Studio)
!C*****
!C  TRNSYS access functions (allow to access TIME etc.)
    USE TrnsysConstants
    USE TrnsysFunctions
    USE mod_lsa1
    USE mod_datautil1
!C-----
!C  REQUIRED BY THE MULTI-DLL VERSION OF TRNSYS
    !DEC$ATTRIBUTES DLLEXPORT :: TYPE446                !SET THE CORRECT
TYPE NUMBER HERE
!C-----
!C  TRNSYS DECLARATIONS
    IMPLICIT NONE !REQUIRES THE USER TO DEFINE ALL VARIABLES BEFORE USING THEM
    DOUBLE PRECISION XIN !THE ARRAY FROM WHICH THE INPUTS TO THIS TYPE WILL BE
RETRIEVED
    DOUBLE PRECISION OUT !THE ARRAY WHICH WILL BE USED TO STORE THE OUTPUTS FROM
THIS TYPE
    DOUBLE PRECISION TIME !THE CURRENT SIMULATION TIME - YOU MAY USE THIS VARIABLE
BUT DO NOT SET IT!
    DOUBLE PRECISION PAR !THE ARRAY FROM WHICH THE PARAMETERS FOR THIS TYPE WILL
BE RETRIEVED
    DOUBLE PRECISION STORED !THE STORAGE ARRAY FOR HOLDING VARIABLES FROM TIMESTEP
TO TIMESTEP
    DOUBLE PRECISION T           !AN ARRAY CONTAINING THE RESULTS FROM THE
DIFFERENTIAL EQUATION SOLVER
    DOUBLE PRECISION DTD T !AN ARRAY CONTAINING THE DERIVATIVES TO BE PASSED TO THE
DIFF.EQ. SOLVER
    INTEGER*4 INFO(15)           !THE INFO ARRAY STORES AND PASSES VALUABLE
INFORMATION TO AND FROM THIS TYPE
    INTEGER*4 NP,NI,NOUT,ND      !VARIABLES FOR THE MAXIMUM NUMBER OF
PARAMETERS,INPUTS,OUTPUTS AND DERIVATIVES
    INTEGER*4 NPAR,NIN,NDER      !VARIABLES FOR THE CORRECT NUMBER OF
PARAMETERS,INPUTS,OUTPUTS AND DERIVATIVES
    INTEGER*4 IUNIT,I TYPE !THE UNIT NUMBER AND TYPE NUMBER FOR THIS COMPONENT
    INTEGER*4 ICNTRL !AN ARRAY FOR HOLDING VALUES OF CONTROL FUNCTIONS WITH THE
NEW SOLVER
    INTEGER*4 NSTORED !THE NUMBER OF VARIABLES THAT WILL BE PASSED INTO AND OUT OF
STORAGE
    INTEGER*4 NSTEP
    CHARACTER*3 OCHECK !AN ARRAY TO BE FILLED WITH THE CORRECT VARIABLE TYPES FOR
THE OUTPUTS
    CHARACTER*3 YCHECK !AN ARRAY TO BE FILLED WITH THE CORRECT VARIABLE TYPES FOR
THE INPUTS
!C-----
!C-----
!C  USER DECLARATIONS - SET THE MAXIMUM NUMBER OF PARAMETERS (NP), INPUTS (NI),
OUTPUTS (NOUT), AND DERIVATIVES (ND) THAT MAY BE SUPPLIED FOR THIS TYPE
    PARAMETER (NP=10,NI=2,NOUT=1,ND=0,NSTEP=2000)
    PARAMETER (NSTORED=(NSTEP*2+6)*2)
!C-----
!C-----
!C  REQUIRED TRNSYS DIMENSIONS

```

```

DIMENSION
XIN(NI),OUT(NOUT),PAR(NP),YCHECK(NI),OCHECK(NOUT),STORED(NSTORED),T(ND),DTDT(ND)
INTEGER NITEMS
!C-----
!C  ADD DECLARATIONS AND DEFINITIONS FOR THE USER-VARIABLES HERE
!C  PARAMETERS
INTEGER :: n_bhes,lu
!C  INPUTS
real :: TIME0, DELT
real :: Q
real, allocatable, dimension(:) :: bhe_dt,Tb_tstep
real, allocatable, dimension(:,:) :: bhe_data,bhe_dist
real :: h,bgdiam,t_ff,soil_k,soil_c
real :: q_step(NSTEP), t_step(NSTEP)
real :: dt, bloque1,bloque2,bloque3,qacc
real :: stime
integer :: status,i,j,k,l,m,n,mode,b,size,n_step,step,step1,kr
character(len=20) :: filename = 'simul.dat'
logical init
!C  GET GLOBAL TRNSYS SIMULATION VARIABLES
TIME0=getSimulationStartTime()
DELT=getSimulationTimeStep()
!C-----
!**** READ IN THE VALUES OF THE PARAMETERS IN SEQUENTIAL ORDER****
n_bhes=PAR(1)      ! number of bhes
h=PAR(2)          ! depth of the BHE
bgdiam=PAR(3)     ! BHE diameter
t_ff=PAR(4)       ! Far field ground temperature
soil_k=PAR(5)     ! Soil thermal conductivity (W/mK)
soil_c=PAR(6)*1000 ! Volumetric soil capacity (kJ/m^3K)
dt=PAR(7)         ! time step for the recalculation of the ground temperature.
If it is set to zero, the input signal "step" says when to recalculate the ground
temperature
kr=PAR(8)         ! Aggregation factor for the load aggregation algorithm
m=PAR(9)          ! Margin value for the load aggregation algorithm
lu=JFIX(PAR(10)+0.1) ! logical unit for the file
!C-----
!****RETRIEVE THE CURRENT VALUES OF THE INPUTS TO THIS MODEL FROM THE XIN ARRAY IN
SEQUENTIAL ORDER****
Q=XIN(1)          ! Heat load injected to the ground (W)
step=XIN(2)       ! Step signal (0 or 1): if dt=0, the LSA type will
recalculate the ground temperature when this signal changes (from 0 to 1 or
viceversa)
IUNIT=INFO(1)
ITYPE=INFO(2)
!C-----
!C  SET THE VERSION INFORMATION FOR TRNSYS
IF(INFO(7).EQ.-2) THEN
INFO(12)=16
RETURN 1
ENDIF
!C-----
!C  DO ALL THE VERY LAST CALL OF THE SIMULATION MANIPULATIONS HERE
IF (INFO(8).EQ.-1) THEN
deallocate(bhe_data)
deallocate(bhe_dist)
deallocate(bhe_dt)
close(lu)
RETURN 1
ENDIF
!C-----
!C  PERFORM ANY 'AFTER-ITERATION' MANIPULATIONS THAT ARE REQUIRED HERE
!C  e.g. save variables to storage array for the next timestep
IF (INFO(13).GT.0) THEN

NITEMS=NSTORED

```

```

        CALL getStorageVars(STORED,NITEMS,INFO)
        DO i=1,(NITEMS/2)
            STORED(i)=STORED((NITEMS/2)+i)
        ENDDO
        CALL setStorageVars(STORED,NITEMS,INFO)
        RETURN 1
    ENDIF
!C-----
!C DO ALL THE VERY FIRST CALL OF THE SIMULATION MANIPULATIONS HERE
!C IF (INFO(7).EQ.-1) THEN
!C SET SOME INFO ARRAY VARIABLES TO TELL THE TRNSYS ENGINE HOW THIS TYPE IS TO WORK
        INFO(6)=NOUT
        INFO(9)=1
        INFO(10)=0 !STORAGE FOR VERSION 16 HAS BEEN CHANGED
!C IN SOME CASES, THE NUMBER OF VARIABLES MAY DEPEND ON THE VALUE OF PARAMETERS
TO THIS MODEL....
        NIN=NI
        NPAR=NP
        NDER=ND
!C CALL THE TYPE CHECK SUBROUTINE TO COMPARE WHAT THIS COMPONENT REQUIRES TO
WHAT IS SUPPLIED IN THE TRNSYS INPUT FILE
        CALL TYPECK(1,INFO,NIN,NPAR,NDER)
!****READ THE COORDINATES OF THE BHEs****
        allocate (bhe_data(INT(n_bhes),2),stat=status)
        bhe_data=0
        call read_data02(bhe_data,filename,lu)
        allocate (bhe_dist(INT(n_bhes),INT(n_bhes)),stat=status)
        allocate(bhe_dt(INT(n_bhes)),stat=status)
        bhe_dt=0
        bhe_dist=0
        do 11 j = 1,n_bhes
            do 12 i = 1,n_bhes
                if(i.ne.j)then
                    bhe_dist(i,j)=sqrt((bhe_data(i,1)-bhe_data(j,1))**2+(bhe_data(i,2)-
bhe_data(j,2))**2)
                else
                    bhe_dist(i,j)=(bgdiam)/2
                endif
            12 continue
        11 continue
!C SET THE NUMBER OF STORAGE SPOTS NEEDED FOR THIS COMPONENT
        NITEMS=NSTORED
        CALL setStorageSize(NITEMS,INFO)
!C RETURN TO THE CALLING PROGRAM
        RETURN 1
    ENDIF
!C-----
!C DO ALL OF THE INITIAL TIMESTEP MANIPULATIONS HERE - THERE ARE NO ITERATIONS AT
THE INITIAL TIME
        IF (TIME .LT. (getSimulationStartTime() + getSimulationTimeStep()/2.D0)) THEN
!C SET THE UNIT NUMBER FOR FUTURE CALLS
            IUNIT=INFO(1)
            ITYPE=INFO(2)
!C PERFORM ANY REQUIRED CALCULATIONS TO SET THE INITIAL VALUES OF THE OUTPUTS HERE
!C ground temperature
            OUT(1)=0
!C PERFORM ANY REQUIRED CALCULATIONS TO SET THE INITIAL STORAGE VARIABLES HERE
            NITEMS=NSTORED
            do i=1,NITEMS
                STORED(i)=0
            enddo
!C PUT THE STORED ARRAY IN THE GLOBAL STORED ARRAY
            CALL setStorageVars(STORED,NITEMS,INFO)
            init= .true.
!C RETURN TO THE CALLING PROGRAM
            RETURN 1

```

```

ENDIF
!C-----
!C *** ITS AN ITERATIVE CALL TO THIS COMPONENT ***
!C-----
!C RETRIEVE THE VALUES IN THE STORAGE ARRAY FOR THIS ITERATION
NITEMS=NSTORED
CALL getStorageVars(STORED,NITEMS,INFO)
DO i=1,NSTEP
    q_step(i)=STORED(i)
    t_step(i)=STORED(NSTEP+1+i)
ENDDO

!C-----
!C *** PERFORM ALL THE CALCULATION HERE FOR THIS MODEL. ***
!C-----
!C ADD YOUR COMPONENT EQUATIONS HERE; BASICALLY THE EQUATIONS THAT WILL
CALCULATE THE OUTPUTS BASED ON THE PARAMETERS AND THE INPUTS. REFER TO CHAPTER 3 OF
THE TRNSYS VOLUME 1 MANUAL FOR DETAILED INFORMATION ON WRITING TRNSYS COMPONENTS.
!***RETRIEVE VALUES FROM THE PREVIOUS TIMESTEP FROM THE STORAGE***
qacc=STORED(NSTEP+1)+Q/h ! The accumulated load in W/m. This load is added up
until it reaches the recalculation time, then is reset to zero
size=STORED(NSTEP*2+2) ! The size of the vectors that store the loads, the
time for each load...
bloque1=STORED(NSTEP*2+3) ! number of type 1 blocks for aggregation of loads
bloque2=STORED(NSTEP*2+4) ! number of type 2 blocks for aggregation of loads
bloque3=STORED(NSTEP*2+5) ! number of type 3 blocks for aggregation of loads
step1=STORED(NSTEP*2+6) ! previous value of the signal step1 (check if changed)
if((dt.eq.0 .and. step.ne.step1))then !If dt=0 and the step signal has
changed, it recalculates the ground temperature and reset the accumulated load
q_step(size+1)=qacc/((TIME-t_step(size+1))/DELT) ! It stores the
accumulated load of the last step in the vector
t_step(size+2)=TIME ! It stores the time at which the recalculation has
been made
qacc=0 ! It resets the accumulated load
size=size+1 !IT increases the size of the vector
bloque1=bloque1+1 !Now there is one type 1 block more
else if(dt.ne.0)then ! If dt is not zero, it recalculates the temperature
when the time is a multiple of the recalculation time step (dt)
if(mod(TIME,dt).eq.0) then
q_step(size+1)=qacc/((TIME-t_step(size+1))/DELT)
t_step(size+2)=TIME
qacc=0
size=size+1
bloque1=bloque1+1
end if
end if
if(bloque1.eq.(kr+m))then ! If the number of type 1 blocks is the the
aggregation factor (kr) plus the margin (m), it assembles the first kr blocks into
one type 2 block.
do i=m,(kr+m-1) !It adds all the loads of the first kr type 1 blocks
multiplied by the time step of each load (W*h/m)
qacc=qacc+q_step(size-i)*(t_step(size-i+1)-t_step(size-i))
enddo
q_step(size-kr-m+1)=qacc/(t_step(size-m+1)-t_step(size-kr-m+1)) !It
changes the q_step array to store the new block 2 load in W/m
do i=0,(m-1)
q_step(size-kr-(m-1-i)+1)=q_step(size-(m-1-i)) ! It sets the values of
q_step and t_step of the margin loads to their new position
t_step(size-kr-(m-1-i)+1)=t_step(size-(m-1-i))
enddo
t_step(size-kr+2)=t_step(size+1)
size=size-kr+1 !It decreases the size of the array because kr loads
have been assembled in one load
bloque1=m !Now there are only m type 1 blocks and one type 2 blocks more
bloque2=bloque2+1
qacc=0
end if

```

```

        if(bloque2.eq.(kr+m))then ! If the number of type 2 blocks is the the
aggregation factor (kr) plus the margin (m), it assembles the first kr blocks into
one type 3 block.
        do i=(2*m),(kr+2*m-1)
            qacc=qacc+q_step(size-i)*(t_step(size-i+1)-t_step(size-i))
        enddo
        q_step(size-kr-2*m+1)=qacc/(t_step(size-2*m+1)-t_step(size-kr-2*m+1))
        do i=0,(2*m-1)
            q_step(size-kr-(2*m-1-i)+1)=q_step(size-(2*m-1-i))
            t_step(size-kr-(2*m-1-i)+1)=t_step(size-(2*m-1-i))
        enddo
        t_step(size-kr+2)=t_step(size+1)
        size=size-kr+1
        bloque2=m
        bloque3=bloque3+1
        qacc=0
    end if
    if(bloque3.eq.(kr+m))then ! If the number of type 3 blocks is the the
aggregation factor (kr) plus the margin (m), it assembles the first kr blocks into
one big block.
        do i=(3*m),kr+3*m-1
            qacc=qacc+q_step(size-i)*(t_step(size-i+1)-t_step(size-i))
        enddo
        q_step(size-kr-3*m+1)=qacc/(t_step(size-3*m+1)-t_step(size-kr-3*m+1))
        do i=0,(3*m-1)
            q_step(size-kr-(3*m-1-i)+1)=q_step(size-(3*m-1-i))
            t_step(size-kr-(3*m-1-i)+1)=t_step(size-(3*m-1-i))
        enddo
        t_step(size-kr+2)=t_step(size+1)
        size=size-kr+1
        bloque3=m
        qacc=0
    endif
if ((dt.eq.0 .and. step.ne.step1) .or. ((dt.ne.0) .and. (mod(TIME,dt).eq.0))) then
!If it is recalculation time, it carries out the supperposition in time and space
and calculates the ground temperature in each BHE
    bhe_dt=0
    do 31 i=1,size
        if (i.eq.1) then
            Q=q_step(i)
        else
            Q=q_step(i)-q_step(i-1)
        end if
        stime=(TIME-t_step(i))*3600
        ! now we start processing the boreholes
        do 25 k=1,n_bhes ! for each borehole
            do 26 l=1,n_bhes ! calculate the dT at all distances (from
other boreholes) and add up
                if(bhe_dist(k,l).gt.0.0)then
                    bhe_dt(k) = bhe_dt(k) +
lsahc_atdist(bhe_dist(k,l),REAL(soil_k),REAL(soil_c),Q,stime,init)
                endif
            init = .false.
            26 continue
            25 continue
            24 continue
        31 continue
    endif
!C-----
!C SET THE STORAGE ARRAY AT THE END OF THIS ITERATION IF NECESSARY
!***THE VALUES OF THE DIFFERENT ARRAYS ARE STORED FOR THE NEXT TIME STEP ****
    NITEMS=NSTORED
    DO i=1,(NSTEP)
        STORED((NSTEP*2+6)+i)=q_step(i)
        STORED((NSTEP*3+7)+i)=t_step(i)
    ENDDO

```

```

STORED(NSTEP*3+7)=qacc
STORED(NSTEP*4+8)=size
STORED(NSTEP*4+9)=bloque1
STORED(NSTEP*4+10)=bloque2
STORED(NSTEP*4+11)=bloque3
STORED(NSTEP*4+12)=step
  CALL setStorageVars(STORED,NITEMS,INFO)
!C-----
!C  SET THE OUTPUTS FROM THIS MODEL IN SEQUENTIAL ORDER AND GET OUT
!C ground temperature
  OUT(1)=sum(bhe_dt)/n_bhes+t_ff ! It calculates the average of the ground
temperature difference of all the BHEs and adds the far field temperature
!C-----
!C  EVERYTHING IS DONE - RETURN FROM THIS SUBROUTINE AND MOVE ON
  RETURN 1
  END
!C-----

```

A.4. Pipe model

The pipe type in TRNSYS used is the type developed in the PhD thesis by Ruiz-Calvo [130] with some improvements: it is possible to simulate both water and MPG (30%) circulating fluids and the calculation of the pressure drop along the pipe, as explained in section 4.3.1.2.

A.4.1. Parameters, inputs and outputs of the pipe TRNSYS type

Table A. 10. Parameters of the pipe TRNSYS type

n	Model Parameters	Units	Min.	Max.
1	Nodes	-	0	Inf.
2	Length	m	0	Inf.
3	Inner diameter	m	0	Inf.
4	Initial temperature	°C	-Inf.	Inf.
5	Roughness	mm	0	Inf.
6	Fluid	-	0	1
7	Number of elbow joints	-	0	Inf.

Table A. 11. Inputs of the pipe TRNSYS type

n	Model Inputs	Units	Min.	Max.
1	Inlet temperature	°C	-Inf.	Inf.
2	Inlet flow rate	kg/hr	0	Inf.
3	Environment temperature	°C	-Inf.	Inf.
4	Thermal losses coefficient	W/(m ² ·K)	0	Inf.

Table A. 12. Outputs of the pipe TRNSYS type

n	Model Outputs	Units	Min.	Max.
1	Outlet temperature	°C	-Inf.	Inf.
2	Outlet flow rate	kg/hr	0	Inf.
3	Pressure drop per meter	Pa/m	0	Inf.
4	Pressure drop	Pa	0	Inf.

A.4.2. Pipe FORTRAN code

```

SUBROUTINE TYPE405 (TIME,XIN,OUT,T,DTDT,PAR,INFO,ICNTRL,*)
C*****
C Object: Pipe
C Simulation Studio Model: Pipe
C Author: Félix Ruiz, modified by Antonio Cazorla
C Editor:
C Date: April 02, 2013 last modified: October 19, 2018
C (Comments and routine interface generated by TRNSYS Studio)
C*****
C TRNSYS access functions (allow to access TIME etc.)
  USE TrnsysConstants
  USE TrnsysFunctions
C-----
C   REQUIRED BY THE MULTI-DLL VERSION OF TRNSYS
  !DEC$ATTRIBUTES DLLEXPORT :: TYPE405 !SET THE CORRECT TYPE NUMBER HERE
C-----
C TRNSYS DECLARATIONS
  IMPLICIT NONE !REQUIRES THE USER TO DEFINE ALL VARIABLES BEFORE USING THEM
  DOUBLE PRECISION XIN !THE ARRAY FROM WHICH THE INPUTS TO THIS TYPE WILL BE
RETRIEVED
  DOUBLE PRECISION OUT !THE ARRAY WHICH WILL BE USED TO STORE THE OUTPUTS FROM
THIS TYPE
  DOUBLE PRECISION TIME !THE CURRENT SIMULATION TIME - YOU MAY USE THIS VARIABLE
BUT DO NOT SET IT!
  DOUBLE PRECISION PAR !THE ARRAY FROM WHICH THE PARAMETERS FOR THIS TYPE WILL
BE RETRIEVED
  DOUBLE PRECISION STORED !THE STORAGE ARRAY FOR HOLDING VARIABLES FROM TIMESTEP
TO TIMESTEP
  DOUBLE PRECISION T1 !AN ARRAY CONTAINING THE RESULTS FROM THE
DIFFERENTIAL EQUATION SOLVER
  DOUBLE PRECISION DTD T !AN ARRAY CONTAINING THE DERIVATIVES TO BE PASSED TO THE
DIFF.EQ. SOLVER
  INTEGER*4 INFO(15) !THE INFO ARRAY STORES AND PASSES VALUABLE
INFORMATION TO AND FROM THIS TYPE
  INTEGER*4 NP,NI,NOUT,ND !VARIABLES FOR THE MAXIMUM NUMBER OF
PARAMETERS,INPUTS,OUTPUTS AND DERIVATIVES
  INTEGER*4 NPAR,NIN,NDER !VARIABLES FOR THE CORRECT NUMBER OF
PARAMETERS,INPUTS,OUTPUTS AND DERIVATIVES
  INTEGER*4 IUNIT,ITYPE !THE UNIT NUMBER AND TYPE NUMBER FOR THIS COMPONENT
  INTEGER*4 ICNTRL !AN ARRAY FOR HOLDING VALUES OF CONTROL FUNCTIONS
WITH THE NEW SOLVER
  INTEGER*4 NSTORED !THE NUMBER OF VARIABLES THAT WILL BE PASSED INTO
AND OUT OF STORAGE
  CHARACTER*3 OCHECK !AN ARRAY TO BE FILLED WITH THE CORRECT VARIABLE
TYPES FOR THE OUTPUTS
  CHARACTER*3 YCHECK !AN ARRAY TO BE FILLED WITH THE CORRECT VARIABLE
TYPES FOR THE INPUTS
C-----
C USER DECLARATIONS - SET THE MAXIMUM NUMBER OF PARAMETERS (NP), INPUTS (NI),
C OUTPUTS (NOUT), AND DERIVATIVES (ND) THAT MAY BE SUPPLIED FOR THIS TYPE
  PARAMETER (NP=7,NI=4,NOUT=4,ND=0)
  integer MAXPOINTS
  PARAMETER (MAXPOINTS=400)
C-----
C   REQUIRED TRNSYS DIMENSIONS
  DIMENSION XIN(NI),OUT(NOUT),PAR(NP),YCHECK(NI),OCHECK(NOUT),
  1 STORED(MAXPOINTS*2),T1(ND),DTDT(ND)
  INTEGER NITEMS
C-----
C ADD DECLARATIONS AND DEFINITIONS FOR THE USER-VARIABLES HERE
C PARAMETERS
  double precision time0,delt
  double precision T(MAXPOINTS), Tini(MAXPOINTS)
  double precision U,L,D,Tenv,Tinit,Tin,flow,Tout,ro,cp,cond

```



```

double precision dx,dt,v,dt_ac,dTin
double precision rug,dP_L,dP,mu,f_D,Re,T_K,L_f
integer i,N,fluid,elbows
double precision, parameter :: pi=3.14159265358979323
C-----
C   GET GLOBAL TRNSYS SIMULATION VARIABLES
TIME0=getSimulationStartTime()
DELT=getSimulationTimeStep()
C-----
N=PAR(1)
L=PAR(2)
D=PAR(3)
Tinit=PAR(4)
rug=PAR(5)
fluid=PAR(6)
elbows=PAR(7)
Tin=XIN(1)
flow=XIN(2)
Tenv=XIN(3)
U=XIN(4)
Tout=Tin
      IUNIT=INFO(1)
      ITYPE=INFO(2)
C-----
C   SET THE VERSION INFORMATION FOR TRNSYS
IF(INFO(7).EQ.-2) THEN
      INFO(12)=16
      RETURN 1
ENDIF
C-----
C   DO ALL THE VERY LAST CALL OF THE SIMULATION MANIPULATIONS HERE
IF (INFO(8).EQ.-1) THEN
      RETURN 1
ENDIF
C-----
C   PERFORM ANY 'AFTER-ITERATION' MANIPULATIONS THAT ARE REQUIRED HERE
C   e.g. save variables to storage array for the next timestep
IF (INFO(13).GT.0) THEN
      NITEMS=N*2
      CALL getStorageVars(STORED,NITEMS,INFO)
      DO i=1,N
          STORED(i)=STORED(N+i)
      ENDDO
      CALL setStorageVars(STORED,NITEMS,INFO)
      RETURN 1
ENDIF
C-----
C   DO ALL THE VERY FIRST CALL OF THE SIMULATION MANIPULATIONS HERE
IF (INFO(7).EQ.-1) THEN
C       SET SOME INFO ARRAY VARIABLES TO TELL THE TRNSYS ENGINE HOW THIS TYPE IS TO
WORK
      INFO(6)=NOUT
      INFO(9)=1
      INFO(10)=0 !STORAGE FOR VERSION 16 HAS BEEN CHANGED
C       SET THE REQUIRED NUMBER OF INPUTS, PARAMETERS AND DERIVATIVES THAT THE USER
SHOULD SUPPLY IN THE INPUT FILE
C       IN SOME CASES, THE NUMBER OF VARIABLES MAY DEPEND ON THE VALUE OF PARAMETERS
TO THIS MODEL...
      NIN=NI
      NPAR=NP
      NDER=ND
C       CALL THE TYPE CHECK SUBROUTINE TO COMPARE WHAT THIS COMPONENT REQUIRES TO
WHAT IS SUPPLIED IN
C       THE TRNSYS INPUT FILE
      CALL TYPECK(1,INFO,NIN,NPAR,NDER)
C       SET THE NUMBER OF STORAGE SPOTS NEEDED FOR THIS COMPONENT

```

```

        NITEMS=N*2
        CALL setStorageSize(NITEMS,INFO)
C      RETURN TO THE CALLING PROGRAM
        RETURN 1
    ENDIF
C-----
C  DO ALL OF THE INITIAL TIMESTEP MANIPULATIONS HERE - THERE ARE NO ITERATIONS AT
THE INITIAL TIME
    IF (TIME .LT. (TIME0 + DELT/2.D0)) THEN
C      SET THE UNIT NUMBER FOR FUTURE CALLS
        IUNIT=INFO(1)
        ITYPE=INFO(2)
C      PERFORM ANY REQUIRED CALCULATIONS TO SET THE INITIAL VALUES OF THE OUTPUTS
HERE
        Tout=Tinit
        OUT(1)=Tout
        OUT(2)=flow
C      PERFORM ANY REQUIRED CALCULATIONS TO SET THE INITIAL STORAGE VARIABLES HERE
        NITEMS=N*2
        DO i=1,N
            STORED(i)=Tinit
        ENDDO
C      PUT THE STORED ARRAY IN THE GLOBAL STORED ARRAY
        CALL setStorageVars(STORED,NITEMS,INFO)
C      RETURN TO THE CALLING PROGRAM
        RETURN 1
    ENDIF
C-----
C  *** ITS AN ITERATIVE CALL TO THIS COMPONENT ***
C-----
C  RETRIEVE THE VALUES IN THE STORAGE ARRAY FOR THIS ITERATION
    NITEMS=N*2
    CALL getStorageVars(STORED,NITEMS,INFO)
    DO i=1,N
        Tini(i)=STORED(i)
    ENDDO
C-----
C  *** PERFORM ALL THE CALCULATION HERE FOR THIS MODEL. ***
C-----
C      ADD YOUR COMPONENT EQUATIONS HERE; BASICALLY THE EQUATIONS THAT WILL
CALCULATE THE OUTPUTS BASED ON THE PARAMETERS AND THE INPUTS. REFER TO CHAPTER 3 OF
THE TRNSYS VOLUME 1 MANUAL FOR DETAILED INFORMATION ON WRITING TRNSYS COMPONENTS.
C  *****
C  * Inicialización de variables *
C  *****
    T_K=(Tini(1)+Tini(N))*0.5+273.15
    if (fluid .eq. 0) then !WATER
        ro=12.36+8.944*T_K-0.02592*T_K**2+0.00002346*T_K**3
        mu=exp(-7.1143-2000.3/T_K+604550/T_K**2)
        cp=-1.03024E-04*T_K**3+1.13872E-01*T_K**2-4.10435E+01*T_K+
.      9.02811E+03
    else !MPG 30%
        ro=539.5+4.928*T_K-0.01515*T_K**2+0.00001357*T_K**3
        mu=exp(-2.4901-5142.2/T_K+1221300/T_K**2)
        cp=2.70720E+00*T_K+3.06317E+03
    endif
    Re=4*(flow/3600)/(pi*D*mu)
    if (flow .gt. 0.0) then
        f_D=8*((8/Re)**12+((2.457*log(((7/Re)**0.9+0.27*rug/D)**(-1))))**16
.      +(37530/Re)**16)**(-1.5))**(1.0/12)
        dP_L=8*f_D*(flow/3600)**2/(pi*pi*D**5*ro)
    else
        dP_L=0
    endif
    L_f=L+elbows*(0.15871+0.02975*D/1000)
    dP=dP_L*L_f

```

```

dx=L/(N-1)
if(flow .le. 0) flow=0
v=flow/(3600*ro*pi*D*D/4)
dt=dx/v*0.99
DELT=DELT*3600
if(DELT .LT. dt) then
dt=DELT
endif
dt_ac=0
dTin=(Tin-Tini(1))/DELT
cond=U*pi*D/(ro*cp*pi*D*D/4)
do while(dt_ac .LT. DELT)
T(1)=dTin*dt+Tini(1)
DO i=2,(N-1)
T(i)=Tini(i)-dt*v/(2*dx)*((Tini(i+1)-Tini(i-1))
-v*dt/dx*(Tini(i+1)-2*Tini(i)+Tini(i-1)))
-dt*cond*(Tini(i)-Tenv)
ENDDO
T(N)=Tini(N)-v*dt/dx*(Tini(N)-Tini(N-1))-dt*cond*(Tini(N)-Tenv)
DO i=1,N
Tini(i)=T(i)
ENDDO
dt_ac=dt_ac+dt
if(dt .GT. (DELT-dt_ac)) then
dt=DELT-dt_ac
endif
enddo
Tout=T(N)
C-----
C SET THE STORAGE ARRAY AT THE END OF THIS ITERATION IF NECESSARY
NITEMS=N*2
DO i=1,N
STORED(N+i)=T(i)
ENDDO
CALL setStorageVars(STORED,NITEMS,INFO)
C-----
C SET THE OUTPUTS FROM THIS MODEL IN SEQUENTIAL ORDER AND GET OUT
OUT(1)=Tout
OUT(2)=flow
out(3)=dP_L
out(4)=dP
C-----
C EVERYTHING IS DONE - RETURN FROM THIS SUBROUTINE AND MOVE ON
RETURN 1
END
C-----

```

A.5. Room Temperature Control (RTC) model

A.5.1. Parameters, inputs and outputs of the RTC TRNSYS type

Table A. 13. Parameters of the RTC TRNSYS type

n	Model Parameters	Units	Min.	Max.
1	Number of rooms	-	0	4
2	Number of time steps	-	0	Inf.
3	dT Hysteresys	delta°C	0	Inf.

Table A. 14. Inputs of the RTC TRNSYS type. The number of inputs 1, 2 and 3 will depend on the number of rooms in parameter 1

n	Model Inputs	Units	Min.	Max.
1·X	Temperature of room X	°C	-Inf.	Inf.
2·X	ON/OFF thermostat of room X	-	0	1
3·X	Setpoint temperature of room X	°C	-Inf.	Inf.
4	season	-	0	1

Table A. 15. Outputs of the RTC TRNSYS type

n	Model Outputs	Units	Min.	Max.
1	Temperature of worst room	°C	-Inf.	Inf.
2	ON/OFF for PID	-	0	1
3	Worst room	-	0	Inf.
4	Setpoint of worst room	°C	-Inf.	Inf.

A.5.2. RTC FORTRAN code

```

SUBROUTINE TYPE440 (TIME,XIN,OUT,T,DTDT,PAR,INFO,ICNTRL,*)
C*****
C Object: Room Temperature Control
C Simulation Studio Model: Room_temperature_control
C Author: IIE
C Editor: Antonio Cazorla-Marin
C Date: diciembre 12, 2018 last modified: diciembre 12, 2018
C (Comments and routine interface generated by TRNSYS Studio)
C*****
C TRNSYS access functions (allow to access TIME etc.)
  USE TrnsysConstants
  USE TrnsysFunctions
C-----
C   REQUIRED BY THE MULTI-DLL VERSION OF TRNSYS
  !DEC$ATTRIBUTES DLLEXPORT :: TYPE440
C-----
C   TRNSYS DECLARATIONS
  IMPLICIT NONE !REQUIRES THE USER TO DEFINE ALL VARIABLES BEFORE USING THEM

  DOUBLE PRECISION XIN !THE ARRAY FROM WHICH THE INPUTS TO THIS TYPE WILL BE
  RETRIEVED
  DOUBLE PRECISION OUT !THE ARRAY WHICH WILL BE USED TO STORE THE OUTPUTS FROM
  THIS TYPE
  DOUBLE PRECISION TIME !THE CURRENT SIMULATION TIME - YOU MAY USE THIS VARIABLE
  BUT DO NOT SET IT!

```

```

      DOUBLE PRECISION PAR !THE ARRAY FROM WHICH THE PARAMETERS FOR THIS TYPE WILL
BE RETRIEVED
      DOUBLE PRECISION STORED !THE STORAGE ARRAY FOR HOLDING VARIABLES FROM TIMESTEP
TO TIMESTEP
      DOUBLE PRECISION T           !AN ARRAY CONTAINING THE RESULTS FROM THE
DIFFERENTIAL EQUATION SOLVER
      DOUBLE PRECISION DTD T !AN ARRAY CONTAINING THE DERIVATIVES TO BE PASSED TO THE
DIFF.EQ. SOLVER
      INTEGER*4 INFO(15)           !THE INFO ARRAY STORES AND PASSES VALUABLE
INFORMATION TO AND FROM THIS TYPE
      INTEGER*4 NP,NI,NOUT,ND      !VARIABLES FOR THE MAXIMUM NUMBER OF
PARAMETERS,INPUTS,OUTPUTS AND DERIVATIVES
      INTEGER*4 NPAR,NIN,NDER     !VARIABLES FOR THE CORRECT NUMBER OF
PARAMETERS,INPUTS,OUTPUTS AND DERIVATIVES
      INTEGER*4 IUNIT,ITYPE !THE UNIT NUMBER AND TYPE NUMBER FOR THIS COMPONENT
      INTEGER*4 ICNTRL            !AN ARRAY FOR HOLDING VALUES OF CONTROL FUNCTIONS
WITH THE NEW SOLVER
      INTEGER*4 NSTORED           !THE NUMBER OF VARIABLES THAT WILL BE PASSED INTO
AND OUT OF STORAGE
      CHARACTER*3 OCHECK          !AN ARRAY TO BE FILLED WITH THE CORRECT VARIABLE
TYPES FOR THE OUTPUTS
      CHARACTER*3 YCHECK          !AN ARRAY TO BE FILLED WITH THE CORRECT VARIABLE
TYPES FOR THE INPUTS
C-----
C   USER DECLARATIONS - SET THE MAXIMUM NUMBER OF PARAMETERS (NP), INPUTS (NI),
C   OUTPUTS (NOUT), AND DERIVATIVES (ND) THAT MAY BE SUPPLIED FOR THIS TYPE
      PARAMETER (NP=3,NI=13,NOUT=4,ND=0,NSTORED=10000)
C-----
C   REQUIRED TRNSYS DIMENSIONS
      DIMENSION XIN(NI),OUT(NOUT),PAR(NP),YCHECK(NI),OCHECK(NOUT),
      ! STORED(NSTORED),T(ND),DTD(ND)
      INTEGER NITEMS
C-----
C   ADD DECLARATIONS AND DEFINITIONS FOR THE USER-VARIABLES HERE
C   PARAMETERS
      integer nr
      integer nTsteps
      double precision dT
C   INPUTS
      DOUBLE PRECISION room_temperature
      DOUBLE PRECISION ON_OFF_room_thermostat
      DOUBLE PRECISION season
C   OTHER VARIABLES
      DOUBLE PRECISION Trooms,switch_th,Tmat,v_slopes,Tsp
      DIMENSION Trooms(4),switch_th(4),v_slopes(4),Tsp(4)
      DIMENSION Tmat(4,6)
      double precision slope, switch_PID,Tworst,dTworst,SPworst
      integer i,j,nTOTAL,nst,n_on,n,room_worst
      double precision TIME0,DELT
C   GET GLOBAL TRNSYS SIMULATION VARIABLES
      TIME0=getSimulationStartTime()
      DELT=getSimulationTimeStep()
C-----
C   READ IN THE VALUES OF THE PARAMETERS IN SEQUENTIAL ORDER
      nr=PAR(1)
      nTsteps=PAR(2)
      dT=PAR(3)
      nst=nTsteps+1
      nTOTAL=nr*nTsteps
C-----
C   RETRIEVE THE CURRENT VALUES OF THE INPUTS TO THIS MODEL FROM THE XIN ARRAY IN
SEQUENTIAL ORDER
      do i=1,nr
         Trooms(i)=XIN(i)
      enddo
      do i=1,nr

```

```

        switch_th(i)=XIN(nr+i)
    enddo
    do i=1,nr
        Tsp(i)=XIN(2*nr+i)
    enddo
    season=XIN(3*nr+1)
        IUNIT=INFO(1)
        ITYPE=INFO(2)
C-----
C   SET THE VERSION INFORMATION FOR TRNSYS
C   IF (INFO(7).EQ.-2) THEN
        INFO(12)=16
        RETURN 1
    ENDIF
C-----
C   DO ALL THE VERY LAST CALL OF THE SIMULATION MANIPULATIONS HERE
C   IF (INFO(8).EQ.-1) THEN
        RETURN 1
    ENDIF
C-----
C   PERFORM ANY 'AFTER-ITERATION' MANIPULATIONS THAT ARE REQUIRED HERE
C   e.g. save variables to storage array for the next timestep
C   IF (INFO(13).GT.0) THEN
        NITEMS=nTOTAL*2
        CALL getStorageVars(STORED,NITEMS,INFO)
        DO i=1,nr
            DO j=1,nTsteps
                STORED((i-1)*nTsteps+j)=STORED(nTOTAL+(i-1)*nTsteps+j)
            ENDDO
        ENDDO

        CALL setStorageVars(STORED,NITEMS,INFO)

        RETURN 1
    ENDIF
C-----
C   DO ALL THE VERY FIRST CALL OF THE SIMULATION MANIPULATIONS HERE
C   IF (INFO(7).EQ.-1) THEN
C   SET SOME INFO ARRAY VARIABLES TO TELL THE TRNSYS ENGINE HOW THIS TYPE IS TO WORK
        INFO(6)=NOUT
        INFO(9)=1
        INFO(10)=0 !STORAGE FOR VERSION 16 HAS BEEN CHANGED

C       SET THE REQUIRED NUMBER OF INPUTS, PARAMETERS AND DERIVATIVES THAT THE USER
C       SHOULD SUPPLY IN THE INPUT FILE IN SOME CASES, THE NUMBER OF VARIABLES MAY DEPEND ON
C       THE VALUE OF PARAMETERS TO THIS MODEL....
        NIN=NI
        NPAR=NP
        NDER=ND
C       CALL THE TYPE CHECK SUBROUTINE TO COMPARE WHAT THIS COMPONENT REQUIRES TO
C       WHAT IS SUPPLIED IN THE TRNSYS INPUT FILE
        CALL TYPECK(1,INFO,NIN,NPAR,NDER)
C       SET THE NUMBER OF STORAGE SPOTS NEEDED FOR THIS COMPONENT
        NITEMS=nTOTAL*2
        CALL setStorageSize(NITEMS,INFO)
C       RETURN TO THE CALLING PROGRAM
        RETURN 1
    ENDIF
C-----
C   DO ALL OF THE INITIAL TIMESTEP MANIPULATIONS HERE - THERE ARE NO ITERATIONS AT
C   THE INITIAL TIME
C   IF (TIME .LT. (getSimulationStartTime() +
C   getSimulationTimeStep()/2.D0)) THEN
C   SET THE UNIT NUMBER FOR FUTURE CALLS
        IUNIT=INFO(1)
        ITYPE=INFO(2)

```

```

C      PERFORM ANY REQUIRED CALCULATIONS TO SET THE INITIAL VALUES OF THE OUTPUTS
HERE
C          slope worst room
              OUT(1)=0
              out(2)=0
              out(3)=0
              out(4)=0
C      PUT THE STORED ARRAY IN THE GLOBAL STORED ARRAY
              CALL setStorageVars(STORED,NITEMS,INFO)
C      RETURN TO THE CALLING PROGRAM
              RETURN 1
ENDIF

C-----
C      *** ITS AN ITERATIVE CALL TO THIS COMPONENT ***
C-----
C      RETRIEVE THE VALUES IN THE STORAGE ARRAY FOR THIS ITERATION
NITEMS=nTOTAL*2
              CALL getStorageVars(STORED,NITEMS,INFO)
              DO i=1,nr
                  DO j=1,nTsteps
                      Tmat(i,j+1)=STORED((i-1)*nTsteps+j)
                  ENDDO
              ENDDO

C-----
C      *** PERFORM ALL THE CALCULATION HERE FOR THIS MODEL. ***
C-----
C      ADD YOUR COMPONENT EQUATIONS HERE; BASICALLY THE EQUATIONS THAT WILL
CALCULATE THE OUTPUTS BASED ON THE PARAMETERS AND THE INPUTS. REFER TO CHAPTER 3 OF
THE TRNSYS VOLUME 1 MANUAL FOR DETAILED INFORMATION ON WRITING TRNSYS COMPONENTS.
              DO i=1,nr
                  Tmat(i,1)=Trooms(i)
                  v_slopes(i)=(Tmat(i,1)-Tmat(i,nst))/(nTsteps*DELT)
              ENDDO
              n_on=sum(switch_th)
              if (n_on .eq. 0) then
                  switch_PID=0
                  room_worst=0
                  Tworst=0
                  SPworst=0
              else
                  switch_PID=1
                  dTworst=dT
                  room_worst=0
                  do i=1,nr
                      if (switch_th(i) .eq. 1) then
                          if ((season .eq. 0) .and.
                          . (Trooms(i) .lt. (Tsp(i)-dT))) then
                              if ((Tsp(i)-Trooms(i)) .ge. dTworst) then
                                  dTworst=Tsp(i)-Trooms(i)
                                  Tworst=Trooms(i)
                                  SPworst=Tsp(i)
                                  room_worst=i
                              endif
                          .
                              elseif ((season.eq.1) .and.
                              . (Trooms(i) .gt. (Tsp(i)+dT))) then
                                  if ((Trooms(i)-Tsp(i)) .ge. dTworst) then
                                      dTworst=Trooms(i)-Tsp(i)
                                      Tworst=Trooms(i)
                                      SPworst=Tsp(i)
                                      room_worst=i
                                  endif
                              endif
                          .
                      endif
                  enddo
                  if (room_worst .eq. 0) then

```

```

        if (season .eq. 0) then
            slope=99
        else
            slope=-99
        endif
        do i=1,nr
            if (switch_th(i) .eq. 1) then
                if ((season .eq. 0) .and.
                    (v_slopes(i) .lt. slope)) then
                    slope=v_slopes(i)
                    Tworst=Rooms(i)
                    SPworst=Tsp(i)
                    room_worst=i
                elseif ((season .eq. 1) .and.
                    (v_slopes(i) .gt. slope)) then
                    slope=v_slopes(i)
                    Tworst=Rooms(i)
                    SPworst=Tsp(i)
                    room_worst=i
                endif
            endif
        enddo
    endif
endif
-----
C  SET THE STORAGE ARRAY AT THE END OF THIS ITERATION IF NECESSARY
C  NITEMS=nTOTAL*2
C  DO i=1,nr
C      DO j=1,nTsteps
C          STORED(nTOTAL+(i-1)*nTsteps+j)=Tmat(i,j)
C      ENDDO
C  ENDDO
C  CALL setStorageVars(STORED,NITEMS,INFO)
-----
C  SET THE OUTPUTS FROM THIS MODEL IN SEQUENTIAL ORDER AND GET OUT
C      slope worst room
C          OUT(1)=Tworst
C          OUT(2)=switch_PID
C          OUT(3)=room_worst
C          out(4)=SPworst
-----
C  EVERYTHING IS DONE - RETURN FROM THIS SUBROUTINE AND MOVE ON
C  RETURN 1
C  END
-----

```


B. Coefficients for the DSHP model

Table B. 1. M1-Summer Air coefficients

\dot{Q}_e		\dot{W}_c	
C0	5.549E+03	C0	-1.272E+02
C1	-5.331E+01	C1	1.756E-04
C2	1.127E+01	C2	1.412E-03
C3	-4.350E-02	C3	2.794E+00
C4	1.247E-01	C4	-1.227E-01
C5	3.997E+01	C5	-9.838E-03
C6	1.697E+00	C6	2.220E-03
C7	-1.494E-01	C7	-5.953E-04
C8	-4.883E-03	C8	-1.935E-08
		C9	-9.442E-04
		C10	2.695E+02
R ²	0.906	R ²	0.959
Error (%)	5.695	Error (%)	7.761

Table B. 2. M2-Summer Ground coefficients

\dot{Q}_c		\dot{Q}_e		\dot{W}_c	
C0	-8.701E+03	C0	-1.295E+04	C0	-9.257E+01
C1	-2.818E+01	C1	-2.854E+01	C1	-1.924E-04
C2	8.045E+01	C2	1.089E+02	C2	1.223E-03
C3	-2.837E-01	C3	-3.829E-01	C3	3.184E+00
C4	2.099E-01	C4	2.626E-01	C4	4.644E-01
C5	2.281E+02	C5	2.892E+02	C5	-1.065E-02
C6	-2.129E+01	C6	-1.372E+01	C6	3.396E-03
C7	-7.987E-01	C7	-1.008E+00	C7	-1.431E-03
C8	6.673E-02	C8	3.563E-02	C8	-3.995E-08
				C9	-1.085E-03
				C10	2.731E+02
R ²	0.976	R ²	0.984	R ²	0.998
Error (%)	6.004	Error (%)	8.835	Error (%)	0.661

Table B. 3. M3-DHW User (Full recovery) coefficients

\dot{Q}_c		\dot{Q}_e		\dot{W}_c	
C0	4.728E+03	C0	9.219E+03	C0	-9.374E+01
C1	-3.939E+01	C1	-5.629E+01	C1	-1.477E-05
C2	3.980E-01	C2	-5.575E+00	C2	9.798E-04
C3	4.338E-03	C3	-1.590E-04	C3	1.487E+00
C4	7.567E-02	C4	1.080E-01	C4	3.600E-01

\dot{Q}_c		\dot{Q}_e		\dot{W}_c	
C5	3.660E+01	C5	6.946E+01	C5	-5.754E-03
C6	1.810E+00	C6	-4.983E+00	C6	3.194E-03
C7	-1.375E-01	C7	-2.500E-01	C7	-6.752E-04
C8	-8.854E-04	C8	-1.229E-03	C8	-4.472E-08
				C9	2.285E-03
				C10	6.716E+02
R ²	0.987	R ²	0.989	R ²	0.986
Error (%)	1.808	Error (%)	1.589	Error (%)	0.893

Table B. 4. M4-Winter Air coefficients

\dot{Q}_c		\dot{W}_c	
C0	-3.185E+03	C0	-1.316E+02
C1	2.157E+01	C1	-2.859E-04
C2	1.474E-01	C2	1.584E-03
C3	-2.111E-03	C3	-1.190E-01
C4	-3.289E-02	C4	5.443E-01
C5	-7.014E+00	C5	3.806E-04
C6	6.112E+00	C6	4.627E-03
C7	2.563E-02	C7	-2.310E-03
C8	-2.267E-02	C8	-3.551E-08
		C9	3.695E-04
		C10	6.263E+02
R ²	0.911	R ²	0.995
Error (%)	5.117	Error (%)	1.545

Table B. 5. M5-Winter Ground coefficients

\dot{Q}_c		\dot{Q}_e		\dot{W}_c	
C0	3.154E+02	C0	1.123E+03	C0	-1.555E+02
C1	-1.415E+01	C1	-2.075E+01	C1	-2.643E-04
C2	8.123E+00	C2	9.253E+00	C2	1.541E-03
C3	-3.063E-02	C3	-3.738E-02	C3	-2.200E+00
C4	5.042E-02	C4	6.635E-02	C4	5.194E-01
C5	1.076E+01	C5	2.405E+01	C5	7.781E-03
C6	1.288E+01	C6	4.528E+00	C6	6.065E-03
C7	-5.095E-02	C7	-9.822E-02	C7	-2.149E-03
C8	-4.422E-02	C8	-1.736E-02	C8	-6.122E-08
				C9	-1.472E-03
				C10	1.122E+03
R ²	0.993	R ²	0.986	R ²	0.989
Error (%)	2.578	Error (%)	4.184	Error (%)	3.157

Table B. 6. M6 and M7 - DHW Air coefficients

\dot{Q}_c		\dot{W}_c	
C0	7.344E+02	C0	-1.572E+02
C1	-8.650E+00	C1	-2.531E-05
C2	1.557E+00	C2	1.632E-03
C3	-7.571E-03	C3	5.410E-02
C4	2.545E-02	C4	7.363E-01
C5	2.206E-01	C5	-3.187E-04
C6	-1.500E+00	C6	3.175E-03
C7	0.000E+00	C7	-8.745E-04
C8	2.444E-03	C8	-4.482E-08
		C9	9.091E-04
		C10	6.345E+02
R ²	0.9458315	R ²	0.985
Error (%)	4.8049643	Error (%)	1.361

Table B. 7. M8 and M9 - DHW Ground coefficients

\dot{Q}_c		\dot{Q}_e		\dot{W}_c	
C0	2.689E+03	C0	3.517E+03	C0	-1.866E+02
C1	-2.350E+01	C1	-2.830E+01	C1	-1.225E-04
C2	1.630E+00	C2	1.001E+00	C2	1.704E-03
C3	-7.443E-03	C3	-7.814E-03	C3	-1.162E+00
C4	5.345E-02	C4	6.260E-02	C4	6.916E-01
C5	4.162E+00	C5	2.329E+01	C5	2.325E-03
C6	2.565E-01	C6	-7.693E-01	C6	6.295E-03
C7	-2.701E-02	C7	-9.410E-02	C7	-2.003E-03
C8	-2.954E-03	C8	-5.991E-04	C8	-7.666E-08
				C9	6.026E-03
				C10	1.251E+03
R ²	0.998	R ²	0.989	R ²	0.953
Error (%)	2.373	Error (%)	4.513	Error (%)	3.703

C. Tribano office building characteristics

Table C. 1. Walls distribution

Wall	Type	Area (m ²)	Category
RICERCA E SVILUPPO (RES)			
North wall	OUTWALL	19.98	EXTERNAL NORTH
Wall production	OUTWALL	19.75	BOUNDARY Production
Partition COMM	INTWALL	25.58	ADJACENT COMM
Partition CORR	INTWALL	18.55	ADJACENT CORR
Floor	INTFLOOR	62.00	BOUNDARY Identical
Roof	ROOF	62.00	EXTERNAL HORIZONTAL
COMMERCIALE (COMM)			
North wall	OUTWALL	11.38	EXTERNAL NORTH
West wall	OUTWALL	27.75	EXTERNAL WEST
Partition AMM	INTWALL	14.88	ADJACENT AMM
Partition RES	INTWALL	25.58	ADJACENT RES
Partition CORR	INTWALL	5.42	ADJACENT CORR
Floor	INTFLOOR	57.00	BOUNDARY Identical
Roof	ROOF	57.00	EXTERNAL HORIZONTAL
AMMINISTRAZIONE (AMM)			
West wall	OUTWALL	11.13	EXTERNAL WEST
Partition COMM	INTWALL	14.88	ADJACENT COMM
Partition META	INTWALL	10.45	ADJACENT META
Partition CORR	INTWALL	12.64	ADJACENT CORR
Floor	INTFLOOR	24.00	BOUNDARY Identical
Roof	ROOF	24.00	EXTERNAL HORIZONTAL
META' SALA INCONTRI (META)			
West wall glazed	OUTWALL	14.07	EXTERNAL WEST
Boundary rest of offices	INTWALL	15.20	BOUNDARY Identical
Partition AMM	INTWALL	10.45	ADJACENT AMM
Partition CORR	INTWALL	15.60	ADJACENT CORR
Floor	INTFLOOR	31.00	BOUNDARY Identical
Roof	ROOF	31.00	EXTERNAL HORIZONTAL
CORRIDOR (CORR)			
Partition RES	INTWALL	18.55	ADJACENT RES
Partition COMM	INTWALL	5.42	ADJACENT COMM
Partition AMM	INTWALL	12.64	ADJACENT AMM
Partition META	INTWALL	15.60	ADJACENT META
Wall production	OUTWALL	32.88	BOUNDARY Production
Rest of offices	INTWALL	16.23	BOUNDARY Identical
Floor	INTFLOOR	90.00	BOUNDARY Identical
Roof	ROOF	90.00	EXTERNAL HORIZONTAL

- BOUNDARY Identical: adiabatic boundary, no heat transfer because the adjacent room temperature is considered equal.
- BOUNDARY Production: adjacent to the Production building, its temperature is considered 18°C in winter and 21°C in summer.

Table C. 2. Windows distribution

Zone	Wall	Type	Area (m ²)
RICERCA E SVILUPPO (RES)	North wall	DOUBLE	5
COMMERCIALE (COMM)	North wall	DOUBLE	3
	West wall	DOUBLE	7
AMMINISTRAZIONE (AMM)	West wall	DOUBLE	2.5
META' SALA INCONTRI (META)	West wall glazed	META_GLASS	13.5

Table C. 3. Walls characteristics

Wall	Layer	Thickness (m)	U-Value (W/(m ² ·K))
OUTWALL	INSULATION	0.140	0.262
	CONCRETE	0.300	
INTWALL	GYPSUM	0.015	2.076
	BRICK	0.150	
	GYPSUM	0.015	
ROOF	INSULATION	0.170	0.211
	CONCRETE	0.200	
	BRICK	0.200	
INTFLOOR	FLOOR	0.005	0.834
	STONE	0.060	
	SILENCE	0.040	
	CONCRETE	0.240	

Table C. 4. Windows characteristics

	U-value (W/(m ² ·K))	g-value (%/100)	Internal shadow	External shadow
DOUBLE	2.3	0.295	0.8 (summer)	-
META_GLASS	1.01	0.281	0.4 (always)	0.6 (summer)

D. Parametrical studies Room temperature control

- Freq. control:
 - 0 (s/r) → water temperature control for the compressor frequency (control on the supply / control on the return).
 - 1 → room temperature control for the compressor frequency.
- Tlimit / SP:
 - SetPoint (°C) if water temperature control in heating (heat) or cooling (cool).
 - Limit in the supply temperature (°C) when room temperature control in heating (heat) or cooling (cool).
- CP IC (Circulation Pump of the Internal Circuit):
 - 0 → fixed speed.
 - 1 (dT) → temperature difference control (dT used).
- Night mode:
 - 0 → No night mode.
 - 1 → Night mode used.
- Tank:
 - 0 → No buffer tank in the internal circuit.
 - 1 → Buffer tank in the internal circuit.
- FCs schedule:
 - 0 → Original working schedule for the fan coils.
 - 1 → Optimized working schedule for the fan coils.

Table D. 1. Parametric analysis. List of simulations

	Freq. control	Tlimit/SP heat	Tlimit/SP cool	CP IC	Night mode	Tank	FCs schedule
1	1	40	12	1	1	1	1
2	1	40	7	1	0	1	1
3	0 (s)	40	12	1	0	1	1
4	1	40	12	1	1	1	1
5	1	40	10	1	1	1	1
6	1	40	7	1	0	1	1
7	1	40	12	1	1	1	0
8	0 (s)	40	12	1	0	1	1
9	1	45	12	1	1	1	1
10	0 (s)	40	10	1	0	1	1

	Freq. control	Tlimit/SP heat	Tlimit/SP cool	CP IC	Night mode	Tank	FCs schedule
11	0 (s)	40	12	1	1	1	1
12	1	40	10	1	1	1	1
13	1	40	7	1	0	1	0
14	1	45	7	1	0	1	1
15	0 (s)	40	12	1	0	1	0
16	1	40	7	1	1	1	1
17	1	40	12	1	1	1	0
18	1	45	12	1	1	1	1
19	1	40	10	1	1	1	0
20	0 (s)	40	12	1	1	1	1
21	1	45	10	1	1	1	1
22	1	45	7	1	0	1	1
23	1	40	7	1	1	1	1
24	0 (s)	40	10	1	0	1	1
25	1	40	7	1	0	1	0
26	1	50	12	1	1	1	1
27	0 (s)	40	10	1	1	1	1
28	1	40	10	1	1	1	0
29	0 (s)	40	12	1	1	1	0
30	1	45	12	1	1	1	0
31	1	40	7	1	1	1	0
32	0 (s)	40	12	1	0	1	0
33	0 (s)	40	7	1	0	1	1
34	0 (s)	40	10	1	0	1	0
35	1	45	10	1	1	1	1
36	0 (s)	45	12	1	0	1	1
37	1	50	12	1	1	1	1
38	1	45	7	1	1	1	1
39	1	45	12	1	1	1	0
40	1	40	7	1	1	1	0
41	1	45	7	1	0	1	0
42	0 (s)	40	10	1	1	1	1
43	0 (s)	40	12	1	1	1	0
44	1	50	10	1	1	1	1
45	1	45	10	1	1	1	0
46	1	45	7	1	1	1	1
47	0 (s)	40	10	1	1	1	0
48	0 (s)	40	7	1	0	1	1
49	0 (s)	45	12	1	0	1	1
50	0 (s)	40	10	1	0	1	0
51	1	45	7	1	0	1	0
52	0 (s)	40	7	1	1	1	1

	Freq. control	Tlimit/SP heat	Tlimit/SP cool	CP IC	Night mode	Tank	FCs schedule
53	0 (s)	45	12	1	1	1	1
54	0 (s)	45	10	1	0	1	1
55	1	50	10	1	1	1	1
56	1	45	10	1	1	1	0
57	1	50	12	1	1	1	0
58	0 (s)	40	7	1	0	1	0
59	1	45	7	1	1	1	0
60	1	50	7	1	1	1	1
61	0 (s)	40	10	1	1	1	0
62	0 (s)	45	12	1	0	1	0
63	1	50	12	1	1	1	0
64	0 (s)	45	12	1	1	1	1
65	0 (s)	40	7	1	1	1	1
66	1	45	7	1	1	1	0
67	1	50	7	1	1	1	1
68	0 (s)	45	10	1	0	1	1
69	1	50	10	1	1	1	0
70	0 (s)	45	10	1	1	1	1
71	0 (s)	40	7	1	1	1	0
72	0 (s)	40	7	1	0	1	0
73	0 (s)	45	12	1	1	1	0
74	0 (s)	45	12	1	0	1	0
75	0 (s)	45	7	1	0	1	1
76	1	50	10	1	1	1	0
77	0 (s)	50	12	1	0	1	1
78	0 (s)	45	10	1	0	1	0
79	1	50	7	1	1	1	0
80	0 (s)	45	10	1	1	1	1
81	0 (s)	40	7	1	1	1	0
82	0 (s)	45	12	1	1	1	0
83	1	50	7	1	1	1	0
84	0 (s)	45	7	1	0	1	1
85	0 (s)	45	10	1	1	1	0
86	0 (s)	50	12	1	0	1	1
87	0 (s)	45	7	1	1	1	1
88	0 (s)	45	10	1	0	1	0
89	0 (s)	50	10	1	0	1	1
90	0 (s)	50	12	1	1	1	1
91	0 (s)	45	7	1	0	1	0
92	1	40	12	0	1	0	1
93	0 (s)	45	10	1	1	1	0
94	1	40	7	0	0	0	1

	Freq. control	Tlimit/SP heat	Tlimit/SP cool	CP IC	Night mode	Tank	FCs schedule
95	0 (s)	50	12	1	0	1	0
96	0 (s)	45	7	1	1	1	1
97	0 (s)	50	12	1	1	1	1
98	0 (s)	50	10	1	0	1	1
99	0 (s)	50	10	1	1	1	1
100	0 (s)	45	7	1	1	1	0
101	1	40	10	0	1	0	1
102	0 (s)	45	7	1	0	1	0
103	0 (s)	50	7	1	0	1	1
104	1	45	12	0	1	0	1
105	0 (s)	50	12	1	1	1	0
106	0 (s)	40	12	0	0	1	1
107	0 (s)	50	12	1	0	1	0
108	1	40	12	0	1	0	0
109	0 (s)	50	10	1	0	1	0
110	1	45	7	0	0	0	1
111	1	45	7	0	0	0	1
112	1	40	7	0	1	0	1
113	0 (s)	50	10	1	1	1	1
114	0 (s)	45	7	1	1	1	0
115	1	40	7	0	0	0	0
116	1	45	10	0	1	0	1
117	1	40	10	0	1	0	0
118	0 (s)	50	12	1	1	1	0
119	1	50	12	0	1	0	1
120	0 (s)	50	7	1	0	1	1
121	0 (s)	40	10	0	0	1	1
122	0 (s)	50	10	1	1	1	0
123	0 (s)	50	7	1	1	1	1
124	0 (s)	40	12	0	1	1	1
125	0 (s)	50	10	1	0	1	0
126	1	45	12	0	1	0	0
127	1	40	7	0	1	0	0
128	1	45	7	0	1	0	1
129	0 (s)	40	12	0	0	1	0
130	1	50	10	0	1	0	1
131	1	50	10	0	1	0	1
132	0 (s)	50	7	1	0	1	0
133	1	45	7	0	0	0	0
134	0 (s)	50	10	1	1	1	0
135	0 (s)	50	7	1	1	1	1
136	1	45	10	0	1	0	0

	Freq. control	Tlimit/SP heat	Tlimit/SP cool	CP IC	Night mode	Tank	FCs schedule
137	0 (s)	40	10	0	1	1	1
138	1	50	7	0	1	0	1
139	0 (s)	40	12	0	1	1	0
140	0 (s)	40	7	0	0	1	1
141	1	50	12	0	1	0	0
142	0 (s)	40	10	0	0	1	0
143	0 (s)	45	12	0	0	1	1
144	0 (s)	50	7	1	1	1	0
145	1	45	7	0	1	0	0
146	0 (s)	50	7	1	0	1	0
147	0 (r)	45	12	0	0	0	1
148	1	50	10	0	1	0	0
149	0 (s)	40	10	0	1	1	0
150	0 (s)	50	7	1	1	1	0
151	0 (s)	40	7	0	1	1	1
152	0 (s)	45	10	0	0	1	1
153	0 (s)	45	12	0	1	1	1
154	1	50	7	0	1	0	0
155	0 (s)	40	7	0	0	1	0
156	0 (s)	45	12	0	0	1	0
157	0 (r)	45	12	0	0	0	0
158	0 (s)	40	7	0	1	1	0
159	0 (s)	45	10	0	1	1	1
160	0 (s)	45	7	0	0	1	1
161	0 (s)	45	12	0	1	1	0
162	0 (s)	50	12	0	0	1	1
163	0 (s)	45	10	0	0	1	0
164	0 (s)	45	10	0	1	1	0
165	0 (s)	45	7	0	1	1	1
166	0 (s)	50	10	0	0	1	1
167	0 (s)	50	12	0	1	1	1
168	0 (s)	45	7	0	0	1	0
169	0 (s)	50	12	0	0	1	0
170	0 (s)	45	7	0	1	1	0
171	0 (s)	50	10	0	1	1	1
172	0 (s)	50	7	0	0	1	1
173	0 (s)	50	12	0	1	1	0
174	0 (s)	50	10	0	0	1	0
175	0 (s)	50	7	0	1	1	1
176	0 (s)	50	10	0	1	1	0
177	0 (s)	50	7	0	0	1	0
178	0 (s)	50	7	0	1	1	0

Table D. 2. Parametric analysis. Power consumption (% respect simulation 1) and number of hours out of comfort in each thermal zone

n	Consumption	RES (h)	COMM (h)	AMM (h)	META (h)
Base case	6.69 MWh	4.18	5.9	0.13	5.93
1	-35.34%	8.7	110.0	286.8	98.7
2	-34.36%	14.8	20.7	1.1	152.1
3	-34.22%	18.2	125.4	283.9	158.6
4	-33.27%	0.4	53.3	149.4	15.2
5	-32.58%	0.7	4.8	79.1	93.3
6	-32.32%	11.0	13.4	0.7	80.7
7	-32.06%	12.2	87.7	201.0	63.3
8	-31.48%	7.7	60.7	147.6	84.5
9	-31.29%	8.2	109.5	286.8	19.1
10	-31.19%	11.1	22.0	75.0	153.1
11	-30.89%	7.6	107.9	283.4	99.9
12	-30.67%	0.4	2.0	8.8	11.5
13	-30.42%	18.2	22.4	3.8	94.3
14	-30.15%	9.8	11.1	1.0	84.1
15	-30.08%	23.3	105.0	198.1	97.2
16	-30.00%	0.7	0.9	0.3	90.8
17	-29.99%	1.2	37.5	84.7	9.3
18	-29.50%	0.2	53.0	149.4	5.6
19	-29.37%	1.5	4.5	32.9	59.6
20	-28.60%	0.2	50.8	147.2	13.1
21	-28.51%	0.2	4.2	79.1	13.5
22	-28.49%	8.6	10.3	0.6	31.2
23	-28.49%	0.4	0.5	0.0	11.5
24	-28.31%	7.7	11.4	7.5	80.9
25	-28.21%	13.8	16.6	1.2	35.1
26	-27.87%	8.2	109.3	286.8	10.2
27	-27.86%	0.6	4.4	74.5	94.3
28	-27.60%	1.2	2.7	3.7	7.3
29	-27.59%	10.6	85.9	197.6	65.0
30	-27.48%	11.4	86.7	200.9	11.0
31	-27.35%	1.5	1.7	2.7	59.6
32	-27.32%	9.8	46.2	83.3	37.0
33	-27.08%	11.1	18.2	0.5	150.7
34	-27.05%	14.1	23.4	31.3	93.6
35	-26.90%	0.2	1.7	8.7	1.9
36	-26.65%	12.2	113.6	283.6	83.4
37	-26.16%	0.2	53.0	149.4	4.8
38	-25.96%	0.2	0.3	0.3	11.1
39	-25.76%	0.7	36.8	84.6	3.8
40	-25.66%	1.2	1.5	0.1	7.3

41	-25.45%	12.7	14.1	3.7	32.4
42	-25.42%	0.2	1.5	7.1	9.5
43	-25.30%	1.0	35.0	82.8	8.2
44	-25.10%	0.2	4.1	79.1	4.6
45	-24.79%	0.7	3.5	32.8	7.3
46	-24.72%	0.2	0.2	0.0	1.9
47	-24.56%	1.4	4.3	30.9	61.3
48	-24.30%	7.7	10.2	0.4	80.9
49	-24.21%	4.8	56.5	147.4	20.9
50	-24.18%	9.8	12.8	3.5	35.0
51	-23.93%	11.4	13.3	1.1	16.2
52	-23.75%	0.6	0.7	0.1	92.0
53	-23.63%	7.1	107.3	283.3	14.8
54	-23.61%	5.1	10.1	74.8	77.9
55	-23.56%	0.2	1.7	8.7	1.1
56	-23.36%	0.7	2.1	3.6	1.8
57	-23.36%	11.2	86.6	200.9	5.5
58	-23.02%	14.1	20.7	0.7	93.6
59	-22.76%	0.7	0.7	2.6	7.3
60	-22.53%	0.2	0.2	0.3	2.2
61	-22.16%	1.0	1.6	3.1	6.1
62	-22.09%	15.6	92.1	197.7	28.4
63	-21.73%	0.6	36.7	84.6	3.2
64	-21.44%	0.1	50.6	147.2	4.3
65	-21.42%	0.2	0.3	0.0	9.5
66	-21.41%	0.7	0.9	0.1	1.8
67	-21.38%	0.2	0.2	0.0	1.1
68	-21.04%	4.8	7.1	7.3	17.3
69	-20.67%	0.5	3.4	32.8	1.8
70	-20.60%	0.1	3.9	74.5	9.3
71	-20.53%	1.4	1.6	0.3	61.3
72	-20.20%	9.8	12.3	0.6	35.0
73	-19.98%	9.5	84.6	197.4	6.6
74	-19.60%	5.6	41.1	82.9	9.1
75	-19.49%	5.1	6.3	0.3	75.5
76	-19.32%	0.6	2.0	3.6	1.2
77	-19.32%	10.8	112.2	283.5	33.6
78	-19.06%	6.3	10.5	31.0	24.8
79	-18.64%	0.5	0.7	2.6	1.8
80	-18.27%	0.1	1.3	7.1	0.7
81	-18.18%	1.0	1.1	0.2	6.5
82	-17.70%	0.1	34.1	82.6	2.8
83	-17.39%	0.6	0.7	0.1	1.2
84	-17.03%	4.8	5.9	0.2	17.3

85	-16.94%	0.2	3.0	30.6	2.9
86	-16.84%	3.4	55.1	147.4	12.2
87	-16.48%	0.1	0.1	0.0	7.0
88	-16.46%	5.6	7.7	3.2	7.0
89	-16.29%	3.7	8.7	74.7	28.0
90	-16.09%	7.1	107.3	283.3	9.4
91	-15.03%	6.3	7.8	0.4	24.7
92	-14.98%	0.3	32.6	103.3	8.5
93	-14.56%	0.1	0.7	2.9	0.8
94	-14.47%	10.4	12.5	0.6	54.4
95	-14.33%	13.1	89.8	197.5	10.8
96	-14.26%	0.1	0.1	0.0	0.7
97	-13.84%	0.0	50.6	147.2	4.1
98	-13.67%	3.4	5.8	7.3	8.6
99	-13.06%	0.0	3.8	74.5	3.9
100	-12.91%	0.2	0.2	0.0	2.9
101	-12.84%	0.3	1.7	4.7	5.4
102	-12.48%	5.6	7.1	0.3	7.0
103	-12.17%	3.7	4.9	0.2	25.7
104	-12.13%	0.2	32.5	103.3	4.6
105	-12.09%	9.2	84.3	197.4	4.8
106	-12.00%	6.6	39.4	100.3	51.1
107	-11.91%	3.5	38.8	82.8	7.7
108	-11.84%	0.8	29.0	62.5	5.8
109	-11.29%	3.8	8.1	30.8	7.2
110	-11.12%	8.0	9.8	0.5	26.2
111	-11.12%	8.0	9.8	0.5	26.2
112	-10.97%	0.3	0.5	0.0	5.4
113	-10.67%	0.0	1.3	7.1	0.4
114	-10.58%	0.1	0.1	0.0	0.8
115	-10.51%	12.3	14.7	0.9	26.6
116	-9.98%	0.2	1.5	4.7	1.5
117	-9.92%	0.8	2.2	3.2	4.6
118	-9.88%	0.0	34.0	82.6	2.4
119	-9.87%	0.2	32.4	103.3	4.1
120	-9.67%	3.4	4.6	0.2	8.6
121	-9.16%	6.6	9.0	4.2	48.2
122	-9.05%	0.0	2.7	30.6	1.2
123	-8.94%	0.0	0.0	0.0	1.5
124	-8.94%	0.1	31.1	100.1	6.4
125	-8.77%	3.5	5.4	3.1	5.7
126	-8.40%	0.5	28.7	62.5	2.6
127	-8.24%	0.8	1.0	0.1	4.6
128	-8.11%	0.2	0.3	0.0	1.5

129	-7.90%	8.2	36.3	59.9	24.8
130	-7.72%	0.2	1.5	4.7	1.0
131	-7.72%	0.2	1.5	4.7	1.0
132	-7.26%	3.8	5.4	0.2	7.2
133	-6.82%	10.2	12.0	0.8	14.0
134	-6.73%	0.0	0.6	2.9	0.4
135	-6.66%	0.0	0.0	0.0	0.4
136	-6.48%	0.5	1.9	3.2	1.4
137	-6.11%	0.1	0.7	4.0	3.6
138	-5.85%	0.2	0.3	0.0	1.0
139	-5.70%	0.4	27.1	59.6	3.5
140	-5.46%	6.6	8.5	0.2	48.2
141	-5.23%	0.5	28.6	62.5	2.3
142	-5.12%	8.2	9.9	3.1	23.7
143	-5.12%	4.2	36.4	100.2	18.9
144	-5.03%	0.0	0.0	0.0	1.2
145	-4.80%	0.5	0.7	0.0	1.4
146	-4.79%	3.5	4.9	0.2	5.7
147	-4.33%	4.1	5.3	2.0	10.4
148	-3.30%	0.4	1.8	3.2	1.2
149	-2.91%	0.4	0.7	2.8	2.4
150	-2.76%	0.0	0.0	0.0	0.4
151	-2.41%	0.1	0.1	0.0	3.6
152	-2.28%	4.2	6.0	4.1	16.0
153	-1.97%	0.0	31.0	100.1	3.4
154	-1.63%	0.5	0.6	0.0	1.2
155	-1.45%	8.2	9.6	0.3	23.7
156	-0.72%	4.7	33.1	59.7	7.5
157	0.00%	4.2	5.9	0.1	5.9
158	0.75%	0.4	0.4	0.0	2.4
159	0.87%	0.0	0.6	4.0	0.5
160	1.43%	4.2	5.5	0.2	16.0
161	1.58%	0.0	26.7	59.6	1.7
162	1.92%	3.1	35.3	100.2	11.2
163	2.06%	4.7	6.7	2.9	6.4
164	4.36%	0.0	0.3	2.8	0.6
165	4.57%	0.0	0.1	0.0	0.5
166	4.76%	3.1	4.9	4.1	8.3
167	5.44%	0.0	30.9	100.1	3.2
168	5.73%	4.7	6.4	0.1	6.4
169	6.72%	2.9	30.8	59.7	6.6
170	8.03%	0.0	0.0	0.0	0.6
171	8.30%	0.0	0.5	4.0	0.3
172	8.46%	3.1	4.4	0.1	8.3

173	9.30%	0.0	26.7	59.6	1.3
174	9.49%	2.9	4.4	2.9	5.5
175	12.00%	0.0	0.0	0.0	0.3
176	12.09%	0.0	0.3	2.8	0.2
177	13.16%	2.9	4.1	0.1	5.5
178	15.76%	0.0	0.0	0.0	0.2

Table D. 3. Parametric analysis. Electric energy consumption of each component (kWh)

n	Compressor	Fan	Parasitic losses	Fan coils	Circulation pump
1	2,972	249	718	202	186
2	2,974	327	718	177	196
3	3,067	241	718	191	184
4	3,031	272	718	193	251
5	3,128	280	718	195	190
6	3,013	347	718	169	282
7	3,146	260	718	235	187
8	3,164	270	718	182	251
9	3,212	292	718	187	188
10	3,241	274	718	183	189
11	3,281	244	718	197	183
12	3,168	303	718	186	264
13	3,201	332	718	208	196
14	3,217	376	718	163	199
15	3,295	253	718	227	186
16	3,271	316	718	185	194
17	3,204	282	718	224	257
18	3,255	307	718	181	257
19	3,299	294	718	224	192
20	3,357	269	718	188	246
21	3,369	324	718	180	193
22	3,234	386	718	158	289
23	3,283	333	718	177	274
24	3,336	305	718	173	266
25	3,247	352	718	199	287
26	3,415	325	718	179	190
27	3,455	277	718	189	188
28	3,330	312	718	214	271
29	3,459	253	718	230	185
30	3,433	297	718	216	189
31	3,411	324	718	214	195
32	3,392	280	718	216	258
33	3,474	327	718	167	194

n	Compressor	Fan	Parasitic losses	Fan coils	Circulation pump
34	3,470	288	718	215	191
35	3,393	337	718	173	270
36	3,533	295	718	175	187
37	3,450	339	718	173	261
38	3,511	359	718	170	196
39	3,472	310	718	208	261
40	3,431	341	718	204	280
41	3,507	374	718	191	199
42	3,529	304	718	179	260
43	3,534	276	718	219	252
44	3,571	357	718	172	194
45	3,585	330	718	205	194
46	3,508	368	718	164	279
47	3,634	289	718	218	190
48	3,551	358	718	156	282
49	3,613	317	718	168	256
50	3,561	318	718	203	274
51	3,513	383	718	184	292
52	3,687	331	718	173	193
53	3,735	292	718	179	185
54	3,707	328	718	167	191
55	3,588	369	718	165	274
56	3,598	340	718	198	274
57	3,693	323	718	204	190
58	3,696	345	718	195	196
59	3,698	361	718	195	197
60	3,714	393	718	162	198
61	3,703	313	718	206	268
62	3,799	302	718	207	188
63	3,724	335	718	197	263
64	3,804	313	718	172	249
65	3,744	358	718	162	276
66	3,700	369	718	188	283
67	3,703	400	718	157	284
68	3,784	352	718	159	271
69	3,846	357	718	193	195
70	3,909	325	718	172	190
71	3,860	346	718	199	195
72	3,773	375	718	183	291
73	3,946	296	718	209	187
74	3,881	322	718	197	262
75	3,940	381	718	151	196
76	3,851	366	718	187	277

n	Compressor	Fan	Parasitic losses	Fan coils	Circulation pump
77	3,991	337	718	165	188
78	3,974	337	718	195	193
79	3,958	387	718	183	198
80	3,976	348	718	163	264
81	3,914	371	718	186	285
82	4,021	315	718	199	255
83	3,952	395	718	177	286
84	4,000	405	718	142	287
85	4,121	331	718	197	191
86	4,076	353	718	159	259
87	4,142	379	718	156	195
88	4,051	360	718	184	278
89	4,164	370	718	158	192
90	4,209	333	718	169	186
91	4,200	394	718	175	198
92	3,013	279	718	180	1,499
93	4,190	352	718	186	271
94	2,993	343	718	161	1,508
95	4,291	342	718	193	189
96	4,192	401	718	146	280
97	4,286	348	718	162	251
98	4,247	388	718	150	274
99	4,383	366	718	161	190
100	4,347	389	718	177	197
101	3,132	307	718	174	1,501
102	4,262	417	718	164	295
103	4,397	423	718	142	197
104	3,189	307	718	171	1,495
105	4,450	334	718	194	187
106	3,225	286	718	172	1,488
107	4,375	354	718	183	264
108	3,192	281	718	208	1,500
109	4,466	378	718	181	193
110	3,197	376	718	153	1,503
111	3,197	376	718	153	1,503
112	3,237	334	718	165	1,504
113	4,458	383	718	153	266
114	4,402	410	718	166	288
115	3,231	345	718	187	1,507
116	3,308	336	718	165	1,497
117	3,299	310	718	200	1,502
118	4,526	346	718	185	256
119	3,323	332	718	166	1,492

n	Compressor	Fan	Parasitic losses	Fan coils	Circulation pump
120	4,463	441	718	133	289
121	3,385	321	718	162	1,493
122	4,625	369	718	182	191
123	4,615	419	718	145	196
124	3,430	283	718	174	1,488
125	4,544	392	718	171	280
126	3,418	304	718	194	1,495
127	3,393	335	718	190	1,504
128	3,413	363	718	156	1,500
129	3,462	297	718	199	1,488
130	3,443	360	718	160	1,494
131	3,443	360	718	160	1,494
132	4,692	435	718	161	199
133	3,471	370	718	174	1,502
134	4,696	384	718	172	272
135	4,673	436	718	136	282
136	3,525	332	718	186	1,497
137	3,590	318	718	165	1,493
138	3,547	387	718	151	1,497
139	3,614	291	718	199	1,488
140	3,588	373	718	146	1,501
141	3,622	325	718	185	1,491
142	3,619	333	718	186	1,493
143	3,665	329	718	159	1,478
144	4,851	427	718	162	197
145	3,619	358	718	176	1,499
146	4,756	449	718	151	297
147	3,633	424	718	147	1,479
148	3,729	353	718	177	1,493
149	3,772	328	718	186	1,493
150	4,907	441	718	152	289
151	3,793	370	718	148	1,501
152	3,825	363	718	150	1,483
153	3,882	321	718	161	1,478
154	3,823	379	718	168	1,495
155	3,819	390	718	167	1,501
156	3,932	334	718	182	1,478
157	3,887	443	718	164	1,479
158	3,972	384	718	167	1,501
159	4,042	356	718	151	1,483
160	4,028	416	718	134	1,491
161	4,096	325	718	182	1,478
162	4,123	359	718	152	1,469

n	Compressor	Fan	Parasitic losses	Fan coils	Circulation pump
163	4,089	371	718	169	1,483
164	4,253	361	718	169	1,483
165	4,246	408	718	135	1,491
166	4,282	394	718	142	1,474
167	4,366	350	718	152	1,469
168	4,289	427	718	150	1,491
169	4,425	359	718	171	1,469
170	4,454	417	718	150	1,491
171	4,528	384	718	143	1,474
172	4,485	446	718	126	1,482
173	4,611	346	718	171	1,469
174	4,581	396	718	158	1,474
175	4,731	437	718	127	1,482
176	4,769	382	718	158	1,474
177	4,781	452	718	139	1,482
178	4,969	439	718	139	1,482